Thèse de doctorat

Université de Limoges

Université de Limoges
ED 615 - Sciences Biologiques et Santé (SBS)
INSERM U1248 IPPRITT

Thèse pour obtenir le grade de
Docteur de l'Université de Limoges
Pharmacologie, infectiologie et sciences du médicament

Présentée et soutenue par
Quentin FAUCHER

Le 13 décembre 2021

Impact de l'hypoxie/réoxygénation sur l'expression et la fonctionnalité des transporteurs tubulaires rénaux

Thèse dirigée par Pierre MARQUET, Chantal BARIN-Le GUELLEC et Roland LAWSON

JURY :

Président du jury
M/M^{me}

Rapporteurs :
M^{me} Marie ESSIG, PU-PH, APHP, Hôpital Ambroise Paré, Département de Néphrologie
M Olivier FARDEL, PU-PH, Pôle Biologie, CHU de Rennes

Examinateurs :
M^{me} Chantal BARIN-Le GUELLEC, MCU-PH, Service de biochimie et biologie moléculaire, CHRU de Tours
M Pierre MARQUET, PU-PH, Service de pharmacologie, toxicologie et pharmacovigilance, CHU de Limoges

À Andrée, Renée, Antoine et Guy

Remerciements

Je remercie l'Université de Limoges, l'École Doctorale Sciences Biologiques et Santé n°615, la Faculté de Médecine et la Faculté des Sciences & Techniques de Limoges de m'avoir formé et octroyé la possibilité et les facilités qui m'ont permis de mener à bien cette thèse.

J'adresse mes remerciements et ma reconnaissance aux membres du jury qui ont accepté d'examiner ce travail.

Au **Dr. Chantal Barin-Le Guellec**, je vous remercie chaleureusement pour la confiance que vous m'avez accordée dès le début de ce travail. Votre pragmatisme et votre objectivité m'ont beaucoup inspiré. Je suis ravi d'avoir pu bénéficier de votre expertise et de votre accompagnement.
Au **Pr. Pierre Marquet**, je vous suis reconnaissant de m'avoir accueilli au sein de votre unité lors de mon stage du Master 1 jusqu' à la fin de cette thèse. J'ai beaucoup appris durant ces années. J'estime avoir eu la chance d'être sous votre supervision éclairée pendant ma thèse.
Au **Dr. Roland Lawson**, je vous remercie d'avoir accepté d'encadrer mon travail en cours de thèse. J'ai apprécié d'être associé à vos recherches, je vous remercie de m'avoir intégré à votre thématique et dans vos projets.

Au **Pr. Marie Essig**, je vous remercie de m'avoir accordé votre confiance à mes débuts. J'accorde de l'importance à votre appréciation de ce travail : un aboutissement de mes premiers pas dans la recherche.
Au **Dr. Bastien Burat**, je te remercie de m'avoir encadré pendant mon Master 1. Ta disponibilité et tes précieux conseils m'ont permis d'apprécier et de réaliser ce travail dès les prémices de cette thèse.

Aux **membres de l'unité INSERM U1248**, à Limoges, je remercie chacun d'entre vous d'avoir rendu possible ce travail tout au long de ces quatre années. J'ai eu la chance de collaborer et d'évoluer au sein de cette unité. J'aspire à pouvoir un jour contribuer à son rayonnement.
Aux **membres de l'unité EA4245**, à Tours, je vous remercie de m'avoir accueilli dans votre unité. J'ai beaucoup apprécié d'échanger et d'apprendre à vos côtés. Je remercie plus particulièrement le **Dr. Stéphanie Chadet** et le **Dr. Marie Piollet** pour leur aide et contribution à la réalisation des expérimentations.

Au **Dr. Florent Di Meo**, je te remercie pour tes conseils, ta disponibilité constante et ton soutien. Tu as grandement participé à mon appréhension initiale et ma compréhension progressive de la recherche.

À **Hélène Arnion**, je te remercie pour ton aide essentielle tout au long de ma thèse. Tes savoirs et savoir-faire ont contribué à l'aboutissement de ce travail.

À **François-Ludovic Sauvage**, je te remercie pour ton aide précieuse dans la réalisation de mes expériences. J'espère que la méthode « sasuke » perdurera.

Au **Dr. Antoine Humeau**, je te remercie pour ton implication dans ce travail. Je te souhaite un « bon début de lecture ».

Au **Dr. Benjamin Chantemargue**, je te remercie pour nos nombreux échanges variés et riches.

À **Emmanuelle Izorche**, je te remercie pour ton aide et ton écoute bienveillante.

À **Karen Poole**, je te remercie pour ton aide permanente et plus particulièrement pour tes corrections de l'anglais.

À **Jean-Sébastien Bernard**, je te remercie pour ton humour quotidien, c'est un réel soutien.

Au **Dr. Nicolas Vedrenne**, je te remercie pour tes conseils avisés.

Au **Dr. Gabin Fabre**, je te remercie pour les échanges que nous avons eus.

À **Émilie Pinault**, je te remercie pour ton aide dans la conduite de cette thèse.

Au **Dr. Hassan Aouad,** j'ai eu la chance de partager ces trois années de thèse avec toi. Je te remercie de m'avoir aidé et soutenu quotidiennement. Je garderai des souvenirs complices de nos échecs, nos doutes, nos rires et nos réussites dans le bureau 240.

À **Tom Nanga**, je te remercie pour ta bienfaisance quotidienne.

Au **Dr. Joseph Berthier**, je te remercie pour ta bonne humeur partagée pendant ces années.

À **Eliés Zarrouk**, je te remercie pour nos nombreux échanges passionnés.

À **Angelika Janaszkiewicz** et **Ágota Tóth**, je vous remercie pour avoir collaboré et sympathisé en anglais.

À **Mehdi Benmameri**, je te remercie pour ta curiosité et ton intérêt pour mes travaux.

À **Roy Lakis**, je te remercie pour nos discussions et tes traductions.

À **Manon Jardou**, je te remercie pour nos discussions et plus particulièrement autour de la vulgarisation.

À **Hugo Alarcan**, je te remercie pour ta patience et ta contribution dans ce travail. Je garde le bon souvenir d'avoir travaillé à tes côtés.

À **Clarisse Brossier**, je te remercie pour ton soutien et ta gaieté. Je suis heureux de t'avoir initié à la recherche et accompagné dans tes travaux.

À **Michael Koczerka**, je te remercie pour ton amitié et ton accueil lors de mes déplacements tourangeaux.

À ma famille et **à mes amis**,

Au terme de ce parcours, je tiens à remercier celles et ceux qui me sont chers. Je vous exprime mes pensées chaleureuses. Je souligne l'intérêt que vous avez porté à mes travaux et qui ont fait l'objet de nombreuses discussions. Les moments passés avec vous en marge de cette thèse m'ont également permis de ménager quelques pauses récréatives et vivifiantes afin de m'éloigner temporairement de ce travail. Aussi, vos contributions, quelles qu'elles soient, m'ont permis de réaliser cette thèse. Je vous remercie infiniment pour votre soutien et la proximité apprenante dont vous m'avez fait bénéficier sans autres distances que celles imposées par la situation sanitaire.

À mes parents,

Je vous exprime ma gratitude et toute mon affection. Votre curiosité spontanée et vos oreilles attentives sont le témoignage de votre sensibilité omniprésente et de votre aide quotidienne.

Droits d’auteurs

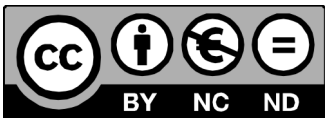

Table des matières

Liste des abréviations

ABC : *ATP-Binding Cassette*

ABM : Agence de la biomédecine

ATP : Adenosine triphosphate

BCRP : *Breast Cancer Resistance Protein*

CHR : Centre Hospitalier Régional

CHRU : Centre Hospitalier Régional Universitaire

DBD: *Donation after Brain Death*

DCD : *Donation after Cardiac Death*

DGF : *Delayed Graft Function*

ECD : *Extanded Criteria Donors*

FSS : *Fluid Shear Stress*

GLUT : *Glucose Transporter*

HMP : *Hypothermic Machine Merfusion*

$HMPO_2$: *active oxygenated* HMP

IGF : *Immediate Graft Function*

iPSC : induced Pluripotent Stem Cells

IR : Ischémie-Reperfusion

IRI : *Ischemia/Reperfusion Injury*

IS : *Indoxyl Sulfate*

LC-MS/MS : Liquid Chromatography-tandem Mass Spectrometry

MATE : *Multidrug And Toxin compound Extrusion*

MEC : Matrice ExtraCellulaire

MRP : *Multidrug Resistance associated Protein*

NMP : *Normothermic Machine Perfusion*

OAT : *Organic Anion Transporter*

OCT : *Organic Cation Transporter*

OMS : Organisation Mondiale de la Santé

P-gp : *P-glycoprotein*

PAH : Para-AminoHippuric acid

PNF : *Primary Non Function*

RMN : Résonnance Magnétique Nucléaire

ROS : *Reactive Oxygen Species*

RSST : *Remote Sensing and Signaling Theory*

SCS : *Static Cold Storage*

SGLT : *Sodium/Glucose coTransporter*

SLC : *SoLute Carrier*

TEA : TétraÉthyl Ammonium

TLDA : *Taqman® Low-Density Array*

TP : Tubule Proximale

Table des illustrations

Introduction générale

Transplantation rénale et prévalence des pathologies rénales

La transplantation rénale est le traitement de référence pour les patients atteints d'insuffisance rénale chronique terminale. Elle leur offre une meilleure qualité de vie et est associée à une réduction de la morbidité et de la mortalité par rapport à la dialyse.

En 2015, Liyanage et coll. avaient estimé que le recours à la thérapie de suppléance aux fonctions épuratrices rénales (dialyse ou transplantation rénale) sera nécessaire à plus de 5 millions de personnes dans le monde d'ici 2030[1]. L'organisation mondiale de la santé (OMS) prévoit une croissance de la mortalité liée aux pathologies rénales jusqu'à 27 décès pour 100 000 personnes en 2060[2]. Cette progression résulte d'un vieillissement de la population et de l'augmentation de la prévalence de pathologies telles que le diabète et l'hypertension[1].

Ces prévisions prédisent un accroissement de la disparité entre le besoin et le nombre d'organes disponibles dans les prochaines décennies. Cette problématique est d'ores et déjà actuelle : pour illustration, en 2020 en France, d'après l'agence de la biomédecine (ABM), le taux de croissance annuel des candidats en liste d'attente a été de 6%. L'augmentation de l'indicateur de pénurie s'élevait à 3,3 receveurs en attente par greffon cette même année contre 2,2 en 2018 et 2019[3]. Sachant que la crise sanitaire liée à l'épidémie SARS-CoV2 a eu un impact sur l'activité de transplantation rénale en 2020.

Donneurs à critères « sous-optimaux » et retard de reprise de fonction

Afin de répondre à la demande croissante d'organes face à un groupe limité de donneurs vivants ou en état de mort encéphalique [*donation after brain death* (DBD)], de nombreux centres de transplantation ont instauré un protocole approuvant le recours à des donneurs dits « sous-optimaux ». Ces derniers incluent les donneurs décédés après arrêt circulatoire [*donation after cardiac death* (DCD)] et les donneurs à critères élargis [*extended criteria donors* (ECD)]. Les ECD correspondent aux donneurs âgés de plus de 60 ans, ou de 50 à 59 ans et présentant au moins deux des trois critères suivants : antécédent d'hypertension artérielle, décès par accident vasculaire cérébral, créatininémie > 1,5 mg/dL[4].

En 2019 et 2020, en France, les ECD représentaient plus de la moitié des donneurs, soit respectivement 52 et 51%. En 2020, les greffes réalisées à partir de donneurs vivants ont continué à baisser, pour la 3^{e} année consécutive, pour atteindre -36% par rapport à 2017[3]. Ces chiffres illustrent l'importance actuelle du recours à ces donneurs dits « marginaux » en transplantation rénale.

Retard de reprise de fonction [Delayed Graft Function (DGF)]

Ces 20 dernières années, les courbes de survie des greffons rénaux révèlent une dégradation de plus en plus précoce, probablement due au recours aux donneurs sous-optimaux. En effet, les greffons issus de ces donneurs sont davantage sujets aux lésions ischémiques. Dans des modèles expérimentaux de transplantation, les reins plus âgés étaient plus susceptibles de subir des lésions ischémiques et ce même lorsque l'ischémie pré-transplantation était brève[5]. Une analyse rétrospective du registre des transplantations australiennes et néo-zélandaises a montré une corrélation entre la fonction du greffon d'une part, le temps total d'ischémie et l'âge du donneur d'autre part. L'incidence de retard de reprise de fonction [*Delayed Graft Function* (DGF)] était plus élevée chez les receveurs de reins de donneurs âgés et pour chaque heure d'ischémie totale, le risque global de perte de greffon augmentait de 2%[6]. Dans une étude déjà ancienne, chez les patients recevant un organe sous-optimal, l'hypertension du donneur était associée de manière indépendante à la DGF. De plus, la DGF et l'hypertension du donneur ont eu un effet négatif sur la fonction du greffon à un an, uniquement pour les greffons sous-optimaux[7].

La DGF est définie comme la nécessité de recours à la dialyse au cours des 7 jours suivant une greffe rénale. Elle est, parmi d'autres, un facteur de risque important d'évolution péjorative du greffon à court (rejet aigu) et à long terme (mauvaise fonction rénale, néphropathie chronique d'allogreffe et perte du greffon)[8–10].

Une analyse, basée sur les données du *Scientific Registry of Transplant Recipients* des États-Unis, de 2000 à 2004, indiquait que la DGF concernait 21% des greffons de donneurs à critères standards, 33% des donneurs à critères élargis (ECD), 40% des donneurs DCD et 55% des donneurs DCD répondant aux critères ECD[11]. En France, sur l'ensemble de la période 2016-2019, le taux de DGF se situait à 27% en cas de donneurs à critères élargis contre 23% et 5% pour les donneurs en état de mort encéphalique et les donneurs vivants, respectivement[3]. Réalisée en 2002, une analyse multivariée montrait que les patients avec une reprise de fonction immédiate du greffon [*immediate graft function* (IGF)] avaient eu une meilleure survie du greffon que ceux avec reprise de fonction lente et qui, eux-mêmes, avaient une meilleure survie que les patients avec une DGF[9]. La conclusion d'une méta-analyse de 34 études réalisées entre 1988 et 2007 était la suivante : les patients atteints de DGF avaient une incidence de 49% de rejets aigus, contre 35% chez les patients non atteints de DGF[8]. Des facteurs influençant la DGF ont été identifiés, parmi lesquels : des paramètres associés au donneur (circonstance du décès et âge)[5,11], des paramètres associés au receveur (sexe, antécédent de diabète, nécessité de dialyse pré-greffe ou taux d'anticorps réactifs plus élevé (>10 %))[12] et des conditions de conservation de l'organe (durée, méthode de conservation et composition de la solution de conservation)[13–16].

Lésions d'ischémie-reperfusion en transplantation rénale

La DGF est une manifestation clinique de l'ischémie-reperfusion (IR) induisant une lésion rénale aiguë [*Ischemia/Reperfusion Injury* (IRI)]. L'IRI est une conséquence fréquente et grave de la transplantation d'organes. Les principales causes et facteurs favorisants sont essentiellement ceux décrits ci-dessus pour la DGF. L'IRI est un processus physiopathologique complexe, multifactoriel, étalé dans le temps et associé à de nombreuses perturbations structurelles et métaboliques (Figure 1). Ces lésions d'IR induisent le développement d'une fibrose interstitielle, un dysfonctionnement microvasculaire et une amplification de la réponse immunitaire locale. Ceux-ci entraînent une altération de la fonction rénale et impactent la survie du greffon à court et potentiellement à long terme[4,17,18].

Le phénomène ischémique

Dès qu'il est prélevé chez le donneur, le greffon est soumis à une période de conservation à +4°C (ischémie froide) dans l'attente d'être transplanté chez le receveur. Le temps d'ischémie froide correspond au délai entre la mise du greffon dans la solution de conservation à +4°C et le déclampage artériel après la réalisation des anastomoses chez le receveur. Une période d'ischémie chaude précède l'ischémie froide. Elle correspond au délai entre le clampage de l'artère du greffon chez le donneur et son immersion dans la solution de conservation.

Au niveau cellulaire, en situation d'hypoxie, la mitochondrie ne peut plus assurer la phosphorylation oxydative nécessaire à la production d'ATP. Un *switch* métabolique s'opère donc au profit de la glycolyse anaérobie pour assurer une production d'ATP minimale (mais insuffisante pour les besoins énergétiques de la cellule). La chute brutale de la quantité d'ATP intracellulaire et l'accumulation de sous-produits du métabolisme anaérobie entraînent une acidose ainsi qu'une hyperosmolarité intracellulaire. La perte de fonction de transporteurs énergie-dépendants, majoritairement la Na^+/K^+-ATPase, induit un afflux de sodium et d'eau aggravant les déséquilibres osmotiques aboutissant à un œdème cellulaire. L'accumulation de calcium intracellulaire, en raison de l'arrêt du pompage du Ca^{2+} hors des cellules et de sa réabsorption limitée par le réticulum endoplasmique, favorise la génération d'espèces réactives de l'oxygène [*reactive oxygen species* (ROS)] au niveau mitochondrial[18–21]. Dans l'ensemble, l'ischémie crée un environnement favorable à de futures lésions délétères lors de la revascularisation des tissus.

La reperfusion tissulaire

À la suite de la revascularisation, les lésions d'ischémie s'accentuent. En effet, la reperfusion ne rétablit pas des conditions physiologiques. Au contraire, elle aggrave les dommages *via* l'activation de plusieurs mécanismes, parmi lesquels la réponse immunitaire adaptative et innée ainsi que les programmes de mort cellulaire. Une étude *in vitro* sur des

cardiomyocytes indiquait que 4% et 17% de la viabilité cellulaire avaient été perdus après respectivement 1 et 4h d'ischémie, mais qu'après 3h de reperfusion, cette perte atteignait 73%[22].

Le retour brutal à un état de normoxie provoque une surproduction de ROS et une réduction de la capacité antioxydante[20,23]. Les ROS contribuent à endommager les bicouches phospholipidiques et le cytosquelette. Cette réoxygénation conduit à différents mécanismes de mort cellulaire tels que l'apoptose et la nécrose[20]. Les cellules nécrotiques favorisent la dénudation des tubules et l'infiltration tissulaire de cellules inflammatoires. Ce phénomène induit une tempête cytokinique, une stimulation du système immunitaire[4,18] et une infiltration des leucocytes dans l'espace interstitiel responsable de l'apparition progressive d'une fibrose interstitielle et d'une atrophie tubulaire. Cette dernière est associée à un dysfonctionnement chronique pouvant mener à la perte totale des fonctions du greffon[24]. L'IR provoque un gonflement des cellules endothéliales et une altération de la cyto-architecture avec pour conséquences une perte des interactions cellules-cellules et une fuite du filtrat glomérulaire[4].

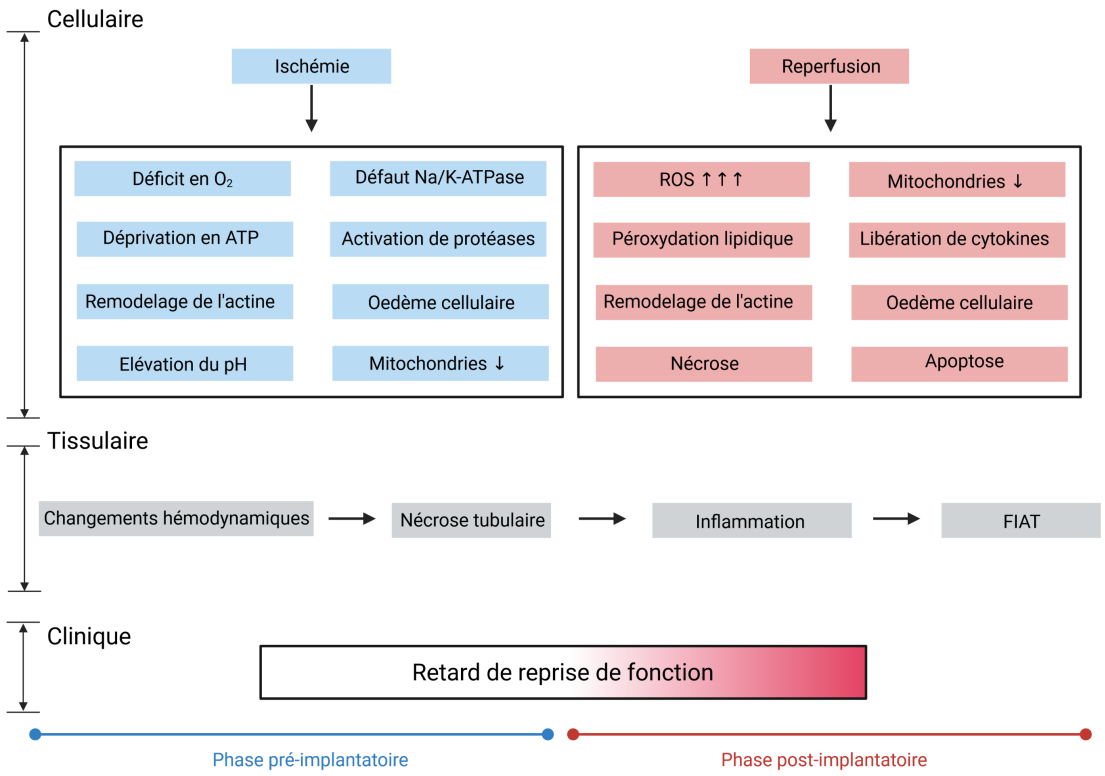

Figure 1 : Lésions d'IR et conséquences en transplantation rénale
L'illustration est inspirée de la référence [4] et a été réalisée avec BioRender.com. FIAT, fibrose interstitielle et atrophie tubulaire ; ROS, *reactive oxygen species*.

Améliorer la qualité du greffon

Pour améliorer la qualité des greffons rénaux, plusieurs stratégies existent à différents temps des phases pré-, per- et post-implantatoires. Au sein de l'unité INSERM U1248 "Pharmacologie & Transplantation", une partie de l'activité de recherche est axée sur l'amélioration de la survie du greffon en aval de la transplantation au moyen de l'optimisation d'utilisation des médicaments immunosuppresseurs. La majeure partie des travaux concerne :

- l'identification des sources pharmacocinétiques et pharmacogénétiques de la variabilité de la réponse entre patients[25,26],
- l'identification de biomarqueurs prédictifs du rejet de greffe[27,28],
- L'étude de la toxicité des immunosuppresseurs[29–31] et de leur suivi thérapeutique[32].

Pour les lésions d'IR, des équipes ont cherché à identifier des mécanismes et des fonctions intracellulaires impliqués dans les dommages (sub) cellulaires, ou des mécanismes tissulaires liés à l'IR, comme cibles thérapeutiques[33–41]. Certaines études sont centrées sur les organes, soit en augmentant le flux sanguin rénal et le débit urinaire, soit en réduisant le gonflement des cellules épithéliales[37–39]. D'autres sur l'échelle cellulaire, et proposent une modulation de l'IRI par des mécanismes métaboliques et anti-inflammatoires, ou à l'aide de molécules aux propriétés antioxydantes[33–36,40,41].

Longtemps délaissée au profit du contrôle du rejet après chirurgie, la période pré-implantatoire apparaît maintenant comme un axe de recherche clé dans ce processus thérapeutique. L'amélioration de la conservation des greffons rénaux concourt à atténuer les lésions d'IR et à anticiper, en amont de la procédure chirurgicale, les éventuelles perturbations post-greffes.

Stratégies pré-implantatoires

Méthodes de conservation

Jusqu'à une époque récente, les greffons rénaux étaient majoritairement conservés de manière statique et à froid [*Static Cold Storage* (SCS)]. Le greffon était placé dans un réservoir entouré de glace et immergé dans une solution de conservation préalablement tempérée à 4°C. Le but est de limiter le métabolisme et l'œdème cellulaire afin que l'organe tolère l'environnement hypoxique[42].

Plusieurs solutions de conservation existent pour cette conservation statique à froid (Annexe 1). Elles ont pour objectifs d'atténuer les lésions ischémiques et d'améliorer ainsi la conservation du tissu rénal[43]. Elles peuvent être réparties en 3 groupes :

- les solutions « intracellulaires » avec [K] > 30mM ; [Na] < 100mM,

- les solutions « extracellulaires » avec [K] < 25mM ; [Na] > 100mM,
- les solutions « intermédiaires » avec [K] et [Na] < 25mM.

Afin de limiter l'œdème cellulaire et interstitiel lié à la condition hypothermique, ces solutions sont supplémentées avec soit des imperméants : des sucres (mannitol, glucose) ou des anions (gluconate), soit des colloïdes (hydroxy-éthyle amidon). Les imperméants préviennent la formation d'un œdème intracellulaire par la pression osmotique qu'ils exercent dans le compartiment vasculaire. Les colloïdes exercent une pression oncotique et préviennent alors la formation d'un œdème interstitiel. Pour prévenir la formation des ROS, divers antioxydants enzymatiques (ex. superoxyde dismutase), non-enzymatiques (ex. acide ascorbique) ou thiolés (ex. glutathion réduit) sont ajoutés dans ces solutions. Enfin, ces solutions sont tamponnées (ex. HEPES) pour atténuer les variations de pH et donc limiter l'acidose (cellulaire et interstitielle)[43]. En 2020, une étude, basée sur le registre français des greffes incluant uniquement des reins conservés en SCS issus de DBD au cours de la période 2010-2014, n'a pas montré de différence significative entre les 5 solutions étudiées vis-à-vis de la survie du greffon à 1 an[44]. Cette étude souligne qu'aucune solution ne présente une supériorité avérée vis-à-vis d'une autre.

La stratégie la plus fréquente actuellement pour la conservation des greffons rénaux « sous-optimaux » est l'utilisation des machines à perfusion hypothermiques [*Hypothermic Machine Perfusion* (HMP)]. Les reins conservés sur HMP sont placés dans un réservoir contenant la solution de conservation tempérée à 4°C. Ce réservoir est entouré d'un bac de glace. Les reins sont ensuite canulés au niveau de l'artère rénale et une pompe de recirculation génère un flux de liquide de perfusion dans le système vasculaire rénal à des pressions subphysiologiques[45] (Figure 2 A/C). L'objectif est de maintenir l'irrigation tissulaire pour assurer une répartition homogène de la température et un maintien des échanges entre le tissu rénal et son environnement. L'utilisation des HMP est associée à de meilleurs résultats, principalement pour les donneurs décédés, avec des taux de DGF réduits et une meilleure survie du greffon[13–15,46]. Sur l'ensemble de la période 2016-2019, en France, le taux de DGF associé aux critères élargis est passé de 37% à 24% en cas de perfusion sur machine[3]. En 2020, en France, 84,4% des greffons ECD ont été mis sur machine de perfusion[3]. Les effets bénéfiques de l'HMP seraient liés à la protection de l'endothélium vasculaire[47] et à la stimulation du métabolisme cellulaire[48].

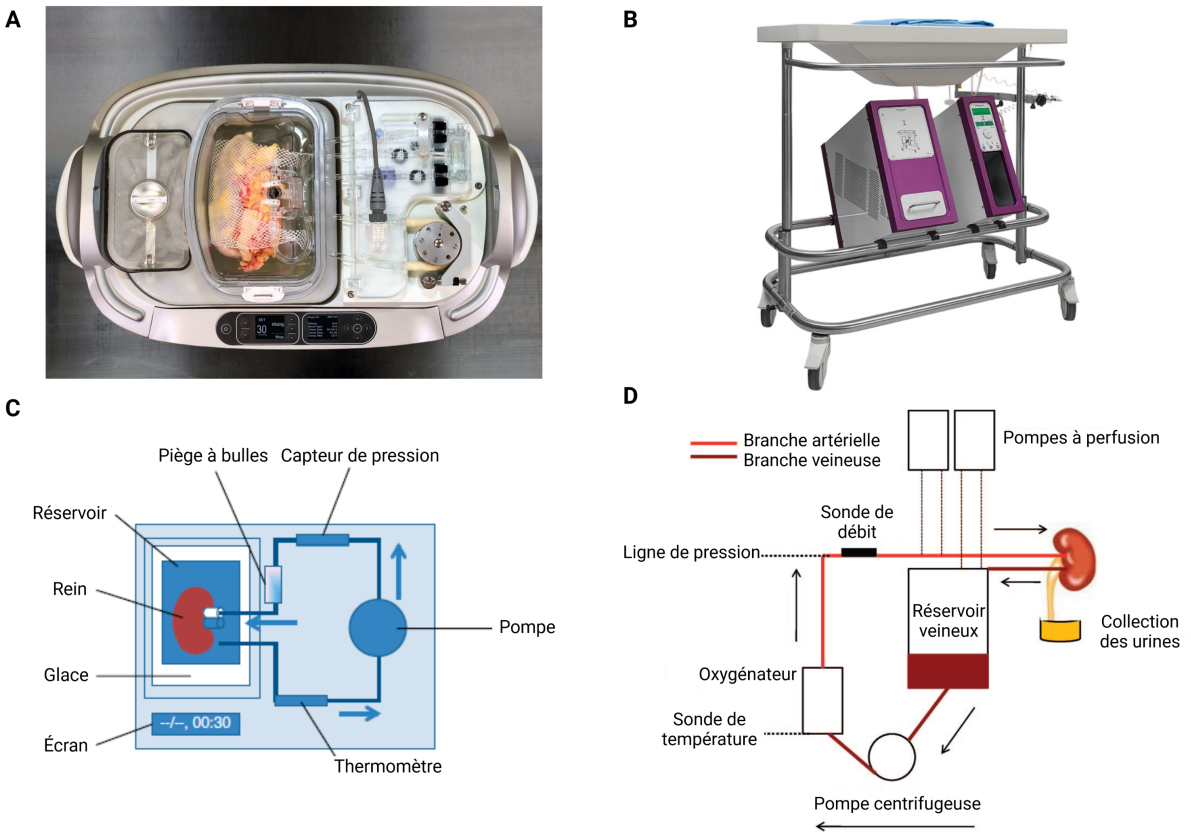

Figure 2 : Différentes stratégies de perfusion des greffons rénaux
(**A**) Machine de perfusion hypothermique LifePort® de Organ Recovery Systems. L'image est publiée avec l'autorisation de ©2021 Organ Recovery Systems, Inc. (**B**) Machine de perfusion normothermique Kidney Assit™ de Organ Assist. L'image est publiée avec l'autorisation de XVIVO Perfusion AB, 2021. (**C-D**) Représentation schématique des machines de perfusion (**C**) hypothermique et (**D**) normothermique. Figure adaptée des références suivantes (**C**) [49] et (**D**) [50]. 'L'illustration a été réalisée avec BioRender.com.

Plus récemment, la machine de perfusion normothermique [*Normothermic Machine Perfusion* (NMP)] est apparue (Figure 2 B/D). Elle permet une perfusion oxygénée et normothermique de l'organe avec l'objectif de rétablir le métabolisme cellulaire pendant sa conservation et d'atténuer les bouleversements métaboliques lors de la reperfusion[51]. Cette technologie est encore très expérimentale et peu répandue. La première transplantation rénale réalisée après conservation du greffon sur machine normothermique a 10 ans à peine[50]. Aucun consensus sur les conditions optimales d'utilisation de ces machines n'a encore été trouvé. Au moment de notre écriture, il n'existe qu'un seul système NMP commercialisé pour le rein (Kidney Assit™ Device de Organ Assist). Le premier cas clinique avec l'utilisation de cette machine a été publié en 2020[52].

Bien que l'utilisation des technologies de perfusion soit prometteuse, les mécanismes cellulaires opérant au cours de la conservation restent mal connus et des études additionnelles

sont nécessaires pour évaluer la qualité des greffons conservés sur machine et anticiper la sévérité des atteintes post-greffes.

Perspectives thérapeutiques et diagnostiques

Aucun biomarqueur fiable et reproductible de la qualité du greffon conservé sur HMP n'existe. À ce jour, la décision de réaliser ou non la transplantation repose sur les paramètres mesurés par la machine. L'analyse pathologique de biopsies systématiques pré-implantatoires est une pratique de plus en plus répandue[53], mais le score pathologique, opérateur-dépendant, n'est pas toujours bien corrélé à la reprise de fonction du greffon. L'étude du contenu des perfusats de greffons conservés sur machine pourrait apporter des informations complémentaires.

Parmi les approches « omiques » non ciblées, la métabolomique s'intéresse à la mesure quantitative des métabolites des systèmes vivants intégrés et de leurs réponses dynamiques aux changements physiologiques et pathologiques. Cette approche a fait l'objet d'un intérêt croissant dans le champ des pathologies rénales[48,54–60]. Des analyses métabolomiques centrées sur les conséquences de l'ischémie ou de l'IR *in vivo*[61–67] ont été effectuées. Les métabolites identifiés confirment le *switch* énergétique et le stress oxydant. Des analyses métabolomiques du liquide de conservation en période pré-greffe pourraient constituer une approche non invasive pour discriminer les lésions d'IR en amont du processus opératoire[65,66]. Elles pourraient ainsi constituer un outil d'évaluation de la qualité des greffons, utilisable pour optimiser les conditions de perfusion et pour rechercher des biomarqueurs du pronostic fonctionnel post-transplantation (IGF/DGF) et du devenir du greffon à long terme[65,66].

L'identification des processus par lesquels ces métabolites se retrouvent dans les solutions de conservation des greffons, l'urine, le plasma ou le tissu rénal, est une nécessité pour comprendre les mécanismes sous-jacents impactés par l'IR. De nombreux métabolites sont liés à un relargage incontrôlé des cellules lésées ou à la réaction inflammatoire, d'autres peuvent illustrer des lésions tubulaires et/ou une altération des fonctions tubulaires rénales.

Cellules tubulaires proximales et transporteurs tubulaires

Les cellules tubulaires proximales, localisées comme leur nom l'indique dans le tubule proximal (Annexe 2), sont les plus sensibles aux lésions d'IR à cause de leur dépendance à l'égard de la phosphorylation oxydative, de leur capacité limitée à utiliser la glycolyse anaérobie et de la grande quantité d'énergie métabolique requise pour le transport membranaire des métabolites essentiels dont ces cellules sont le siège. De nombreux métabolites endogènes (ex. intermédiaires du cycle de Krebs, acides aminés, glucose) et des

molécules de signalisation (ex. les nucléotides cycliques ou les prostaglandines) sont substrats de divers transporteurs de solutés (*Solute carrier* (SLC)) et de transporteurs ABC (*ATP-binding cassette*). La régulation de l'expression et/ou de la fonction des transporteurs membranaires est donc essentielle à la clairance rénale de leurs substrats et à la régulation de l'homéostasie métabolique des tissus.

L'ischémie subie par le greffon lors de sa conservation s'accompagne, entre autres mécanismes lésionnels, d'une altération fonctionnelle des transporteurs tubulaires. Compte tenu du rôle majeur des transporteurs dans la fonction rénale, une altération de leur activité pourrait en partie expliquer les perturbations fonctionnelles du greffon chez le receveur et favoriser des perturbations métaboliques globales et une surexposition médicamenteuse en période post-greffe immédiate. Les profils métabolomiques différentiels du perfusat des greffons pourraient refléter des modulations d'activité des transporteurs et permettre d'anticiper des complications futures associées à leur dysfonction en période post-greffe.

Chapitre I. **Revue de littérature sur les lésions d'ischémie-reperfusion, les transporteurs tubulaires proximaux et la transplantation rénale**

Afin de comprendre l'impact de la modulation IR-dépendante des transporteurs sur la fonction rénale post-greffe, nous avons réalisé un état des lieux des connaissances relatives aux effets des lésions d'IR sur les transporteurs tubulaires proximaux. En préambule, nous avons présenté leur fonctionnement ainsi que leur rôle prépondérant dans les processus de sécrétion et de réabsorption tubulaire. Enfin, nous avons exposé les conséquences possibles d'une perturbation des transporteurs tubulaires dans le contexte de la transplantation rénale.

Au travers de cette revue de la littérature, nous souhaitions établir le rationnel de notre étude. Afin d'envisager les conséquences théoriques que les lésions d'IR pourraient avoir sur la fonction rénale post-transplantation, nous avons fait la synthèse des différentes études qui traitent de l'impact de l'ischémie et de l'IR sur l'expression et/ou l'activité des transporteurs tubulaires *in vitro*, *in vivo* et chez l'homme. Enfin, nous avons souhaité comprendre en quoi une modulation de leurs fonctions pourrait améliorer la survie du greffon.

I.1. Article de revue de littérature : Effects of Ischemia-Reperfusion on Tubular Cell Membrane Transporters and Consequences in Kidney Transplantation

Journal of
Clinical Medicine

MDPI

Review

Effects of Ischemia-Reperfusion on Tubular Cell Membrane Transporters and Consequences in Kidney Transplantation

Quentin Faucher [1], Hugo Alarcan [1], Pierre Marquet [1,2] and Chantal Barin-Le Guellec [1,3,4,*]

1 IPPRITT UMR1248, Université de Limoges, INSERM, F-87042 Limoges, France; quentin.faucher@unilim.fr (Q.F.); hugo.alarcan@unilim.fr (H.A.); pierre.marquet@unilim.fr (P.M.)
2 Department of Pharmacology and Toxicology, CHU Limoges, F-87042 Limoges, France
3 Laboratory of Biochemistry and Molecular Biology, CHU Tours, F-37000 Tours, France
4 Department of Pharmacology, Université de Tours, F-37044 Tours, France
* Correspondence: chantal.barin-leguellec@univ-tours.fr

Received: 6 July 2020; Accepted: 6 August 2020; Published: 12 August 2020

Abstract: Ischemia-reperfusion (IR)-induced acute kidney injury (IRI) is an inevitable event in kidney transplantation. It is a complex pathophysiological process associated with numerous structural and metabolic changes that have a profound influence on the early and the late function of the transplanted kidney. Proximal tubular cells are particularly sensitive to IRI. These cells are involved in renal and whole-body homeostasis, detoxification processes and drugs elimination by a transporter-dependent, transcellular transport system involving Solute Carriers (SLCs) and ATP Binding Cassettes (ABCs) transporters. Numerous studies conducted mainly in animal models suggested that IRI causes decreased expression and activity of some major tubular transporters. This could favor uremic toxins accumulation and renal metabolic alterations or impact the pharmacokinetic/toxicity of drugs used in transplantation. It is of particular importance to understand the underlying mechanisms and effects of IR on tubular transporters in order to improve the mechanistic understanding of IRI pathophysiology, identify biomarkers of graft function or promote the design and development of novel and effective therapies. Modulation of transporters' activity could thus be a new therapeutic opportunity to attenuate kidney injury during IR.

Keywords: ischemia/reperfusion injury; kidney transplantation; renal tubular transporters; drug transporters; toxin elimination

1. Introduction

For patients with end-stage renal disease, transplantation is a treatment of choice, providing a much better quality of life. To overcome the gap between a growing need for organs and the limited number of living or brain-dead donors, most centers are increasingly using sub-optimal donors, i.e., presenting with circulatory death or other expanded donation criteria. However, kidneys retrieved from such donors are more prone to Ischemia-Reperfusion (IR)-Induced acute kidney injury (IRI), Delayed Graft Function (DGF), and generally have shorter graft survival [1]. In the context of solid organ transplantation, IRI is strongly correlated to morbidity. Tissue and cellular hypoxia begin as soon as the organ is removed and the hypoxic phenomenon extends during graft storage in the preservation fluid. Graft lesions then increase after transplantation, secondary to revascularization. IRI is a complex pathophysiological process, associated with numerous structural and metabolic changes, arising from a complicated interaction between renal hemodynamics, inflammatory cytokines, endothelial and tubular cell injuries. These processes in turn favor short and potentially long-term graft failure [2–8].

The proximal tubule is more sensitive to IRI than other kidney structures. Proximal tubular cells express many multispecific transporters, belonging to either the SoLute Carrier (SLC) or ATP-Binding Cassette (ABC) families. They are involved in the reabsorption and secretion of various endogenous and exogenous compounds, according to their locations, i.e., on the basolateral (blood) or apical (urine) sides. These substrates comprise electrolytes (e.g., Na^+, Cl^-, K^+, Ca^{2+}), glucose, amino acids, several important anions (e.g., phosphate and citrate), uremic toxins (e.g., *p*-cresol, indoxyl sulfate, hippuric acid) as well as xenobiotics, some of which are used during the post-transplantation period (e.g., immunosuppressants, antibiotics, antiviral drugs). Owing to the bi-directional exchange they allow, proximal tubular cells are involved in renal and whole-body homeostasis, detoxification processes and xenobiotic clearance [9–11]. The effects of IR on the metabolism and structure of proximal tubular cells have been widely studied [12,13], but its effects on expression and activity of membrane transporters is less known and has not been reviewed so far. This article reviews current knowledge about the impact of IR on the expression and activity of SLC and ABC renal tubular cell membrane transporters. Its ambition is also to help to figure out new therapeutic approaches to prevent or reduce IRI-dependent alterations of transporter's activity.

2. Coordinated and Bidirectional Transcellular Transport in Proximal Tubular Cells

Proximal tubular cells ensure trans-epithelial exchanges by means of their singular cyto-architecture and coordinated transport system. These polarized cells possess a basolateral membrane, in relation to systemic circulation, and an apical membrane made of elongated microvilli, in contact with the glomerular filtrate. Several transmembrane transporters, which mainly belong to the SLC and the ABC families, ensure coordinated movements of their substrates across tubular cells (Figure 1) [9,14,15].

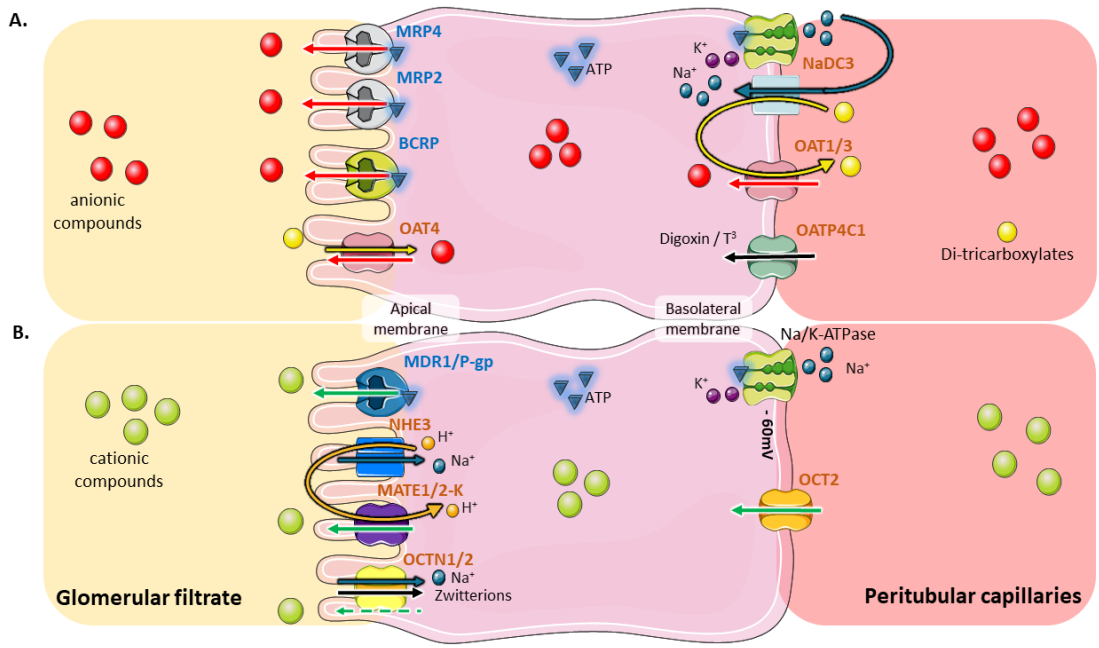

Figure 1. Bidirectional transporter-dependent transfer of anionic (**A**) or cationic (**B**) compounds within proximal tubular cells. (**A**) The elimination of organic anions (OA^-) mainly depends on a coordinated transfer mediated by OAT1/3 (*SLC22A6* and *SLC22A8*) and MRP2/4 (*ABCC2* and *ABCC4*). The transport of OA^- at the basolateral side of tubular cells by OATs uses a tertiary active transport system. The Na^+/K^+-ATPase pumps sodium out of the cell. This creates the gradient by which Na^+/dicarboxylate cotransporters (NaDC3/*SLC13A3*) drive the uptake of Na^+ and α-ketoglutarate and other dicarboxylates into the cell. High intracellular concentration of dicarboxylates produces the outward driving force enabling influx of organic substrates by OATs exchangers. This antiport transfer results in the entry of endogenous OA^- or xenobiotics into the tubular cell. A member of the OATP

family, OATP4C1 (*SLCO4C1*), also contributes to the basolateral entry of anionic molecules including cAMP, digoxin, ouabain, and thyroid hormones (T^3) [16,17]. The OA^- that have reached the intracellular compartment are then excreted at the apical pole through a ATP-dependent primary active transport depending mainly on MRP2, MRP4 and BCRP (*ABCG2*) [14,16,18]. At the apical membrane, OAT4 (*SLC22A11*) promotes a bidirectional transport which allows the reabsorption of some OA^- including sulfate conjugates against the efflux of dicarboxylates such as α-ketoglutarate [19]. (**B**) Organic cations (OC^+) pass through the basolateral membrane via an electrogenic uniport transport, driven by the negative internal potential created by the Na^+/K^+-ATPase. This transport mostly involves the OCT2 member of the SLC family (*SLC22A2*) [20]. At the apical membrane, MATE1 (*SLC47A1*) and MATE2-K (*SLC47A2*), coupled with Na^+/H^+ exchangers like NHE3 (*SLC9A3*), mediate the secretion of OC^+: the protons released into the tubular lumen are taken up by OC^+/H^+ exchangers, promoting an input of H^+ which is counterbalanced by an output of organic cations [15]. Other transporters of the SLC family are expressed at the apical membrane, including OCTN1 (*SLC22A4*) and OCTN2 (*SLC22A5*), which ensure the Na^+-dependent reabsorption of zwitterions and facilitated secretion of OC^+ [21]. MDR1/P-gp (*ABCB1*), an ABC family transporter located at the apical side, is also involved in the removal of organic cations and xenobiotics [9]. Artwork was designed using Servier Medical Art by Servier licensed under CC BY 3.0 (https://smart.servier.com).

The SLC superfamily includes a large number of polyspecific transporters, some of which are intensively expressed at the renal level. Among the most expressed ones, are organic cations facilitative uniporters (OCTs), organic anion/dicarboxylate exchangers (OATs), Na^+/zwitterion cotransporters (OCTNs), uric acid exchanger (URAT1), Na^+/phosphate (NaPi-IIa/NaPi-IIc) or Na^+/dicarboxylate (NaDC3) cotransporters, sodium-independent organic anion transporters (OATPs) and multi-drug and toxin extrusion transporters (MATEs) [22–24]. ABC transporters, which promote ATPase-coupled unidirectional transport of their substrates, are also widely expressed at the apical membrane of tubular cells. The most expressed tubular ABC transporters are multidrug resistance protein 1 (P-gp, MDR1), multidrug resistance-associated proteins 2,4 (MRP2,4) and breast cancer resistance protein (BCRP) [14,25].

3. Role of Tubular Transporters in Maintaining Renal Cells' Equilibrium, Tissue Homeostasis, Detoxification Processes and Drug Elimination

Following glomerular filtration, numerous solutes (e.g., amino acids, glucose, potassium, phosphate, bicarbonate, low-molecular-weight proteins, tricarboxylic acid (TCA) intermediates) are reabsorbed in the proximal tubule to prevent excessive losses of vital metabolites. Tubular cells are also in charge of the urinary elimination of various in-excess endogenous metabolites. As SCLS and ABCs tubular transporters are involved in the tubular transfer of a vast number of small molecules, including inorganic ions, metabolites, nutrients and signaling molecules [9], they have a major role in controlling tissue and cell homeostasis (Figure 2). It is worth noting that the activity of the sodium-potassium pump (Na^+/K^+-ATPase), located at the basolateral pole, provides the electrochemical gradient necessary for tubular movements of electrolytes and solutes in all tubular segments [26]. As shown in Figure 2, tubular transporters coordinate the harmonized, bi-directional transport of their endogenous substrates. The vectorial reabsorption of glucose, as well as the cooperative interaction of some transporters of the amino acid transport system, illustrates this phenomenon.

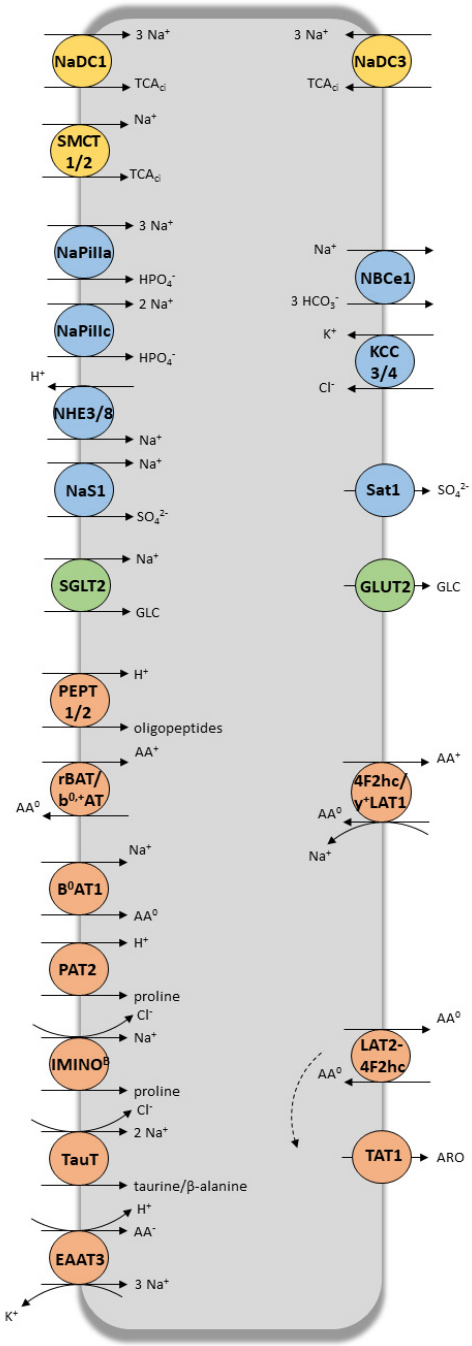

Figure 2. TCA cycle intermediates (yellow), electrolytes (blue), glucose (green) and peptides (orange) SLCs super-family transporters expressed at apical (left) and basolateral (right) membrane of tubular proximal cells. TCA_{ci}, TCA cycle intermediates; Ur, urate; GLC, glucose; AA^{-}, anionic amino acids; AA^{0}, neutral amino acids; AA^{+}, dibasic amino acids; ARO, aromatic amino acids. Artwork was designed using Servier Medical Art by Servier licensed under CC BY 3.0 (https://smart.servier.com).

As well as their role in homeostasis described above, SLCs and ABCs transporters are also involved in detoxification processes by contributing to the renal handling of metabolic wastes, environmental chemicals and uremic toxins [27]. Uremic toxins are compounds normally eliminated by the kidney, which accumulate in the case of chronic kidney disease, causing several complications, including nephropathy [11]. The list of these molecules is available on the network of the European Uremic Toxin Workgroup (http://www.uremic-toxins.org). This list contains more than 150 substances

derived from dietary protein breakdown, endogenous metabolic pathways or the gut microbiome [27]. They are divided into three classes based on their chemical properties: (i) small water-soluble, non-protein-bound solutes, with a molecular weight less than 500 Da (e.g., urea, creatinine, uric acid); (ii) middle size molecules (e.g., parathyroid hormone); and (iii) small protein-bound solutes (e.g., *p*-cresol, indoxyl sulfate, hippuric acid) [27,28]. Even if most of these toxins can be removed from the body by glomerular filtration, elimination of the protein-bound uremic toxins depends predominantly on tubular transporters' activity [27]. Table 1 presents the main uremic toxins handled by multi-specific tubular transporters, of which OAT1 and OAT3 are the most important. Although numerous studies have documented the specificities of certain SLC transporters for these protein-bound uremic solutes/toxins, their apical efflux into urine and their excretion by ABC transporters are less well known.

Renal tubular transporters are also responsible for the handling of many drugs, some of which are used in kidney transplantation. Ivanyuk et al. recently reviewed current knowledge on the role and clinical relevance of tubular transporters in drug therapy [29]. Many other reviews are available for a comprehensive understanding of this topic, and interested readers are referred to corresponding references [9,10,18,30–33]. Table 1 presents a list of the main xenobiotics handled by renal transporters (Table 1).

Table 1. Main endogenous metabolites, uremic toxins and drugs handled by renal tubular transporters.

Part 1—Transporters of Endogenous Metabolites					
Transporter	**Gene**	**Location**	**Transport Mode**	**Endogenous Substrates**	**References**
Inorganic Ions					
NaPi-IIa	*SLC34A1*	Apical	Na^+/phosphate co-transporter	Na^+; Pi	[24]
NaPi-IIc	*SLC34A3*	Apical	Na^+/phosphate co-transporter	Na^+; Pi	
NHE3	*SLC9A3*	Apical	Na^+/H^+ exchanger	Na^+; H^+	[34]
NBCe1	*SLC4A4*	Basolateral	Na^+/HCO_3^- co-transporter	Na^+; HCO_3^-	[35]
KCC3	*SLC12A6*	Basolateral	K^+-Cl^- cotransporter	K^+; Cl^-	[36]
KCC4	*SLC12A7*	Basolateral	K^+-Cl^- cotransporter	K^+; Cl^-	
NaS1	*SLC13A1*	Apical	Na^+-SO_4^{2-}-cotransporter	Na^+; SO_4^{2-}	[37]
Sat1	*SLC26A1*	Basolateral	sulfate anion transporter	SO_4^{2-}	
Glucose					
SGLT1	*SLC5A1*	Apical	Na^+/glucose co-transporter	Na^+; glucose	[38]
SGLT2	*SLC5A2*	Apical	Na^+/glucose co-transporter	Na^+; glucose	
GLUT1	*SLC2A1*	Basolateral	passive transport	glucose	
GLUT2	*SLC2A2*	Basolateral	passive transport	glucose	
Peptides, amino acids					
PEPT1	*SLC15A1*	Apical	H^+/oligopeptide cotransporters	oligopeptides	[39]
PEPT2	*SLC15A2*	Apical	H^+/oligopeptide cotransporters	oligopeptides	
Neutral amino acids (AA0)					
B^0AT1	*SLC6A19*	Apical	Na^+-neutral amino acid co-transporter	AA^0	[40]
TauT	*SLC6A6*	Apical	Na^+-dependent co-transporter	taurine; β-alanine; (GABA)	[40,41]
$IMINO^B$	*SLC6A20*	Apical	Na^+-Cl^--dependent co-transporter	proline; hydroxyproline	[40]
PAT2	*SLC36A2*	Apical	H^+-dependent symporter	glycine; alanine; proline	[40]
LAT2-4F2hc	*SLC7A8*/*SLC3A2*	Basolateral	antiporter	ARO; AA^0	[42,43]
TAT1	*SLC6A10*	Basolateral	uniporter	ARO	
Cationic amino acids (AA+)					
rBAT/$b^{0,+}$AT	*SLC3A1*/*SLC7A9*	Apical	amino acids exchanger	AA^+; AA^0	[44,45]
4F2hc/y^+LAT1	*SLC3A2*/*SLC7A7*	Basolateral	Na^+-dependent amino acids exchanger	AA^+; AA^0	[46]
Anionic amino acids (AA−)					
EAAT3	*SLC1A1*	Basolateral	K^+-Na^+/H^+/amino acids exhanger	L-glutamate; L-aspartate	[40]
Tricarboxylic acid (TCA) intermediates					
NaDC1	*SLC13A2*	Apical	Na^+/di-tricarboxylate co-transporter	TCA cycle (e.g., succinate, citrate, α-ketoglutarate, fumarate)	[47]
NaDC3	*SLC13A3*	Basolateral	Na^+/di-tricarboxylate co-transporter	TCA cycle (e.g., succinate, citrate, α-ketoglutarate, fumarate)	
SMCT1	*SLC5A8*	Apical	high-affinity Na^+-coupled co-transporter	lactate; pyruvate; nicotinate	[48]
SMCT2	*SLC5A12*	Apical	low-affinity Na^+-coupled co-transporter	lactate; pyruvate; nicotinate	

Table 1. *Cont.*

Part 2—Transporters of Uremic Toxins and Drugs			
Transporter	**Endogenous Substrates**	**Uremic Toxins**	**Drugs**
		Organic anions (OA^-)	
		OAT Family	
OAT1; OAT2; OAT3; OAT4	mono-carboxylates (e.g., butyrate, lactate, propionate, pyruvate, 3-hydroxybutyrate, benzoate, 3-hydroxypropionate, 3-hydroxyisobutyrate); di-carboxylates (e.g., α-ketoglutarate, *N*-acetylaspartate); short-chain fatty acids (e.g., hexanoate, heptanoate and octanoate); prostaglandins (PGE2 and PGF2α); cyclic nucleotides (cAMP and cGMP); folate; nicotinate; tryptophan metabolites (quinolinate and kynurenate); purine metabolites (xanthine and hypoxanthine); adenine, adenosine, cytidine, guanidine, guanosine, inosine; hormones (estrone-3-sulfate, 17β-estradiol-3-sulfate, ß-estradiol-3-sulfate, β-estradiol-3,7-disulfate and DHEAS) [22,49,50]	uremic toxins (indoxyl sulfate, *p*-cresol, *p*-cresyl sulfate, indole-acetate, uric acid, creatinine, kynurenic acid, orotic acid, benzoate, trimethylamine *N*-Oxide (TMAO), 3-carboxy-4-methyl-5-propyl-2-furanpropionate (CMPF)); environmental toxins (mercury conjugate, ochratoxin A and aristolochic acid) [9,27,28,51]	Antivirals (adefovir, tenofovir, aciclovir, ciclofovir, cidofovir, lamivudine, stavudine); Non steroidals anti-inflammatory; Methotrexate; Diuretics (furosemide, bumetanide, hydrochlorothiazide); Angiotensin II receptors blockers (candesartan, valsartan, losartan …); β-lactams (penicillins chepalosporines …); Other antibiotics (tetracycline, ciprofloxacine); H2-antihistaminics (cimetidine, ranitidine, famotidine …); ACE inhibitors (captopril, quinaprine); HMG-coA reductor inhibitors (fluvastatin, pravastatin, simvastatin); Oral antidiabetics (glibenclamide …); mycophenolic acid glucuronide; Uricosuric-drugs (probenecid, benzbromarone) [9,29,30,52]
OATP Family			
OATP4C1	thyroid hormones (T^3), cAMP [50]	asymmetric dimethylarginine (ADMA), guanidine succinate (GSA), and trans-aconitate [27]	Digoxin, ouabaine, methotrexate [29]
MRP Family			
MRP2; MRP4	glutathione, conjugated glutathione; bilirubin glucuronides and other metabolites (LTC4, E217βG, reduced glutathione (GSH)); cyclic nucleotides and ADP; prostaglandins (PGE1, PGE2); thromboxane B2 (TBX2); proinflammatory leukotrienes B4 et C4 (LTB4, LTC4); estradiol glucuronide (E217βG); folic acid [53,54]	kynurenic acid, probably indoxyl sulfate and hippuric acid [27]	Antivirals (tenofovir); Non steroidals anti-inflammatory; Methotrexate; Diuretics (furosemide); Angiotensin II receptors blockers; β-lactams [29]

Table 1. *Cont.*

Part 2—Transporters of Uremic Toxins and Drugs			
Transporter	**Endogenous Substrates**	**Uremic Toxins**	**Drugs**
BCRP Family			
BCRP	Vitamins (folic acid, B2, K3) estrone-3 sulfate, dehydroepiandrosterone sulfate, E217βG [55]	Urate, kynurenic acid, indoxyl sulfate, hippuric acid, *p*-cresyl sulfate and *p*-cresyl glucuronide [27,56,57]	Corticosteroids conjugates; Antineoplasics (mitoxantrone, methotrexate, irinotecan …); Antiretroviral nucleosides (AZT, lamivudine …); Fluoroquinolones; Statins (rosuvastatin); sulfasalazine; ITK (imatinib, gefitinib, nilotinib) [29,55]
Organic cations (OC^+)			
OCT Family			
OCT2	choline, thiamine, L-carnitine [31]	polyamine uremic toxins (e.g., cadaverine, putrescine, spermine and spermidine); guanidino group (e.g., creatinine, guanidine or methylguanidine) [27,58]	Metformin; Cisplatin; H2-antihistaminics (cimetidine, famotidine, ranitidine …); antivirals; β blockers (pindolol …); Calcium channel blockers; Antiarrhythmics (procainamide, dofetilide …); Antimalarials; Varenicline; Amantadine; Memantine [29,31]
OCTN1; OCTN2	ergothionein; L-carnitine, choline [22,59]		Verapamil; Quinidine; Gabapentine; β-lactams (cephaloridine, cefepime); Valproic acid [10,29]
MATE Family			
MATE1; MATE2	6β-hydroxycortisol, E3S, *N*-methylnicotinamide (NMN), L-Arginine and thiamine [60]	guanidine, creatinine and ADMA [60]	Corticosteroids; Metformin; Cimetidine; Platinum compounds; Antibiotics (cefalexine, cephradine); H2-antihistaminics (cimetidine); Memantine [10,29]
MDR Family			
MDR1/P-gp	Anticancer drugs (methotrexate, anthacyclines, campthecins, taxanes …); Digoxin; Cardiovascular agents (valsartan, quinidine, nifedipine, verapamil); Immunosuppressant (ciclosporine, tacrolimus); Corticosteroids (corticosterone, dexamethasone); Antibactrial (erythromycine); Antiretrovirals (ritonavir, saquinavir); Phenobarbital; Phenytoin; Statins (lovastatin, simvastatin); H1-antihistaminic (fexofenadine); Anticoagulants (dabigatran); ITK inhibitors (imatinib, gefitinib); Antiepileptics (Topiramate); Analgesics (morphine) [9,10,29,32]		

Non-exhaustive list of endogenous and exogenous substrates handled by tubular transporters. Not all substrates of the OAT family are transported by each member of this family. For P-gp, we have represented only the xenobiotics transported.

4. Effects of IRI on Renal SLC and ABC Proximal Tubular Transporters

Proximal tubular cells are particularly sensitive to IR-induced injury [4,61–63] because of the high metabolic energy required for membrane transport of essential metabolites, their strong dependence on oxidative phosphorylation and their limited ability to utilize anaerobic glycolysis [61,62]. Numerous alterations affect tubular proximal cells during IRI [2,5,61,62], whether structural (e.g., actin cytoskeleton remodeling [64,65], brush-border membrane disruption [66], loss of cell polarity, loss of tight junctions [62] and rupture in the continuity of the phospholipid bilayer [61]) or functional (e.g., mitochondrial swelling and impaired mitochondrial respiratory capacity [62], deprivation in intracellular ATP [67], modification of calcium and sodium homeostasis [5]). It is thus relevant to hypothesize that cells with sub-lethal injuries have a reduced capacity for transcellular transport of their endogenous and exogenous substrates (Figure 3). Several studies actually provided insights in this matter by analyzing the effects on transporters expression and/or function of ischemia alone, or ischemia followed by reperfusion. Others have indirectly evaluated transport activity by measuring plasma or urinary metabolite content in conditions of, and after recovery from, I and/or IR.

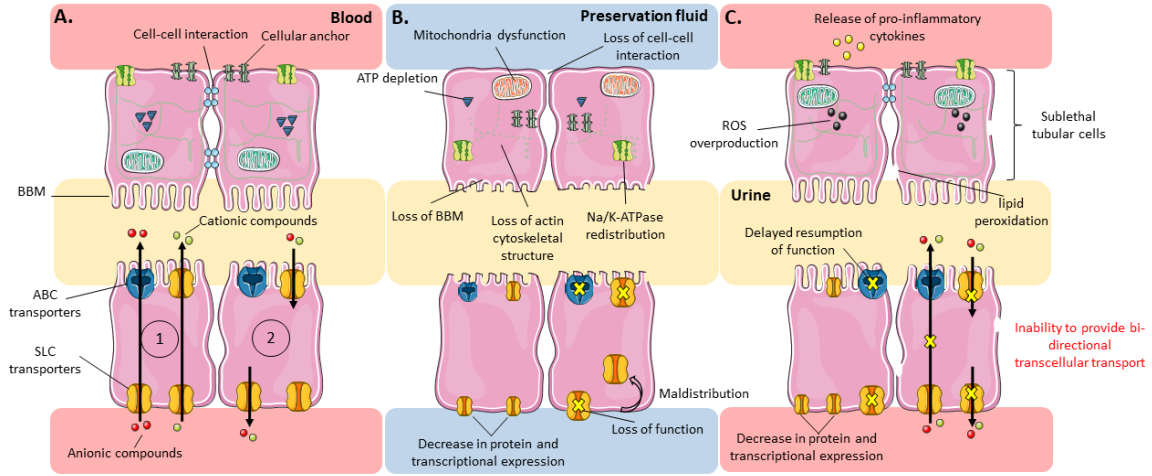

Figure 3. Evolution of subcellular structures and expression/function of tubular transporters under physiological and ischemia-reperfusion conditions focused on sublethal tubular cells. Evolution of subcellular structures (top) and expression/function of tubular transporters (bottom) under (**A**) physiological, (**B**) ischemic and (**C**) reperfusion conditions, focused on sublethal tubular cells. (1) Tubular secretion; (2) Tubular reabsorption. ABC and SLC transporters are distinguished by their shape and do not represent specific members of their respective families. Artwork was designed using Servier Medical Art by Servier licensed under CC BY 3.0 (https://smart.servier.com).

4.1. Effects of Ischemia (I) and/or Ischemia-Reperfusion/Reoxygenation (IR) on Transporters' Expression and/or Function

Several studies, conducted either in vitro or in vivo, have evaluated whether and how tubular transporters are modulated by I and/or IR. They mainly focused on the transport of electrolytes, metabolites and drugs and were all conducted at 37 °C, thus evaluating the effects of warm ischemia. In this section, we present the major tubular transporters whose activity or expression is modulated by IR. IRI and associated kidney dysfunction have numerous deleterious clinical consequences in transplant patients. However, allograft dysfunction is multifactorial and transporters only account for a small piece of the puzzle. Although it is very difficult to make direct links in such a complex process, there is evidence that transporters are involved in part of the electrolyte and acid-base disorders encountered after kidney transplantation [68]. Connections between transporter's modulation and related consequences on graft outcomes or on toxins and xenobiotic accumulation are further discussed in the next chapters.

4.1.1. Effects on Solute Carriers (SLC)

Several studies have analyzed the consequences of I or IR on Na^+-dependent uptake of compounds by tubular cells. Brush-border membrane vesicles isolated from mouse kidneys subjected to different conditions of ischemia/reperfusion showed decreased ^{32}Pi uptake after 15, 30 and 60 min of ischemia induced by renal arterial clamping. This correlated with a decrease in protein expression of the NaPi-II cotransporter. The uptake of ^{32}Pi and NaPi-II expression only reappeared after 2 h of reperfusion following 30 min of ischemia, but was not restored when ischemia lasted 60 min [69].

In rats subjected to 15 and 30 min of renal ischemia, NHE3 mRNA in the kidney cortex significantly decreased after 12 h of reperfusion and was still low after 24 h. The transcriptional expression of NHE3 was less severely affected after 15 min clamping than 30 min[99]. Other authors showed decreased NHE3 transcripts and protein expression in rat cortex and medulla for up to 10 days after reperfusion, following 40 min of ischemia [70]. Kwon et al. examined the abundance of several Na^+-coupled transporters in rats subjected to different ischemia (30, 40 and 60 min) and reperfusion (1–5 days) time durations. After 1 day of reperfusion following 30 min of ischemia, they saw a decrease in protein expression of NHE3, NaPi-IIa and Na^+/K^+-ATPase, paralleling an increase in urinary excretion of Na^+. Five days after 30 min of ischemia, urinary excretion of Na^+ normalized but the renal expression of Na^+ transport proteins had incompletely recovered. Sixty minutes of ischemia induced stronger changes in these parameters on day 1, with no recovery on day 5 [71].

Several studies in rats have demonstrated that renal ischemia is also associated with a transient decrease in glucose transport activity on proximal tubule brush border vesicles, due to decreased SGLT2 expression at the apical membrane [72,73]. Glucose reabsorption was significantly reduced in the post-ischemia period, with partial recovery after 4 h [72].

Similar results were obtained with SLC transporters involved in xenobiotic clearance and detoxification processes [74]. Many studies showed decreased clearance of uremic toxins using a rat model of ischemic acute renal failure [75–77]. Matsuzaki et al. showed that IR (30-min bilateral clamping of renal arteries followed by 6, 12, 24 or 48 h of reperfusion) was associated with a significant increase in the concentration of indoxyl sulfate in serum, proportional to reperfusion time duration [77]. This paralleled a significant decrease in rOAT1 and rOAT3 mRNAs and protein expression. A decrease in the uptake of PAH and estrone sulfate was also observed in renal slices taken from these rats at 48 h of reperfusion, consistent with the decreased rOAT1 and rOAT3 protein expression at that time. Schneider et al. also showed that 45 min of renal ischemia is accompanied by a downregulation of protein and transcriptional expression of rOAT1 and rOAT3, with an early decrease (as early as 6 h after the start of reperfusion) followed by a partial recovery at 24 h and a complete restoration at 72 h [76]. These results were corroborated using an in vitro model of hypoxia-reoxygenation, showing that 2 h of hypoxia induced a significant decrease of basolateral fluorescein uptake 48 hours after reoxygenation [78].

Regarding organic cations, the renal clearance of tetraethylammonium (TEA) was significantly lower in rats exposed to IR (48 h of reperfusion following 30 min bilateral arterial clamping), as compared to control animals. In addition, the authors found a significant decrease in the uptake of TEA by renal slices isolated from these rats. However, the concentration of TEA in the kidney was significantly elevated in rats exposed to IR, suggesting a concomitant decrease of its efflux transport. This altered TEA transport was associated with significant decreases in rOCT2 and rMATE1 mRNAs and protein expression, the latter transporter being indeed the most severely affected [79]. A significant decrease in rOCT1 and rOCT2 mRNAs and protein expression was also observed 24 h after 45-min bilateral clamping of the renal arteries in rats [80]. The uptake of methyl-4-phenylpyridinium, a prototypical OCT substrate, was also reduced in the authors' in vitro IRI model [80]. In mouse models of either syngenic or allogeneic kidney transplantation, a significant decrease in rOCT1 mRNA and protein expression was observed at day 4 post-transplantation in both conditions [81], whereas decreased rOCT2 mRNA and protein expression was only observed in allogeneic transplantation. This suggests a link between the immune response and the downregulation of some tubular transporters.

In humans, Corrigan et al. determined the effect of post-ischemic lesions on PAH clearance and PAH extraction rate, by measuring renal blood flow using magnetic resonance imaging [82]. The study included 44 kidney transplant patients in whom PAH clearance was measured at 1–3 h and then at 7 days after transplantation. PAH clearance decreased independently of renal plasma flow, confirming that active proximal secretion of PAH is impaired in kidney transplant patients. This strongly suggests that organic anion transporters are dysfunctional after an ischemic insult, although their expression was not measured in this study. In this regard, Kwon et al. performed an immuno-histochemical analysis with confocal microscopy of hOAT1 on biopsies from 10 cadaveric donor renal allografts, taken 1 hour after reperfusion following a total ischemic time of 1574 ± 72 min [83]. They found diverse abnormal cell localizations of OAT1, characterized by variable patterns of misdistribution between basolateral membrane and cytoplasm. In a subset of patients in whom PAH net tubular secretion was measured at post-operative day 4 ± 1, a trend to more severe hOAT1 misdistribution was seen in patients with the lowest PAH clearances. Nonetheless, even subjects with misdistribution or absent hOAT1 were still able to secrete PAH, probably because hOAT3 is less severely altered by ischemia than hOAT1.

4.1.2. Effects on ABC Transporters

Contrary to SLCs, information on the effects of IR on renal ABC drug transporters is limited. In their above-described study showing decreased rOAT1,3 expression and function up to 48 h after reperfusion, Matsuzaki et al. found a transient increase in the amount of mRNA encoding Mdr1 after 6 and 12 h of reperfusion, with a return to basal values at 24 h. At 48 h of reperfusion, rMdr1 mRNA level and P-gp protein expression were identical to those of control animals [77]. Following 30 min bilateral clamping of renal arteries in a mouse model, Huls et al. found that some transporters genes were up-regulated and others downregulated 7 days after ischemia [84]. In particular, there was an increase in the mRNA levels of the *ABCB1*, *ABCB11* and *ABCC4* genes but a decrease for *abca3*, *abcc2* and *abcg2*. For each of them, the expression levels had returned to baseline at day 14. A significant decrease in the protein expression of *ABCA3*, *ABCB44* and *ABCB11* and *ABCC2* was observed 7 days after reperfusion, suggesting differential modulation of various ABC transporters during ischemia-reperfusion in the kidney. The opposite pattern between *ABCC4* and *ABCB11* transcripts and expression of the respective proteins suggests post-transcriptional regulatory mechanisms. We hypothesize that this differential regulation of ABC transporters during IR results from the regeneration process, which takes place after ischemic injury as an adaptive response to maintain homeostasis.

4.1.3. Possible Mechanisms Underlying Membrane Transporter Dysfunction during I or I/R

As detailed above, experimental and clinical studies clearly show that IR induces decreased transport activities of most renal SLC transporters and has differential effects on ABC transporters. Reduced tubular uptake of substrates from blood along with up-regulation of P-gp and other ABC transporters has the potential to decrease the amount of potentially harmful substrates in the proximal tubular epithelium. However, after this brief quiescence, resumption of the activity of transporters in the post-ischemic phase ensures the entry of various metabolites essential to the viability of tubular cells. Overall, tubular transporters are mechanistically involved in cell dysfunction during IR but their restoration protects the organ after IR [85]. It is worth mentioning that the kinetics of transcriptional events and of protein expression generally differ. Most authors showed a rapid restoration of mRNAs encoding rOAT1 and rOAT3 and a slower recovery of protein expression after reperfusion [76]. In allograft recipients, kidney secretory function measured by PAH extraction is greatly reduced 1–3 h after reperfusion and generally restored within about 7 days, except in some patients who present with sustained acute kidney injury [82]. Several mechanisms might explain such time-dependent modulation of the expression and/or activity of tubular transporters under these conditions.

Although most studies have linked decreased activity of SLCs to decreased expression at the transcriptional or protein level, we recalled above that SLC-mediated transport directly depends on

the activity of the Na^+/K^+-ATPase pump, whose expression and activity is markedly depressed in the ischemic kidney [61,65,71]. The decreased inward Na^+ gradient in renal tubular cells reduces the outward gradient of α-ketoglutarate and other di-tricarboxylates, and then the influx of OATs substrates. Regarding OCTs, the Na^+/K^+-ATPase defect reduces the inside-negative electric potential, which is the driving force of OC^+ influx. The loss of function of NHE3 at the apical pole, which limits availability of the co-substrate necessary for MATEs-mediated transport, probably plays a role too. Similarly, ischemia-associated ATP depletion could be a cause of dysfunction of the ATP-dependent ABC transporters [25].

Transporter activity can also be regulated by modification of protein expression, posttranslational regulation, oligomerization, protein trafficking, epigenetics and non-genomic pathways, triggered by hormones and/or growth factors [14,86,87]. The mechanism governing the transcriptional regulation of transporters by IR is not fully understood but, as for other genes, it probably depends on specific transcription factors. The genomic response to hypoxia depends primarily on the Hypoxia Inducible Factor (HIF-1), which binds to Hypoxia-Response Elements (HRE) on the promoter of target genes and orchestrates their transcription [88]. Several studies demonstrated the importance of HIF in renal protection against IRI [89–91]. Other studies highlighted a potential link between HIF and transporters' regulation [92,93]. Besides the HIF-1 pathway, the recently identified ischemia/reperfusion-inducible protein (IRIP) was shown to negatively regulate the activities of various transporters, including OCT1-2-3, MATE1, OAT1 and Pgp [94–96]. Some authors suggested that the abnormal expression and distribution of rat and human OAT1 may be related to the activation of protein kinase C (PKC), which downregulates hOAT1-mediated transport through carrier internalization from the cell membrane [83,97,98]. In line with this hypothesis, it was shown that prostaglandin-E2, a COX metabolite favored by IR, specifically downregulates OAT at the transcriptional level by acting via the E prostanoid receptor type 4 (EP4), subsequently activating PKA [99].

4.2. Effects of I and/or IR on Tubular Transport Functions as Evaluated by Metabolomics Studies

Several metabolomics analyses were conducted to study the consequences of I or IR in vivo. Based on the identification of metabolites differentially affected in the pre-ischemic, ischemic and reperfusion periods, this approach was used to elucidate the underlying biochemical processes and to identify biomarkers [100–106]. The metabolites usually found to be altered reflect the change in energetic pathways (i.e., a switch from the glycolytic pathway to fatty acid beta-oxidation feeding the TCA cycle), or belong to oxidative stress pathways [63]. However, as most of these metabolites are substrates of transporters, their concentration in graft preservation solutions, urine, plasma or renal tissue may also be related to tubular injuries and/or altered transporter function.

Analysis of the preservation solution during hypothermic perfusion machine (HPM) or static cold storage (SCS) revealed that numerous metabolites, not initially present in the solutions, were detected less than 1 h after the begin of conservation period. There were also significant changes in the concentration of constituents of the preservation solutions. These changes may point out at products of metabolism being released from the kidney and substances being removed by the kidney to supply ongoing cell processes, respectively. This could be related to a rupture of the epithelium integrity, cell death or changes in subcellular energy production, but also to global and/or selective (dys)-function of tubular transport systems in ischemic conditions. By comparing, in paired porcine kidneys, the ratio of tissue-to-perfusion fluid levels of metabolites between SCS and HPM conditions, Nath et al. showed that, while a number of metabolites were released during storage in the two conditions, several (e.g., alanine, succinate, tyrosine and leucine) exhibited much less tissue accumulation with HPM than with SCS, suggesting that some cellular transport processes remained active during perfusion [107]. Similarly, rapid glutathione depletion in the conservation fluid during HPM is likely to reflect cellular uptake of this protective antioxidant. Another ex situ organ preservation method, called Normothermic Machine Perfusion (NMP), is the subject of renewed interest. It intends to mimic physiological

conditions in the human body and has shown promising results [108,109]. However, to the best of our knowledge, no metabolomic study has yet been conducted on perfusion fluid coming from NMP.

Recently, Stryjak et al. [106] studied the influence of long-term ischemia (2, 4, 6 and 21 h of static cold preservation) on tissue quality using an in situ kidney metabolomics analysis in rabbits. They found significant variation in the tissue content of numerous compounds as compared to the baseline. These metabolites belong to various biochemical pathways, including those involved in reactive oxygen species (ROS) production or amino-acid metabolism. This study confirms the time-dependent impact of ischemia on renal metabolic balance, as already observed for the expression and functionality of transporters. However, the lack of concomitant analysis of the perfusion fluid hinders drawing conclusions on the added contribution of altered transport versus pure metabolic disturbances.

Wei et al. explored the metabolome in the plasma and in the kidney cortex and medulla from a mouse model of warm IR [101]. Various catabolites of amino acids and fatty acids (3-indoxyl sulfate, *p*-cresol sulfate, glycine- or acetyl-conjugates) normally excreted in urine, peaked in plasma as early as 2 h after reperfusion. This, together with the significant accumulation of urate in the kidney tissue, may reflect decreased tubular transport by OATs and MATEs, respectively. At the time of the most severe injury (48 h), markedly decreased concentrations of metabolites related to energetic (glucose, free fatty acids, amino acids), purine and other major metabolic pathways were found in the kidney tissue and plasma. This may primarily be due to the lack of oxygen and nutrient supply and to mitochondrial dysfunction, but one cannot rule out decreased tubular reabsorption of these metabolites. Rising levels of PGs in kidney tissue over reperfusion time [101] may reflect inflammation, a well-known component of IR, but also decreased tubular organic anion secretion. Finally, using unilateral clamping of renal artery in a swine model, Malagrino et al. found numerous metabolites in serum or urine able to discriminate between the pre-ischemic and ischemic periods [100]. Using pathway analysis, these metabolites were related to amino-acids degradation and to several molecular and cellular functions including, among others, lipid metabolism, biochemistry of small molecules, and molecular transport. By comparing nuclear protein content of ischemic and non-ischemic kidney tissue, the authors were able to rebuild a network of metabolic processes during IR. Unfortunately, they did not analyze whether or not membrane transporters were differentially modulated in ischemic vs. non-ischemic kidneys.

Altogether, these studies demonstrate that IR is accompanied by the disruption of several metabolic pathways (glucose, lipid and nucleotide metabolism, TCA cycle), which translates into variations of metabolomic profiles in biological fluids and/or tissues. Although the role that disruption of tubular transporters plays in some of the metabolomic variations observed has not been firmly demonstrated, it cannot be overlooked as they regulate cell exchanges and provide for kidney energy needs.

5. Consequences of IR-Induced Modulation of Renal Transporters in the Post-Transplantation Period

The evolution of the expression and activity of renal tubular transporters SLCs and ABCs under the effect of IR in kidney transplantation is an important field of research. It may help to better understand and characterize tubular cell dysfunctions associated with IR and thus understand graft outcome. As presented above, SLCs and ABCs transporters contribute to the homeostasis of endogenous and/or exogenous substances and IR-induced modulation of their functions can (i) disrupt the reabsorption of essential nutrients (ii) cause cytotoxicity in proximal tubular cells (iii) promote local inflammation during reperfusion (iv) induce disturbances in other organs of the body, or (v) modify drug pharmacokinetics and/or toxicity, all these processes being potentially deleterious for the graft and the recipient.

5.1. Alteration of the Graft Itself

As described previously, IR is accompanied by an apical redistribution of the Na^+/K^+-ATPase pump and of NHE3, leading to decreased apical reabsorption of Na^+ [110]. Higher urinary concentration of

Na^+ results in decreased glomerular filtration through the tubulo-glomerular feedback that helps to limit Na^+ and fluid loss. This phenomenon may serve to protect the vulnerable tubules, but reduction of glomerular filtration rate favors renal failure [63]. Tubular reabsorption of Na^+ is normally followed by osmotic reabsorption of water by aquaporins 1 and 3, which have also been found to be dysregulated by IR [111]. In addition, IR disrupts the close coordination between Na^+ absorption at the apical membrane and its efflux at the basolateral membrane, which is needed to prevent increased osmotic pressure and swelling of the cell.

In a more general context, acute loss of renal function in AKI results in multiple disturbances in fluid, electrolyte and acid-base homeostasis. For example, the kidneys normally excrete fixed non-volatile acids resulting from the catabolism of dietary proteins to maintain acid–base homeostasis. AKI is often associated with metabolic acidosis showing a disruption of this balance, linked to the retention of organic anions [112].

During tissue reoxygenation, the ROS overproduction is deleterious to proximal tubular cells and the graft [8]. Radical scavenging is normally accomplished by intracellular antioxidants, including many TCA cycle metabolites that indirectly help to maintain sufficient glutathione levels by increasing NADPH production [113]. Ergothionein has antioxidant properties that contribute in decreasing ROS production and local inflammation in the post-transplant period [114]. L-carnitine also has antioxidant and protective effects in tissues with oxidative damage and its administration 30 min before reperfusion had protective effects against I/R-induced AKI [115–117]. A disruption of the functionality of the OCTNs, OATs and NaDCs transporters during the post-transplant period can disrupt reabsorption of these antioxidants from urine. A study showed that succinate is responsible for the production of mitochondrial ROS during reperfusion [118]. Hypoxia-dependent succinate accumulation is also associated with a shift in the equilibrium of many TCA cycle metabolites, including oxaloacetate, fumarate, α-ketoglutarate, aspartate, citrate and isocitrate [119]. The equilibrium between elimination and reabsorption of TCA cycle intermediates in ischemic conditions thus appears to be an important phenomenon in reperfusion lesions. OAT1, OAT2, OAT3 and NaDC3 at the basolateral pole and NaDC1 at the apical membrane ensure intra/extra-cellular exchanges of these intermediaries at the tubular level. A recent study in mice treated with a continuous infusion of β-hydroxybutyrate (a ketone body, substrate of OAT1) before and after IRI, showed that it has a protective effect against acute renal IR injuries [120]. It implies that, without supplementation, decreased intracellular availability of β-hydroxybutyrate may favor tubular injury. Interestingly, the renoprotective effect sustained for up to 24 h after infusion is stopped. The authors postulated that it resulted from long-acting effects of β-hydroxybutyrate on epigenetic regulation of several genes controlling pyroptosis. We may also hypothesize a role for tubular transporters, acting in cooperation to maintain high intracellular levels of β-hydroxybutyrate. Overall, we hypothesize that perturbation of transmembrane transport, responsible for the intracellular disequilibrium of metabolites necessary for the energetic pathways and/or the protection against free radicals, is a key mechanism of IRI-induced AKI.

Other authors highlighted the importance of epithelial cell maladaptive repair mechanisms in the promotion of pathological phenotypes in kidney transplant recipients, characterized among others by interstitial fibrosis, tubular atrophy and capillary rarefaction [121–123]. While tubular epithelium repair may obviously improve tubular transport functions, tubular transporters might also play a role in tubular epithelium repair [14,124] by maintaining homeostasis in sublethal tubular cells, thus favoring progressive tubular repopulation with nonlethally injured cells [125,126].

Besides, recent studies suggested that transporters of the SLC22 family participate in a wide network of communication between various systems of the organism. Based on the distribution of OATs across organs and on the diversity and specificities of their substrates, a phenomenon of "remote sensing and signaling" was suggested, by which cooperation between transporters with different tissue expression patterns helps to maintain whole-body homeostasis [9,127–129]. The presence of a multi-scale network of transporters, together with possible compensatory up-regulation between transporters at the renal level [130], could have repercussions in normal physiology and pathophysiology

of the transplanted organ and of the whole organism [61]. In this sense, a frequent consequence of reperfusion after localized tissue ischemia is injury to other organ systems, so-called distant or remote organ injury (ROI) [131–133], including hepatic changes after renal IR injury [134,135].

5.2. Accumulation of Toxic Substances

IR-induced modulation of tubular renal transporters leads to an accumulation of toxic substances in the post-transplantation period, which may have prejudicial consequences on graft function or outcome. Understanding how these transporters are modulated along time and deciphering the consequences of increased exposure to uremic toxins or other toxic compounds may be useful for the monitoring of renal transplant recipients and the development of new therapeutic strategies. As previously mentioned in this paper, many studies showed a decreased clearance of uremic toxins, either anionic (e.g., indoxyl sulfate, PAH, estrone sulfate) or cationic (TEA, guanidine), that paralleled the decreased expression of their corresponding transporters [76,77,79,100]. In turn, their clearance also normalized in parallel to the transporters activity's restoration [76,77].

In recent years, important progress has been made in the understanding and characterization of the toxicity of uremic toxins, especially for *p*-cresol and indoxyl sulfate. An in vitro study evaluated the effects on endothelial cell proliferation in a large panel of uremic solutes (guanidine compounds, polyamines, oxalate, myoinositol, urea, uric acid, creatinine, indoxyl sulfate, indole-3-acetic acid, *p*-cresol, hippuric acid, and homocysteine). It demonstrated that *p*-cresol and indoxyl sulfate reduced endothelial cell proliferation and wound repair, in a dose-dependent manner for *p*-cresol [136]. Indoxyl sulfate, at concentrations found in uremic patients, also induces the production of oxidative stress radicals in endothelial cells [137]. As recently described by Huang et al., PAH also promotes endothelial dysfunction by increasing ROS production, thus possibly accelerating tubular damage [138]. Moreover, uremic toxins can also have a direct impact on the expression of tubular cell transporters. Indeed, Brandoni et al. found that exposure of a suspension of proximal tubular cells to urea led to a significant decrease in OAT1 and OAT3 protein abundance in cell membranes, in a concentration-dependent manner [139]. Therefore, the direct effect of uremic toxins on transporters function, whose expression is already decreased, may have a synergistic effect on their accumulation, together with that of other endogenous or exogenous substrates.

In renal transplant patients, evaluating the particular role of altered tubular transport on graft dysfunction and rejection is difficult, as it is far from being the sole mechanism involved in these complications. Nevertheless, Knoflach et al. showed that PAH concentrations increased in patients who experienced acute renal allograft rejection and decreased rapidly after successful antirejection treatment [140]. Similarly, Corrigan et al. confirmed that secretion of PAH is impaired for at least 7 days, even after the onset of GFR recovery [82]. Impaired secretion of PAH may arise from decreased transporter expression but may also involve a competitive inhibitory mechanism. Indeed, uremic toxins and other products normally eliminated by the kidneys (or by hemodialysis) accumulate in blood in the first few hours or days after transplantation. These toxins can limit the renal excretion of each other by competitively inhibiting transporters.

In a rat model of chronic renal failure (CRF), the overload of PAH and indoleacetic acid accelerated the loss of kidney function, glomerular sclerosis and tubulointerstitial injury [141]. Numerous studies in patients with CRF showed that uremic toxin accumulation leads to various complications including endothelial senescence [142], atherogenesis [143], cardiovascular diseases [144,145] or increased risk of all-cause mortality [144,146]. In CRF, these toxins accumulate for very long periods, making their toxicity particularly critical. As their accumulation in the transplanted patient is reversible, owing to the restoration of glomerular filtration and transporter's function, their deleterious effects should be less important. However, these putative uremic toxins are poorly filtered across dialysis membranes because they are protein bound and current dialysis therapy does not correct the full spectrum of uremic toxicity [27]. Therefore, in the context of IR-induced AKI, residual tubular transporter function may contribute to the attenuation of acute kidney dysfunction in the immediate post-transplant period.

5.3. Impact on Drugs Used in Transplanted Patients

Downregulation of renal tubular transporters induced by IR, together with subsequent accumulation of uremic toxins may modulate the pharmacokinetics of several drugs, leading to decreased clearance and risk of increased toxicity in the early post-transplantation period. Functional alteration in renal excretion is of particular clinical importance for drugs with a narrow therapeutic range, such as immunosuppressants.

Generally, inhibition of basolateral uptake transporters causes an increase in the systemic concentration of their substrates, while inhibition of apical efflux transporters can cause an increase in intracellular concentrations, leading to possible nephrotoxicity. However, information about pharmacokinetic alterations resulting from decreased function of renal tubular transporters for drugs used in renal transplantation is limited. Tacrolimus, cyclosporine, sirolimus and everolimus undergo hepatic metabolism and are mainly eliminated in the bile. Others, like corticosteroids or mycophenolate mofetil, are conjugated in the liver and subsequently eliminated by the kidney, as inactive metabolites. This suggests that alteration of renal transporters should not be a major factor involved in the pharmacokinetics or toxicity of the parent compounds. However, renal tubular transporters are partially involved in the urine excretion of the unchanged fraction of tacrolimus and cyclosporin that are substrates of P-gp [10,29,32], of corticosteroids conjugates that are substrates of P-gp, BCRP and MATEs [10,29,32,147], and of mycophenolic acid glucuronide, a substrate of OAT3 [52] and MRP2 [148]. Moreover, as stated above, the hepatic disposition of these drugs can be impaired in renal transplantation due to competitive mechanisms arising from uremic toxin accumulation. Thus, the potential effect of renal tubular transporter's alteration on these drugs, albeit indirect for a large part, should not be ignored.

Some studies evaluated the particular role of renal P-gp on calcineurin inhibitors' toxicity in kidney transplantation, with controversial results [149–152]. In a prospective cohort of 252 adult renal allograft recipients receiving tacrolimus, Naesens et al. found that the absence of P-gp expression (evaluated by immunohistochemistry) and the combined donor-recipient homozygosity for the c.C3435T variant in *ABCB1* gene (possibly responsible for altered conformation and function of P-gp [153]) were associated with more chronic allograft damage [149]. The presence of this variant in the donor has also been associated with cyclosporine nephrotoxicity in a case-control study [150]. However, other authors found no such association [152] or even the opposite [151]. Due to its wide expression on numerous tissues, it is very difficult to evaluate the part of tubular P-gp in the global role it may have on calcineurin inhibitors' pharmacokinetics. Hence, to date, no clear conclusion can be drawn about IR-induced P-gp dysfunction and the risk of calcineurin inhibitors' toxicity.

Interestingly, immunosuppressants also have inhibitory effects on various transporters. OAT1 and OAT3 are inhibited by mycophenolic acid, while MRP2 and MRP4 are inhibited by mycophenolic acid, tacrolimus, cyclosporine and hydrocortisone [154,155], suggesting that the fraction of these compounds reaching the kidney could have a synergistic effect with IR on the decreased function of tubular transporters. As mentioned before, a reduced expression of tubular OCT1 and OCT2 was observed after allogeneic kidney transplantation in rats [81]. The authors confirmed that cyclosporine A, without being itself a substrate of OCTs, had inhibitory effects on their activity and could also possibly lead to drug–drug interactions.

It is well known that sirolimus and calcineurin inhibitors, mostly cyclosporine, are involved in numerous drug–drug interactions [156–159]. An in vitro study conducted on human renal epithelial cells showed that P-gp protects renal epithelial cells from cyclosporine toxicity and that sirolimus inhibits P-gp-mediated efflux of cyclosporine, leading to intracellular accumulation of the drug. This suggests that the renal P-gp could play a role in the potentiation of cyclosporine nephrotoxicity by sirolimus [160].

It has been demonstrated that cyclosporine increases mycophenolic acid glucuronide exposure via the inhibition of its biliary excretion by MRP2 [161]. However, El-Sheik et al. demonstrated on rat kidney homogenates that cyclosporine also interferes with mycophenolic acid renal excretion by

inhibiting its renal glucuronidation and the subsequent MRP2-mediated transport of mycophenolic acid glucuronide [162].

Thus, kidney transplant recipients are exposed to transporter-mediated drug–drug interactions but also drug-metabolites and drug-toxins interactions, which can amplify the consequences of IR-induced transporter dysfunction [163].

Pharmacokinetic consequences of impaired transporter expression have been studied, or can be anticipated, for drugs other than immunosuppressors. For example, the AUC and the half-life of famotidine were two-fold higher in IR rats than in sham operated controls, in line with downregulation of OCT2 and MATE1 [79]. Regarding anionic drugs, Sakurai et al. showed that cefazolin elimination correlated with *OAT3* mRNA levels in patients with renal disease [164]. Concerning the antibiotics commonly used in renal transplantation, trimethoprim, generally combined with sulfamethoxazole, is eliminated unchanged by renal excretion and is a substrate of MATE1 and MATE2 [165], suggesting that intrarenal accumulation of this drug could occur in response to their downregulation. On the contrary, downregulation of OATs at the basolateral membrane could decrease the renal uptake and accumulation of antivirals such as acyclovir, thereby reducing tubular toxicity. Generally speaking, IR-induced transporter' alterations may impair the pharmacokinetics of numerous drugs, independently of, or in addition to, altered glomerular filtration.

6. Modulation of Transporter's Function for Improving Graft Outcome

Different therapeutic approaches were proposed to reduce renal IRI, targeting various stages of transplantation: (i) before transplantation, by pre-treatment of livings donor (mostly dietary preconditioning) or conditioning of deceased donors before organ harvesting; (ii) during graft preservation, by using hypothermic or normothermic perfusion machines (the latter necessitating the use of an oxygen carrier) or by adding therapeutic agents to the preservation fluid; (iii) after transplantation, by modulating the recipient' treatment [166].

Storage on NMP, which maintains organs at physiological temperature, restores normal cellular processes and allows kidneys to maintain their function. Hosgood and Nicholson found that 1 h of NMP improved early graft function of kidneys from extended criteria donors [167]. Moreover, Kaths et al. showed in a porcine model that prolonged periods of NMP improved graft function with significantly lower serum creatinine values and significantly higher creatinine clearance when compared with SCS [168]. This conservation technology enhances the functionality of the graft in the post-transplant period and could better preserve tubular transporters' activity prior to reperfusion. However, as NPM is still technologically challenging with only limited pilot human studies available up until now [169], its effects on membrane transporters has not yet been evaluated.

While many therapeutic agents have been tested and are effective in animals to prevent or combat IRI, none has been implanted in routine clinical practice yet [166,170]. Most of them target major pathways of IR such as inflammation, energetic metabolism, oxidative stress or coagulation and rely on supplementation of the preservation fluid with a therapeutic agent, gene therapy or cell therapies [171]. Other studies presented below and summarized in Table 2 evaluated how the harmful effects of IR can be minimized and renal recovery improved through modulation of transporters function (Table 2) [172–181]. Therefore, future research should be directed to increase the contribution of IR-induced transporter's modulation in order to improve the implementation of new therapeutics or the development of new diagnostic markers.

Table 2. Summary of treatments used against Ischemia-Reperfusion-Injury, acting through modulation of transporters activities.

Treatment	Action	Model (Species/Organ)	References
tNKA(β)	Enhances Na^+/K^+-ATPase activity	Rat/Kidney	[172]
Ouabain	Preserves Na^+/K^+-ATPase activity	Rat/Heart	[173]
Indomethacin	Prevents OAT1 and OAT3 downregulation, increases PAH excretion	Rat/Kidney	[174]
Meclofenamate	Prevents OAT1 and OAT3 downregulation (induced by Protaglandin E2), Decreases indoxyl-sulfate hepatic production	Rat/Kidney, Liver	[175]
Ceftriaxone	Upregulates and increases SGLT1 activity	Rat/Brain	[176]
5-(*N*-ethyl-*N*-isopropyl) amiloride	Inhibits NHE	Mice/Kidney	[177]
S3226	Inhibits NHE3	Rat/Kidney	[178]
Side population cells	Cells which constitutively express BCRP	Mice/Kidney	[179]
Liopoxin analog	Restores expression of genes differentially expressed by IRI, including OCT1 and aquaporin 1	Mice/Kidney	[180]
Pravastatin	Upregulates OATP4C1	Rat/Kidney	[181]

Gong et al. demonstrated in vitro that truncated Na^+/K^+-ATPase β (tNKAβ) could activate the NKA α subunit and thus enhance the activity of the Na^+/K^+-ATPase. They then showed on a rat model that the tNKAβ-treated group (2 h before reperfusion) exhibited significant improvement in renal function, with lower serum creatinine and blood urea nitrogen (BUN) levels on postoperative days 1–6 [172]. Belliard et al. showed in rat heart preparations exposed to 30 min of ischemia followed by 30 min of reperfusion that preconditioning with a sub-inotropic concentration of the cardiac glycoside ouabain prevented ischemia-induced alterations of the Na^+/K^+-ATPase and was associated with better contractile function [173]. Schneider et al. also demonstrated that, after bilateral clamping of renal arteries in rats, intraperitoneal injection of indomethacin (inhibiting the IR-dependent increase in PGE_2) prevented the downregulation of rOAT1 and rOAT3 transporter expression during reperfusion and resulted in an increased PAH net excretion [174]. They also demonstrated that the beneficial effects of indomethacin on renal function in IR conditions were related to the increased expression of the OAT1 and OAT3 transporters [85]. Similarly, intravenous administrations of meclofenamate in a rat model of IR had a nephroprotective effect by restoring the renal expression of rOAT1 and rOAT3 [175]. However, Yamashita et al. demonstrated in uninephrectomized mice undergoing left renal artery clamping, that pre-ischemic treatment (but not post-ischemic) with 5-(*N*-ethyl-*N*-isopropyl) amiloride, an inhibitor of NHE, attenuated IR-induced renal dysfunction [177]. NHE3 seemed to be involved in the development and progression of post-ischemic renal injury, probably by increasing Na^+/Ca^{2+} intracellular concentrations during ischemia. Similar results were found with a NHE3 selective inhibitor (S3226) in a rat model of IR [178].

Genetic deletion of SGLT1 was recently found to improve recovery of kidney function on day 14 in a mouse model of renal IR and was associated with a reduced tubular injury score [182]. These studies clearly demonstrate that modulation of transporter activity during ischemic periods and/or reperfusion is accompanied by an attenuation of ischemic damage. However, the nature of this beneficial modification, whether accentuation or inhibition of activity, may depend on the transporters and more precisely on substrate specificity for the transporters.

Other potential therapies could depend on tubular transporter function. Side population (SP) cells, a stem-cell rich population found in the kidney that constitutively expresses BCRP, significantly improved renal function after bilateral clamping of renal arteries in mice [179]. The therapeutic potential of SP cells was reduced by pretreatment with verapamil, an inhibitor of BCRP, suggesting that this transporter contributes to the nephroprotective effect of SP. Kieran et al. evaluated the modification of the transcriptomic response to renal IRI by a lipoxin analog previously found to have nephroprotective effects in a murine model of IRI [180]. They found that this analog could restore the expression of many genes either downregulated or upregulated by IR. Although the effect of this lipoxin analog is not limited to a specific family of genes, this study showed that the expression level

of renal transporters such as OCT1 or aquaporin 1 was restored. The PKC inhibitor, sotrastaurin, ameliorated ischemia-reperfusion organ damage and promoted cytoprotection in a model of extended renal cold preservation followed by transplantation [183]. It is interesting to remember that activation of PKC downregulates hOAT1-mediated transport through transporter internalization from the cell membrane [83,97,98], and to put forward the hypothesis that the beneficial effects observed in this study could be related to a restoration or non-loss of function of OAT1.

Some years ago, pravastatin was shown to reduce the levels of specific uremic toxins (asymmetric dimethylarginine, guanidine succinate and trans-aconitate) in the plasma [181]. After administration of pravastatin, the mRNA level of rat slco4c1 was significantly increased in the kidney. Similarly, the application of pravastatin potentiated (by 1.73-fold) the *SLCO4C1* (OATP4C1) mRNA in human kidney proximal cells. Altogether, these data suggest that pravastatin increased ADMA and *trans*-aconitate excretion in the proximal tubules, via SLCO4C1 up-regulation. The authors showed that statins function as a nuclear receptor ligand, recruiting the AhR-XRE system and upregulating SLCO4C1 transcription. Whether this mechanism also applies to other kidney transporters has not yet been studied further. Another transcriptomics therapeutic target of interest is HIF-1. Pharmacological induction of HIF can be obtained using molecules that stabilize HIF or that inactivate prolyl hydroxylase domains (PHD) involved in HIF-1 degradation in the proteasome [86,184–186]. Interestingly, Hagos et al. found that PHD inhibitors are taken up into the tubular cells by OAT1 and OAT3 and released in urine by OAT4 [86]. This suggests that the downregulation of OATs during I/R could modulate the effectiveness of therapeutic agents like PHD inhibitors. Hence, therapeutic strategies aiming to modulate transcriptional or posttranscriptional mechanisms in tubular cells using pharmacological agents are potentially limited by associated factors [63].

7. Conclusions

IRI is a complex and important problem in kidney transplantation. Development of therapeutic strategies is critical due to the increasing use of marginal grafts, more susceptible to the injury processes. Elucidating the pathophysiological mechanisms of IRI may allow designing potential therapies. In this paper, we have assessed the impact of IR on major SLC and ABC transporters by selecting the most relevant papers published on this topic. Most of them showed that SLCs are downregulated during ischemic periods and recover with a delay upon reperfusion. In contrast, the literature points to a lack of knowledge regarding ABC transporters. Although we did not conduct a true systematic review to find all the relevant studies on the topic, we made a thorough analysis of the literature and completed the search by reading the most relevant references cited in these papers. This work allowed us to gather the still fragmentary knowledge concerning the impact of the IR on the tubular transporters. However, improved understanding of the modulation of these transporters by IR would contribute to better characterizing its clinical impact and anticipating renal function recovery. In our opinion, altered functionality of renal tubule transporters by IR and subsequent disruptions in the equilibrium of endogenous and exogenous substrates may participate in lesions that occur during kidney transplantation procedure. Protection and/or restoration of transport activity could be part of multiple treatment strategy at various time points during the donation, preservation and transplantation to reduce IRI and its consequences. It may represent an important research area for the improvement of short and long-term graft outcomes.

Author Contributions: Conceptualization, C.B.-L.G., Q.F., P.M.; methodology, C.B.-L.G. and P.M.; validation, C.B.-L.G. and P.M.; investigation, Q.F. and H.A.; resources, Q.F. and H.A.; data curation, Q.F., H.A. and C.B.-L.G.; writing—original draft preparation, Q.F., H.A. and C.B.-L.G.; writing—review and editing, Q.F., H.A., C.B.-L.G. and P.M.; supervision, C.B.-L.G. and P.M.; project administration, C.B.-L.G. and P.M. All authors have read and agreed to the published version of the manuscript.

Funding: This research received no external funding.

Acknowledgments: The authors thank the Nouvelle Aquitaine Region and INSERM for their financial support. The authors are grateful to Karen Poole for correcting the English.

Conflicts of Interest: The authors have no conflict of interest to declare.

References

1. Wong, G.; Teixeira-Pinto, A.; Chapman, J.R.; Craig, J.C.; Pleass, H.; McDonald, S.; Lim, W.H. The Impact of Total Ischemic Time, Donor Age and the Pathway of Donor Death on Graft Outcomes After Deceased Donor Kidney Transplantation. *Transplantation* **2017**, *101*, 1152–1158. [CrossRef]
2. Chen, C.-C.; Chapman, W.C.; Hanto, D.W. Ischemia-reperfusion injury in kidney transplantation. *Front. Biosci. (Elite Ed.)* **2015**, *7*, 117–134.
3. Menke, J.; Sollinger, D.; Schamberger, B.; Heemann, U.; Lutz, J. The effect of ischemia/reperfusion on the kidney graft. *Curr. Opin. Organ Transplant.* **2014**, *19*, 395–400. [CrossRef]
4. Ponticelli, C. Ischaemia-reperfusion injury: A major protagonist in kidney transplantation. *Nephrol. Dial. Transplant.* **2014**, *29*, 1134–1140. [CrossRef]
5. Salvadori, M.; Rosso, G.; Bertoni, E. Update on ischemia-reperfusion injury in kidney transplantation: Pathogenesis and treatment. *World J. Transplant.* **2015**, *5*, 52–67. [CrossRef]
6. Venkatachalam, M.A.; Weinberg, J.M.; Kriz, W.; Bidani, A.K. Failed Tubule Recovery, AKI-CKD Transition, and Kidney Disease Progression. *J. Am. Soc. Nephrol.* **2015**, *26*, 1765–1776. [CrossRef]
7. Zhao, H.; Alam, A.; Soo, A.P.; George, A.J.T.; Ma, D. Ischemia-Reperfusion Injury Reduces Long Term Renal Graft Survival: Mechanism and Beyond. *EBioMedicine* **2018**, *28*, 31–42. [CrossRef]
8. Nieuwenhuijs-Moeke, G.J.; Pischke, S.E.; Berger, S.P.; Sanders, J.S.F.; Pol, R.A.; Struys, M.M.R.F.; Ploeg, R.J.; Leuvenink, H.G.D. Ischemia and Reperfusion Injury in Kidney Transplantation: Relevant Mechanisms in Injury and Repair. *J. Clin. Med.* **2020**, *9*, 253. [CrossRef]
9. Nigam, S.K.; Wu, W.; Bush, K.T.; Hoenig, M.P.; Blantz, R.C.; Bhatnagar, V. Handling of Drugs, Metabolites, and Uremic Toxins by Kidney Proximal Tubule Drug Transporters. *Clin. J. Am. Soc. Nephrol.* **2015**, *10*, 2039–2049. [CrossRef]
10. George, B.; You, D.; Joy, M.S.; Aleksunes, L.M. Xenobiotic transporters and kidney injury. *Adv. Drug Deliv. Rev.* **2017**, *116*, 73–91. [CrossRef]
11. Risso, M.A.; Sallustio, S.; Sueiro, V.; Bertoni, V.; Gonzalez-Torres, H.; Musso, C.G. The Importance of Tubular Function in Chronic Kidney Disease. *Int. J. Nephrol. Renov. Dis.* **2019**, *12*, 257–262. [CrossRef] [PubMed]
12. Kalogeris, T.; Baines, C.P.; Krenz, M.; Korthuis, R.J. Cell biology of ischemia/reperfusion injury. *Int. Rev. Cell Mol. Biol.* **2012**, *298*, 229–317. [PubMed]
13. Sheridan, A.M.; Bonventre, J.V. Cell biology and molecular mechanisms of injury in ischemic acute renal failure. *Curr. Opin. Nephrol. Hypertens.* **2000**, *9*, 427–434. [CrossRef] [PubMed]
14. Masereeuw, R.; Russel, F.G.M. Regulatory pathways for ATP-binding cassette transport proteins in kidney proximal tubules. *AAPS J.* **2012**, *14*, 883–894. [CrossRef] [PubMed]
15. Skorecki, K.; Chertow, G.; Marsden, P.; Taal, M.; Yu, A. *Brenner and Rector's The Kidney, (2 Volume Set)*, 10th ed.; Elsevier: Philadelphia, PA, USA, 2015.
16. El-Sheikh, A.A.K.; Masereeuw, R.; Russel, F.G.M. Mechanisms of renal anionic drug transport. *Eur. J. Pharmacol.* **2008**, *585*, 245–255. [CrossRef]
17. Otani, N.; Ouchi, M.; Hayashi, K.; Jutabha, P.; Anzai, N. Roles of organic anion transporters (OATs) in renal proximal tubules and their localization. *Anat. Sci. Int.* **2017**, *92*, 200–206. [CrossRef]
18. Yin, J.; Wang, J. Renal drug transporters and their significance in drug–drug interactions. *Acta Pharm. Sin. B* **2016**, *6*, 363. [CrossRef]
19. Ekaratanawong, S.; Anzai, N.; Jutabha, P.; Miyazaki, H.; Noshiro, R.; Takeda, M.; Kanai, Y.; Sophasan, S.; Endou, H. Human organic anion transporter 4 is a renal apical organic anion/dicarboxylate exchanger in the proximal tubules. *J. Pharmacol. Sci.* **2004**, *94*, 297–304. [CrossRef]
20. Motohashi, H.; Sakurai, Y.; Saito, H.; Masuda, S.; Urakami, Y.; Goto, M.; Fukatsu, A.; Ogawa, O.; Inui, K. Gene expression levels and immunolocalization of organic ion transporters in the human kidney. *J. Am. Soc. Nephrol.* **2002**, *13*, 866–874.
21. Koepsell, H.; Endou, H. The SLC22 drug transporter family. *Pflug. Arch.* **2004**, *447*, 666–676. [CrossRef]
22. Koepsell, H. The SLC22 family with transporters of organic cations, anions and zwitterions. *Mol. Asp. Med.* **2013**, *34*, 413–435. [CrossRef] [PubMed]

23. Pelis, R.M.; Wright, S.H. SLC22, SLC44, and SLC47 transporters-organic anion and cation transporters: Molecular and cellular properties. *Curr. Top. Membr.* **2014**, *73*, 233–261. [PubMed]
24. Farrow, E.G.; White, K.E. Recent Advances in Renal Phosphate Handling. *Nat. Rev. Nephrol.* **2010**, *6*, 207–217. [CrossRef]
25. Srikant, S.; Gaudet, R. Mechanics and pharmacology of substrate selection and transport by eukaryotic ABC exporters. *Nat. Struct. Mol. Biol.* **2019**, *26*, 792–801. [CrossRef] [PubMed]
26. Aperia, A.; Fryckstedt, J.; Holtbäck, U.; Belusa, R.; Cheng, X.J.; Eklöf, A.C.; Li, D.; Wang, Z.M.; Ohtomo, Y. Cellular mechanisms for bi-directional regulation of tubular sodium reabsorption. *Kidney Int.* **1996**, *49*, 1743–1747. [CrossRef] [PubMed]
27. Masereeuw, R.; Mutsaers, H.A.M.; Toyohara, T.; Abe, T.; Jhawar, S.; Sweet, D.H.; Lowenstein, J. The kidney and uremic toxin removal: Glomerulus or tubule? *Semin. Nephrol.* **2014**, *34*, 191–208. [CrossRef] [PubMed]
28. Wu, W.; Bush, K.T.; Nigam, S.K. Key Role for the Organic Anion Transporters, OAT1 and OAT3, in the in vivo Handling of Uremic Toxins and Solutes. *Sci. Rep.* **2017**, *7*, 4939. [CrossRef]
29. Ivanyuk, A.; Livio, F.; Biollaz, J.; Buclin, T. Renal Drug Transporters and Drug Interactions. *Clin. Pharm.* **2017**, *56*, 825–892. [CrossRef]
30. Burckhardt, G. Drug transport by Organic Anion Transporters (OATs). *Pharmacol. Ther.* **2012**, *136*, 106–130. [CrossRef]
31. Koepsell, H. Organic Cation Transporters in Health and Disease. *Pharmacol. Rev.* **2020**, *72*, 253–319. [CrossRef]
32. Sharom, F.J. The P-glycoprotein multidrug transporter. *Essays Biochem.* **2011**, *50*, 161–178. [CrossRef] [PubMed]
33. Liu, X. SLC Family Transporters. *Adv. Exp. Med. Biol.* **2019**, *1141*, 101–202. [PubMed]
34. Fenton, R.A.; Poulsen, S.B.; de la Mora Chavez, S.; Soleimani, M.; Dominguez Rieg, J.A.; Rieg, T. Renal tubular NHE3 is required in the maintenance of water and sodium chloride homeostasis. *Kidney Int.* **2017**, *92*, 397–414. [CrossRef] [PubMed]
35. Soleimani, M.; Burnham, C.E. Physiologic and molecular aspects of the Na+:HCO3− cotransporter in health and disease processes. *Kidney Int.* **2000**, *57*, 371–384. [CrossRef] [PubMed]
36. Mercado, A.; Vázquez, N.; Song, L.; Cortés, R.; Enck, A.H.; Welch, R.; Delpire, E.; Gamba, G.; Mount, D.B. NH2-terminal heterogeneity in the KCC3 K+-Cl- cotransporter. *Am. J. Physiol. Ren. Physiol.* **2005**, *289*, F1246–F1261. [CrossRef]
37. Markovich, D. Physiological roles of renal anion transporters NaS1 and Sat1. *Am. J. Physiol. Ren. Physiol.* **2011**, *300*, F1267–F1270. [CrossRef]
38. Ghezzi, C.; Loo, D.D.F.; Wright, E.M. Physiology of renal glucose handling via SGLT1, SGLT2 and GLUT2. *Diabetologia* **2018**, *61*, 2087–2097. [CrossRef]
39. Smith, D.E.; Clémençon, B.; Hediger, M.A. Proton-coupled oligopeptide transporter family SLC15: Physiological, pharmacological and pathological implications. *Mol. Asp. Med.* **2013**, *34*, 323–336. [CrossRef]
40. Verrey, F.; Singer, D.; Ramadan, T.; Vuille-dit-Bille, R.N.; Mariotta, L.; Camargo, S.M.R. Kidney amino acid transport. *Pflug. Arch.* **2009**, *458*, 53–60. [CrossRef]
41. Turner, R.J. beta-Amino acid transport across the renal brush-border membrane is coupled to both Na and Cl. *J. Biol. Chem.* **1986**, *261*, 16060–16066.
42. Park, S.Y.; Kim, J.-K.; Kim, I.J.; Choi, B.K.; Jung, K.Y.; Lee, S.; Park, K.J.; Chairoungdua, A.; Kanai, Y.; Endou, H.; et al. Reabsorption of neutral amino acids mediated by amino acid transporter LAT2 and TAT1 in the basolateral membrane of proximal tubule. *Arch. Pharm. Res.* **2005**, *28*, 421–432. [CrossRef] [PubMed]
43. Vilches, C.; Boiadjieva-Knöpfel, E.; Bodoy, S.; Camargo, S.; López de Heredia, M.; Prat, E.; Ormazabal, A.; Artuch, R.; Zorzano, A.; Verrey, F.; et al. Cooperation of Antiporter LAT2/CD98hc with Uniporter TAT1 for Renal Reabsorption of Neutral Amino Acids. *J. Am. Soc. Nephrol.* **2018**, *29*, 1624–1635. [CrossRef]
44. Mora, C.; Chillarón, J.; Calonge, M.J.; Forgo, J.; Testar, X.; Nunes, V.; Murer, H.; Zorzano, A.; Palacín, M. The rBAT gene is responsible for L-cystine uptake via the b0,(+)-like amino acid transport system in a "renal proximal tubular" cell line (OK cells). *J. Biol. Chem.* **1996**, *271*, 10569–10576. [CrossRef] [PubMed]
45. Fernández, E.; Carrascal, M.; Rousaud, F.; Abián, J.; Zorzano, A.; Palacín, M.; Chillarón, J. rBAT-b(0,+)AT heterodimer is the main apical reabsorption system for cystine in the kidney. *Am. J. Physiol. Ren. Physiol.* **2002**, *283*, F540–F548. [CrossRef] [PubMed]

46. Torrents, D.; Estévez, R.; Pineda, M.; Fernández, E.; Lloberas, J.; Shi, Y.B.; Zorzano, A.; Palacín, M. Identification and characterization of a membrane protein (y+L amino acid transporter-1) that associates with 4F2hc to encode the amino acid transport activity y+L. A candidate gene for lysinuric protein intolerance. *J. Biol. Chem.* **1998**, *273*, 32437–32445. [CrossRef]
47. Bergeron, M.J.; Clémençon, B.; Hediger, M.A.; Markovich, D. SLC13 family of Na^+-coupled di- and tri-carboxylate/sulfate transporters. *Mol. Asp. Med.* **2013**, *34*, 299–312. [CrossRef]
48. Gopal, E.; Umapathy, N.S.; Martin, P.M.; Ananth, S.; Gnana-Prakasam, J.P.; Becker, H.; Wagner, C.A.; Ganapathy, V.; Prasad, P.D. Cloning and functional characterization of human SMCT2 (SLC5A12) and expression pattern of the transporter in kidney. *Biochim. Biophys. Acta* **2007**, *1768*, 2690–2697. [CrossRef]
49. Eraly, S.A.; Vallon, V.; Vaughn, D.A.; Gangoiti, J.A.; Richter, K.; Nagle, M.; Monte, J.C.; Rieg, T.; Truong, D.M.; Long, J.M.; et al. Decreased Renal Organic Anion Secretion and Plasma Accumulation of Endogenous Organic Anions in OAT1 Knock-out Mice. Available online: http://www.jbc.org (accessed on 7 May 2019).
50. Burckhardt, G.; Burckhardt, B.C. In vitro and in vivo evidence of the importance of organic anion transporters (OATs) in drug therapy. *Handb. Exp. Pharmacol.* **2011**, *201*, 29–104.
51. Bush, K.T.; Wu, W.; Lun, C.; Nigam, S.K. The drug transporter OAT3 (SLC22A8) and endogenous metabolite communication via the gut-liver-kidney axis. *J. Biol. Chem.* **2017**, *292*, 15789–15803. [CrossRef]
52. Uwai, Y.; Motohashi, H.; Tsuji, Y.; Ueo, H.; Katsura, T.; Inui, K. Interaction and transport characteristics of mycophenolic acid and its glucuronide via human organic anion transporters hOAT1 and hOAT3. *Biochem. Pharmacol.* **2007**, *74*, 161–168. [CrossRef]
53. Russel, F.G.M.; Koenderink, J.B.; Masereeuw, R. Multidrug resistance protein 4 (MRP4/ABCC4): A versatile efflux transporter for drugs and signalling molecules. *Trends Pharmacol. Sci.* **2008**, *29*, 200–207. [CrossRef] [PubMed]
54. Van de Water, F.M.; Masereeuw, R.; Russel, F.G.M. Function and regulation of multidrug resistance proteins (MRPs) in the renal elimination of organic anions. *Drug Metab. Rev.* **2005**, *37*, 443–471. [CrossRef] [PubMed]
55. Liu, X. ABC Family Transporters. *Adv. Exp. Med. Biol.* **2019**, *1141*, 13–100. [PubMed]
56. Mutsaers, H.A.M.; Caetano-Pinto, P.; Seegers, A.E.M.; Dankers, A.C.A.; van den Broek, P.H.H.; Wetzels, J.F.M.; van den Brand, J.A.J.G.; van den Heuvel, L.P.; Hoenderop, J.G.; Wilmer, M.J.G.; et al. Proximal tubular efflux transporters involved in renal excretion of p-cresyl sulfate and p-cresyl glucuronide: Implications for chronic kidney disease pathophysiology. *Toxicol. In Vitro* **2015**, *29*, 1868–1877. [CrossRef] [PubMed]
57. Dehghan, A.; Köttgen, A.; Yang, Q.; Hwang, S.-J.; Kao, W.L.; Rivadeneira, F.; Boerwinkle, E.; Levy, D.; Hofman, A.; Astor, B.C.; et al. Association of three genetic loci with uric acid concentration and risk of gout: A genome-wide association study. *Lancet* **2008**, *372*, 1953–1961. [CrossRef]
58. Kimura, N.; Masuda, S.; Katsura, T.; Inui, K. Transport of guanidine compounds by human organic cation transporters, hOCT1 and hOCT2. *Biochem. Pharmacol.* **2009**, *77*, 1429–1436. [CrossRef]
59. Bacher, P.; Giersiefer, S.; Bach, M.; Fork, C.; Schömig, E.; Gründemann, D. Substrate discrimination by ergothioneine transporter SLC22A4 and carnitine transporter SLC22A5: Gain-of-function by interchange of selected amino acids. *Biochim. Biophys. Acta* **2009**, *1788*, 2594–2602. [CrossRef]
60. Nies, A.T.; Damme, K.; Kruck, S.; Schaeffeler, E.; Schwab, M. Structure and function of multidrug and toxin extrusion proteins (MATEs) and their relevance to drug therapy and personalized medicine. *Arch. Toxicol.* **2016**, *90*, 1555–1584. [CrossRef]
61. Sharfuddin, A.A.; Molitoris, B.A. Pathophysiology of ischemic acute kidney injury. *Nat. Rev. Nephrol.* **2011**, *7*, 189–200. [CrossRef]
62. Basile, D.P.; Anderson, M.D.; Sutton, T.A. Pathophysiology of Acute Kidney Injury. *Compr. Physiol.* **2012**, *2*, 1303–1353.
63. Guellec, C.B.-L.; Largeau, B.; Bon, D.; Marquet, P.; Hauet, T. Ischemia/reperfusion-associated tubular cells injury in renal transplantation: Can metabolomics inform about mechanisms and help identify new therapeutic targets? *Pharmacol. Res.* **2018**, *129*, 34–43. [CrossRef]
64. Du, J.; Zhang, L.; Yang, Y.; Li, W.; Chen, L.; Ge, Y.; Sun, C.; Zhu, Y.; Gu, L. ATP depletion-induced actin rearrangement reduces cell adhesion via p38 MAPK-HSP27 signaling in renal proximal tubule cells. *Cell. Physiol. Biochem.* **2010**, *25*, 501–510. [CrossRef] [PubMed]
65. Molitoris, B.A.; Dahl, R.; Geerdes, A. Cytoskeleton disruption and apical redistribution of proximal tubule Na(+)-K(+)-ATPase during ischemia. *Am. J. Physiol.* **1992**, *263*, F488–F495. [CrossRef] [PubMed]

66. Khundmiri, S.J.; Asghar, M.; Khan, F.; Salim, S.; Yusufi, A.N. Effect of reversible and irreversible ischemia on marker enzymes of BBM from renal cortical PT subpopulations. *Am. J. Physiol.* **1997**, *273*, F849–F856. [CrossRef] [PubMed]
67. Collard, C.D.; Gelman, S. Pathophysiology, clinical manifestations, and prevention of ischemia-reperfusion injury. *Anesthesiology* **2001**, *94*, 1133–1138. [CrossRef]
68. Pochineni, V.; Rondon-Berrios, H. Electrolyte and Acid-Base Disorders in the Renal Transplant Recipient. *Front. Med. (Lausanne)* **2018**, *5*, 5. [CrossRef]
69. Khundmiri, S.J.; Asghar, M.; Banday, A.A.; Khan, F.; Salim, S.; Levi, M.; Yusufi, A.N.K. Effect of ischemia reperfusion on sodium-dependent phosphate transport in renal brush border membranes. *Biochim. Biophys. Acta* **2005**, *1716*, 19–28. [CrossRef]
70. Di Sole, F.; Hu, M.-C.; Zhang, J.; Babich, V.; Bobulescu, I.A.; Shi, M.; McLeroy, P.; Rogers, T.E.; Moe, O.W. The reduction of Na/H exchanger-3 protein and transcript expression in acute ischemia-reperfusion injury is mediated by extractable tissue factor(s). *Kidney Int.* **2011**, *80*, 822–831. [CrossRef]
71. Kwon, T.H.; Frøkiaer, J.; Han, J.S.; Knepper, M.A.; Nielsen, S. Decreased abundance of major Na(+) transporters in kidneys of rats with ischemia-induced acute renal failure. *Am. J. Physiol. Ren. Physiol.* **2000**, *278*, F925–F939. [CrossRef]
72. Johnston, P.A.; Rennke, H.; Levinsky, N.G. Recovery of proximal tubular function from ischemic injury. *Am. J. Physiol.* **1984**, *246*, F159–F166. [CrossRef]
73. Molitoris, B.A.; Kinne, R. Ischemia induces surface membrane dysfunction. Mechanism of altered Na+-dependent glucose transport. *J. Clin. Investig.* **1987**, *80*, 647–654. [CrossRef] [PubMed]
74. Saito, H. Pathophysiological regulation of renal SLC22A organic ion transporters in acute kidney injury: Pharmacological and toxicological implications. *Pharmacol. Ther.* **2010**, *125*, 79–91. [CrossRef] [PubMed]
75. Bischoff, A.; Bucher, M.; Gekle, M.; Sauvant, C. PAH clearance after renal ischemia and reperfusion is a function of impaired expression of basolateral Oat1 and Oat3. *Physiol. Rep.* **2014**, *2*, e00243. [CrossRef]
76. Schneider, R.; Sauvant, C.; Betz, B.; Otremba, M.; Fischer, D.; Holzinger, H.; Wanner, C.; Galle, J.; Gekle, M. Downregulation of organic anion transporters OAT1 and OAT3 correlates with impaired secretion of para-aminohippurate after ischemic acute renal failure in rats. *Am. J. Physiol. Ren. Physiol.* **2007**, *292*, F1599–F1605. [CrossRef] [PubMed]
77. Matsuzaki, T.; Watanabe, H.; Yoshitome, K.; Morisaki, T.; Hamada, A.; Nonoguchi, H.; Kohda, Y.; Tomita, K.; Inui, K.; Saito, H. Downregulation of organic anion transporters in rat kidney under ischemia/reperfusion-induced acute [corrected] renal failure. *Kidney Int.* **2007**, *71*, 539–547. [CrossRef]
78. Sauvant, C.; Schneider, R.; Holzinger, H.; Renker, S.; Wanner, C.; Gekle, M. Implementation of an in vitro model system for investigation of reperfusion damage after renal ischemia. *Cell. Physiol. Biochem.* **2009**, *24*, 567–576. [CrossRef]
79. Matsuzaki, T.; Morisaki, T.; Sugimoto, W.; Yokoo, K.; Sato, D.; Nonoguchi, H.; Tomita, K.; Terada, T.; Inui, K.; Hamada, A.; et al. Altered pharmacokinetics of cationic drugs caused by down-regulation of renal rat organic cation transporter 2 (Slc22a2) and rat multidrug and toxin extrusion 1 (Slc47a1) in ischemia/reperfusion-induced acute kidney injury. *Drug Metab. Dispos.* **2008**, *36*, 649–654. [CrossRef]
80. Schneider, R.; Meusel, M.; Betz, B.; Kersten, M.; Möller-Ehrlich, K.; Wanner, C.; Koepsell, H.; Sauvant, C. Nitric oxide-induced regulation of renal organic cation transport after renal ischemia-reperfusion injury. *Am. J. Physiol. Ren. Physiol.* **2011**, *301*, F997–F1004. [CrossRef]
81. Ciarimboli, G.; Schröter, R.; Neugebauer, U.; Vollenbröker, B.; Gabriëls, G.; Brzica, H.; Sabolić, I.; Pietig, G.; Pavenstädt, H.; Schlatter, E.; et al. Kidney transplantation down-regulates expression of organic cation transporters, which translocate β-blockers and fluoroquinolones. *Mol. Pharm.* **2013**, *10*, 2370–2380. [CrossRef]
82. Corrigan, G.; Ramaswamy, D.; Kwon, O.; Sommer, F.G.; Alfrey, E.J.; Dafoe, D.C.; Olshen, R.A.; Scandling, J.D.; Myers, B.D. PAH extraction and estimation of plasma flow in human postischemic acute renal failure. *Am. J. Physiol.* **1999**, *277*, F312–F318. [CrossRef]
83. Kwon, O.; Hong, S.-M.; Blouch, K. Alteration in renal organic anion transporter 1 after ischemia/reperfusion in cadaveric renal allografts. *J. Histochem. Cytochem.* **2007**, *55*, 575–584. [CrossRef] [PubMed]
84. Huls, M.; van den Heuvel, J.J.M.W.; Dijkman, H.B.P.M.; Russel, F.G.M.; Masereeuw, R. ABC transporter expression profiling after ischemic reperfusion injury in mouse kidney. *Kidney Int.* **2006**, *69*, 2186–2193. [CrossRef] [PubMed]

85. Schneider, R.; Meusel, M.; Betz, B.; Held, C.; Möller-Ehrlich, K.; Büttner-Herold, M.; Wanner, C.; Gekle, M.; Sauvant, C. Oat1/3 restoration protects against renal damage after ischemic AKI. *Am. J. Physiol. Ren. Physiol.* **2015**, *308*, F198–F208. [CrossRef]
86. Hagos, Y.; Schley, G.; Schödel, J.; Krick, W.; Burckhardt, G.; Willam, C.; Burckhardt, B.C. α-Ketoglutarate-related inhibitors of HIF prolyl hydroxylases are substrates of renal organic anion transporters 1 (OAT1) and 4 (OAT4). *Pflug. Arch.* **2012**, *464*, 367–374. [CrossRef] [PubMed]
87. Paulusma, C.C.; Kothe, M.J.; Bakker, C.T.; Bosma, P.J.; van Bokhoven, I.; van Marle, J.; Bolder, U.; Tytgat, G.N.; Oude Elferink, R.P. Zonal down-regulation and redistribution of the multidrug resistance protein 2 during bile duct ligation in rat liver. *Hepatology* **2000**, *31*, 684–693. [CrossRef] [PubMed]
88. Ke, Q.; Costa, M. Hypoxia-inducible factor-1 (HIF-1). *Mol. Pharmacol.* **2006**, *70*, 1469–1480. [CrossRef] [PubMed]
89. Hill, P.; Shukla, D.; Tran, M.G.B.; Aragones, J.; Cook, H.T.; Carmeliet, P.; Maxwell, P.H. Inhibition of hypoxia inducible factor hydroxylases protects against renal ischemia-reperfusion injury. *J. Am. Soc. Nephrol.* **2008**, *19*, 39–46. [CrossRef]
90. Conde, E.; Alegre, L.; Blanco-Sánchez, I.; Sáenz-Morales, D.; Aguado-Fraile, E.; Ponte, B.; Ramos, E.; Sáiz, A.; Jiménez, C.; Ordoñez, A.; et al. Hypoxia inducible factor 1-alpha (HIF-1 alpha) is induced during reperfusion after renal ischemia and is critical for proximal tubule cell survival. *PLoS ONE* **2012**, *7*, e33258. [CrossRef]
91. Chen, Y.; Jiang, S.; Zou, J.; Zhong, Y.; Ding, X. Silencing HIF-1α aggravates growth inhibition and necrosis of proximal renal tubular epithelial cell under hypoxia. *Ren. Fail.* **2016**, *38*, 1726–1734. [CrossRef]
92. Comerford, K.M.; Wallace, T.J.; Karhausen, J.; Louis, N.A.; Montalto, M.C.; Colgan, S.P. Hypoxia-inducible factor-1-dependent regulation of the multidrug resistance (MDR1) gene. *Cancer Res.* **2002**, *62*, 3387–3394.
93. Zapata-Morales, J.R.; Galicia-Cruz, O.G.; Franco, M.; Martinez, Y.; Morales, F. Hypoxia-inducible factor-1α (HIF-1α) protein diminishes sodium glucose transport 1 (SGLT1) and SGLT2 protein expression in renal epithelial tubular cells (LLC-PK1) under hypoxia. *J. Biol. Chem.* **2014**, *289*, 346–357. [CrossRef] [PubMed]
94. Jiang, W.; Prokopenko, O.; Wong, L.; Inouye, M.; Mirochnitchenko, O. IRIP, a new ischemia/reperfusion-inducible protein that participates in the regulation of transporter activity. *Mol. Cell. Biol.* **2005**, *25*, 6496–6508. [CrossRef] [PubMed]
95. Li, Q.; Yang, H.; Peng, X.; Guo, D.; Dong, Z.; Polli, J.E.; Shu, Y. Ischemia/Reperfusion-inducible protein modulates the function of organic cation transporter 1 and multidrug and toxin extrusion 1. *Mol. Pharm.* **2013**, *10*, 2578–2587. [CrossRef] [PubMed]
96. Prokopenko, O.; Mirochnitchenko, O. Ischemia-reperfusion-inducible protein modulates cell sensitivity to anticancer drugs by regulating activity of efflux transporter. *Am. J. Physiol. Cell Physiol.* **2009**, *296*, C1086–C1097. [CrossRef] [PubMed]
97. Kwon, O.; Wang, W.-W.; Miller, S. Renal organic anion transporter 1 is maldistributed and diminishes in proximal tubule cells but increases in vasculature after ischemia and reperfusion. *Am. J. Physiol. Ren. Physiol.* **2008**, *295*, F1807–F1816. [CrossRef] [PubMed]
98. Wolff, N.A.; Thies, K.; Kuhnke, N.; Reid, G.; Friedrich, B.; Lang, F.; Burckhardt, G. Protein kinase C activation downregulates human organic anion transporter 1-mediated transport through carrier internalization. *J. Am. Soc. Nephrol.* **2003**, *14*, 1959–1968. [CrossRef]
99. Preising, C.; Schneider, R.; Bucher, M.; Gekle, M.; Sauvant, C. Regulation of Expression of Renal Organic Anion Transporters OAT1 and OAT3 in a Model of Ischemia/Reperfusion Injury. *Cell. Physiol. Biochem.* **2015**, *37*, 1–13. [CrossRef]
100. Malagrino, P.A.; Venturini, G.; Yogi, P.S.; Dariolli, R.; Padilha, K.; Kiers, B.; Gois, T.C.; Motta-Leal-Filho, J.M.; Takimura, C.K.; Girardi, A.C.C.; et al. Metabolomic characterization of renal ischemia and reperfusion in a swine model. *Life Sci.* **2016**, *156*, 57–67. [CrossRef]
101. Wei, Q.; Xiao, X.; Fogle, P.; Dong, Z. Changes in metabolic profiles during acute kidney injury and recovery following ischemia/reperfusion. *PLoS ONE* **2014**, *9*, e106647. [CrossRef]
102. Jouret, F.; Leenders, J.; Poma, L.; Defraigne, J.-O.; Krzesinski, J.-M.; de Tullio, P. Nuclear Magnetic Resonance Metabolomic Profiling of Mouse Kidney, Urine and Serum Following Renal Ischemia/Reperfusion Injury. *PLoS ONE* **2016**, *11*, e0163021. [CrossRef]

103. Chihanga, T.; Ma, Q.; Nicholson, J.D.; Ruby, H.N.; Edelmann, R.E.; Devarajan, P.; Kennedy, M.A. NMR spectroscopy and electron microscopy identification of metabolic and ultrastructural changes to the kidney following ischemia-reperfusion injury. *Am. J. Physiol. Ren. Physiol.* **2018**, *314*, F154–F166. [CrossRef] [PubMed]
104. Bon, D.; Billault, C.; Claire, B.; Thuillier, R.; Hebrard, W.; Boildieu, N.; Celhay, O.; Irani, J.; Seguin, F.; Hauet, T. Analysis of perfusates during hypothermic machine perfusion by NMR spectroscopy: A potential tool for predicting kidney graft outcome. *Transplantation* **2014**, *97*, 810–816. [CrossRef] [PubMed]
105. Guy, A.J.; Nath, J.; Cobbold, M.; Ludwig, C.; Tennant, D.A.; Inston, N.G.; Ready, A.R. Metabolomic analysis of perfusate during hypothermic machine perfusion of human cadaveric kidneys. *Transplantation* **2015**, *99*, 754–759. [CrossRef]
106. Stryjak, I.; Warmuzińska, N.; Bogusiewicz, J.; Łuczykowski, K.; Bojko, B. Monitoring of the influence of long-term oxidative stress and ischemia on the condition of kidney using solid phase microextraction chemical biopsy coupled with liquid chromatography high resolution mass spectrometry. *J. Sep. Sci.* **2020**, *43*, 1867–1878. [CrossRef]
107. Nath, J.; Smith, T.B.; Patel, K.; Ebbs, S.R.; Hollis, A.; Tennant, D.A.; Ludwig, C.; Ready, A.R. Metabolic differences between cold stored and machine perfused porcine kidneys: A 1H NMR based study. *Cryobiology* **2017**, *74*, 115–120. [CrossRef] [PubMed]
108. DiRito, J.R.; Hosgood, S.A.; Tietjen, G.T.; Nicholson, M.L. The future of marginal kidney repair in the context of normothermic machine perfusion. *Am. J. Transplant.* **2018**, *18*, 2400–2408. [CrossRef]
109. Weissenbacher, A.; Vrakas, G.; Nasralla, D.; Ceresa, C.D.L. The future of organ perfusion and re-conditioning. *Transpl. Int.* **2019**, *32*, 586–597. [CrossRef]
110. Woroniecki, R.; Ferdinand, J.R.; Morrow, J.S.; Devarajan, P. Dissociation of spectrin-ankyrin complex as a basis for loss of Na-K-ATPase polarity after ischemia. *Am. J. Physiol. Ren. Physiol.* **2003**, *284*, F358–F364. [CrossRef]
111. Fernández-Llama, P.; Andrews, P.; Turner, R.; Saggi, S.; Dimari, J.; Kwon, T.H.; Nielsen, S.; Safirstein, R.; Knepper, M.A. Decreased abundance of collecting duct aquaporins in post-ischemic renal failure in rats. *J. Am. Soc. Nephrol.* **1999**, *10*, 1658–1668.
112. Miltényi, M.; Tulassay, T.; Körner, A.; Szabó, A.; Dobos, M. Tubular dysfunction in metabolic acidosis. First step to acute renal failure. *Contrib. Nephrol.* **1988**, *67*, 58–66.
113. Liu, J.; Litt, L.; Segal, M.R.; Kelly, M.J.S.; Pelton, J.G.; Kim, M. Metabolomics of oxidative stress in recent studies of endogenous and exogenously administered intermediate metabolites. *Int. J. Mol. Sci.* **2011**, *12*, 6469–6501. [CrossRef] [PubMed]
114. Halliwell, B.; Cheah, I.K.; Drum, C.L. Ergothioneine, an adaptive antioxidant for the protection of injured tissues? A hypothesis. *Biochem. Biophys. Res. Commun.* **2016**, *470*, 245–250. [CrossRef] [PubMed]
115. Mishra, A.; Reddy, I.J.; Gupta, P.S.P.; Mondal, S. L-carnitine Mediated Reduction in Oxidative Stress and Alteration in Transcript Level of Antioxidant Enzymes in Sheep Embryos Produced In Vitro. *Reprod. Domest. Anim.* **2016**, *51*, 311–321. [CrossRef] [PubMed]
116. Ribas, G.S.; Vargas, C.R.; Wajner, M. L-carnitine supplementation as a potential antioxidant therapy for inherited neurometabolic disorders. *Gene* **2014**, *533*, 469–476. [CrossRef] [PubMed]
117. Liu, Y.; Yan, S.; Ji, C.; Dai, W.; Hu, W.; Zhang, W.; Mei, C. Metabolomic changes and protective effect of (L)-carnitine in rat kidney ischemia/reperfusion injury. *Kidney Blood Press. Res.* **2012**, *35*, 373–381. [CrossRef]
118. Chouchani, E.T.; Pell, V.R.; Gaude, E.; Aksentijević, D.; Sundier, S.Y.; Robb, E.L.; Logan, A.; Nadtochiy, S.M.; Ord, E.N.J.; Smith, A.C.; et al. Ischaemic accumulation of succinate controls reperfusion injury through mitochondrial ROS. *Nature* **2014**, *515*, 431–435. [CrossRef] [PubMed]
119. Chinopoulos, C. Which way does the citric acid cycle turn during hypoxia? The critical role of α-ketoglutarate dehydrogenase complex. *J. Neurosci. Res.* **2013**, *91*, 1030–1043. [CrossRef]
120. Tajima, T.; Yoshifuji, A.; Matsui, A.; Itoh, T.; Uchiyama, K.; Kanda, T.; Tokuyama, H.; Wakino, S.; Itoh, H. β-hydroxybutyrate attenuates renal ischemia-reperfusion injury through its anti-pyroptotic effects. *Kidney Int.* **2019**, *95*, 1120–1137. [CrossRef]
121. Ferenbach, D.A.; Bonventre, J.V. Mechanisms of maladaptive repair after AKI leading to accelerated kidney ageing and CKD. *Nat. Rev. Nephrol.* **2015**, *11*, 264–276. [CrossRef]
122. Andrade, L.; Rodrigues, C.E.; Gomes, S.A.; Noronha, I.L. Acute Kidney Injury as a Condition of Renal Senescence. *Cell Transplant.* **2018**, *27*, 739–753. [CrossRef]

123. Qi, R.; Yang, C. Renal tubular epithelial cells: The neglected mediator of tubulointerstitial fibrosis after injury. *Cell Death Dis.* **2018**, *9*, 1126. [CrossRef] [PubMed]
124. Huls, M.; Russel, F.G.M.; Masereeuw, R. The Role of ATP Binding Cassette Transporters in Tissue Defense and Organ Regeneration. *J. Pharm. Exp. Ther.* **2009**, *328*, 3–9. [CrossRef] [PubMed]
125. Humphreys, B.D.; Czerniak, S.; DiRocco, D.P.; Hasnain, W.; Cheema, R.; Bonventre, J.V. Repair of injured proximal tubule does not involve specialized progenitors. *Proc. Natl. Acad. Sci. USA* **2011**, *108*, 9226–9231. [CrossRef] [PubMed]
126. Berger, K.; Moeller, M.J. Mechanisms of epithelial repair and regeneration after acute kidney injury. *Semin. Nephrol.* **2014**, *34*, 394–403. [CrossRef] [PubMed]
127. Ahn, S.-Y.; Nigam, S.K. Toward a systems level understanding of organic anion and other multispecific drug transporters: A remote sensing and signaling hypothesis. *Mol. Pharmacol. Exp.* **2009**, *76*, 481–490. [CrossRef]
128. Rosenthal, S.B.; Bush, K.T.; Nigam, S.K. A Network of SLC and ABC Transporter and DME Genes Involved in Remote Sensing and Signaling in the Gut-Liver-Kidney Axis. *Sci. Rep.* **2019**, *9*. [CrossRef]
129. Nigam, S.K.; Bush, K.T. Uraemic syndrome of chronic kidney disease: Altered remote sensing and signalling. *Nat. Rev. Nephrol.* **2019**, *15*, 301–316. [CrossRef]
130. Chen, C.; Slitt, A.L.; Dieter, M.Z.; Tanaka, Y.; Scheffer, G.L.; Klaassen, C.D. Up-regulation of Mrp4 expression in kidney of Mrp2-deficient TR- rats. *Biochem. Pharmacol.* **2005**, *70*, 1088–1095. [CrossRef]
131. Shiao, C.-C.; Wu, P.-C.; Huang, T.-M.; Lai, T.-S.; Yang, W.-S.; Wu, C.-H.; Lai, C.-F.; Wu, V.-C.; Chu, T.-S.; Wu, K.-D.; et al. Long-term remote organ consequences following acute kidney injury. *Crit. Care* **2015**, *19*, 438. [CrossRef]
132. Dépret, F.; Prud'homme, M.; Legrand, M. A Role of Remote Organs Effect in Acute Kidney Injury Outcome. *Nephron* **2017**, *137*, 273–276. [CrossRef]
133. Kao, C.-C.; Yang, W.-S.; Fang, J.-T.; Liu, K.D.; Wu, V.-C. Remote organ failure in acute kidney injury. *J. Formos. Med. Assoc.* **2019**, *118*, 859–866. [CrossRef] [PubMed]
134. Serteser, M.; Koken, T.; Kahraman, A.; Yilmaz, K.; Akbulut, G.; Dilek, O.N. Changes in hepatic TNF-alpha levels, antioxidant status, and oxidation products after renal ischemia/reperfusion injury in mice. *J. Surg. Res.* **2002**, *107*, 234–240. [CrossRef] [PubMed]
135. Vaghasiya, J.D.; Sheth, N.R.; Bhalodia, Y.S.; Jivani, N.P. Exaggerated Liver Injury Induced by Renal Ischemia Reperfusion in Diabetes: Effect of Exenatide. *Saudi J. Gastroenterol.* **2010**, *16*, 174–180. [CrossRef] [PubMed]
136. Dou, L.; Bertrand, E.; Cerini, C.; Faure, V.; Sampol, J.; Vanholder, R.; Berland, Y.; Brunet, P. The uremic solutes p-cresol and indoxyl sulfate inhibit endothelial proliferation and wound repair. *Kidney Int.* **2004**, *65*, 442–451. [CrossRef]
137. Dou, L.; Jourde-Chiche, N.; Faure, V.; Cerini, C.; Berland, Y.; Dignat-George, F.; Brunet, P. The uremic solute indoxyl sulfate induces oxidative stress in endothelial cells. *J. Thromb. Haemost.* **2007**, *5*, 1302–1308. [CrossRef]
138. Huang, M.; Wei, R.; Wang, Y.; Su, T.; Li, P.; Chen, X. The uremic toxin hippurate promotes endothelial dysfunction via the activation of Drp1-mediated mitochondrial fission. *Redox Biol.* **2018**, *16*, 303–313. [CrossRef]
139. Brandoni, A.; Torres, A.M. Altered Renal Expression of Relevant Clinical Drug Transporters in Different Models of Acute Uremia in Rats. Role of Urea Levels. *Cell. Physiol. Biochem.* **2015**, *36*, 907–916. [CrossRef]
140. Knoflach, A.; Binswanger, U. Serum hippuric acid concentration in renal allograft rejection, ureter obstruction, and tubular necrosis. *Transpl. Int.* **1994**, *7*, 17–21. [CrossRef]
141. Satoh, M.; Hayashi, H.; Watanabe, M.; Ueda, K.; Yamato, H.; Yoshioka, T.; Motojima, M. Uremic toxins overload accelerates renal damage in a rat model of chronic renal failure. *Nephron Exp. Nephrol.* **2003**, *95*, e111–e118. [CrossRef]
142. Oliva-Damaso, E.; Oliva-Damaso, N.; Rodriguez-Esparragon, F.; Payan, J.; Baamonde-Laborda, E.; Gonzalez-Cabrera, F.; Santana-Estupiñan, R.; Rodriguez-Perez, J.C. Asymmetric (ADMA) and Symmetric (SDMA) Dimethylarginines in Chronic Kidney Disease: A Clinical Approach. *Int. J. Mol. Sci.* **2019**, *20*, 3668. [CrossRef]
143. Gondouin, B.; Cerini, C.; Dou, L.; Sallée, M.; Duval-Sabatier, A.; Pletinck, A.; Calaf, R.; Lacroix, R.; Jourde-Chiche, N.; Poitevin, S.; et al. Indolic uremic solutes increase tissue factor production in endothelial cells by the aryl hydrocarbon receptor pathway. *Kidney Int.* **2013**, *84*, 733–744. [CrossRef] [PubMed]

144. Barreto, F.C.; Barreto, D.V.; Canziani, M.E.F. Uremia Retention Molecules and Clinical Outcomes. *Contrib Nephrol.* **2017**, *191*, 18–31. [PubMed]
145. Liabeuf, S.; Cheddani, L.; Massy, Z.A. Uremic Toxins and Clinical Outcomes: The Impact of Kidney Transplantation. *Toxins (Basel)* **2018**, *10*, 229. [CrossRef] [PubMed]
146. Massy, Z.A.; Liabeuf, S. Middle-Molecule Uremic Toxins and Outcomes in Chronic Kidney Disease. *Contrib. Nephrol.* **2017**, *191*, 8–17. [PubMed]
147. Mao, Q.; Unadkat, J.D. Role of the breast cancer resistance protein (BCRP/ABCG2) in drug transport-an update. *AAPS J.* **2015**, *17*, 65–82. [CrossRef]
148. Patel, C.G.; Ogasawara, K.; Akhlaghi, F. Mycophenolic acid glucuronide is transported by multidrug resistance-associated protein 2 and this transport is not inhibited by cyclosporine, tacrolimus or sirolimus. *Xenobiotica* **2013**, *43*, 229–235. [CrossRef]
149. Naesens, M.; Lerut, E.; de Jonge, H.; Van Damme, B.; Vanrenterghem, Y.; Kuypers, D.R.J. Donor age and renal P-glycoprotein expression associate with chronic histological damage in renal allografts. *J. Am. Soc. Nephrol.* **2009**, *20*, 2468–2480. [CrossRef]
150. Hauser, I.A.; Schaeffeler, E.; Gauer, S.; Scheuermann, E.H.; Wegner, B.; Gossmann, J.; Ackermann, H.; Seidl, C.; Hocher, B.; Zanger, U.M.; et al. ABCB1 genotype of the donor but not of the recipient is a major risk factor for cyclosporine-related nephrotoxicity after renal transplantation. *J. Am. Soc. Nephrol.* **2005**, *16*, 1501–1511. [CrossRef]
151. Moore, J.; McKnight, A.J.; Döhler, B.; Simmonds, M.J.; Courtney, A.E.; Brand, O.J.; Briggs, D.; Ball, S.; Cockwell, P.; Patterson, C.C.; et al. Donor ABCB1 variant associates with increased risk for kidney allograft failure. *J. Am. Soc. Nephrol.* **2012**, *23*, 1891–1899. [CrossRef]
152. Woillard, J.-B.; Gatault, P.; Picard, N.; Arnion, H.; Anglicheau, D.; Marquet, P. A donor and recipient candidate gene association study of allograft loss in renal transplant recipients receiving a tacrolimus-based regimen. *Am. J. Transplant.* **2018**, *18*, 2905–2913. [CrossRef]
153. Kimchi-Sarfaty, C.; Oh, J.M.; Kim, I.-W.; Sauna, Z.E.; Calcagno, A.M.; Ambudkar, S.V.; Gottesman, M.M. A "silent" polymorphism in the MDR1 gene changes substrate specificity. *Science* **2007**, *315*, 525–528. [CrossRef] [PubMed]
154. El-Sheikh, A.A.K.; Greupink, R.; Wortelboer, H.M.; van den Heuvel, J.J.M.W.; Schreurs, M.; Koenderink, J.B.; Masereeuw, R.; Russel, F.G.M. Interaction of immunosuppressive drugs with human organic anion transporter (OAT) 1 and OAT3, and multidrug resistance-associated protein (MRP) 2 and MRP4. *Transl Res.* **2013**, *162*, 398–409. [CrossRef] [PubMed]
155. Nies, A.T.; Cantz, T.; Brom, M.; Leier, I.; Keppler, D. Expression of the apical conjugate export pump, Mrp2, in the polarized hepatoma cell line, WIF-B. *Hepatology* **1998**, *28*, 1332–1340. [CrossRef] [PubMed]
156. Zimmerman, J.J.; Harper, D.; Getsy, J.; Jusko, W.J. Pharmacokinetic interactions between sirolimus and microemulsion cyclosporine when orally administered jointly and 4 hours apart in healthy volunteers. *J. Clin. Pharm.* **2003**, *43*, 1168–1176. [CrossRef]
157. Emoto, C.; Vinks, A.A.; Fukuda, T. Risk Assessment of Drug-Drug Interactions of Calcineurin Inhibitors Affecting Sirolimus Pharmacokinetics in Renal Transplant Patients. *Ther. Drug Monit.* **2016**, *38*, 607–613. [CrossRef]
158. Podder, H.; Stepkowski, S.M.; Napoli, K.L.; Clark, J.; Verani, R.R.; Chou, T.C.; Kahan, B.D. Pharmacokinetic interactions augment toxicities of sirolimus/cyclosporine combinations. *J. Am. Soc. Nephrol.* **2001**, *12*, 1059–1071.
159. Kahan, B.D. Efficacy of sirolimus compared with azathioprine for reduction of acute renal allograft rejection: A randomised multicentre study. The Rapamune US Study Group. *Lancet* **2000**, *356*, 194–202. [CrossRef]
160. Anglicheau, D.; Pallet, N.; Rabant, M.; Marquet, P.; Cassinat, B.; Méria, P.; Beaune, P.; Legendre, C.; Thervet, E. Role of P-glycoprotein in cyclosporine cytotoxicity in the cyclosporine-sirolimus interaction. *Kidney Int.* **2006**, *70*, 1019–1025. [CrossRef]
161. Hesselink, D.A.; van Hest, R.M.; Mathot, R.A.A.; Bonthuis, F.; Weimar, W.; de Bruin, R.W.F.; van Gelder, T. Cyclosporine interacts with mycophenolic acid by inhibiting the multidrug resistance-associated protein 2. *Am. J. Transplant.* **2005**, *5*, 987–994. [CrossRef]

162. El-Sheikh, A.A.K.; Koenderink, J.B.; Wouterse, A.C.; van den Broek, P.H.H.; Verweij, V.G.M.; Masereeuw, R.; Russel, F.G.M. Renal glucuronidation and multidrug resistance protein 2-/ multidrug resistance protein 4-mediated efflux of mycophenolic acid: Interaction with cyclosporine and tacrolimus. *Transl. Res.* **2014**, *164*, 46–56. [CrossRef]
163. Nigam, S.K. What do drug transporters really do? *Nat. Rev. Drug Discov* **2015**, *14*, 29–44. [CrossRef] [PubMed]
164. Sakurai, Y.; Motohashi, H.; Ueo, H.; Masuda, S.; Saito, H.; Okuda, M.; Mori, N.; Matsuura, M.; Doi, T.; Fukatsu, A.; et al. Expression levels of renal organic anion transporters (OATs) and their correlation with anionic drug excretion in patients with renal diseases. *Pharm. Res.* **2004**, *21*, 61–67. [CrossRef] [PubMed]
165. Kito, T.; Ito, S.; Mizuno, T.; Maeda, K.; Kusuhara, H. Investigation of non-linear Mate1-mediated efflux of trimethoprim in the mouse kidney as the mechanism underlying drug-drug interactions between trimethoprim and organic cations in the kidney. *Drug Metab. Pharmacol.* **2019**, *34*, 87–94. [CrossRef] [PubMed]
166. Saat, T.C.; van den Akker, E.K.; IJzermans, J.N.M.; Dor, F.J.M.F.; de Bruin, R.W.F. Improving the outcome of kidney transplantation by ameliorating renal ischemia reperfusion injury: Lost in translation? *J. Transl. Med.* **2016**, *14*, 20. [CrossRef]
167. Nicholson, M.L.; Hosgood, S.A. Renal transplantation after ex vivo normothermic perfusion: The first clinical study. *Am. J. Transplant.* **2013**, *13*, 1246–1252. [CrossRef]
168. Kaths, J.M.; Cen, J.Y.; Chun, Y.M.; Echeverri, J.; Linares, I.; Ganesh, S.; Yip, P.; John, R.; Bagli, D.; Mucsi, I.; et al. Continuous Normothermic Ex Vivo Kidney Perfusion Is Superior to Brief Normothermic Perfusion Following Static Cold Storage in Donation After Circulatory Death Pig Kidney Transplantation. *Am. J. Transplant.* **2017**, *17*, 957–969. [CrossRef]
169. Kataria, A.; Magoon, S.; Makkar, B.; Gundroo, A. Machine perfusion in kidney transplantation. *Curr. Opin. Organ Transplant.* **2019**, *24*, 378–384. [CrossRef]
170. Chatterjee, P.K. Novel pharmacological approaches to the treatment of renal ischemia-reperfusion injury: A comprehensive review. *Naunyn Schmiedebergs Arch. Pharmacol.* **2007**, *376*, 1–43. [CrossRef]
171. Chatauret, N.; Thuillier, R.; Hauet, T. Preservation strategies to reduce ischemic injury in kidney transplantation: Pharmacological and genetic approaches. *Curr. Opin. Organ Transplant.* **2011**, *16*, 180–187. [CrossRef]
172. Gong, H.; Sun, J.; Xue, W.; Tian, P.; Ding, X.; Yan, H.; Li, Y.; Zheng, J. Protective effect of truncated Na+/K+-ATPase β on ischemia/reperfusion-induced renal injury in rats. *Exp. Biol. Med. (Maywood)* **2014**, *239*, 677–685. [CrossRef]
173. Belliard, A.; Gulati, G.K.; Duan, Q.; Alves, R.; Brewer, S.; Madan, N.; Sottejeau, Y.; Wang, X.; Kalisz, J.; Pierre, S.V. Ischemia/reperfusion-induced alterations of enzymatic and signaling functions of the rat cardiac Na+/K+-ATPase: Protection by ouabain preconditioning. *Physiol. Rep.* **2016**, *4*. [CrossRef] [PubMed]
174. Schneider, R.; Meusel, M.; Renker, S.; Bauer, C.; Holzinger, H.; Roeder, M.; Wanner, C.; Gekle, M.; Sauvant, C. Low-dose indomethacin after ischemic acute kidney injury prevents downregulation of Oat1/3 and improves renal outcome. *Am. J. Physiol. Ren. Physiol.* **2009**, *297*, F1614–F1621. [CrossRef] [PubMed]
175. Saigo, C.; Nomura, Y.; Yamamoto, Y.; Sagata, M.; Matsunaga, R.; Jono, H.; Nishi, K.; Saito, H. Meclofenamate elicits a nephropreventing effect in a rat model of ischemic acute kidney injury by suppressing indoxyl sulfate production and restoring renal organic anion transporters. *Drug Des. Dev. Ther.* **2014**, *8*, 1073–1082.
176. Verma, R.; Mishra, V.; Sasmal, D.; Raghubir, R. Pharmacological evaluation of glutamate transporter 1 (GLT-1) mediated neuroprotection following cerebral ischemia/reperfusion injury. *Eur. J. Pharmacol.* **2010**, *638*, 65–71. [CrossRef] [PubMed]
177. Yamashita, J.; Ohkita, M.; Takaoka, M.; Kaneshiro, Y.; Matsuo, T.; Kaneko, K.; Matsumura, Y. Role of Na+/H+ exchanger in the pathogenesis of ischemic acute renal failure in mice. *J. Cardiovasc. Pharmacol.* **2007**, *49*, 154–160. [CrossRef] [PubMed]
178. Hropot, M.; Juretschke, H.P.; Langer, K.H.; Schwark, J.R. S3226, a novel NHE3 inhibitor, attenuates ischemia-induced acute renal failure in rats. *Kidney Int.* **2001**, *60*, 2283–2289. [CrossRef]
179. Liu, W.-H.; Liu, H.-B.; Gao, D.-K.; Ge, G.-Q.; Zhang, P.; Sun, S.-R.; Wang, H.-M.; Liu, S.-B. ABCG2 protects kidney side population cells from hypoxia/reoxygenation injury through activation of the MEK/ERK pathway. *Cell Transplant.* **2013**, *22*, 1859–1868. [CrossRef]

180. Kieran, N.E.; Doran, P.P.; Connolly, S.B.; Greenan, M.-C.; Higgins, D.F.; Leonard, M.; Godson, C.; Taylor, C.T.; Henger, A.; Kretzler, M.; et al. Modification of the transcriptomic response to renal ischemia/reperfusion injury by lipoxin analog. *Kidney Int.* **2003**, *64*, 480–492. [CrossRef]
181. Toyohara, T.; Suzuki, T.; Morimoto, R.; Akiyama, Y.; Souma, T.; Shiwaku, H.O.; Takeuchi, Y.; Mishima, E.; Abe, M.; Tanemoto, M.; et al. SLCO4C1 transporter eliminates uremic toxins and attenuates hypertension and renal inflammation. *J. Am. Soc. Nephrol.* **2009**, *20*, 2546–2555. [CrossRef]
182. Nespoux, J.; Patel, R.; Hudkins, K.L.; Huang, W.; Freeman, B.; Kim, Y.C.; Koepsell, H.; Alpers, C.E.; Vallon, V. Gene deletion of the Na+-glucose cotransporter SGLT1 ameliorates kidney recovery in a murine model of acute kidney injury induced by ischemia-reperfusion. *Am. J. Physiol. Ren. Physiol.* **2019**, *316*, F1201–F1210. [CrossRef]
183. Fuller, T.F.; Kusch, A.; Chaykovska, L.; Catar, R.; Pützer, J.; Haller, M.; Troppmair, J.; Hoff, U.; Dragun, D. Protein kinase C inhibition ameliorates posttransplantation preservation injury in rat renal transplants. *Transplantation* **2012**, *94*, 679–686. [CrossRef] [PubMed]
184. Nangaku, M.; Rosenberger, C.; Heyman, S.N.; Eckardt, K.-U. Regulation of hypoxia-inducible factor in kidney disease. *Clin. Exp. Pharmacol. Physiol.* **2013**, *40*, 148–157. [CrossRef] [PubMed]
185. Shu, S.; Wang, Y.; Zheng, M.; Liu, Z.; Cai, J.; Tang, C.; Dong, Z. Hypoxia and Hypoxia-Inducible Factors in Kidney Injury and Repair. *Cells* **2019**, *8*, 207. [CrossRef] [PubMed]
186. Eltzschig, H.K.; Eckle, T. Ischemia and reperfusion—From mechanism to translation. *Nat. Med.* **2011**, *17*, 1391–1401. [CrossRef]

Objectifs de la thèse

L'atténuation des lésions d'IR, et par conséquent de leur influence sur les fonctions rénales post-greffe, permettrait d'améliorer la survie des greffons. Notre revue de la littérature ayant confirmé que les transporteurs tubulaires pouvaient constituer un mécanisme central de ces lésions ou de leurs conséquences, les objectifs de nos recherches ont été de :

- (i) déterminer si et comment les transporteurs membranaires des cellules tubulaires proximales sont affectés par les lésions d'IR,
- (ii) définir la cinétique de leur modulation,
- (iii) identifier des biomarqueurs spécifiques de la fonction de ces transporteurs.

Dans ce but, un premier axe de recherche a consisté à caractériser les profils métabolomiques de perfusats et l'expression des transporteurs tubulaires de greffon issus de donneurs ECD, à la fin de leur conservation sur HMP. Il s'est agi plus spécifiquement : (1) d'étudier l'évolution des profils métabolomiques en fonction de la durée de perfusion pour comprendre les mécanismes lésionnels et (2) de rechercher si des variations d'expression des transporteurs tubulaires existaient dans ce contexte et si oui, si elles pouvaient expliquer les évolutions métaboliques. En complément, nous avons étudié si l'expression des transporteurs et les variations métaboliques survenant au cours de la conservation sur HMP étaient prédictives de la reprise de fonction du greffon. Ce travail de recherche clinique était inscrit dans les objectifs de l'étude pilote RENALIFE enregistrée dans ClinicalTrials.gov sous l'identifiant NCT03024229. Un second axe de recherche a consisté à étudier les profils métabolomiques et l'expression des transporteurs sur un modèle cellulaire soumis à différents temps d'hypoxie et d'hypoxie/réoxygénation. Cette étude fondamentale avait pour but d'étudier la cinétique des effets de l'hypoxie/réoxygénation sur les transporteurs et le métabolome, afin d'objectiver le lien éventuel entre la perturbation du métabolome endogène et la modulation des transporteurs.

Ce travail translationnel repose donc sur une étude clinique et une étude expérimentale. Il avait pour but de mieux appréhender le phénomène physiopathologique des lésions d'IR et de mieux comprendre la modulation des transporteurs par l'IRI afin de caractériser son impact clinique et d'anticiper la récupération de la fonction rénale. Nous présupposons que l'altération de la fonctionnalité des transporteurs et les perturbations de l'équilibre des substrats endogènes et exogènes qui en découlent, peuvent participer aux lésions qui surviennent lors de la procédure de transplantation rénale. La protection et/ou la restauration de l'activité des transporteurs pourraient faire partie d'une stratégie de prévention multiple à différents moments, du prélèvement, de la préservation de l'organe jusqu'à la période post-transplantation, afin de réduire l'IRI et ses conséquences.

Chapitre II. **Impact de l'ischémie et de l'hypoxie-réoxygénation sur l'expression et l'activité des transporteurs tubulaires**

II.1. Hypothèses

Notre revue bibliographique a dressé un bilan des connaissances actuelles de la modulation IR-dépendante des transporteurs tubulaires. La majorité des études étaient réalisées sur des modèles précliniques d'ischémie chaude, induite par un clampage artériel d'une durée inférieure à 1h, impliquant une privation en oxygène et en nutriments des tissus. Peu d'études ont été menées sur une cinétique d'ischémie ou sur des temps longs. Par conséquent, nous avons souhaité tester l'hypothèse suivante : la durée d'ischémie initiale impacte non seulement l'expression des transporteurs pendant l'ischémie, mais également le retour à un niveau d'expression (et/ou de fonctionnalité) basale lors de la reperfusion.

Les études répertoriées dans la littérature traitaient principalement des transporteurs de la super-famille SLC dits de « médicaments », bien que les cellules tubulaires proximales expriment à leur surface un grand nombre d'autres transporteurs membranaires, aux rôles prépondérants. Les substrats pris en charge par ces transporteurs sont mono-spécifiques (ex. glucose ; SGLT2 (apical), GLUT2 (basal)), ou multi-spécifiques (ex. acide urique ; OAT1/3 (basal), MRP4, BCRP, URTA1 (apical)). Par conséquent, le transport tubulaire transcellulaire présente une « plasticité » due à une activité compensatrice des transporteurs entre eux. Une observation consolidée par la récente RSST (*Remote Sensing and Signalling Theory*) que l'on pourrait traduire par « théorie de la détection et de la signalisation à distance ». Cette théorie est basée, entre autres, sur la présence de transporteurs multi-spécifiques dans différents organes qui, ensemble, forment un réseau de communication multi-échelle et adaptatif permettant de maintenir, voire de rétablir, l'homéostasie de l'organisme (Figure 3). Les souris Sglt1$^{-/-}$ (KO pour ce transporteur) ont une meilleure récupération de la fonction rénale après clampage de l'artère rénale que les souris sauvages. A l'inverse, c'est la restauration d'OAT1/3 induite par un agent pharmacologique, l'indométacine, qui présentait ce même effet néphroprotecteur. Cela suggère que l'effet des transporteurs sur la reprise de fonction rénale peut être opposé, et pourrait dépendre de la nature de leurs substrats. Nous avons donc ciblé un large spectre de transporteurs, dont des transporteurs impliqués dans la réabsorption tubulaire, notamment dans le transport coordonné des acides aminés (ex. B0AT1 (*SLC6A19*), LAT1 (*SLC7A5*), PEPT2 (*SLC15A2*)), peu étudiés jusqu'à présent.

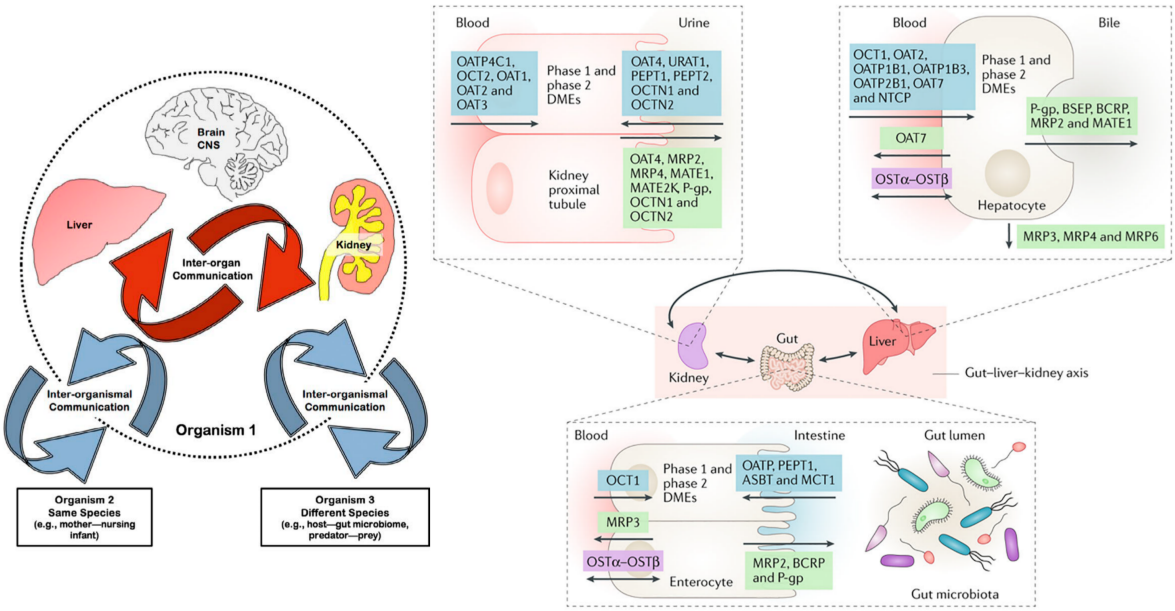

Figure 3 : Illustration de la « théorie de la détection et de la signalisation à distance » (RSST) développée par Nigam et coll.
Figure adaptée des références [68,69]. L'illustration a été réalisée avec BioRender.com.

La modulation fonctionnelle des transporteurs en période post-greffe immédiate pourrait créer un « embouteillage compétitif » entre les substrats. Les toxines urémiques et les xénobiotiques pourraient avoir une action inhibitrice synergique perturbant le mouvement des métabolites endogènes. Cette hypothèse est étayée par des observations récentes selon lesquelles des toxines urémiques peuvent entrer en compétition avec des médicaments couramment utilisés dans la gestion de l'insuffisance rénale chronique[70].

Dans ce travail, nous avons donc testé l'hypothèse d'une relation étroite entre la modulation des systèmes de transport tubulaire et les perturbations du métabolome endogène causées par l'IR, chez l'homme. En effet, les différences entre les espèces en ce qui concerne le métabolisme et la fonction des transporteurs, pourraient limiter l'extrapolation des résultats expérimentaux à la clinique[71,72].

II.2. Impact de l'ischémie sur le contenu métabolique et l'expression des transporteurs de greffons rénaux conservés sur HMP

II.2.1. Résumé

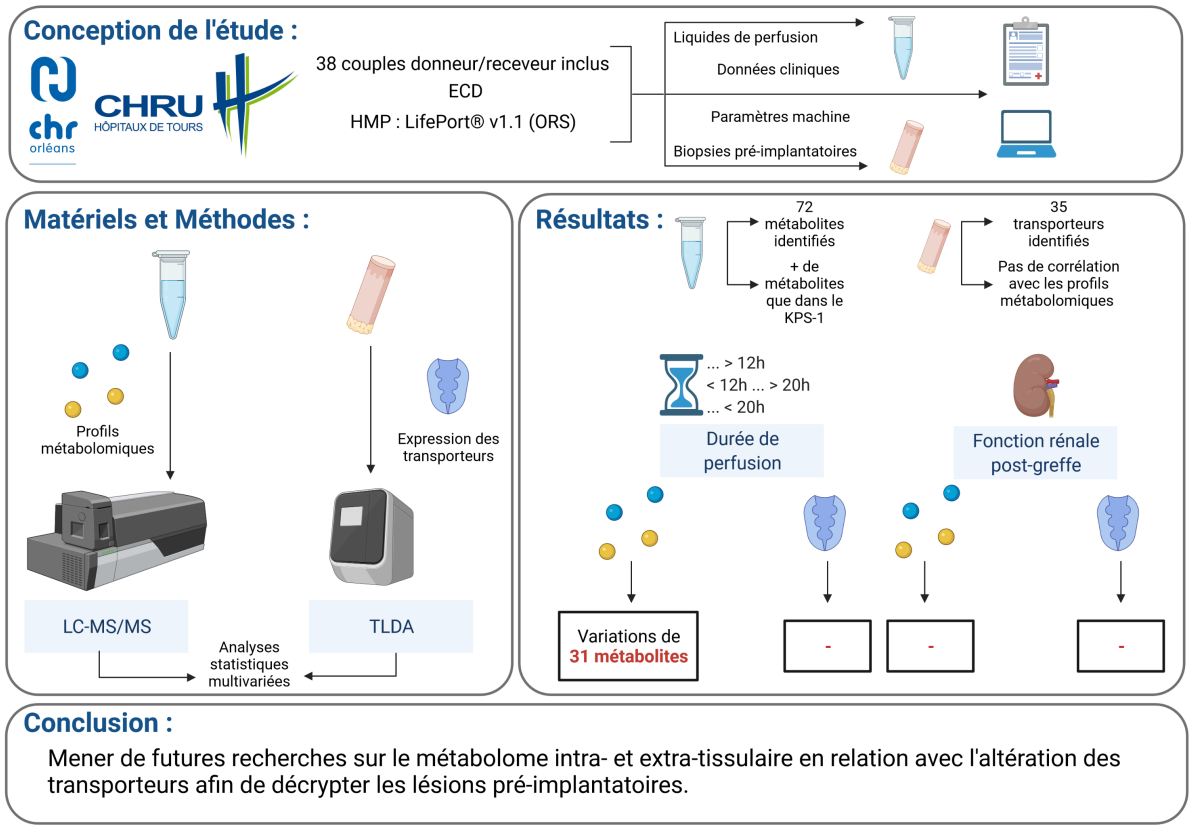

Figure 4 : Résumé graphique de l'article expérimental 1
L'illustration a été réalisée avec BioRender.com. ECD, *extanded criteria donors*; LC-MS/MS, *liquid chromatography-tandem mass spectrometry*; ORS, *Organ Recovery Systems*; TLDA, *Taqman Low-Density Array*.

L'étude clinique RENALIFE était une étude pilote coordonnée par le service d'urologie du CHRU de Tours en association avec le CHR d'Orléans. L'objectif était d'évaluer l'impact des lésions ischémiques subies par des greffons rénaux, issus de ECD et conservés sur HMP, sur la qualité de reprise de la fonction rénale chez les patients receveurs. En 2014, Bon et coll. ont démontré, dans un modèle d'auto-transplantation chez le porc, le potentiel du profilage métabolomique des perfusats de greffon pendant la période pré-implantatoire comme outil de diagnostic rapide des résultats de la greffe[65]. Guy et coll. ont confirmé son potentiel en 2015 sur une cohorte de patients transplantés[66]. Le protocole RENALIFE avait pour objectif de compléter ces études antérieures par (i) l'exploration du métabolome par chromatographie en phase liquide couplée à la spectrométrie de masse en tandem (LC-MS/MS) au lieu de la spectrométrie de résonnance magnétique nucléaire (RMN), (ii) l'exploration de reins humains au lieu de modèles animaux et (iii) l'exploration de l'effet de temps de perfusion plus longs. À l'instar des études citées, nous souhaitions identifier des métabolites dans le milieu de

conservation comme potentiels biomarqueurs non-invasifs et prédictifs de la fonction du greffon. Nous avons également évalué l'expression transcriptionnelle des transporteurs tubulaires sur les biopsies pré-implantatoires collectées juste en amont de la procédure chirurgicale. Notre hypothèse initiale était la suivante : certains métabolites discriminants vis-à-vis de la durée de perfusion ou du devenir du greffon, identifiés dans les liquides de perfusion, sont substrats de transporteurs tubulaires et pourraient témoigner de leur perte d'activité. En d'autres termes, la perte de fonction des transporteurs constituerait un phénomène explicatif (au moins partiel) des variations métaboliques observées. De plus, nous avons testé le caractère prédictif de l'expression des transporteurs tubulaires sur la fonction rénale post-greffe. Les critères d'inclusion et d'exclusion ainsi que les différents prélèvements réalisés et les données cliniques recueillies dans le cadre de cette étude sont synthétisés en Figure 5.

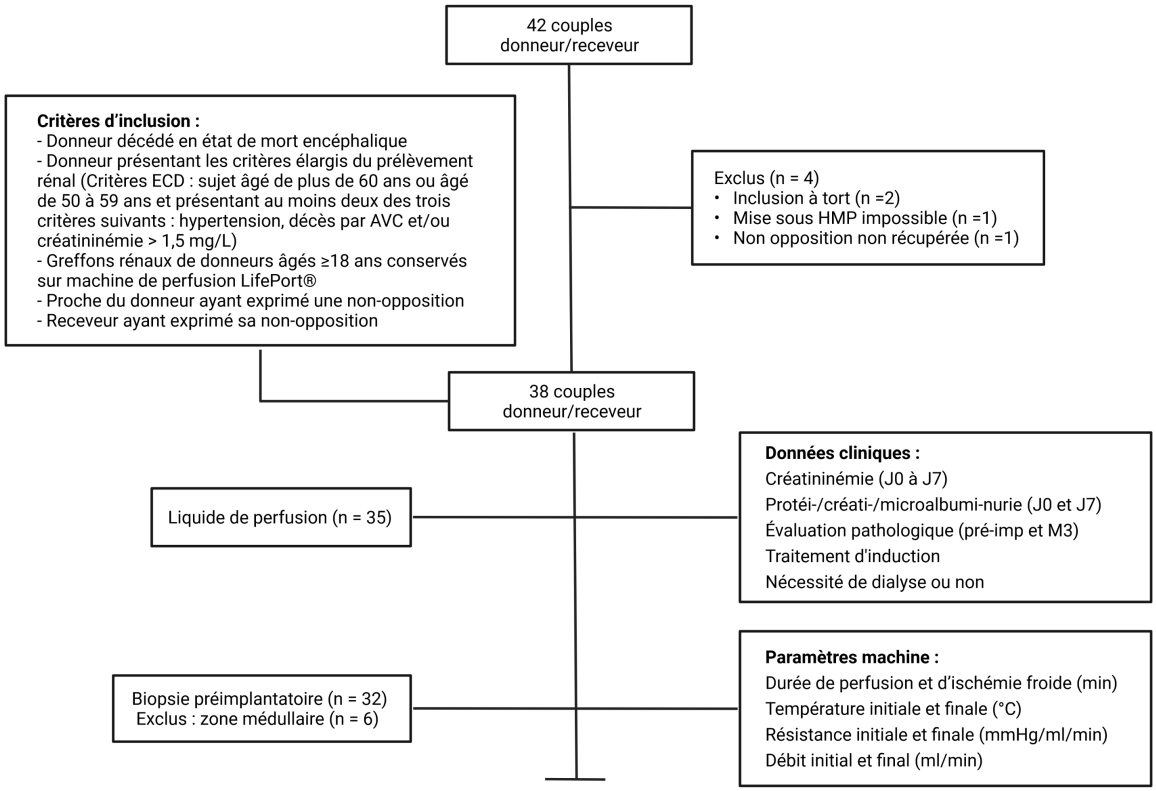

Figure 5 : Diagramme de flux de l'essai clinique RENALIFE
L'illustration a été réalisée avec BioRender.com.

Nous avons identifié 31 métabolites dont la quantité variait en fonction de la durée de perfusion. Certains d'entre eux n'avaient encore jamais été détectés dans ce contexte. Cependant, les signatures métabolomiques et l'expression des transporteurs tubulaires, évaluée pour la première fois dans ce contexte, ne montraient pas de lien statistique avec la fonction rénale post-greffe. De plus, les variations métabolomiques observées en fonction du

temps de perfusion n'étaient pas corrélées avec l'expression des transporteurs. Nous proposons la conduite de nouvelles études cliniques ou translationnelles évaluant en plus les perturbations métaboliques dans le tissu rénal, afin d'étudier ces relations avec plus de précision.

II.2.2. Article expérimental 1 : Perfusate metabolomics content and tubular transporters expression during kidney graft preservation by hypothermic machine perfusion

Les *Supplementary Data* de l'article expérimental 1 sont disponibles en Annexe 3.

Perfusate metabolomics content and tubular transporters expression during kidney graft preservation by hypothermic machine perfusion

Quentin Faucher[1*], Hugo Alarcan[1,2*], François-Ludovic Sauvage[1], Lionel Forestier[3], Elodie Miquelestorena-Standley[4,5], Lydie Nadal-Desbarats[6], Hélène Arnion[1], Jean-Christophe Venhard[7], Nicolas Brichart[8], Franck Bruyère[9], Pierre Marquet[1,10], and Chantal Barin-Le Guellec[1,2#]

#corresponding author.

***These authors contributed equally.**

Affiliations:

1: IPPRITT UMR1248, Université de Limoges, INSERM, Limoges, France
2: Service de biochimie et biologie moléculaire, CHRU de Tours, Tours, France
3: BISCEm, US 042 INSERM-UMS 2015 CNRS, Université de Limoges, Limoges, France.
4: Service d'anatomie et cytologie pathologiques, Hôpital Trousseau, CHRU Tours, Tours, France
5: EA4245, Transplantation, Immunologie, Inflammation, Université de Tours, 37000 Tours, France
6: UMR 1253, iBrain, Université de Tours, INSERM, 37000 Tours, France
7 : Coordination hospitalière des prélèvements d'organes et de tissus, CHRU de Tours, Tours, France
8: Service de chirurgie urologique, CHR Orléans, Orléans, France
9: Service d'urologie, hôpital Bretonneau, CHRU Tours, Tours, France
10: Service de pharmacologie, toxicologie et pharmacovigilance, CHRU Limoges, Limoges, France

Correspondance information:
Chantal Barin-Le Guellec
Service de Biochimie et Biologie Moléculaire, CHU Bretonneau, 2 boulevard Tonnellé 37044 Tours, France
chantal.barin-leguellec@univ-tours.fr

Clinical Trial Notation: Metabolomics in assessing the quality of kidney transplants retained on a Lifeport® Perfusion Machine (RENALIFE), ClinicalTrials.gov NCT03024229

AUTHORSHIP PAGE

Q.F.: Participated in research design, data collection, analysis and interpretation, and the writing of the article. **H.A.:** Participated in research design, data collection, analysis and interpretation, and the writing of the article. **F.L.S.:** Participated in data analysis, and the writing of the article. **L.F.:** Participated in data analysis, and article review. **E.M.S.:** Participated in data collection and article review. **L.N.:** Participated in data analysis and article review. **H.A(2):** Participated in data analysis, and article review. **J.C.V.**: Participated in research design and data collection. **N.B.:** Participated in research design and data collection. **F.B.:** Participated in research design and data collection. **P.M.:** Participated in research design, data analysis and interpretation, and article review. **C.B.L.G.:** Participated in research design, data collection, analysis and interpretation, and the writing of the article.

Disclosure: The authors have no conflicts of interest to declare.

Funding: funding for this research was provided by Organ Recovery System.

ABBREVIATIONS PAGE

ABC, ATP-binding cassette. CIM, clustered image maps. DGF, delayed graft function. ECD, expanded criteria donors. FC, fold change. FDR, false discovery rate. HMP, hypothermic machine perfusion. IGF, immediate graft function. IRI, ischemia-reperfusion injury. LC-MS/MS, liquid chromatography/tandem mass spectrometry. NMR, nuclear magnetic resonance. PCA, principal component analysis. PLS, partial least squares. PLS-DA, partial least squares discriminant analysis. RF, random forest. RIN, RNA integrity number. SCS, static cold storage. SLC, solute carrier

Abstract

Background: Ischemia-related injury during the pre-implantation period impacts kidney graft outcome. Evaluating these lesions by a non-invasive approach before transplantation could help to understand the mechanisms of graft injury and identify potential biomarkers predictive of graft outcomes. This study aims to determine metabolomic content of graft perfusion fluids and its dependence on preservation time and to explore whether tubular transporters are possibly involved in the metabolomics variations observed.

Methods: Kidneys were stored on hypothermic perfusion machines. We evaluated the metabolomic profiles of perfusion fluids (n=35) using Liquid Chromatography coupled with tandem Mass Spectrometry and studied the transcriptional expression of tubular transporters on pre-implantation biopsies (n=26). We used univariate and multivariate analyses to assess the impact of perfusion time on these parameters and their relationship with graft outcome.

Results: Seventy-two metabolites were found in preservation fluids at the end of perfusion, of which 40% were already present in the native conservation solution. We observed an increase of 23 metabolites with longer perfusion time and a decrease for 8. The predictive model for time-dependent variation of metabolomics content showed good performance (R^2= 76%, Q^2= 54%, accuracy= 41%, permutations test significant). Perfusion time had no effect on the mRNA expression of transporters. We found no correlation between metabolomics and transporters expression. Neither the metabolomics profile nor the transporters expression were predictive of graft outcome.

Conclusion: Our results open the way for further studies, focusing on both intra- and extra-tissue metabolome, to investigate whether transporter alterations can explain the variations observed in pre-implantation period.

KEYWORDS: hypothermic machine perfusion, metabolomic, renal transplantation, tubular membrane transporters, PLS-DA

Introduction

Kidney transplantation is the treatment of choice for patients suffering from end-stage renal diseases. According to the World Health Organization, the death rate from kidney diseases will continue to increase to reach 27 deaths per 100 000 people by 2060[1], while the use of renal replacement therapy (i.e. dialysis or kidney transplantation) worldwide will reach ±5 million people by 2030[2]. With regard to this increase of renal diseases, the gap between the demand for organs and the limited group of donors will continue to widen. To overcome this issue, many centers are gradually accepting sub-optimal donors, including donation after circulatory death and Extended Criteria Donors (ECD). However, kidneys retrieved from such donors are more prone to Ischemia-Reperfusion Injury (IRI) and Delayed Graft Function (DGF) in the post-transplant period[3]. IRI is a multifactorial pathophysiological process incumbent to the transplantation procedure and a major cause of DGF, which in turn increases the risk of short- and long-term poor graft outcomes[4–7]. For these sub-optimal donors, Hypothermic Machine Perfusion (HMP), an *ex vivo* circulating, hypoxic environment, is recommended for kidney preservation, as compared to static cold storage (SCS), in order to reduce DGF rates and improve graft survival[8]. However, reliable tools are needed for the evaluation of graft quality during HMP preservation. Metabolomic analysis of the perfusion fluid provides the possibility to reveal potential biomarkers of graft quality or predictive of transplantation outcomes, but also to inform about the cellular mechanisms occurring during organ perfusion[9]. The few studies previously conducted on this topic showed a variation of the metabolomic content according to the perfusion time: mainly an increase of lactate and amino-acids and a decrease of glutathione[10–12]. These variations suggest metabolites are uptaken or released by the kidney during its preservation. Renal tubular membrane transporters (mainly of the SoLute Carrier (SLC) and ATP Binding-Cassette (ABC) families) play

a major role in cell and tissue homeostasis owing to the bidirectional, transcellular exchanges they are involved in. Alteration of their activity, previously demonstrated (mainly for SLC) during ischemia or ischemia/reperfusion[13,14], could be responsible for some metabolic variations observed during organ perfusion, but also have deleterious consequences for the graft outcomes[15]. Concerning the predictive value of the perfusion fluid metabolomic content, controversial results have been found and a recent review suggests that further studies are needed[16].

The objectives of the present clinical study were to determine the metabolomic contents of perfusion fluids collected at the end of kidney graft perfusion on HMP and the transcriptional expression of renal tubular transporters on graft biopsies taken at the same time. We aimed to explore the relationships between ischemia duration, *ex situ* metabolites, transporters expression and graft outcome. To the best of our knowledge, this is the first evaluation of the potential impact of membrane transporter alterations on the variations of the perfusion fluid metabolomic contents observed during graft preservation by HMP.

Materials and Methods

A more detailed description of the materials and methods is available in the Supplementary Digital Content (SCD, "Material and Methods")

As part of the clinical research project "RENALIFE" (ClinicalTrials.gov NCT03024229), 38 kidneys taken from ECD were included. Organs were stored on HMP LifePort® Kidney Transporter 1.0 (Organ Recovery Systems) with KPS-1® (Organ Recovery System) as preservation solution. HMP parameters (temperature, flow, resistance) were recorded during kidney conservation and a perfusate sample was collected at the end of perfusion (storage at -20°C after centrifugation: 3000g, 10min). Preimplantation biopsy (targeting the renal cortex)

was performed and split in two, with one fragment embedded in paraffin after fixation for anatomopathological evaluation and the other stored at -20°C. Serum creatinine and clinical events were recorded up to 7 days and 3 months respectively. Immediate Graft Function (IGF) was characterized by a serum creatinine ≤ 250 µmol/L on day 7 without the need for dialysis and Delayed Graft Function (DGF) by the necessity of dialysis within the first 7 days. Mass spectrometry chromatographic analysis was performed using a LCMS-8060 tandem mass spectrometer (Shimadzu) and the package "Method Package for Cell Culture Profiling Ver.2" (Shimadzu). Infusion of pure substances was performed to add some molecules to the package. Perfusates were analyzed in duplicate and native KPS-1 was injected to determine its basal composition. A COBAS 6000 analyzer (Roche Diagnostics) was used to determine sodium, potassium, calcium, phosphate, chloride, bicarbonate, urea, creatinine, and glucose concentrations and add them to the previous metabolites.

Graft RNA was extracted from frozen pre-implantation biopsies. After quantification and integrity evaluation, retro-transcription was performed. Taqman Low Density Array (TLDA) cards were used to determine the transcriptional expression of 35 membrane tubular transporters , 3 aquaporins, 2 Na/K-ATPase sub-units (Supplementary table 1 for probe sets) and 4 housekeeping gene candidates (*NME4, CHFR, C16ORF62* and *NASP*) chosen according to the literature[17]. Undetermined or > 35 Ct values were replaced by 35. Transporters expression was analyzed by the comparative $2^{-\Delta Ct}$ method with ΔCt = Ct (target gene) – Ct (mean of the housekeeping genes finally retained)[18]. Then $2^{-\Delta Ct}$ were normalized by log2 transformation. Three housekeeping genes (*NME4*, *CHFR* and *C16ORF62*) were finally selected using Genorm[19] and Normfinder[20].

To explore the impact of ischemia duration on the perfusate metabolomics contents and tubular transporters expression, grafts were allocated to 3 different perfusion duration groups: < 12h, between 12 and 20h, and > 20h.

Statistical analysis involved univariate followed by multivariate analysis (Principal Component Analysis (PCA) , Partial Least Squares discriminant analysis (PLS-DA), Partial Least Squares (PLS), Random Forest (RF), in accordance with standard approaches for metabolomic analyzes[21]). The MetaboAnalyst 5.0 computational platform (www.metaboanalyst.ca/faces/home.xhtml) was used for all the analyses except for PLS which was performed using the MixOmics package (version 1.6.3) in R (version 4.0.2).

Results

1. Study population

Thirty-eight donor-recipients couples were included (Table 1). All donors were brain dead and ECD. The median perfusion and cold ischemia time was 831.5 and 1020 min, respectively.

2. Perfusate metabolomic content and transcriptional expression of tubular transporters

2.1. *Metabolomic content of graft perfusion fluid*

In the 35 perfusion liquids available, 72 different metabolites were identified, 66 with LC-MS/MS (Supplementary Table 2) and 6 with COBAS analyzer. All of them were present in each sample, with a few exceptions (Table 2). Twenty-nine of them were already present in the native KPS-1. At the end of perfusion, 6 were increased (inosine, guanosine, xanthosine, 5-methyl adenosine, tryptophan and riboflavin) and 10 were decreased (gluconic acid, methionine sulfoxide, glucosamine, oxidized glutathione, adenine, 2-Ketoisovaleric acid, 3-Methyl-2-oxovaleric acid, D-gluconic acid sodium salt, D-Ribose and deoxycytidine

monophosphate) as compared to native KPS-1. Forty-three metabolites were exclusively found in the graft perfusates. These metabolites belong mainly to the amino-acids metabolism pathways (Supplementary Figure S1).

2.2. Transcriptional expression of tubular transporters in pre-implantation biopsies

Thirty-four biopsies were available for RNA extraction. Eight were excluded: 2 because of RNA yield and 6 because they contained renal medulla. The mean RIN value for the 26 biopsies retained was 5.4 +/- 2.4. All the transporters of interest were identified in these biopsies. We found high expression correlations between them (Supplementary Figure S2).

3. Impact of perfusion duration on metabolomic profiles and transporter expression

3.1. *Metabolomics variations according to perfusion duration*

Univariate analysis showed that 31 features were significantly (FDR<0.05) different between the perfusion duration groups (Figure 1). Twenty-three metabolites increased with longer perfusion durations (*e.g.* lactate or leucine) but 8 decreased (*e.g.* glutathione or inosine). PCA unsupervised analysis showed good separation of the scores between the two extreme groups (<12 h and >20 h), whereas group 2 overlapped with the others. Fifty-two percent of the variation was explained by the first and second components (Figure 2A). Similarly, the PLS-DA score plot (first two components) showed complete separation between groups 1 and 3, but overlap with group 2 (Figure 2B). Cross-validation showed good performances: goodness-of-fit (R^2) = 76%, predictive cumulative variation (Q^2) = 54% and accuracy = 41%. The model was significant according to the permutation test ($p<0.05$), supporting the absence of overfitting. The most important metabolites for the model are shown in Figure 2C. Significant pathways based on the important metabolites (VIP value > 0.8) are listed in Supplementary Figure S3.

3.2. Transporter expression according to perfusion duration

The transcriptional expression of transporters according to the perfusion duration was not significantly different in univariate analysis. The PLS-DA model performance was: R^2 = 34%, negative Q^2 and accuracy = 30%, and the permutation test was not significant (Figure 3).

4. Correlation between transporters expression and metabolomic content

Correlation between transporters expression and metabolomic content was investigated by PLS regression. The Clustered Image Maps (CIM) of the model is displayed in Figure 4. It does not show patterns of correlation between metabolites and transporters. The maximal positive and negative correlations were weak: 0.54 and -0.54, respectively.

5. Predictive biomarkers of graft outcome

Considering the low rate of patients with DGF (13.2%, n=5), we enhanced the statistical power of graft recovery analysis by comparing patients with and without IGF (serum creatinine > 250 µM on Day7, with or without dialysis). No significant differences were found between IGF (n=29) and non-IGF (n=9) recipients regarding the clinical parameters (*e.g.* age, sex, induction therapy), machine parameters recorded (temperature, resistive index, flow rate), cold ischemia time or biopsy pathological evaluation (Table 1).

5.1. *Metabolomics in assessing the quality of kidney grafts*

Univariate analysis showed that 4-hydroxyproline (Fold Change (FC): 0.31, raw p-value: 0.13) and alanine (FC: 0.73, raw p-value: 0.15) tended to be lower in perfusion fluids of non-IGF patients (Figure 5A). PLS-DA allowed visual separation between IGF and non-IGF on the scoreplot of the first two components (Figure 5B), with correct accuracy (69 %) and R^2 (36%), but negative Q^2. The permutation test was not significant. Random forest analysis, a tree-

based machine-learning algorithm adapted to small size datasets, was used to find a better model. The out-of bag error (samples wrongly predicted) was 23% for the overall dataset, but 100% of non-IGF samples were predicted as IGF, showing that the model was unable to predict graft recovery (Figure 5C).

5.2. *Transcriptomic extraction of transporters according to graft quality*

Univariate analysis did not identify any transporter able to discriminate between IGF and non-IGF (data not shown). Similarly, PLS-DA failed to predict graft recovery in our cohort, as evidenced by an overlap between the two groups (Figure 6A): the yielded R^2=26% and accuracy = 69%, with a negative Q^2. The permutation test was not significant. Random forest analysis showed poor prediction of non-IGF patients: 5 of the 6 non-IGF cases were misclassified as IGF (Figure 6B).

Discussion

This clinical study aimed to better characterize the metabolic variations occurring during organ preservation on HMP through metabolic profiling of the fluid collected at the end of perfusion. We observed marked modifications of the metabolomic content, with regard to the native preservation fluid (KPS-1®), but also as a function of perfusion duration, which is a surrogate of the cold ischemia time duration. We also investigated the transcriptional expression of tubular transporters to explore if variations in their activity could be linked with metabolic variations seen during machine perfusion. However, we did not observe any particular pattern between the expression of any transporter and the metabolic profiles or perfusion duration. Finally, we evaluated the predictive ability of perfusate metabolites and tubular transporters mRNA expression as potential biomarkers of graft function by comparing IGF and non-IGF patients and found none.

Maintained metabolic activity of grafts stored on perfusion machine

We determined the relative concentrations of 72 metabolites, some of which, to our knowledge, had never been studied in this context. We observed a marked difference in metabolomic profiles between the perfusate collected at the end of perfusion and the native fluid KPS-1 (Table 2). We found 29 metabolites in KPS-1, which is more than its theoretical composition. Among these, some showed decreased quantities at the end of perfusion, suggesting they were reabsorbed or consumed by the kidney, while others increased (Table 2). The 43 other metabolites, mainly amino-acids (Supplementary Figure 1), were exclusively detected in the fluid at the end of perfusion. Metabolites that appeared, or increased from basal value, were released by the graft, which can be related to sustained metabolic activity, ischemic damages, or both.

Modifications occur during preservation on HMP

Understanding ischemic phenomena occurring during graft preservation remains a leading issue in renal transplantation for the improvement of graft management. However, our understanding of the metabolic activity occurring during kidney preservation on HMP is still partial. Only a few studies have analyzed kidney graft *in situ* or perfusate metabolomics[10–12,22]. They aimed to identify early predictive biomarkers of graft function and investigate the underlying mechanisms. Our work attempted to consolidate and complement previous studies by: (i) the use of LC-MS/MS instead of NMR[10–12]; (ii) the exploration of human kidneys instead of pig[10] or rabbit models[22]; and (iii) the exploration of longer perfusion times[11,12]. Among the 72 metabolites analyzed, the concentration of 8 them significantly decreased when the perfusion time increased (Figure 1), including glutathione and oxidized glutathione. This decrease had already been described by ^{1}H-NMR analyses of perfusates in both humans

and pig[10–12]. Glutathione is involved in free radicals scavenging and its decrease sensitizes the graft to IRI. We also found an increased level of lactic acid, choline and some amino-acids (*e.g.* valine, alanine, glycine and glutamic acid) as a result of longer perfusion. These observations are consistent with previous results obtained by Bon *et al.*, who reported an increase in concentrations of these metabolites in porcine kidney perfusates between 2h and 22h perfusion[10]. Increased lactic acid simply reflects anaerobic glycolysis occurring in a hypoxic environment and increased amino-acids may reflect intracellular release. Most of our findings are consistent with those previously published, except for some. For example, the level of glucose and inosine increased with perfusion time in the study by Guy *et al.*, whereas it was unchanged and decreased in ours. However, these authors explored two early time points: 45 min vs. 4 hours, while the first quartile of our perfusion duration was already about 10 hours. The usefulness of following the kinetics of metabolites has been demonstrated recently, using solid phase microextraction and LC/MS for *in situ* kidney metabolomics analysis at five sequential time points in a rabbit model: immediately following removal of the donor's kidneys and after 2, 4, 6 and 21 hours of SCS[22]. The authors found that metabolites related to various metabolic pathways, including amino-acids and purine metabolism, significantly increased during the first hours of kidney preservation, whereas a decrease occurred with longer perfusion durations. However, their methodology (*in situ*, limited number of samples, SCS conservation) hampers the direct comparison with our results. Nevertheless, we also observed at the extra-tissue level that the amounts of some intermediates of purine metabolism such as adenine, inosine and guanosine decreased, while that of xanthine increased, with perfusion time. The results observed here most likely illustrate that kidneys with longer ischemia consume more adenine and inosine and produce more xanthine in response to ATP deprivation. To the best of our knowledge, other metabolites (*e.g.* taurine,

niacinamide or glucosamine) and their association with perfusion duration had never been studied in this context.

Weak correlation between metabolites in the perfusate and tubular transporters

The metabolomic signatures observed over perfusion time reflect sustained metabolic activities by kidneys stored on HMP, but the underlying mechanisms are currently poorly understood. Some metabolites are physiologically reabsorbed or secreted through specific membrane tubular transporters[15]. Their sensitivities to ischemia[15,23] and potentially altered activity could explain a part of the *ex situ* metabolomic variations observed. A decrease at the mRNA and protein levels of *SLC22A6* (OAT1) and *SLC22A8* (OAT3), involved in the uptake of organic anions, was observed after 30 minutes of ischemia in the rat[13] and similar results were found for *SLC22A1* (OCT1) and *SLC22A2* (OCT2), involved in organic cation uptake, also in a rat model[14]. Considering the limited quantity and quality of RNA we chose a TLDA approach for transcriptional expression determination, since it only requires small quantities of RNA and is able to amplify small cDNA fragments. We successfully determined the transcriptional expression of all targeted genes. However, no association was observed between transporter expression and perfusion duration (Figure 3). Previous works suggest that the downregulation of membrane transporters occurs since only after 30 min of warm ischemia[23]. In our study, some transporter alterations may have occurred before the biopsy, which was done after the warm ischemia period and after at least 176 min of perfusion. We might have confirmed this hypothesis with non-ischemic biopsy controls, but we could not obtain any. It is also possible that some transporters are not affected by ischemia during preservation by HMP.

We did not find any particular correlation with the metabolomic profile in the perfusion fluid, even for well-known transporter/substrate couples (*e.g.,* SGLT2/glucose or OAT1/PAH) and

amino-acid transport systems (Figure 4). In HMP, the perfusion fluid irrigates both the basolateral and apical poles of the tubule, whereas the function of transporters and thus the identification of variations reflecting their activity is highly dependent on a polarized environment. Moreover, the transcriptional expression of transporters alone cannot perfectly reflect their real activity, but we could not evaluate their protein expression (because of too low amounts of proteins) or cellular localization (due to histological fixation). Globally, these results call for further studies, evaluating both the intra- and extra-tissue metabolome in relation to the expression, localization and functions of transporters (e.g. based on transporter-specific labeled substrates) as a function of ischemia time, to uncover potential relationships between transporters and metabolites during kidney graft perfusion. However, it is worth mentioning that such studies may still be confounded by injury-induced cellular release of metabolites.

Metabolomic signatures and expression of tubular transporters do not predict IGF

The present study also aimed to identify non-invasive biomarkers predictive of graft outcomes that could be measured in the pre-implantation period. Actually, reliable biomarkers would be instrumental to optimize patient management and graft outcome. Assessment of graft quality in the transplantation period is currently based on perfusion parameters such as the restrictive index or the flow rate, and pathological evaluation of a preimplantation biopsy. However, these indicators are not sufficiently reliable to safely discard a graft. Accordingly, in our study, no indicators predicted post-transplant graft function (data not shown). Rapid determination of the perfusate metabolomic profile in the preimplantation period would be convenient and adapted to clinical routine. The proof of concept was brought by Bon *et al.* in a porcine renal auto-transplantation model where valine, alanine, glutathione and glutamate

concentrations in the perfusion fluid were correlated with serum creatinine at 3 months[10]. Guy *et al.* also found in a human cohort that glucose and inosine concentrations were lower in the perfusate of DGF kidneys, while leucine was higher[11]. In our study, we did not identify any metabolite or multivariate model predictive of graft recovery (Figure 5). We did not replicate previous results, maybe due to the differences of perfusion durations explored and given that in the study by Guy *et al.*, cadaveric kidneys arrived at their unit on SCS before being transferred to HMP, whereas in our study the kidneys retrieved from each donor were put directly on HMP. Moreover, the metabolites identified previously were not the same between the two studies.

The relative heterogeneity and the small size of our cohort probably limited the predictive ability of the metabolome. Also, the low DGF rate (13.2%) of ECD donors' kidneys preserved with the LifePort® Kidney Transporter in our cohort (as compared with a DGF rate of 30 % for SCS in France in 2017[24]) supported the utility of HMP for such donors, but limited the statistical power of our study. However, our negative result is in line with a recent systematic review that highlighted the lack of accuracy and hindsight of metabolomics in human kidney graft perfusates[16]. The evaluation of perfusate metabolomics variations might still be relevant[25], since it recently suggested a higher *de novo* metabolic activity of kidneys preserved on machine versus SCS[26], or it could highlight the metabolic variations occurring with oxygen supplementation[27,28] or pharmacological agents[29,30].

Finally, we aimed to determine if the expression of tubular transporters in our cohort could predict early post-transplant graft outcomes. To the best of our knowledge, no study has yet been conducted in this regard. Our results do not support evaluating transporters

transcriptional expression at the end of kidney graft HMP, with the aim of predicting graft function.

Conclusion

In summary, we did not find any predictive biomarkers of graft function in the perfusate metabolome or among tubular transporter mRNAs of human kidneys stored on HMP. However, we observed marked differences between the metabolomics profiles collected at the end of perfusion and the perfusion liquid initial composition, which reflects persistence of a metabolic activity during HMP. Moreover, the concentration of many metabolites was modified after the longer perfusions, mostly in agreement with the literature but also for some metabolites that have never been studied in this context so far. The transcriptional expression of 40 membrane transporters determined at the same time was not correlated with the variations of these metabolites or with perfusion time. We suggest conducting further translational studies, to evaluate the ratio of tissue-to-perfusion fluid concentrations of metabolites as well as tubular transporter activity to decipher the deleterious mechanisms associated with ischemia in the pre-implantation period.

Bibliography

1. World Health Organization. Projections of mortality and causes of death, 2016 to 2060. Accessed May 13, 2021. https://www.who.int/healthinfo/global_burden_disease/projections/en/

2. Liyanage T, Ninomiya T, Jha V, et al. Worldwide access to treatment for end-stage kidney disease: a systematic review. *The Lancet*. 2015;385(9981):1975-1982. doi:10.1016/S0140-6736(14)61601-9

3. Wong G, Teixeira-Pinto A, Chapman JR, et al. The Impact of Total Ischemic Time, Donor Age and the Pathway of Donor Death on Graft Outcomes After Deceased Donor Kidney Transplantation. *Transplantation*. 2017;101(6):1152-1158. doi:10.1097/TP.0000000000001351

4. Chen C-C, Chapman WC, Hanto DW. Ischemia-reperfusion injury in kidney transplantation. *Front Biosci (Elite Ed)*. 2015;7:117-134.

5. Gill J, Dong J, Rose C, Gill JS. The risk of allograft failure and the survival benefit of kidney transplantation are complicated by delayed graft function. *Kidney Int*. 2016;89(6):1331-1336. doi:10.1016/j.kint.2016.01.028

6. Nieuwenhuijs-Moeke GJ, Pischke SE, Berger SP, et al. Ischemia and Reperfusion Injury in Kidney Transplantation: Relevant Mechanisms in Injury and Repair. *Journal of Clinical Medicine*. 2020;9(1):253. doi:10.3390/jcm9010253

7. Salvadori M, Rosso G, Bertoni E. Update on ischemia-reperfusion injury in kidney transplantation: Pathogenesis and treatment. *World J Transplant*. 2015;5(2):52-67. doi:10.5500/wjt.v5.i2.52

8. Peng P, Ding Z, He Y, Zhang J, Wang X, Yang Z. Hypothermic Machine Perfusion Versus Static Cold Storage in Deceased Donor Kidney Transplantation: A Systematic Review and Meta-Analysis of Randomized Controlled Trials. *Artif Organs*. 2019;43(5):478-489. doi:10.1111/aor.13364

9. Barin-Le Guellec C, Largeau B, Bon D, Marquet P, Hauet T. Ischemia/reperfusion-associated tubular cells injury in renal transplantation: Can metabolomics inform about mechanisms and help identify new therapeutic targets? *Pharmacol Res*. 2018;129:34-43. doi:10.1016/j.phrs.2017.12.032

10. Bon D, Billault C, Claire B, et al. Analysis of perfusates during hypothermic machine perfusion by NMR spectroscopy: a potential tool for predicting kidney graft outcome. *Transplantation*. 2014;97(8):810-816. doi:10.1097/TP.0000000000000046

11. Guy AJ, Nath J, Cobbold M, et al. Metabolomic analysis of perfusate during hypothermic machine perfusion of human cadaveric kidneys. *Transplantation*. 2015;99(4):754-759. doi:10.1097/TP.0000000000000398

12. Nath J, Guy A, Smith TB, et al. Metabolomic Perfusate Analysis during Kidney Machine Perfusion: The Pig Provides an Appropriate Model for Human Studies. *PLoS One*. 2014;9(12). doi:10.1371/journal.pone.0114818

13. Matsuzaki T, Watanabe H, Yoshitome K, et al. Downregulation of organic anion transporters in rat kidney under ischemia/reperfusion-induced acute [corrected] renal failure. *Kidney Int*. 2007;71(6):539-547. doi:10.1038/sj.ki.5002104

14. Matsuzaki T, Morisaki T, Sugimoto W, et al. Altered pharmacokinetics of cationic drugs caused by down-regulation of renal rat organic cation transporter 2 (Slc22a2) and rat multidrug and toxin extrusion 1 (Slc47a1) in ischemia/reperfusion-induced acute kidney injury. *Drug Metab Dispos*. 2008;36(4):649-654. doi:10.1124/dmd.107.019869

15. Faucher Q, Alarcan H, Marquet P, Barin-Le Guellec C. Effects of Ischemia-Reperfusion on Tubular Cell Membrane Transporters and Consequences in Kidney Transplantation. *J Clin Med*. 2020;9(8). doi:10.3390/jcm9082610

16. Guzzi F, Knight SR, Ploeg RJ, Hunter JP. A systematic review to identify whether perfusate biomarkers produced during hypothermic machine perfusion can predict graft outcomes in kidney transplantation. *Transplant International*. 2020;33(6):590-602. doi:https://doi.org/10.1111/tri.13593

17. Wang Z, Lyu Z, Pan L, Zeng G, Randhawa P. Defining housekeeping genes suitable for RNA-seq analysis of the human allograft kidney biopsy tissue. *BMC Med Genomics*. 2019;12(1):86. doi:10.1186/s12920-019-0538-z

18. Schmittgen TD, Livak KJ. Analyzing real-time PCR data by the comparative C(T) method. *Nat Protoc*. 2008;3(6):1101-1108. doi:10.1038/nprot.2008.73

19. Vandesompele J, De Preter K, Pattyn F, et al. Accurate normalization of real-time quantitative RT-PCR data by geometric averaging of multiple internal control genes. *Genome Biol*. 2002;3(7):RESEARCH0034. doi:10.1186/gb-2002-3-7-research0034

20. Andersen CL, Jensen JL, Ørntoft TF. Normalization of real-time quantitative reverse transcription-PCR data: a model-based variance estimation approach to identify genes suited for normalization, applied to bladder and colon cancer data sets. *Cancer Res*. 2004;64(15):5245-5250. doi:10.1158/0008-5472.CAN-04-0496

21. Chong J, Wishart DS, Xia J. Using MetaboAnalyst 4.0 for Comprehensive and Integrative Metabolomics Data Analysis. *Curr Protoc Bioinformatics*. 2019;68(1):e86. doi:10.1002/cpbi.86

22. Stryjak I, Warmuzińska N, Bogusiewicz J, Łuczykowski K, Bojko B. Monitoring of the influence of long-term oxidative stress and ischemia on the condition of kidney using solid phase microextraction chemical biopsy coupled with liquid chromatography high resolution mass spectrometry. *J Sep Sci*. Published online February 18, 2020. doi:10.1002/jssc.202000032

23. Kwon O, Wang W-W, Miller S. Renal organic anion transporter 1 is maldistributed and diminishes in proximal tubule cells but increases in vasculature after ischemia and reperfusion. *Am J Physiol Renal Physiol*. 2008;295(6):F1807-1816. doi:10.1152/ajprenal.90409.2008

24. Agence de la biomédecine - Le rapport annuel médical et scientifique 2017. Accessed October 15, 2019. https://www.agence-biomedecine.fr/annexes/bilan2017/accueil.htm

25. Kvietkauskas M, Zitkute V, Leber B, Strupas K, Stiegler P, Schemmer P. The Role of Metabolomics in Current Concepts of Organ Preservation. *International Journal of Molecular Sciences*. 2020;21(18):6607. doi:10.3390/ijms21186607

26. Nath J, Smith TB, Patel K, et al. Metabolic differences between cold stored and machine perfused porcine kidneys: A 1H NMR based study. *Cryobiology*. 2017;74:115-120. doi:10.1016/j.cryobiol.2016.11.006

27. Darius T, Vergauwen M, Smith TB, et al. Influence of Different Partial Pressures of Oxygen During Continuous Hypothermic Machine Perfusion in a Pig Kidney Ischemia-reperfusion Autotransplant Model. *Transplantation*. 2020;104(4):731-743. doi:10.1097/TP.0000000000003051

28. Patel K, Smith TB, Neil DAH, et al. The Effects of Oxygenation on Ex Vivo Kidneys Undergoing Hypothermic Machine Perfusion. *Transplantation*. 2019;103(2):314-322. doi:10.1097/TP.0000000000002542

29. Hosgood SA, Hoff M, Nicholson ML. Treatment of transplant kidneys during machine perfusion. *Transpl Int*. 2021;34(2):224-232. doi:10.1111/tri.13751

30. Franzin R, Stasi A, Fiorentino M, et al. Renal Delivery of Pharmacologic Agents During Machine Perfusion to Prevent Ischaemia-Reperfusion Injury: From Murine Model to Clinical Trials. *Front Immunol*. 2021;12. doi:10.3389/fimmu.2021.673562

Acknowledgments

The authors thank the Nouvelle Aquitaine Region, INSERM and the Organ Recovery System for their financial support. The authors are grateful to Karen Poole for correcting English and Etienne Broggi for his valuable input during the initiation of the project.

Table 1: Characteristics of kidney graft donors, recipients and storage conditions

	Overall (n=38)	IGF (n=29)	non-IGF (n=9)	*P*	*Unknown (N,(%))*
Donor:					
Age (years):	67.5 (61.75-75)	65 (60.5-75)	70 (67-77)	0.28	
Sex (N,(%)):					
F	21 (55.3%)	14 (48.3%)	7 (77.8%)	0.15	
M	17 (44.8)	15 (51.7 %)	2 (22.2)		
Donation after brain death (N,(%)):	38 (100%)	29 (100.0%)	9 (100.0%)	1	
Expanded Criteria donors (N,(%)):	38 (100%)	29 (100.0%)	9 (100.0%)	1	
Recipient:					
Age (years):	65.5 (57-72)	65 (56.5-69)	72 (61-73)	0.20	
Sex (N,(%)):					
F	13 (34.2%)	11 (37.9%)	2 (22.2%)	0.4562	
M	25 (65.8 %)	18 (62.1 %)	7 (77.8 %)		
Ethnicity (N,(%)):				0.89	1 (2.6%)
Caucasian	30 (78.9%)	22 (75.9%)	8 (88.9 %)		
Afroamerican	2 (5.3%)	1 (3.4%)	1 (11.1 %)		
Other	4 (10.5%)	4 (13.8%)	0 (0,0 %)		
Renal disease :					
Diabetes mellitus	9 (23.7 %)	6 (20.7%)	3 (33.3 %)		
Hypertension	14 (36.8%)	9 (31.0%)	5 (55.6%)		
Glomerulopathy	2 (5.3%)	1 (3.4%)	1 (11.1 %)		
Tubulointerstitial nephropathy	3 (7.9%)	1 (3.4%)	2 (22.2%)		
Polycystic kidney disease	6 (15.8%)	5 (17.2%)	1 (11.1 %)		
Other	16 (42.1%)	13 (44.8%)	3 (33.3 %)		
Number of Transplantation (N,(%)):				1	
1	35 (92.1%)	26 (89.7%)	9 (100.0%)		
>1	3 (7.9%)	3 (10.3%)	0 (0.0%)		
Dialysis before transplantation (N,(%)) :	34 (89.5%)	25 (86.2%)	9 (100.0%)	0.55	
Induction therapy (N,(%)):					
Thymoglobulin	11 (28.9%)	10 (34.5%)	1 (11.1%)		
IL2R antibody	27 (71.0%)	19 (65.5%)	8 (88.9%)		
Maintenance therapy (N,(%)):					
MMF-Corticosteroids-CNI	32 (84.2%)	24 (82.8%)	8 (88.9%)		
MMF-Corticosteroids	3 (7.9%)	2 (6.9%)	1 (11.1%)		
Corticosteroids-CNI-imTOR	2 (5.3%)	2 (6.9%)	0 (0.0%)		
Corticosteroids-CNI	1 (2.6%)	1 (3.4%)	0 (0.0%)		
Death (N,%):	1 (2.6%)	1 (3.4%)	0 (0.0%)	1	
Banff Classification (pre-implantation biopsies) (N,(%)):				0.50	10 (26.3)
Normal	17 (44.7%)	12 (41.4%)	5 (55.6%)		
Acute tubular injury	10 (26.3%)	9 (31.0%)	1 (11.1%)		
Interstitial fibrosis/tubular atrophy	1 (2.6%)	1 (3.4%)	0 (0.0%)		
Graft rejection (N,(%)):					

Total	2 (5.3%)	1 (3.4%)	1 (11.1%)		
Antibody-mediated rejection	2	1	1		
T cell-mediated rejection	0	0	0		
Storage conditions:					
Perfusion duration (min):	831.5 (622.75-1031.25)	911 (603-1146)	675 (646-882)	0.45	
Cold ischemia duration (min):	1020 (810-1231.5)	1046 (812.5-1287)	875 (810-1065)	0.29	
Initial Temperature (°C):	2.8 (2.3-5.8)	2.85 (2.15-6.625)	2.5 (2.25-3.1)	0.58	3 (7.9%)
End Temperature (°C):	2.6 (2.2 -4.2)	2.75 (2.275-4.925)	2.5 (2.1-2.85)	0.35	3 (7.9%)
Decrease Temperature (°C):	0.1 (-0.4-1.3)	0.15 (-0.425-1.625)	0.1 (-0.45-1.05)	0.68	3 (7.9%)
Initial Resistance (mmHg/ml/min):	0.45 (0.3-0.8)	0.5 (0.2-0.8)	0.4 (0.3-0.95)	0.49	2 (6.4%)
End Resistance (mmHg/ml/min):	0.2 (0.1-0.2)	0.2 (0.1-0.2)	0.2 (0.2-0.3)	0.26	3 (7.9%)
Decrease Resistance (mmHg/ml/min):	0.2 (0.1-0.6)	0.15 (0.075-0.6)	0.2 (0.1-0.65)	0.52	3 (7.9%)
Initial Flow (ml/min):	60 (31-91)	57.5 (34.5-113)	60 (26-82.5)	0.41	3 (7.9%)
End Flow (ml/min):	111 (82-136)	117 (91-147.75)	97 (73-113.5)	0.16	3 (7.9%)
Increase Flow (ml/min):	43 (4-82)	51.5 (-2.5-97.5)	42 (20.5-74.5)	0.99	3 (7.9%)

Data reported as: "Median (Quartiles)" or " N,(%)", with p-values from Fisher's exact tests or Wilcoxon tests, as appropriate *Significant at $p < 0.05$. CNI, calcineurin inhibitor; MMF, mycophenolate mofetil; imTOR, mammalian target of rapamycin inhibitor

Table 2: Metabolomic contents of commercial and end-of-perfusion KPS-1 preservation fluid

Detected in KPS-1 and perfusates			Only detected in perfusates
Increased	**Unchanged**	**Decreased**	
Inosine	Sodium #	Gluconic acid #	O-Phosphoethanolamine
Guanosine	Potassium #	Methionine sulfoxide	Cystine
Xanthosine	Calcium #	Glucosamine	Aspartic acid
Tryptophan	Phosphates	Oxidized glutathione	Serine
Riboflavin	Glucose #	Adenine #	4-Hydroxyproline
5-Methylthioadenosine	Glutathione #	2-Ketoisovaleric acid	Cystathionine
	Hexose #	3-Methyl-2-oxovaleric acid	Glycine
	Pipecolic acid	D gluconic acid sodium salt #	Threonine
	Thymine	D-Ribose #	Glutamic acid
	Thymidine	Deoxycytidine monophosphate	Alanine
	Biotin		Ornithine
	D-Mannitol		Proline
	4-Pyridoxic acid		2-Aminoethanol
			Lysine
			Histidine
			Lactic acid
			Arginine
			Uracil
			Uric acid
			Choline
			5-Glutamylcysteine
			Xanthine
			Hypoxanthine
			Valine
			Uridine
			Methionine
			Niacinamide
			Tyrosine
			Adenosine
			Pyridoxal*
			4-Aminobenzoic acid**
			Isoleucine
			Leucine
			Phenylalanine
			Kynurenine**
			alpha-keto-glutarate
			Creatinine
			L-Carnitine
			PAH**
			Taurine
			1-Methylhistidine

Anthranilic acid**
Urea

*present only in a few patients, ** < LOQ in a few patients, # listed as constituents of KPS1

Figure legends:

Figure 1: Univariate analysis of metabolites in perfusates according to perfusion duration. Only the metabolites with significant differences between groups are displayed in this figure. Comparisons were made using Kruskal-Wallis tests and adjusted for multiple testing by the FDR method. Group 1 (blue box): perfusion duration < 12 hours; Group 2 (green box): perfusion duration between 12 and 20 hours; Group 3 (red box): perfusion duration > 20 hours. Box plots are grouped according to compound classes: (A.) amino-acids and their metabolites, (B.) vitamins, (C.) nucleic acids and their metabolites, (D.) TCA Cycle and lactate, (E.) others.

Figure 2: Multivariate analysis showing variations of metabolomic profiles according to perfusion duration. Group 1 (blue squares): perfusion duration < 12 hours; Group 2 (green triangles): perfusion duration between 12 and 20 hours; Group 3 (red dots): perfusion duration > 20 hours (A.) PCA scores plot showing separation between groups 1 and 3 but not with group 2. Principal component PC1 described 40% of the variation and PC2 11.5%. (B.) PLS-DA scores plot showing good separation between the 3 groups. (C.) Most important features for PLS-DA based on the (VIP) values; boxes on the right indicate the way of variation. PCA: Principal Component Analysis; PLS-DA: Partial Least Squares - Discriminant Analysis; VIP: Variable Influence on Projection.

Figure 3: Variations of mRNA expression of tubule transporter according to perfusion duration. PLS-DA scores plot showed no separation between the 3 groups. PLS-DA model yielded poor performance with cross-validation (R^2 = 34%, Q^2 = -39% and accuracy = 30%) and the permutation test (p-value = 0.95). Group 1 (blue squares): perfusion duration < 12 hours;

Group 2 (green triangles): perfusion duration between 12 and 20 hours; Group 3 (red dots): perfusion duration > 20 hours

Figure 4: Clustered Image Maps of the relationships between transporters and metabolites (sPLS method). The red and blue colors indicate positive and negative correlations respectively, whereas yellow indicates no significant correlation. CIM: Clustered Image Maps; sPLS: sparse Partial Least Squares

Figure 5: Assessment of IGF based on metabolomic profiles. Univariate analysis (A.) Volcano plot showing a decreased tendency of 4-Hydroxyproline and Alanine in non-IGF (red boxes) versus IGF (Immediate Graft Function; green boxes) patients (FC threshold of 1.2 and raw p-value of 0.2). Multivariate analysis (B.) The PLS-DA scores plot shows incomplete separation between groups with correct accuracy (70 %) and R^2 (36%), but poor predictability (Q^2 = -0.31). The permutation test was not significant (p = 0.6). (C.) Random Forest (RF) Classification showing the error rate for the overall dataset and for each class. PLS-DA; Partial Least Squares - Discriminant Analysis.

Figure 6: Assessment of IGF based on mRNA expression of tubule transporters. Multivariate analysis (A.) PLS-DA scores plot showing an overlap between graft recovery statuses and poor performance diagnostics (R^2=26%, accuracy = 69% and Q^2 = -1.28). The permutation test was not significant (p = 0.5) (B.) Random Forest (RF) Classification showing the overall error rate and for each class: the model has a poor predictability for non-IGF patients. PLS-DA; Partial Least Squares - Discriminant Analysis.

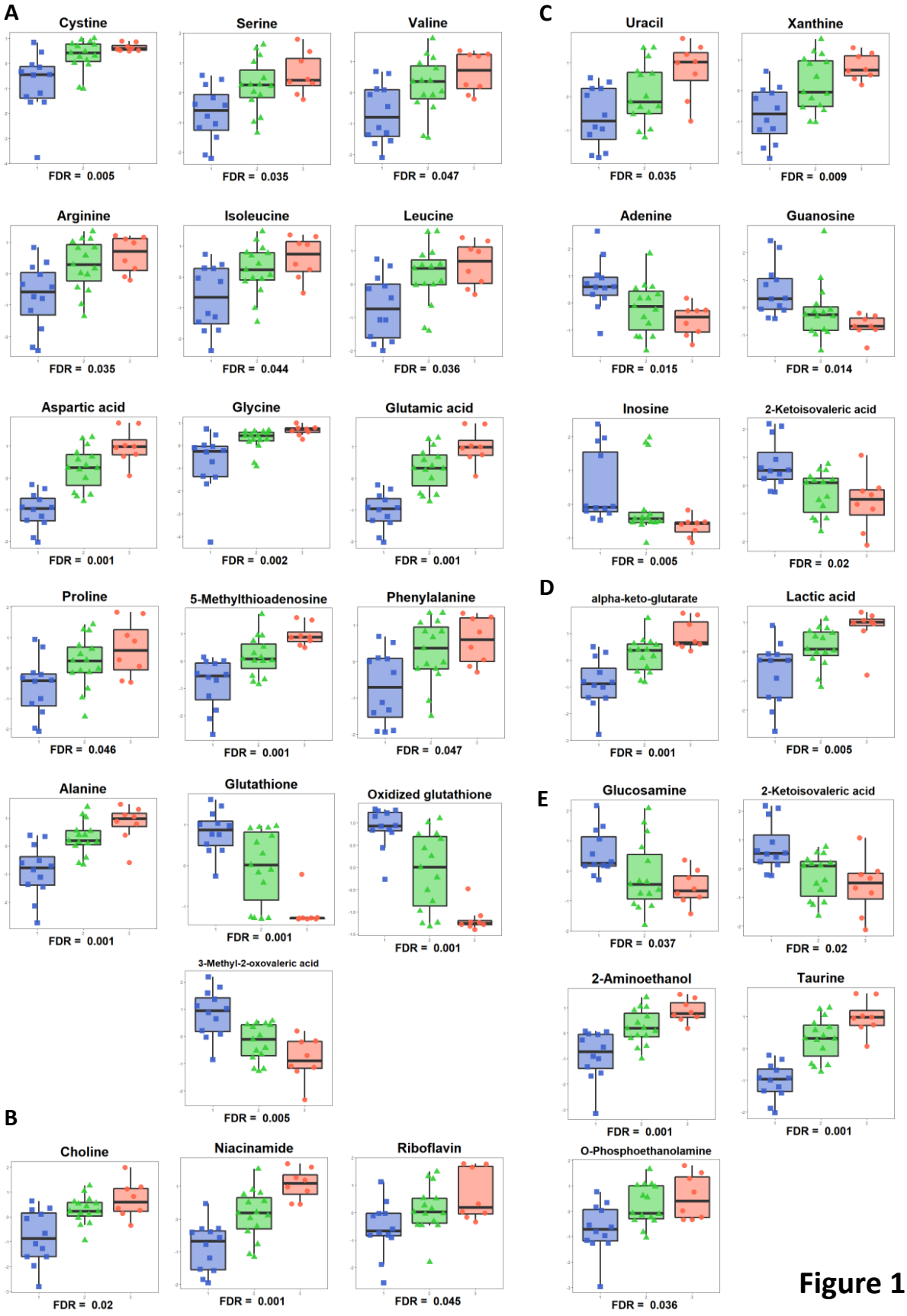

Figure 1

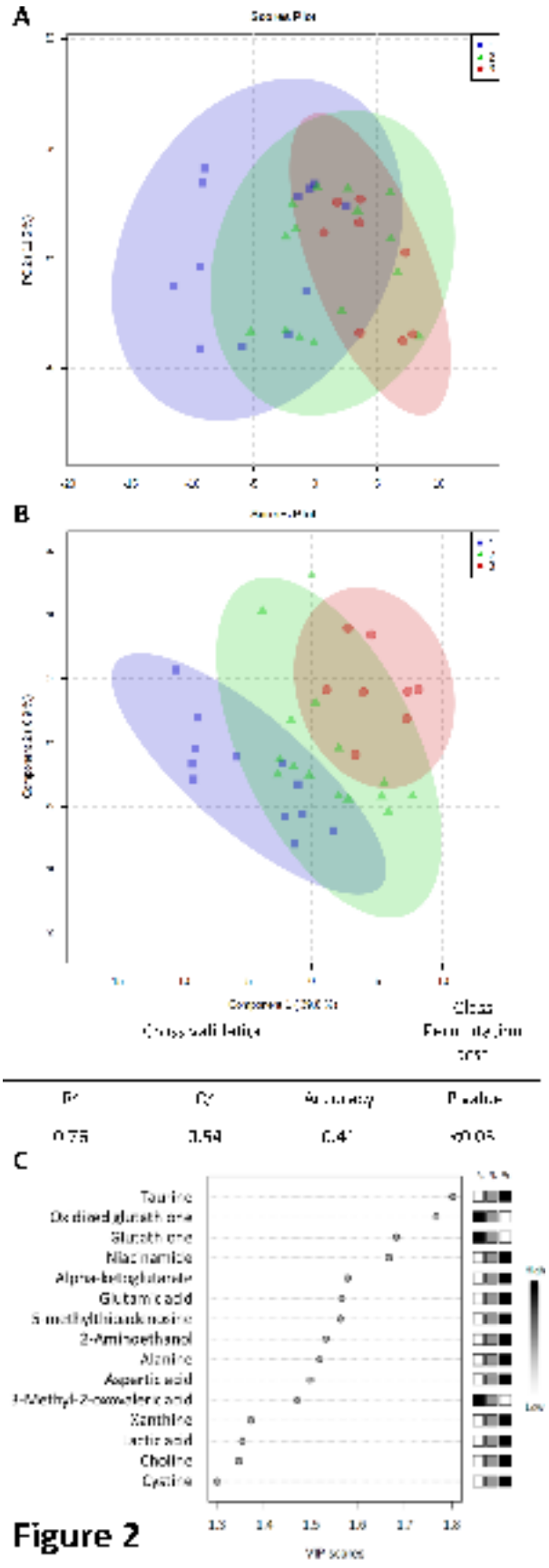

Figure 2

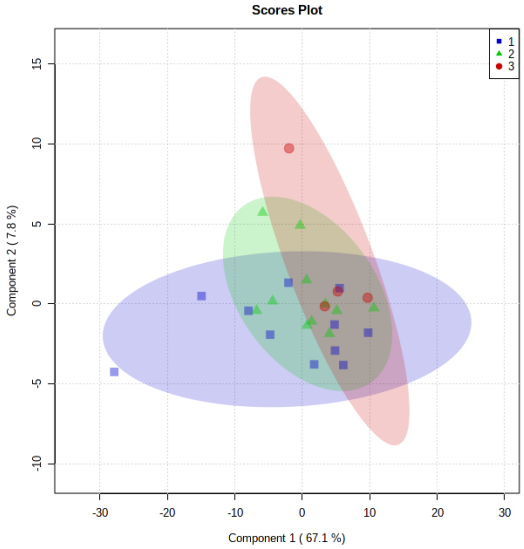

	Cross validation		Class Permutation test
R^2	Q^2	Accuracy	P value
0.34	-0,39	0.30	0.95

Figure 3

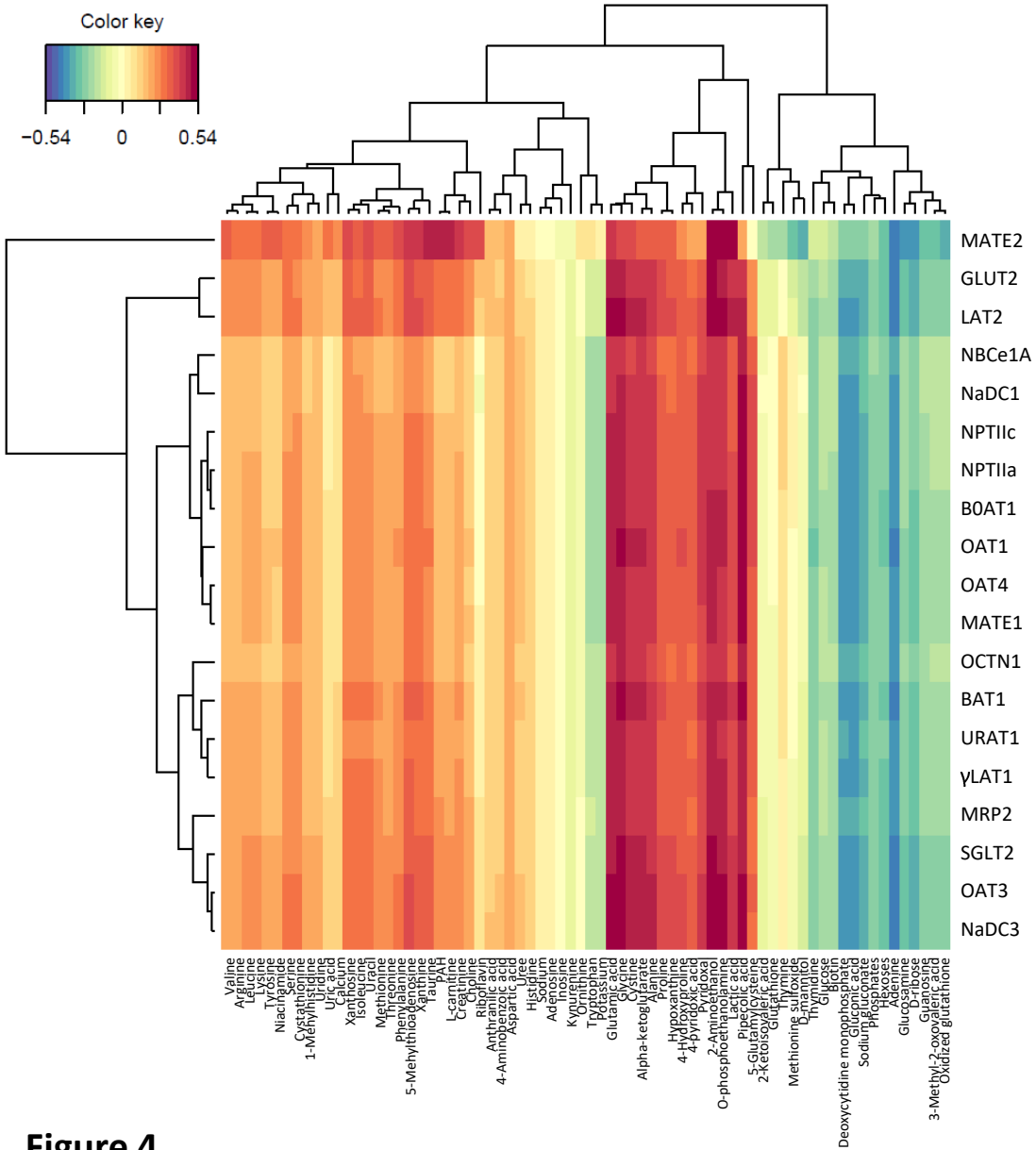

Figure 4

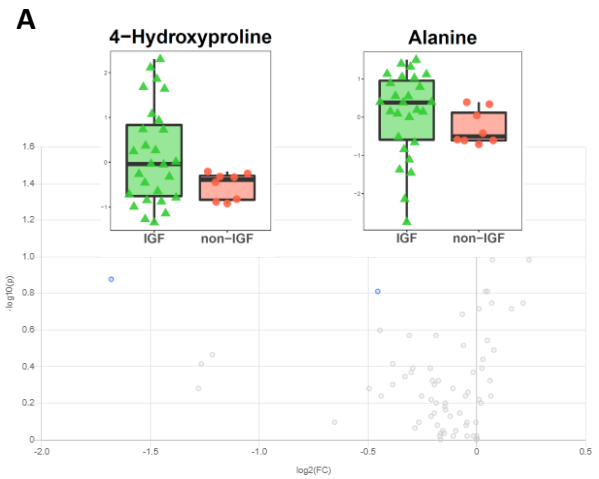

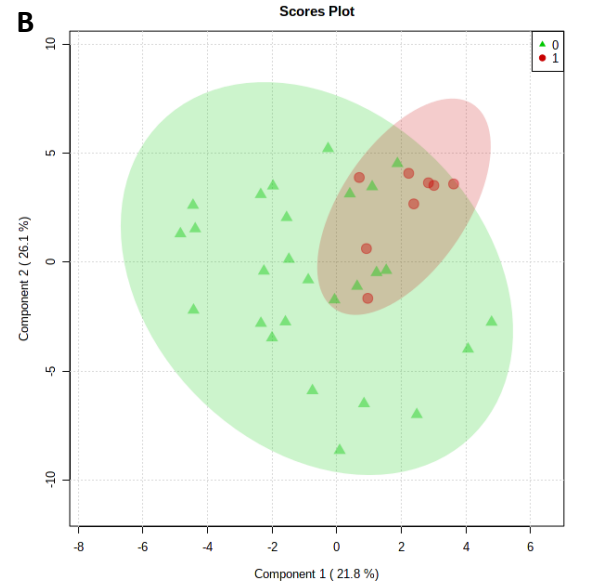

Cross validation			Class Permutation test
R^2	Q^2	Accuracy	P value
0.36	-0.31	0.69	0.6

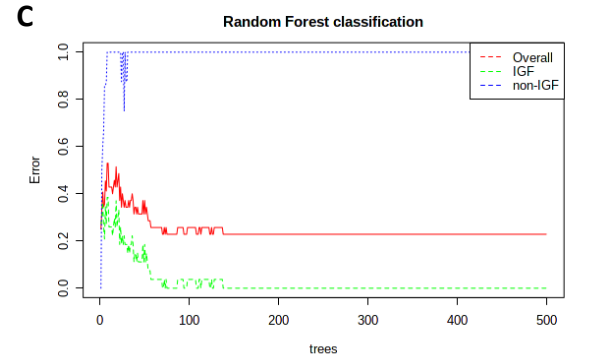

Figure 5

A

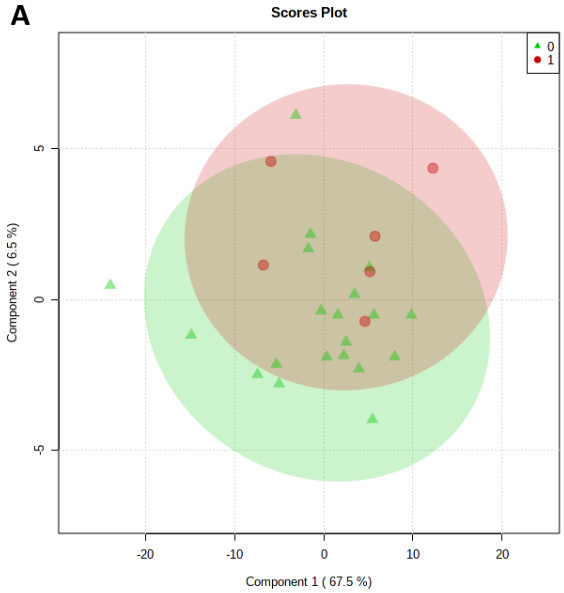

Cross validation		Class Permutation test	
R^2	Q^2	Accuracy	P value
0.26	-1,28	0.69	0.5

B

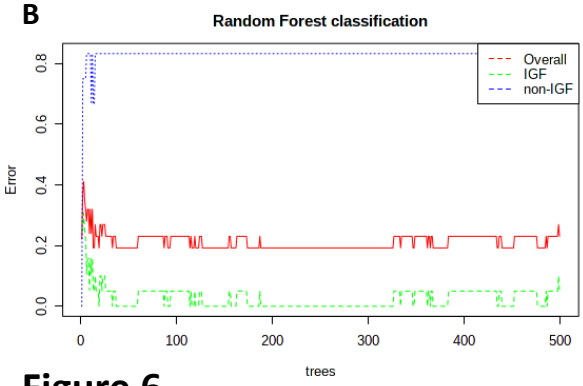

Figure 6

II.2.3. Discussion et perspectives

II.2.3.1. Investigations complémentaires

La recherche clinique RENALIFE a fait l'objet de plusieurs rapports d'études : un premier auprès du fournisseur de la machine de perfusion (*Organ Recovery Systems*) et un second auprès du CHRU de TOURS (PHAO-2015). Ce dernier a également été transmis aux autorités réglementaires, en vertu de la décision du 08/02/2021 de l'agence nationale de sécurité du médicament et des produits de santé.

Des analyses réalisées dans le cadre de ce projet n'ont pas été mentionnées dans l'article présenté ci-dessus. Des analyses métabolomiques des liquides de perfusion par spectrométrie RMN ont été menées à l'aide d'un RMN Bruker AVANCE III HD (Bruker), pour lequel le proton résonne à 600MHz, par la plateforme PST-ASB « Analyses des Systèmes Biologiques » de l'Université de Tours. En effet, il est préconisé de multiplier les techniques spectrométriques pour les analyses métabolomiques afin d'augmenter le spectre de détection des métabolites[73]. Toutefois, l'analyse en RMN s'est révélée peu contributive au regard de l'analyse LC-MS/MS. Les modèles d'analyse statistique multivariée développés par la plateforme PST-ASB à partir des données RMN seules n'ont pas révélé non plus de métabolites biomarqueurs de la fonction rénale post-greffe. Notre étude met en avant l'intérêt de la spectrométrie de masse pour l'analyse du métabolome puisque son utilisation, initialement en complément de la RMN, a permis d'identifier beaucoup plus de métabolites.

Afin de disposer d'échantillons contrôles pour évaluer les effets de la conservation des reins sur HMP, nous avons également réalisé une demande *ad hoc* de mise à disposition de biopsies de tissus sains de rein auprès du CRBioLim (le Centre de Ressources Biologiques du CHU de Limoges). Cette demande a reçu l'aval du Comité Médico Scientifique du CRBioLim et a été enregistrée sous le n° 2020-002 le 13/02/2020. Conformément à la réglementation, les prélèvements utilisés dans ce projet étaient issus de patients préalablement informés et qui n'avaient pas émis d'opposition à leur utilisation à des fins de recherche. Le recueil des biopsies a été constitué à partir de néphrectomies pour cancer avec un pistolet de biopsie 16 gauge, dans des conditions similaires à celles de l'étude RENALIFE. Des biopsies fraîches ont été récupérées pour être stockées directement à -20°C, afin de déterminer la variation d'expression des transporteurs tubulaires en situation d'ischémie (patient RENALIFE) par rapport au tissu présumé non ischémié (CRBioLim). Malheureusement, nous avons constaté qu'en amont de leur conservation, les biopsies du CRBioLim avaient subi une phase d'ischémie chaude de durée variable rendant leur utilisation en tant que contrôles inappropriée.

Dans l'étude RENALIFE, d'autres fragments de ces biopsies ont été fixés dans le formol tamponné 4%, l'alcool formol acide acétique (AFA), le liquide de Bouin ou le liquide de Dubosc (Bouin alcoolique). Ces biopsies fixées devaient également servir à la mise au point de techniques d'immunohistochimie, mais la trop faible quantité de matériel biologique recueilli par biopsie a rendu impossible la réalisation de coupes histologiques, très consommatrices de tissu. Nous avons donc priorisé l'étude transcriptomique, plus complète au regard du nombre de transporteurs ciblés. De plus, l'hétérogénéité des fixateurs utilisés pour l'évaluation pathologique aurait empêché la comparaison de l'ensemble des patients entre eux, lors des analyses d'immunohistochimie.

Au vu des résultats que nous avons obtenus, nous proposons la conduite d'une nouvelle étude clinique sur une cohorte de patients transplantés, avec pour objectif l'évaluation de l'expression transcriptionnelle et protéique, ainsi que la localisation des transporteurs tubulaires, à différent temps de conservation. Cette étude devra inclure des tissus rénaux non-ischémiés afin d'objectiver clairement les modifications induites par les conditions de conservation. En post-opératoire, l'étude des transporteurs est plus complexe. Ils semblent retourner à une fonctionnalité/expression basale dans les heures/jours qui suivent la revascularisation. Leur évaluation à partir des biopsies systématiques collectées à 1 ou 3 mois n'est donc pas pertinente. La future étude pilote devra inclure la réalisation d'une biopsie per-transplantation systématique dédiée, elle aussi, à l'étude de l'expression et de la localisation des transporteurs tubulaires. Cette étude clinique permettra de statuer sur la modulation des transporteurs par l'ischémie et l'IR chez l'Homme et orientera les recherches futures dans ce domaine.

II.2.3.2. Perspectives pour l'analyse du métabolome dans *le liquide de conservation* en période pré-implantatoire

Dans la discussion de notre article, nous affirmons que l'étude du métabolome dans le liquide de conservation en période pré-implantatoire reste pertinente. Le caractère prédictif du métabolome à l'égard de la fonction rénale post-greffe était difficilement évaluable dans notre étude en raison de la faible incidence de DGF et de la petite taille des échantillons. D'autres études, avec un nombre plus conséquent de patients inclus, devront être menées en ce sens. Dans cette discussion, nous traçons aussi des perspectives d'utilisation sur d'autres supports, détaillés ci-après.

II.2.3.2.1. Perfusion hypothermique oxygénée

Avec l'avènement des machines de perfusion, de nombreuses stratégies de conservation ont émergé. Au cours de la dernière décennie, l'oxygénation pré-implantatoire a généré un intérêt croissant. Darius et al ont récemment fait la synthèse des différentes

stratégies et des applications cliniques de cette oxygénation additionnelle[74]. L'oxygénation pendant la conservation sur HMP est aussi appelé *active oxygenated* HMP ($HMPO_2$). L'oxygénation sur HMP a montré un effet bénéfique sur la fonction rénale et la fibrose interstitielle évaluées après 2 semaines et 3 mois post-transplantation, respectivement, sur un modèle d'auto-transplantation de DCD chez le porc[75]. De nombreuses études ont été menées sur un modèle d'auto-transplantation porcin en cas d'ischémie-reperfusion[76–79]. Elles ont toutes conclu à une meilleure récupération rénale des greffons conservés sur HMP en présence d'oxygène. L'oxygénation sur HMP était associée à une stimulation du métabolisme aérobie favorisant l'activité du cycle de Krebs et la production d'ATP intra-tissulaire[76]. Un consensus quant au pourcentage d'oxygène à appliquer (hyper-oxygénation ou oxygénation atmosphérique) lors de la perfusion n'a pas encore été trouvé. Chez l'Homme, l'essai clinique COMPARE (ISRCTN32967929) a comparé les effets de l'oxygénation (100% O_2) par rapport à la non-oxygénation en HMP. Cet essai international multicentrique (106 paires de reins issus de DCD ont été transplantées chez des receveurs éligibles) a montré que l'oxygénation pendant la perfusion améliore la fonction rénale et réduit les complications post-opératoires sévères[80]. D'autres études cliniques, en cours, testent les effets de l'oxygénation lors de la conservation sur HMP[81,82]. Son utilisation en période pré-implantatoire induit un maintien du métabolisme aérobie et probablement un profil métabolomique différent de la conservation sur HMP standard. Nous supposons que le contenu métabolique du perfusat des greffons conservés sur $HMPO_2$ sera différent de celui des greffons conservés sur machines HMP standard. Par conséquent, l'analyse de ce contenu par une approche complémentaire (RMN et MS) non ciblée reste toujours pertinente en tant qu'outil diagnostic pré-implantatoire et non-invasif. L'inclusion d'un nombre conséquent de patients et d'une cohorte de validation augmentera la précision et la force de l'étude. L'utilisation combinée de biomarqueurs métabolomiques présent dans le liquide de conservation et de facteurs de risques ou prédicteurs cliniques pourrait constituer un outil pronostic mixte.

II.2.3.2.2. Machine de perfusion normothermique

L'utilisation des machines de perfusion normothermique fait également l'objet de nombreux travaux. Hosgood et coll. ont été les pionniers de la perfusion rénale *ex vivo* normothermique en utilisant un perfusat à base de sang appauvri en leucocytes chez le porc[83]. Ces solutions de conservation sont les plus couramment utilisées pour les NMP. En plus de leur capacité de transport d'oxygène, le flux de globules rouges favorise la fonction physiologique des cellules endothéliales. Des études expérimentales s'affranchissent de ces solutions à base de globules rouges par l'utilisation de milieux acellulaires[84,85]. En plus des transporteurs d'oxygènes protéiques ou non-protéiques, diverses substances sont ajoutées dans ces solutions (ex. colloïdes, vasodilatateurs, corticostéroïdes, antibiotiques à large

spectre). Cependant, la composition de ces solutions de conservation n'est pas encore standardisée[51]. La durée de perfusion normothermique est aussi source de débats. Le groupe de recherche de Sarah Hosgood a établi un protocole avec une période de 1h de NMP[86] à la suite d'une conservation hypothermique et précédant la procédure chirurgicale ; *a contrario* Kaths et coll. ont démontré qu'une perfusion normothermique continue sur leur modèle NEVKP (*normothermic ex-vivo kidney perfusion*) était plus performante qu'une perfusion de courte durée en fin de procédure, vis-à-vis de la récupération rénale à court terme[87]. L'absence d'application clinique et de consensus sur le temps de perfusion et la composition du perfusat ne permettent pas d'envisager, à l'heure actuelle, une étude randomisée des profils métabolomiques dans le liquide de conservation avec l'objectif d'identifier des biomarqueurs prédictifs de la fonction post-greffe. En revanche, de nombreux travaux expérimentaux visant à optimiser le conditionnement et la fenêtre d'action des NMP s'appuient sur l'utilisation des méthodes « omics », comme par exemple les analyses protéomiques et transcriptomiques récentes sur un modèle d'auto-transplantation porcin[88,89]. L'analyse métabolomique des perfusats constitue une approche complémentaire à la compréhension et à l'optimisation des conditions de conservation normothermiques.

II.2.3.3. Perspectives méthodologiques

L'un des principaux enjeux de la métabolomique présente et future est de proposer une couverture du métabolome la plus large possible, ce qui nécessite de combiner diverses plateformes de chimie analytique. Celles-ci incluent les technologies de spectrométrie de masse [LC-MS, GC-MS (*gas chromatography-mass spectrometry*), CE-MS (*capillary electrophoresis–mass spectrometry*), IMS-MS (*ion-mobility spectrometry–mass spectrometry*)] et la RMN. L'amélioration des bases de données spectrales favorisera la faisabilité et l'automatisation de la déconvolution spectrale, tandis que l'amélioration des méthodes statistiques et les analyses de voies favoriseront l'intégration et l'interprétation des données métabolomiques. L'objectif de cette partie n'est pas de présenter l'ensemble des méthodologies actuelles et futures associées à la métabolomique. En ce sens, nous recommandons la lecture de la revue récente de David S Wishart[73].

II.2.3.4. Métabolisme endogène et modulation d'expression des transporteurs tubulaires

Comme évoqué dans la discussion de l'article, nos résultats suggèrent la conduite d'autres études qui évalueront les profils métabolomiques intra/extra-tissulaires et l'expression des transporteurs tubulaires pour étudier leurs relations éventuelles avec plus de précision. Ces recommandations ont été appliquées à l'étude fondamentale que nous présenterons ci-après puisque nous avons évalué l'impact de l'hypoxie et de l'hypoxie/réoxygénation sur les profils métaboliques endogènes extra et intra-cellulaire, ainsi que sur l'expression des

transporteurs. Nous avons également pris en considération la cinétique des variations métaboliques et/ou des transporteurs. L'absence de variations de la quantité de glucose dans les profils métabolomiques des perfusats en fonction de la durée de perfusion nous a amené à considérer le maintien d'une forte concentration en glucose sur nos modèles hypoxiques *in vitro*.

II.3. Impact de l'hypoxie et l'hypoxie/réoxygénation sur le métabolome extra/intracellulaire et l'expression des transporteurs tubulaires

II.3.1. Résumé

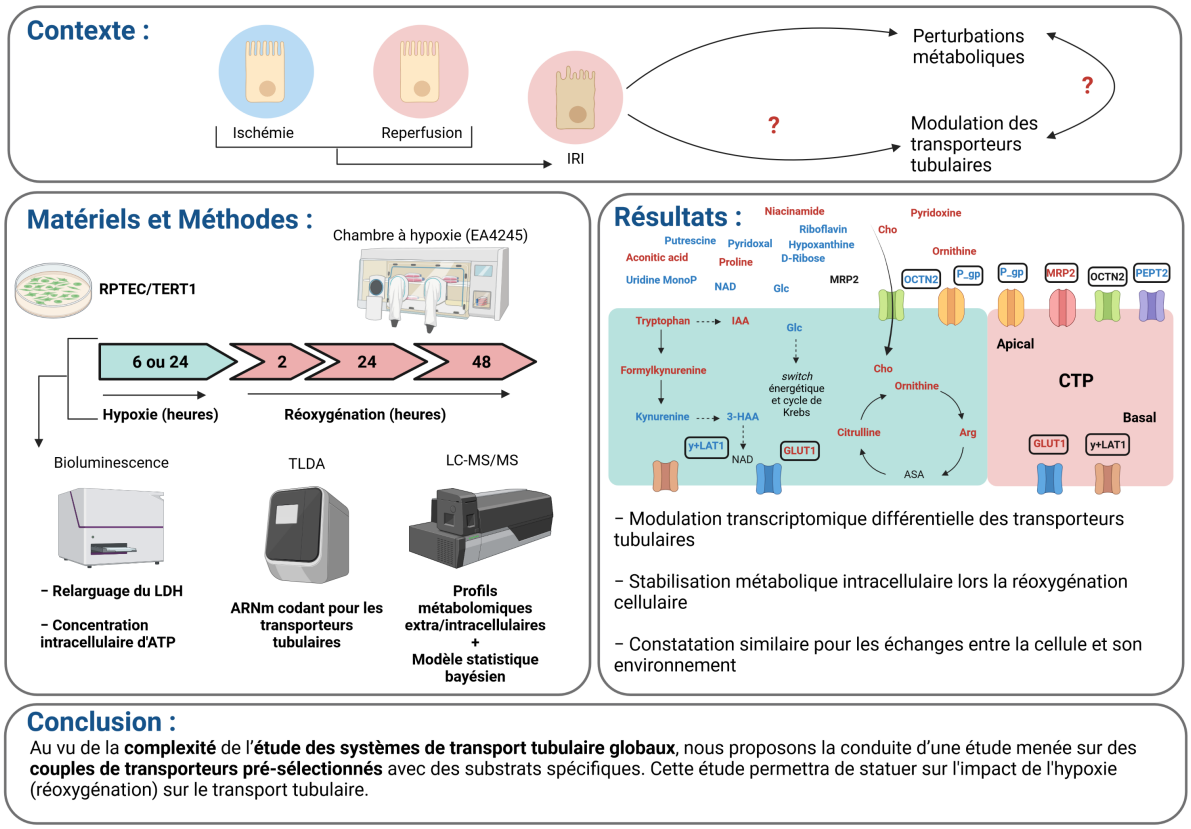

Figure 6 : Résumé graphique de l'article expérimental 2
L'illustration a été réalisée avec BioRender.com. CTP, cellules tubulaires ; LC-MS/MS, *liquid chromatography-tandem mass spectrometry*; LDH, lactate déshydrogénase ; TLDA, *Taqman Low-Density Array*.

Dans cette étude exploratoire réalisée à partir d'une lignée cellulaire humaine, nous avons évalué l'impact de l'hypoxie et de l'hypoxie/réoxygénation sur les systèmes de transport tubulaires et la composition du métabolome extra/intracellulaire. Nous souhaitions tester l'hypothèse d'une modulation hypoxie-dépendante des transporteurs tubulaires et la cinétique de cette modulation lors de la réoxygénation cellulaire. Aussi, nous avons étudié l'influence de la durée d'hypoxie sur cette modulation. La caractérisation des profils métabolomiques

extra/intracellulaires répondait à deux objectifs. Le premier consistait à décrire les variations induites par l'hypoxie et l'hypoxie/réoxygénation, le second à évaluer leur corrélation avec l'expression des transporteurs tubulaires en tant que phénomène explicatif additionnel aux variations métaboliques induites par l'hypoxie et l'hypoxie/réoxygénation.

Une cinétique d'hypoxie (6 et 24 heures) et de réoxygénation (2, 24 et 48 heures après hypoxie) a été réalisée sur des cellules RPTEC/TERT1 *via* l'utilisation d'une chambre à hypoxie disponible au sein du laboratoire EA4245 T2I (Faculté de Médecine de l'Université de Tours).

L'analyse transcriptomique par une approche TLDA a révélé un mécanisme de régulation transcriptionnel hypoxie-dépendant des transporteurs dans les cellules tubulaires proximales. Les transporteurs sont affectés différemment par ce mécanisme sous-jacent. La majorité de ceux constituant le système de transport des acides aminés [EAAT3 (*slc1a1*), 4F2hc (*slc3a2*) et LAT2 (*slc7a8*)], ainsi que le transporteur NaDC3 (*slc13a3*), ne sont pas affectés par l'hypoxie et l'hypoxie/réoxygénation. Le profil d'expression de certains des autres transporteurs est modifié pendant l'hypoxie [y^+LAT1 (*slc7a7*) et OCTN2 (*slc22a5)*], pendant la réoxygénation [MRP2 (*abcc2*), PEPT1/2 (*slc15a1/2*), OATP4C1 (*slco4c1*)], ou par les deux [P-gp (*abcb1*) et GLUT1 (*slc2a1*)]. Après une hypoxie de 6 et 24 heures suivie d'une réoxygénation de 48 heures, plus aucune variation significative des quantités de transcrits n'était observée (sauf pour OATP4C1). Ce résultat a révélé la nature transitoire de cette régulation transcriptionnelle.

La composition métabolique extra/intracellulaire en conditions d'hypoxie et d'hypoxie/réoxygénation a été déterminée par un protocole d'analyse métabolomique en LC-MS/MS. Au moyen d'une approche de modélisation bayésienne, nous avons mis en évidence que l'hypoxie s'accompagne d'un switch énergétique vers la glycolyse anaérobie (ex. augmentation de l'acide lactique, de l'acide pyruvique et de l'acide succinique), d'une altération de la voie de la kynurénine (ex. augmentation du tryptophane, de la formylkynurénine et de l'acide indole 3-acétique) et du cycle de l'urée (ex. augmentation de l'ornithine, de l'arginine, et de la cytidine). Ces perturbations métaboliques intracellulaires étaient accentuées lors d'une hypoxie prolongée. La réoxygénation cellulaire s'accompagnait d'un retour rapide à un niveau métabolique basal et à une stabilisation des échanges entre la cellule et son environnement. La modulation des transporteurs n'était pas corrélée avec les variations métaboliques observées. Cette absence de lien suscite plusieurs interprétations : (i) l'altération des transporteurs n'affecte pas le métabolome endogène ; (ii) la méthode métabolomique semi-ciblée utilisée ne couvrait pas un spectre suffisamment large de métabolites ;

(iii) l'expression transcriptionnelle n'est pas représentative des perturbations fonctionnelles des transporteurs ; ou (iv) des mécanismes compensatoires entre transporteurs maintiennent l'homéostasie du métabolome.

La complexité de l'étude globale des systèmes de transport tubulaires, nous amène à préconiser la conduite de nouvelles études ciblées sur des couples de transporteurs présélectionnés. L'utilisation de substrats spécifiques de ces transporteurs permettra d'étudier avec plus de précision l'impact de l'hypoxie/réoxygénation sur la fonctionnalité de ces derniers.

II.3.2. Article expérimental 2 : Impact of hypoxia and reoxygenation on the extra/intracellular metabolome and transporter expression in kidney tubular cells

Les *Supplementary Data* de l'article expérimental 2 sont disponibles en Annexe 4.

Impact of hypoxia and reoxygenation on the extra/intracellular metabolome and transporter expression in kidney tubular cells

Quentin Faucher[1], Stéphanie Chadet[2], Antoine Humeau[1,3], François-Ludovic Sauvage[1], Hélène Arnion[1], Sébastien Roger[2], Roland Lawson[1], Pierre Marquet[1,3,#], Chantal Barin-Le Guellec[1,4]

 # corresponding author.

Affiliations:

1: Pharmacology & Transplantation, UMR1248, Université de Limoges, INSERM, Limoges, France
2: EA4245, Transplantation, Immunologie, Inflammation, Université de Tours, 37000 Tours, France
3: Service de pharmacologie, toxicologie et pharmacovigilance, CHRU Limoges, Limoges, France
4: Service de biochimie et biologie moléculaire, CHRU de Tours, Tours, France

Correspondence information:
Prof. Pierre Marquet, Department of Pharmacology, Toxicology and Pharmacovigilance

University Hospital of Limoges, CBRS, 2 rue Bernard Descottes, 87000 Limoges, France

Email: pierre.marquet@unilim.fr

Tel: +33 555 05 64 18

Abstract

Background:

Ischemia-reperfusion injury induces several perturbations that alter immediate kidney graft function after transplantation and may affect long-term graft outcomes. Given the IRI-dependent metabolic disturbances previously reported, we hypothesized that proximal tubular transporters in charge of endogenous as well as exogenous substrates may be involved in these lesions during the pre-and post-implantation steps.

Methods:

Human proximal tubular cells were cultured in hypoxia for 6 or 24 hours, each followed by 2, 24 or 48 hours under normoxic culture conditions. We used TaqMan Low-Density Array to investigate the transcriptomic modulation of membrane transporters. Using semi-targeted LC-MS/MS profiling, we determined the extracellular and intracellular metabolome composition under hypoxia and following reoxygenation. We identified significant metabolic variations by means of statistical modeling.

Results:

The expression profile of some tubular transporters was impacted either during hypoxia (y+LAT1 (slc7a7) and OCTN2 (slc22a5)), during reoxygenation (MRP2 (abcc2), PEPT1/2 (slc15a1/2), rBAT (*slc3a1*), and OATP4C1 (slco4c1)), or under both conditions (P-gp (abcb1) and GLUT1 (slc2a1)). The P-gp and GLUT1 transcripts increased ((fold change) = 2.93 and 4.11, respectively) after 2-hour reoxygenation preceded by 24-hour hypoxia. We observed a downregulation (FC = 0.42) of y^+LAT1 (*slc7a7*) after 24-hour hypoxia and of PEPT2 (*slc15a2*) and rBAT after 24-hour hypoxia followed by 2-hour reoxygenation (FC = 0.40 and 0.33, respectively). Metabolomics investigation showed that hypoxia and hypoxia duration (in hours) altered the energetic and kynurenine pathways. However, intracellular metabolic homeostasis was promptly restored after reoxygenation, as were the exchanges between the cells and their extracellular environment.

Conclusion:

Altogether, our study provides insight into the transcriptomic response of the different tubular transporters to hypoxia and reoxygenation. No correlation was found between the expression of transporters and the metabolic variations observed. Given the complexity of studying the global transport systems in kidney tubular cells, we propose that further transport studies focus on targeted transporters, employing specific substrates.

Introduction

Kidney transplantation is the gold standard treatment for patients with end-stage renal disease. Given the high prevalence of kidney diseases[1], the gap between the needs and the number of available organs will continue to rise. According to the ABM (agence de la biomédecine)[2], the shortage indicator in France reached 3.3 recipients per available graft in 2020, against 2.2 in 2019 and 2018. Faced to a growing shortage of available organs, transplantation centers are broadening the criteria for organ acceptability by allowing the procurement of "sub-optimal" donors including donors after cardiac death and extended criteria donors (ECD). However, kidneys from these donors are more prone to favor Ischemia-Reperfusion Injury (IRI)[3,4], which is a frequent and serious complication in kidney transplantation, associated with delayed graft function in the post-implantation period. IRI is a complex pathophysiological, multifactorial and prolonged in time process, associated with numerous structural and metabolic disturbances. IR lesions induce the development of interstitial fibrosis and amplification of the local immune response with impairment of renal function and graft outcomes[4–6]. The need for more high-risk donors and subsequent increased probability of ischemia lesions requires improved understanding and alleviation of these lesions. Metabolomic profiling analyses focusing on ischemia or IR *in vivo* have been performed[7–10]. Numerous metabolites identified in perfusion solutions or bio-fluids are related to release from injured cells and to the inflammatory response. Other metabolites may arise from tubular damage and/or impaired renal tubular function. Tubular cells are the most sensitive to IRI, especially since a high energy level is required for the substrates exchange from blood to urine or *vice versa*. These trans-epithelial movements are governed mainly by the coordinated activity of tubular transporters of the SLCs (Solute Carriers) and ABCs (ATP-Binding Cassette) super-family[11,12]. Lesions associated with ischemia are accompanied by a functional alteration of tubular transporters. These alterations, observed in pre-clinical models of warm ischemia, are prolonged during reperfusion and could influence graft outcomes. Given the major role of transporters in renal and organism homeostasis, alterations in their activity could partially explain the delay in the recovery of graft function in the recipient, constitute a risk of global metabolic disturbances as well as toxins and drug overexposure in the immediate post-transplant period[11,12]. We conducted an exploratory study in a human cell line to determine the impact of hypoxia and reoxygenation on the expression of tubular transporters and on intra and extra-intracellular metabolome composition.

Results

Hypoxia-induced adaptive responses in PTC

We found a significant decrease of ATP intracellular concentration in PTC of -88.3% after 6 hours of hypoxia (0.08 ± 0.02 vs 0.77 ± 0.05 nmol/µg protein; *** p= 0.0002 (Figure 1 A)) as compared to normoxia (data not shown). There was also a significant decrease of -92.6% after 24 hours of hypoxia (0.06 ± 0.01 vs 0.82 ± 0.03; **** p< 0.0001 (Figure 1 A)). There was no noticeable cytotoxicity as compared to normoxia at T0 and after 6 hours of hypoxia alone or followed by 2, 24, or 48 hours of reoxygenation, as it reached a maximum of 6.31 ± 0.6 % after 48 hours of reoxygenation. No difference was observed at T0 and after 24 hours of hypoxia alone either. In contrast, we found a significant increase in cytotoxicity after 2 hours (9.46 ± 1.39 vs 3.96 ± 0.61; ** p= 0.0025), 24 hours (14.14 ± 2.79 vs 5.66 ± 0.35; * p= 0.0116) and 48-hour reoxygenation (16.9 ± 3.02 vs 8.23 ± 0.73; * p= 0.0162) as compared to normoxia. We did not observe significant differences in LDH release in normoxia over time (Figure 1 B). Figure 1C shows the metabolic signature of Krebs cycle intermediates and anaerobic glycolysis (Figure 1 C).

Expression of tubular transporters

H and H/R conditions did not induce RNA degradation, as shown by mean RIN values of 9.7 +/- 0.01 for N, H, and H/R conditions (data not show). Among the targeted genes, we did not detect s*lc22a6*, *slc22a7*, *slc22a8*, *slc22a11*, *slc2a2*, *slc5a1*, *slc47a2, slc47a1*, *slc22a2*, *slc13a2*, *slc22a12* and *abcg2*. Heatmap representation shows the different transporter expression patterns (fold-change (FC)) in the H and H/R conditions as compared to their respective N control (Figure 2 A). Each group of transporters is presented on an individual heatmap (Figure 2 B-F). The fold-change values are summarized in Supplemental Table 1. We have focused on the relevant variations since sporadic variations could be false positives.

We observed downregulation of all aquaporins after 24-hour hypoxia (FC = 0.37 for AQP1, 0.06 for AQP2, and 0.42 for AQP3) (Figure 2 F). Downregulation was likely maintained up to 48 hours of reoxygenation for AQP1 (FC = 0.54) and AQP2 (FC = 0.23) and up to 2 hours for AQP3 (FC = 0.32). For AQP2 we observed a downregulation at 6-hour hypoxia (FC = 0.54) followed by an upregulation after 24 hours (FC = 2.20) further accentuated after 48-hour reoxygenation (FC = 10.77). Regarding ABC transporters (Figure 2 B), the amount of transcripts coding for P-gp (abcb1) did not vary after 6hour hypoxia, whereas a decreasing trend was observed after 24 hours (FC = 0.51) of hypoxia and up to 24-hour reoxygenation (FC = 0.30 after 2 hours and 0.58 after 24 hours). The amount of transcripts encoding MRP2 (*abcc2*) increased (FC = 2.93) after 2-hour reoxygenation preceded by 24-hour hypoxia.

For the amino acid transport system (Figure 2 D), we observed a downregulation (FC = 0.42) of y^+LAT1 (*slc7a7*) after 24-hour hypoxia and of PEPT2 (*slc15a2*) and rBAT (*slc3a1*) after 2-hour reoxygenation preceded by 24-hour hypoxia (FC = 0.40 and 0.33, respectively). For the latter, we also observed an increase after 48-hour reoxygenation preceded by 6-hour hypoxia (FC = 2.08). We observed an increased quantity of transcripts encoding for GLUT1 (*slc2a1*) after 6 (FC = 10.56) and 24-hour hypoxia (FC = 8.58), and even after 2-hour reoxygenation (FC = 4.11) (Figure 2 C). There was a decreasing trend for OCTN2 (*slc22a5*) after 24 hours of hypoxia (FC = 0.51) as well as a decrease for OATP4C1 (*slco4c1*) and OCT1 (slc22a1) after 48-hour reoxygenation preceded by 24-hour hypoxia (FC = 0.41 and 0.36, respectively). In Figure 2 G is represented the “physiological” variation of transcriptional expression in normoxic conditions.

Metabolomic profiling under H and H/R conditions

We also assessed normoxia conditions alone to document the "physiological” variation kinetics of the PTC metabolome. Results are summarized in SD statistical analysis - "Metabolomic_description". We also documented the stability of the internal standard (2-Isopropylmalic acid) which validates the reproducibility of our mass spectrometry analyses (SD statistical analysis - "Metabolomic_description").

Intracellular metabolome

Intracellular metabolome profiling showed that some metabolites were more abundant after 6-hour hypoxia, *e.g.* indole-3-acetic acid, lactic acid, 2-Aminoadipic acid (Figure 3 A), or 24-hour hypoxia, *e.g*. indole-3-acetic acid, lactic acid, choline (Figure 3 B), compared to their respective normoxic control. Others are decreased after 6-hour, *e.g.* thymine, adenosine, citric acid (Figure 3 A), or 24-hour hypoxia, *e.g.* cytidine monophosphate, deoxycytidine, xanthosine (Figure 3 B). Metabolites that increase or decrease upon reoxygenation (2, 24, and 48 hours) following 6 or 24-hour hypoxia are summarized in Table 1 – Part 1. Some metabolites increased with hypoxia duration *e.g.* citrulline, arginine, uridine, whereas others decreased *e.g.* pyridoxal phosphate, N-acetylaspartic acid, 2-aminoadipic acid (Figure 3 C). We also compared the metabolomic profiles during reoxygenation following 24 versus 6-hour hypoxia. After 2-hour reoxygenation we found a higher amount of uridine, phenylalanine and tryptophan, in contrast to lower deoxycytidine and glutathione. No metabolites were significantly over- or under-abundant after 24-hour reoxygenation and only hypoxanthine was found in higher quantities after 48-hour reoxygenation. All the results of the intracellular metabolomic analyses are presented in SD statistical analysis - "Metabolomic_intracellular". Pathway analyses showed that the metabolites dysregulated after 6-hour hypoxia belonged mainly to the metabolism of alanine, aspartate and glutamate on the one hand, and glutathione and purine on the other (Figure 3

D). After 24 hours reoxygenation, dysregulated metabolites were mainly involved in the phenylalanine, tyrosine and tryptophan biosynthesis pathway (Figure 3 E). Besides, this pathway is the most discriminative between the 6 and 24-hour hypoxia conditions (Figure 3 F).

Extracellular metabolome

We investigated the metabolomics profile of the native medium under N, H, and H/R to document any degradation or generation of metabolites. When compared to the results obtained on the extracellular medium, these data help to distinguish non-cellular dependent processes from those resulting from reabsorption, secretion or release by cells. The results are summarized in SD statistical analysis - "Metabolomic_native". Extracellular metabolome profiling showed that some metabolites were more abundant after 6 hours (lactic acid, ornithine, cytidine, aconitic acid and adenosine) (Figure 4 A) and 24 hours (lactic acid, ornithine, niacinamide, succinic acid, glutamic acid, choline, pyridoxine, proline and aconitic acid) (Figure 4 B) of hypoxia compared to their respective normoxic control. Others were decreased after 6-hour (hexoses, uridine monophosphate, argininosuccinic acid, riboflavin, and pyridoxal) (Figure 4 A) and 24-hour hypoxia (hypoxanthine, D-ribose, hexoses, uridine monophosphate, putrescine, riboflavin, pyridoxal) (Figure 4 B). Metabolites that increase or decrease in the supernatant upon reoxygenation (2, 24 and 48 hours) following 6 or 24-hour hypoxia relative to their respective controls are summarized in Table 1 – Part 2. Some metabolites were found in higher levels after 24 hours than 6 hours of hypoxia (lysine, niacinamide, pyridoxine, choline, proline) and others in lower levels (adenosine, hexoses, uridine monophosphate, cytidine, hypoxanthine, putrescine) (Figure 4 C). Upon reoxygenation preceded by 24-hour hypoxia, none of the metabolites were found in higher or lower quantities in the extracellular medium as compared to reoxygenation period preceded by 6-hour hypoxia (SD statistical analysis - "Metabolomic_extracellular").

Discussion

We conducted an exploratory study to determine the effect of oxygen deprivation on the expression profiles of tubular transporters and its influence on intra- and extra-cellular metabolome. Some transporters showed transcriptional down- or upregulation during prolonged hypoxia. We then investigated whether there was a relationship with the PTC endogenous metabolome. We found a rapid return to equilibrium of the metabolome upon cell reoxygenation and only weak disruption of exchanges between the cell and its environment. These results suggest that in our conditions, the impact hypoxia and reoxygenation has on the expression of tubular transporters does not significantly translate on cellular metabolome modification (Figure 5).

H conditions lead to adaption of PTC

Albeit the impact of IR or ischemia on the expression of tubular transporters had already been documented using pre-clinical models, few studies were conducted on hypoxia/reoxygenation kinetics using human cells line. We opted for two hypoxia durations (6 hours for brief and 24 hours for prolonged hypoxia) according to the above-mentioned clinical study[13], where cold ischemia duration was on average 1020 minutes (810-1231.5 min). Given previous observations in this clinical study indicating no variation of glucose in graft preservation fluids according to ischemia duration, we chose to study oxygen deprivation only. We found that hypoxia (6 and 24 hours) did not induce uncontrolled death of PTCs, and that these cells appeared to be more sensitive to prolonged hypoxia upon reoxygenation (Figure 1 B). The intracellular ATP concentration falls after oxygen deprivation and is stabilized during the hypoxic period tanks to an anaerobic energetic switch (Figure 1 A). We identified variations of some anaerobic glycolysis and TCA cycle intermediates, characteristic of ischemia. Among them, lactic and pyruvic acid exhibited increasing dysregulation with hypoxia duration (Figure 1 C). Other variations related to energy production were observed, in particular the glutathione metabolism pathway and ATP breakdown (Figure 3 A/D).

Expression of membrane transporters

We aimed to determine if hypoxia induces a global perturbation of the tubular transporter-dependent transport system. Moreover, we hypothesized that hypoxia duration affects the expression of transporters but also their recovery under reoxygenation. Our transcriptomic study presents some limitations though, including a lack of robustness highlighted by the different variations observed with different MRP4 primers, the alternate of and/or isolated up- and down-regulation phenomena (AQP3, NBCe1 (*slc4a4*), NaPiIIc (*slc34a3*), OCT1 (*slc22a1*), rBAT (*slc3a1*), MRP1 (*abcc1*) and SGLT2 (*slc5a2*))), and the high variability observed in normoxic conditions over time (Figure 2 G). For this reason, we will only discuss a few robust variations.

For aquaporins (AQP1 and AQP2) we observed a downregulation only after 24-hour hypoxia and it persists during reoxygenation. For AQP2, the upregulation observed after 24 and 48-hour reoxygenation preceded by 6-hour hypoxia suggests a subsequent compensation mechanism. After 24-hour hypoxia, we only observed this mechanism after more than 48-hour oxygenation. This downregulation of AQP1 and AQP2 during hypoxia might be explained by the necessity for PTCs to decrease water uptake to prevent cellular edema.

The transcripts encoding several tubular transporters were not detected in our conditions. Among them, OAT1/OAT2/OAT3 and GLUT2 were previously described as missing in this cell model[14], whereas OCT2, MATE1, MATE2, and BCRP were detected in previous studies[14,15]. Unfortunately, the absence of OAT1/3, OCT2, and MATE1 hampered the validation of previous observations in animal

models. Indeed, Matsuzaki et al. observed a decreased of rOAT1 and rOAT3 protein expression after 48-hour reperfusion preceded by 30min of warm ischemia in rats[16]. Schneider et al. found a significant decrease in rOCT1 and rOCT2 mRNAs and protein expression after 24-hour reoxygenation preceded by 45-min bilateral clamping of the renal arteries in rats[17]. Many studies mostly reported downregulations of SLCs during ischemia[11,12]. Our results showed a similar tendency, except for GLUT1 (*slc2a1*). We observed that some transporters were not affected by hypoxia or reoxygenation, especially those of the amino acid transport system (*e.g.* EAAT3 (*slc1a1*) 4F2hc (*slc3a2*), LAT2 (*slc7a8*)) and NaDC3 (*slc13a3*) (Figure 2 A-E). Differential hypoxia-dependent modifications of the mRNA expression of ABC transporters (up-regulation for MRP2 and down-regulation for P-gp after 2-hour reoxygenation) was observed. . Interestingly, the expression profile of some transporters is modified either during hypoxia (y^+LAT1 (*slc7a7*) and OCTN2 (*slc22a5*), or during reoxygenation (MRP2 (*abcc2*), PEPT1/2 (*slc15a1/2*), OATP4C1 (*slco4c1*), or both (P-gp (*abcb1*) and GLUT1 (*slc2a1*)). We did not observe any significant variation of transcript quantities after 48-hour reoxygenation preceded by 6 and 24-hour hypoxia (except for OATP4C1), showing the transient nature of transporters' expression perturbations. However, the recovery of transcriptional expression during reoxygenation does not necessarily imply the absence of protein variations, since the kinetics of transcriptional events and protein expression generally differ[11].

Variations in transporter expression during hypoxia and reoxygenation could be linked with other hypoxia-dependent perturbations. Based on the modulation of transporter expression we suggested that it could be involved in the metabolic disturbances induced by hypoxia and reoxygenation.

Evolution of extra/intra-cellular metabolomic profiles under H and H/R

As mentioned in the introduction, IRI induces ischemia-dependent metabolic disturbance and also a post-reperfusion metabolic collapse[18]. We performed a semi-targeted profiling of the endogenous metabolome to determine its evolution under hypoxia and reoxygenation conditions, to decipher the underlying mechanisms of IRI and highlight possible endogenous metabolite/transporter relationships.

Intracellular metabolome

We assessed the time-dependent intracellular metabolic changes under hypoxia and reoxygenation. In addition of the well-known perturbation of the energetic pathway mentioned above, we found an alteration of the kynurenine pathway, involved in *de novo* biosynthesis of the coenzyme NAD and sensitivite to the redox balance[19]. The decrease in kynurenine and 3-HAA was observed after 6 and 24-hour hypoxia. The increase of kynurenic acid during brief hypoxia and the increase of

tryptophan and formylkynurenine after 24 hours suggest a progressive requirement for the kynurenine-(3-HAA) pathway to maintain NAD coenzyme levels, since the impairment of *de novo* NAD biosynthesis is an aggravating risk factor for AKI[20]. Indole-3-acetic acid, another tryptophan-derived metabolite, was also found in higher quantities after 6 and 24-hour hypoxia. Hypoxia and its duration also impacted the urea cycle.

A reversion to the aerobic energy metabolism occurred and stabilization was observed promptly after cellular reoxygenation. It is worth mentioning that the metabolome variations were highly time-dependent and did not necessarily reflect the underlying (pathway or transport) disorders. Additional fluxomic approaches could provide further information on the metabolic fluxes (fluxome) and thus the underlying mechanisms of reoxygenation perturbations in PTCs[21]. However, this rapid equilibrium shows that hypoxia at 37°C did not induce a large-scale metabolic perturbation of PTCs upon reoxygenation. This result supports the use of normothermic machine perfusion in transplantation. This method tends to mitigate the metabolic gap between hypoxia and reoxygenation by maintaining metabolic activity in the pre-implantation period[22]. However, the absence of data obtained in a hypothermic environment hampers a direct comparison between these two conditions in our study.

Extracellular metabolome

Analyzing the extracellular metabolome under hypoxia and reoxygenation conditions was meant to understand the mechanisms associated with IR and identify metabolites potentially reflecting transport activities. The absence of H/R inducing cytotoxicity implies that extracellular metabolic changes are not related to release by cell lysis. The decrease in extracellular glucose quantity under hypoxic conditions and up to 48 hours of reoxygenation, indicates consumption linked to anaerobic glycolysis. The secretion of lactic and pyruvic acid over the same timeline confirms this energetic switch. We also observed a higher amount of choline in the medium, but only after 24 hours of hypoxia. Since choline is reabsorbed by PTCs, this variation could be related to a decrease in its reabsorption during prolonged exposure to hypoxia. Increased ornithine concentration reflects the cellular increase in the urea cycle. As for the intracellular metabolome during reoxygenation, few variations were found in the exchanges between the cell and its extracellular environment, indicating the rapid adaptability of cellular pathways and transport activities to maintain homeostasis.

Transcriptomal expression of membrane transporters and metabolomic variations

In this study, we assessed in parallel the intra/extracellular profiles of metabolites and the mRNA expression of transporters to investigate their interdependence, as proposed in a previous clinical study[13].

We found an increase in transcriptional GLUT1 expression under hypoxia (6 and 24 hours). GLUT1 is involved in the systemic reabsorption of glucose at the basolateral pole of PTC. Its overexpression is inconsistent with intracellular glucose uptake.

Kynurenic acid is a metabolite excreted by MRP4 and BCRP[23]. The transient increase in its intracellular amount suggests a modulation of its transporter-dependent excretion under hypoxia. However, extracellular kynurenic acid did not vary under hypoxic conditions, rather suggesting increased degradation or decreased production of this metabolite. On the other hand, we observed a decrease in choline reabsorption only after 24-hour hypoxia. Choline is reabsorbed at the apical membrane by OCTN2[24]. The tendency for OCTN2 downregulation after 24-hour hypoxia may explain the disturbance of choline reabsorption. However, the intracellular choline concentration remained elevated in hypoxia, suggesting other compensatory mechanisms. Choline reabsorption was roughly unchanged after 2 and 24-hour reoxygenation preceded by prolonged hypoxia, but declined after 48 hours, suggesting a sustained downregulation of OCTN2 with a possible compensation of OCTN1 during the early hours of reoxygenation. Hypoxia and reoxygenation did not induce any disturbance in amino acid secretion or reabsorption, suggesting that the modulation of expression of some transporters did not influence the global homeostasis of these functions.

Overall, we did not find any transporter-related metabolic variation. This can be explained by (i) the consumption or production of endogenous transporters' substrates by metabolic cycles, (ii) a shift between transcriptomic and protein expression and (iii) a compensation by other transporters. It is worth mentioning that the expression of some transporters can directly influence the cellular production of endogenous metabolites. Vriend *et al*. showed that the OAT1 and OAT3 expression affects cellular energy metabolism and the synthesis of α-ketoglutarate[25]. Similar studies could be undertaken based on the hypoxia-sensitive transporters identified here to determine the impact of their expression on the endogenous metabolite production.

The influence of ischemia on tubular transporters expression during kidney conservation has not been extensively studied in humans. Kown *et al.* reported a misdistribution of hOAT1 on post-ischemic biopsies obtained 1 hour after reperfusion during transplant operation[26]. We demonstrated that the transcriptomic expression of the transporters was not different according to graft preservation duration on a perfusion machine in a cohort of transplant patients[13]. The transporter perturbations observed in pre-clinical models during reperfusion may be more related to protein impairment or malfunction and to perturbations of the handling of "systemic" substrates, than to transcriptomic expression. The limited ability to study transporters in 2D cell models is the major limitation of this work[27,28]. The recent development of a protocol to generate induced pluripotent stem cell (iPSC)-

derived renal proximal tubule-like cells is a promising alternative to improve the relevance of cellular models[29]. A more physiological system with cells cultured in a microfluidic device to form 3D proximal tubules will be considered to further study tubular transcellular transport functionality[28,30]. IR-mimicking micro-perfusion systems could be based on recently proposed models[31,32]. These studies should also investigate the possible interaction between uremic toxins, drugs and endogenous metabolites to shed light on the impact of tubular transporter disruption on the recovery of renal transplant function. Isotope-labeled exogenous substrates may permit to unravel the influence of transporters on substrate transport and the underlying metabolic pathways[33].

Further studying the ischemia-dependent modulations of transporters is important in the context of pre-implantation graft preservation on hypothermic and normothermic machines, where the disruption of transporter functions could impact the therapeutic efficacy of exogenous molecules added in the perfusion fluid, as pre-graft therapies[34].

Conclusion

We have studied the impact of hypoxia and hypoxia/reoxygenation on the transcriptional expression of a large number of SLCs and ABCs transporters constituting the harmonized and vectorial membrane transport systems of human proximal tubular cells. This study shows dysregulations of the transcriptional expression of transporters in PTCs during oxygen deprivation. The underlying molecular mechanisms are unclear, but their effects on transporters can be sustained or appear during early reoxygenation, and are sensitive to hypoxia duration. Cellular reoxygenation was accompanied by a rapid return to metabolic equilibrium. We did not find any relationship between perturbations among a large set of endogenous metabolites and transporters' expression. This highlights the limitation of isolated systems to study cells' metabolic and transport functions together. Studying the global tubular transport system and metabolic disturbances is challenging due to the large numbers of transporters and substrates involved, and to the multispecific nature of numerous substrates. Given this complexity, we call for further studies targeting a pre-selected transcellular transport using specific substrates. These studies could help to better investigate the connection between membrane transport and metabolic disturbances under hypoxia/reoxygenation.

Methods

Chemicals and reagents

Dulbecco's Modified Eagle's Medium F-12 Nutrient mixture (Ham) (DMEM/F-12 (1:1) (1X) + GlutaMAX™ – I, #31331-028), Dulbecco's phosphate buffered saline (PBS, #14190-144) all from Gibco™, BCA protein assay KIT (23225, Pierce™) and Taqman Low Density Array® (TLDA) cards were purchased from Thermofisher Scientific. The list of probe sets and manufacturer's code for TaqMan

probes are listed in Supplementary Table 1. G-148 (#04727878001), Cell Lytic (#C2978)), Discovery HS F5-3 column (150 x 2.1 mm d.i., 3 µm) (#567503-U), 2-Isopropylmalic acid (#333115), α-ketoglutaric acid (#75890), D-gluconic acid sodium salt (#G9005), D-Mannitol (#M4125), D-Ribose (#R7500), Magnesium D-gluconate hydrate (#G9130), and Taurine (#T0625) were purchased from Sigma-Aldrich. Finally, hTERT Immortalized RPTEC Growth kit (#ACS-4007) was purchased from ATCC.

Cell culture condition

RPTEC/TERT1 human proximal tubular cells (ATCC® CRL-4031™) were expanded in 175cm^2 flasks at 37°C with 5% CO_2 in a serum-free hormonally-defined medium (RPTECm) consisting of a mixture of DMEM/F-12(1:1) (1X) + GlutaMAX™, supplemented with a commercially available growth kit (hTERT Immortalized RPTEC Growth kit (ATCC®), and 0.1 mg/mL G-418. Cells were subcultured after establishing a contact-inhibited monolayer and reseeded at 100% confluence density in plastic culture plates. Before the start of the experiments, cells were grown for at least 14 days to reach a differentiated state with medium replacement three times per week in agreement with the literature[14,15,35]. RPTEC/TERT1 exhibit uniform cobblestone-like appearance with dome formation. For Hypoxia (H) and Hypoxia/Reoxygenation (H/R) experiments, RPTEC/TERT1 differentiated cells were submitted to 6 hours or 24-hour hypoxia (1% O_2, 5% CO_2 , RPTECm) in a hypoxia chamber (INVIVO2 200, Ruskinn Technology, AWEL internaltional) at the partners' laboratory EA4245 T2I (Tours, France). RPTECm were equilibrated overnight in the hypoxia chamber before the experiment. Hypoxic incubations were followed or not by several periods of reoxygenation (21% O_2, 5% CO_2, RPTECm). For each H or H/R culture condition, a control with a similar normoxic (N) culture period (21% O2, 5% CO2, RPTECm) was performed, to take into account the variation related to culture timing and duration. For the normoxic controls of hypoxic conditions without reoxygenation, the medium was equilibrated overnight before the experimentation. The specific culture conditions for each experiment (cell density, culture area, oxygenation level, sample collection) are summarized in Figure 6. RPTEC/TERT1 cells were used at passages 20–30.

ATP concentration measurement

After incubation (Figure 1 A), cells were washed with ice cold PBS and then lysed with 300 µL of Cell Lytic (Sigma-Aldrich) for 10 min at room temperature under agitation. Cell lysates were transferred to 1.5 mL tubes and incubated on ice for 30 min before centrifugation at 4°C at 17,500*g* during 15 min. Supernatants were stored at -80°C. Intracellular ATP quantification was performed by bioluminescence using the ATP determination kit (A22066, Invitrogen™) following the manufacturer's instructions. Briefly, 10 µL supernatant of each sample and 90 µL of reaction mix were loaded into a white-bottom 96-well plate. The plate was incubated for 15 minutes in the dark under agitation and then measured on PerkinElmer EnSpire® Multimode Plate Reader. Protein content was estimated using the BCA

protein assay following the manufacturer's instructions. Intracellular ATP concentration was expressed as nmol per µg of protein. One experiment was performed in triplicate.

LDH release

After each incubation time (Figure 1 B), 2 µL of supernatant was collected and stored at -20°C in q.s. 100µL LDH buffer (200mM Tris-HCl (pH = 7.3), 10% Glycerol and 1% BSA). The LDH concentration was determined using the LDH-Glo™ Cytotoxicity Assay kit (J2380, Promega Corporation) following the manufacturer's instructions. Briefly, the samples were diluted 10-fold in LDH buffer before loading 50µL of each sample into a white-bottom 96-well plate. The 5% Triton X-100 samples were diluted 20-fold. Fifty µL of reaction buffer were added before 45 min incubation in the dark. Luminescence was measured on PerkinElmer EnSpire® Multimode Plate Reader. Results were expressed as percentage of cytotoxicity related to the 5% Triton X-100 treatment as 100% cytotoxicity. Four independent experiments were performed each in quadruplicate.

Transcriptional expression of tubular transporters

For each incubation condition, RNA was extracted using the Nucleospin RNA/Protein kit (740933.50, Macherey-Nagel), according to the manufacturer's instructions. Extracts were then stored at -80°C until analysis. RNA concentration in the extracts was estimated using Qubit 4.0 with the Qubit™ RNA BR Assay Kit (Q10210, Invitrogen™). RNA quality was assessed by RNA Integrity Number (RIN) determination with Agilent RNA 6000 Pico kit and a Bioanalyzer 21 000 (Agilent). One µg RNA from each duplicates were pooled and the concentration was estimated. cDNA was synthesized from 1 µg RNA using the High-capacity cDNA Reverse Transcription kit (4368814, Applied Biosystems™), according to the manufacturer's instructions. For each sample, a mix containing 200 ng cDNA diluted in RNAse-free water q.s. 55µL and 55 µL TaqMan® Universal Master Mix II was prepared. One hundred µL of this reaction mix was then loaded to each slot of the TLDA card. After double centrifugation at 1,200 rpm for 1 min, the card was sealed and subsequently analyzed using Polymerase Chain Reaction (PCR) QuantStudio 12K with mix-UNG Amperase with the following the program conditions: 50°C for 2 min, 95°C for 10 min and 40 cycles of 95°C for 15 s followed by 60°C for 1 min. Using custom-designed TLDA cards we investigated the mRNA level of 40 genes coding mostly for tubular transporters and 4 housekeeping genes candidates (NME4, CHFR, C16orf62 and NASP) chosen according to the literature[36]. The mRNA expression of tubular transporters was then analyzed by the comparative $2^{-\Delta\Delta Ct}$ method with NME4, CHFR, and C16orf62 as housekeeping genes. Two independent experiments were performed in duplicate. Only genes with a proper amplification curve were included in our analysis. Heat maps were built with the software MeV_4_9_0.

Metabolomic profiling

Differentiated RPTEC/TERT1 cells were incubated under different conditions of H, H/R or N. At the end of the incubation periods the supernatants were collected (extraction of extracellular metabolites) and cells lysed (extraction of intracellular metabolites). The native medium was collected at each incubation time, as well as before and after overnight equilibration (Figure 1 C). For each independent experiment, a novel RPTECm was prepared before the incubations. For metabolomics investigations, three independent experiments were performed in triplicate.

Extraction of extracellular metabolites

Metabolite extraction was performed following the recommendations of the LC-MS/MS "Method Package for Cell Culture Profiling Ver.2" protocol (Shimadzu). The supernatants collected were centrifuged at 3,000 g for 1 min at room temperature to pellet suspended cell debris. One hundred µL of the supernatant were added to 200 µL of acetonitrile and 20 µL of internal standard (2-isopropylmalic acid [0.5 mmol/L]) solution, and strongly stirred. After centrifugation at room temperature for 15 min at 15,000*g*, the supernatant was diluted 1/10 in ultrapure water and transferred to a vial before injection of 3µL into the analytical system.

Extraction of Intracellular metabolites

The intracellular metabolite extraction protocol was adapted from a previously published method[37]. Briefly, cells were washed with ice-cold PBS and then lysed with 2 ml of 80% (vol/vol) methanol in ultrapure H_2O containing the internal standard (2-Isopropylmalic acid [0.5 mmol/L]) at 1/1000th (cooled to − 80 °C), and incubated for 20 minutes at -80°C. Each well was then scrapped with a cell scraper. Nine hundred microliters of the cell lysate/methanol mixture was transferred into a 2mL tube and 900µL in another. Each tube was centrifuged at 11,000*g* for 10 min at 4°C to pellet cell debris. The metabolite-containing supernatant was transferred into a new 1.5mL tube and evaporated to dryness in a vacuum concentrator at ambient temperature. The extract was then solubilized with 55 µL of ultrapure H_2O. The content of couples of tubes corresponding to the same sample was pooled. One hundred µL were transferred into vials for injection into the analytical system.

LC-MS/MS-metabolomic analysis

Mass spectrometry analysis was performed using a LCMS-8060 (Shimadzu) tandem mass spectrometer operated following the LC-MS/MS "Method Package for Cell Culture Profiling Ver.2" method (Shimadzu). For analysis of compounds not initially included in this kit, infusion of pure substances was performed and the retention time, relevant ion transitions and compound name were added to the list of compounds to analyze. The complete list of metabolites screened in this study is available in

Supplementary Table 3. For each transition analyzed, only well-defined chromatographic peaks were considered. Raw spectrometric data sets were normalized (area ratio (AR)) to the intensity of 2-isopropylmalic acid as internal standard. For further details on mass spectrometry analysis, please refer to the supplementary section "LC-MS/MS parameters".

Statistical analysis

Statistical analysis of Figure 1 data was performed using the unpaired t test with or without Welch's correction as implemented in GraphPad Prism (v. 5.04). For more details on all statistical tests performed, please refer to "Supplementary Table 4 - Summary of statistical analyses".

In order to study the variations in the concentration of metabolites inherent to hypoxia and hypoxia/reoxygenation we normalized the AR in hypoxia (reoxygenation) by the AR in normoxia. We could not divide by the mean value, because some metabolites were missing in normoxia. Thus, we divided by the sum of AR in normoxia and hypoxia resulting in the Normalized Area Ratio (NAR) (Figure 7).

Modeling was processed independently for the intracellular and extracellular media, with the R 4.1.0 software and the brms 2.16.1 package. The response variable was the NAR in hypoxic condition, and was modeled using a Gaussian family. The explanatory variables were hypoxia duration (oxie_t), reoxygenation duration (reox_t) and metabolites (metabolite). The model formula in brms was:

NAR ~ 0 + Intercept + oxie_t + mo(reox_t) + oxie_t:mo(reox_t) + (oxie_t:reox_t || metabolite), sigma ~ metabolite.

The effect of reoxygenation was modelled as a monotonic effect (mo), which means that the relative abundance of a metabolite can decrease or increase during reoxygenation, but it cannot increase and decrease or vice-versa. The monotonic effect of reoxygenation can be different for each preceding hypoxia duration (oxie_t:mo(reox t)). The interaction effect between hypoxia and reoxygenation durations is metabolite-dependent (oxie_t:reox_t || metabolite). The correlations of coefficients within the grouping factor were not modelled (||). The standard deviation of the Gaussian distribution of NAR was estimated for each metabolite (sigma ~ metabolite). The modeling estimations were performed using Markov chain Monte-Carlo with 4 chains and 20000 iterations including 10000 warmups and a thinning rate of 20. The samples were drawn using No-U-Turn sampler with a target average acceptance probability of 0.95. The priors for each parameter are presented in Supplementary Table 5. Detailed statistical analyses, as well as the scripts used are available in: https://ippritt_inserm-u1248.gitlab.io/2021_faucher_sd_statistics_metabolomics/.

Acknowledgments

The authors thank the Nouvelle Aquitaine Region and INSERM for their financial support, and BISCEm US042 INSERM—UMS 2015 CNRS, Molecular Analysis Platform for technical support. The authors are grateful to Karen Poole for correcting English, and Jean-Sebastien Bernard and Marie Piollet for helping with the experiments.

References

1. WHO | Projections of mortality and causes of death,
2016 to 2060. *WHO* http://www.who.int/healthinfo/global_burden_disease/projections/en/.
2. Agence de la biomédecine. Rapport annuel d'activité de l'agence de la biomédecine relatif à la greffe rénale (2020). https://rams.agence-biomedecine.fr/sites/default/files/pdf/2021-08/ABM_PG_Organes_Rein2020.pdf (2021).
3. Wong, G. *et al.* The Impact of Total Ischemic Time, Donor Age and the Pathway of Donor Death on Graft Outcomes After Deceased Donor Kidney Transplantation. *Transplantation* **101**, 1152–1158 (2017).
4. Zhao, H., Alam, A., Soo, A. P., George, A. J. T. & Ma, D. Ischemia-Reperfusion Injury Reduces Long Term Renal Graft Survival: Mechanism and Beyond. *EBioMedicine* **28**, 31–42 (2018).
5. Nieuwenhuijs-Moeke, G. J. *et al.* Ischemia and Reperfusion Injury in Kidney Transplantation: Relevant Mechanisms in Injury and Repair. *Journal of Clinical Medicine* **9**, 253 (2020).
6. Chen, C.-C., Chapman, W. C. & Hanto, D. W. Ischemia-reperfusion injury in kidney transplantation. *Front Biosci (Elite Ed)* **7**, 117–134 (2015).
7. Malagrino, P. A. *et al.* Metabolomic characterization of renal ischemia and reperfusion in a swine model. *Life Sci.* **156**, 57–67 (2016).
8. Jouret, F. *et al.* Nuclear Magnetic Resonance Metabolomic Profiling of Mouse Kidney, Urine and Serum Following Renal Ischemia/Reperfusion Injury. *PLoS ONE* **11**, e0163021 (2016).
9. Stryjak, I., Warmuzińska, N., Bogusiewicz, J., Łuczykowski, K. & Bojko, B. Monitoring of the influence of long-term oxidative stress and ischemia on the condition of kidney using solid phase

microextraction chemical biopsy coupled with liquid chromatography high resolution mass spectrometry. *J Sep Sci* (2020) doi:10.1002/jssc.202000032.

10. Nath, J. *et al.* Metabolic differences between cold stored and machine perfused porcine kidneys: A 1H NMR based study. *Cryobiology* **74**, 115–120 (2017).

11. Faucher, Q., Alarcan, H., Marquet, P. & Barin-Le Guellec, C. Effects of Ischemia-Reperfusion on Tubular Cell Membrane Transporters and Consequences in Kidney Transplantation. *J Clin Med* **9**, (2020).

12. Barin-Le Guellec, C., Largeau, B., Bon, D., Marquet, P. & Hauet, T. Ischemia/reperfusion-associated tubular cells injury in renal transplantation: Can metabolomics inform about mechanisms and help identify new therapeutic targets? *Pharmacol. Res.* **129**, 34–43 (2018).

13. Faucher, Q. *et al.* Perfusate metabolomics content and tubular transporters expression during kidney graft preservation by hypothermic machine perfusion. *medRxiv* 2021.09.27.21264167 (2021) doi:10.1101/2021.09.27.21264167.

14. Secker, P. F., Schlichenmaier, N., Beilmann, M., Deschl, U. & Dietrich, D. R. Functional transepithelial transport measurements to detect nephrotoxicity in vitro using the RPTEC/TERT1 cell line. *Arch. Toxicol.* **93**, 1965–1978 (2019).

15. Aschauer, L., Carta, G., Vogelsang, N., Schlatter, E. & Jennings, P. Expression of xenobiotic transporters in the human renal proximal tubule cell line RPTEC/TERT1. *Toxicol In Vitro* **30**, 95–105 (2015).

16. Matsuzaki, T. *et al.* Downregulation of organic anion transporters in rat kidney under ischemia/reperfusion-induced acute [corrected] renal failure. *Kidney Int.* **71**, 539–547 (2007).

17. Schneider, R. *et al.* Nitric oxide-induced regulation of renal organic cation transport after renal ischemia-reperfusion injury. *Am. J. Physiol. Renal Physiol.* **301**, F997–F1004 (2011).

18. Lindeman, J. H. *et al.* Results of an explorative clinical evaluation suggest immediate and persistent post-reperfusion metabolic paralysis drives kidney ischemia reperfusion injury. *Kidney Int* **98**, 1476–1488 (2020).

19. González Esquivel, D. *et al.* Kynurenine pathway metabolites and enzymes involved in redox reactions. *Neuropharmacology* **112**, 331–345 (2017).

20. Poyan Mehr, A. *et al.* De novo NAD+ biosynthetic impairment in acute kidney injury in humans. *Nat. Med.* **24**, 1351–1359 (2018).

21. Cortassa, S. *et al.* From Metabolomics to Fluxomics: A Computational Procedure to Translate Metabolite Profiles into Metabolic Fluxes. *Biophys J* **108**, 163–172 (2015).

22. Elliott, T. R., Nicholson, M. L. & Hosgood, S. A. Normothermic kidney perfusion: An overview of protocols and strategies. *Am J Transplant* **21**, 1382–1390 (2021).

23. Dankers, A. C. A. *et al.* Hyperuricemia influences tryptophan metabolism via inhibition of multidrug resistance protein 4 (MRP4) and breast cancer resistance protein (BCRP). *Biochimica et Biophysica Acta (BBA) - Molecular Basis of Disease* **1832**, 1715–1722 (2013).

24. Koepsell, H., Lips, K. & Volk, C. Polyspecific organic cation transporters: structure, function, physiological roles, and biopharmaceutical implications. *Pharm. Res.* **24**, 1227–1251 (2007).

25. Vriend, J. *et al.* Organic anion transporters 1 and 3 influence cellular energy metabolism in renal proximal tubule cells. *Biol. Chem.* **400**, 1347–1358 (2019).

26. Kwon, O., Hong, S.-M. & Blouch, K. Alteration in renal organic anion transporter 1 after ischemia/reperfusion in cadaveric renal allografts. *J. Histochem. Cytochem.* **55**, 575–584 (2007).

27. Fransen, M. F. J. *et al.* Bioprinting of kidney in vitro models: cells, biomaterials, and manufacturing techniques. *Essays Biochem* EBC20200158 (2021) doi:10.1042/EBC20200158.

28. Wilmer, M. J. *et al.* Kidney-on-a-Chip Technology for Drug-Induced Nephrotoxicity Screening. *Trends Biotechnol.* **34**, 156–170 (2016).

29. Chandrasekaran, V. *et al.* Generation and characterization of iPSC-derived renal proximal tubule-like cells with extended stability. *Sci Rep* **11**, 11575 (2021).

30. Jansen, J. *et al.* Bioengineered kidney tubules efficiently excrete uremic toxins. *Sci Rep* **6**, 26715 (2016).

31. Giraud, S., Thuillier, R., Cau, J. & Hauet, T. In Vitro/Ex Vivo Models for the Study of Ischemia Reperfusion Injury during Kidney Perfusion. *International Journal of Molecular Sciences* **21**, 8156 (2020).

32. Zamorano, M. *et al.* Tackling Ischemic Reperfusion Injury With the Aid of Stem Cells and Tissue Engineering. *Frontiers in Physiology* **12**, 1436 (2021).

33. Nath, J. *et al.* (13)C glucose labelling studies using 2D NMR are a useful tool for determining ex vivo whole organ metabolism during hypothermic machine perfusion of kidneys. *Transplant Res* **5**, 7 (2016).

34. Hosgood, S. A., Hoff, M. & Nicholson, M. L. Treatment of transplant kidneys during machine perfusion. *Transpl Int* **34**, 224–232 (2021).

35. Aschauer, L. *et al.* Delineation of the Key Aspects in the Regulation of Epithelial Monolayer Formation. *Mol Cell Biol* **33**, 2535–2550 (2013).

36. Wang, Z., Lyu, Z., Pan, L., Zeng, G. & Randhawa, P. Defining housekeeping genes suitable for RNA-seq analysis of the human allograft kidney biopsy tissue. *BMC Med Genomics* **12**, 86 (2019).

37. Yuan, M., Breitkopf, S. B., Yang, X. & Asara, J. M. A positive/negative ion-switching, targeted mass spectrometry-based metabolomics platform for bodily fluids, cells, and fresh and fixed tissue. *Nat Protoc* **7**, 872–881 (2012).

Tables

Table 1: Metabolomic profiling under hypoxia/reoxygenation incubation

Part 1: Intracellular environment						
H (hours)	6			24		
R (hours)	2	24	48	2	24	48
Metabolites	Lactic acid Phenylalanine Uridine Putrescine Hexoses	ASA Adenine Putrescine	ASA Adenine Putrescine	Lactic acid Pyridoxal Desoxycytidine Citric acid Putrescine	ASA Lactic acid Adenine Adenosine Xanthosine Guanosine	ASA Lactic acid Hypoxanthine Adenine Adenosine
Part 2: Extracellular environment						
H (hours)	6			24		
R (hours)	2	24	48	2	24	48
Metabolites	Lactic acid Pyruvic acid Hexoses Uridine	Lactic acid Pyruvic acid Pyridoxine Uridine Desoxycytidine Hexoses	Lactic acid Pyruvic acid Pyridoxine Hexoses Uridine	Lactic acid Pyruvic acid Pyridoxal Uridine	Lactic acid Pyruvic acid Pyridoxine Hexoses	Lactic acid Pyruvic acid Pyridoxine Proline Choline Hexoses

Metabolites are in red (abundance increased) or blue (abundance decreased). ASA; arginosuccinic acid; H, hypoxia; R, reoxygenation

Figures legends

Figure 1: Hypoxia-reoxygenation conditions

(**A**) Intracellular ATP concentration, expressed as nmol/µg of protein, in differentiated hRPTEC/TERT1 cells after 6 hours (left graph) or 24 hours (right graph) of N or H. Data are presented as aligned dot plot with mean ± s.e.m, ***$p < 0.001$, ****$p < 0.0001$ by unpaired *t*-test (n= one independent experiment in triplicate). (**B**) LDH released over time by differentiated hRPTEC/TERT1 cells after either 6 hours (left panel) or 24 hours (right panel) hypoxia (blue circles) and then submitted to reoxygenation (red circles). Green circles correspond to control experiments under normoxia. Data are represented by aligned dot plot line at median that correspond to the percentage of cytotoxicity relative to Triton X-100 treatment as 100% cytotoxicity. The percentage of cytotoxicity of H and H/R was compared to their respective control (N), *p< 0.05, **p < 0.01 by unpaired t-test with Welch's correction (n= four independent experiments in quadruplicate). (**C**) Intracellular metabolomic analysis of H-incubated cells compare to N. The percentage of H compared to N (green dotted line) is represented by the blue aligned dot plot with mean ± s.e.m for metabolites of glycolysis and TCA cycle, **p < 0.01, ***p < 0.001, ****p < 0.0001 by unpaired t-test with Welch's correction. Comparison between H-incubated cells during 6 and 24 hours was performed, ##p < 0.01, ###p < 0.001 by unpaired t-test with Welch's correction. Hypoxia during 6h and 24h have their own independent N control (n= three independent experiments in triplicate).

Figure 2: Transcriptional expression of tubular transporters under H and H/R conditions

Heat map representation of TLDA results. Heat map shows the global gene fold change expression pattern according to (**A-F**) H and H/R conditions, and (**G**) N condition. In (G), the different normoxia conditions are compared to 6-hour normoxia to show the time-dependent variation of transporter expression. Shades of yellow indicate upregulation while shades of blue indicate downregulation. Black color indicates unchanged expression. Color intensity reflect the higher fold change value (n= two independent experiments in duplicate). ABC, ATP-Binding Cassette; AQP, aquaporins; Na/K-ATPase subunits; AA, amino acid; OI, organic ions.

Figure 3: Intracellular metabolomic profiling under H and H/R conditions

(**A-B**) Posterior predictive distribution of metabolites in condition of (**A**) 6 and (**B**) 24-hour hypoxia without réoxygénation, in the intracellular environment. The points are the mean, and thick and thin segments are respectively the 80% and 98% credible intervals of the posterior distribution. The green line (mean) and rectangles (80% and 98% credible intervals) are the posterior predictive distribution irrespective of metabolite. Metabolites are in red (over abundant) or blue (under abundant) if their 98% credible intervals don't cross the 98% credible interval for all the metabolites. (**C**) Difference of posterior predictive distribution in 24 and 6-hour hypoxia of metabolites after 2-hour reoxygenation. The points are the mean, thick and thin segments are respectively the 80% and 98% credible intervals of the posterior distribution. The green line (mean) and rectangles (80% and 98% credible intervals) are the posterior predictive distribution irrespective of metabolite. Metabolites are in red (over abundant) or blue (under abundant) if their 98% credible intervals don't cross the 98% credible interval for all the metabolites. (**D-F**) Pathway analysis based on discriminant metabolites after (**D**)

6-hour hypoxia, (**E**) 24-hour hypoxia or (**F**) between 6 and 24-hour hypoxia. Larger circles farther from the y axis and orange-red color show higher impact of pathway. AAG, alanine, aspartate and glutamate metabolism; PTT, phenylalanine, tyrosine and tryptophan biosynthesis.

Figure 4: Extracellular metabolomic profiling under H and H/R conditions

(**A-B**) Posterior predictive distribution of metabolites in condition of (**A**) 6 and (**B**) 24-hour hypoxia without reoxygenation, in the extracellular environment. The points are the mean, and thick and thin segments are respectively the 80% and 98% credible intervals of the posterior distribution. The green line (mean) and rectangles (80% and 98% credible intervals) are the posterior predictive distribution irrespective of metabolite. Metabolites are in red (over abundant) or blue (under abundant) if their 98% credible intervals don't cross the 98% credible interval for all the metabolites. (**C**) Difference of posterior predictive distribution in 24 and 6-hour hypoxia of metabolites after 2-hour reoxygenation. The points are the mean, thick and thin segments are respectively the 80% and 98% credible intervals of the posterior distribution. The green line (mean) and rectangles (80% and 98% credible intervals) are the posterior predictive distribution irrespective of metabolite. Metabolites are in red (over abundant) or blue (under abundant) if their 98% credible intervals don't cross the 98% credible interval for all the metabolites.

Figure 5: Impact of hypoxia on metabolomics profiles and of hypoxia/reoxygenation on the mRNA expression or tubular transporters

Overview of metabolomic and transporter perturbations in H-incubated PTCs during (**A**) 6 and (**B**) 24 hours. PTC in blue represents hypoxia and in red the first two hours of reoxygenation. For reoxygenation, we have only represented transporters variations. The metabolites and transporters in red increase, blue decrease, and black are unchanged compared to normoxia. 3-AA, 3-hydroxyanthranylic acid; IAA, indole-3-acetic acid; Arg, arginine; ASA, arginosuccinic acid; Cho, choline; Glc, glucose; MonoP, monophosphate; NAD, nicotinamide adenine dinucleotide.

Figure 6: Culture and sampling conditions for each type of experiments

Listing and picture of culture and sampling conditions for (**A**) intracellular ATP concentration estimation (n= one experiment in triplicate). (**B**) Intracellular LDH release estimation (n= four independent experiments in quadruplicates for H/R and N conditions, and in triplicates for 5% Triton X-100). Five samples were taken at different time for each condition (i.e. H/R or N) and one for 5% Triton X-100 that correspond to RPTECm 5% Triton X-100. (**C**) Metabolomic profiling (n= three experiments in triplicates for each condition). This experiment is composed of 16 conditions consisting of 2 H conditions, 3 R conditions (per H condition) and 8 N conditions. (**D**) Transporters expression (n= two experiments in duplicates for each condition). This experiment is composed of 16 conditions consisting of 2 H conditions, 3 R conditions (per H condition) and 8 N conditions. NM; Native Medium.

Figure 7: Principle of NAR normalization for the statistical analysis of metabolomics profiles

The normalized area ratio (NAR) in hypoxia corresponds to the relative contribution of the area ratio (AR), in %, to the quantity of the metabolite in both normoxia and hypoxia for each combination of environment (intra or extracellular), hypoxia and reoxygenation duration, metabolite and experiment. It varied between 0 (the area ratio did not contribute to the metabolite quantity in the condition) to 100 (the area ratio contributed alone for the metabolite in the condition). The expected value for an equivalent quantity of the metabolite in hypoxia compared to normoxia was 100 / 6 (= 16.7), which means that each area ratio (3 in hypoxia and 3 in normoxia for each experiment) equally contributed to the metabolite quantity. The expected maximal value was 100/3 (= 33.3), which means that the metabolite quantity was equally in the three hypoxia data and did not identify in each normoxia data. The undetected metabolites in both normoxia and hypoxia in one experiment are considered 100/6, which means that each area ratio equally contributed to the absence of the metabolite.

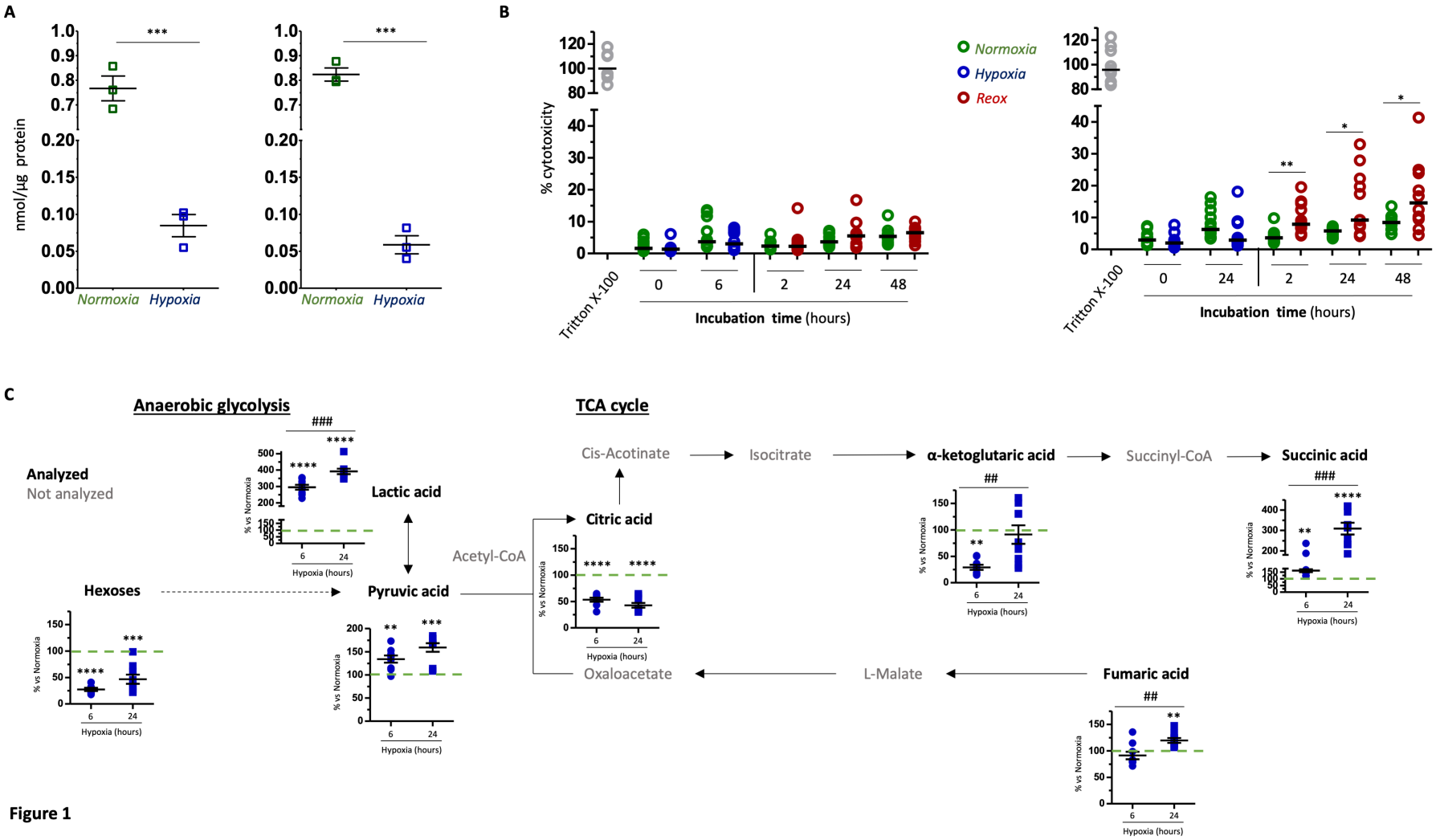

Figure 1

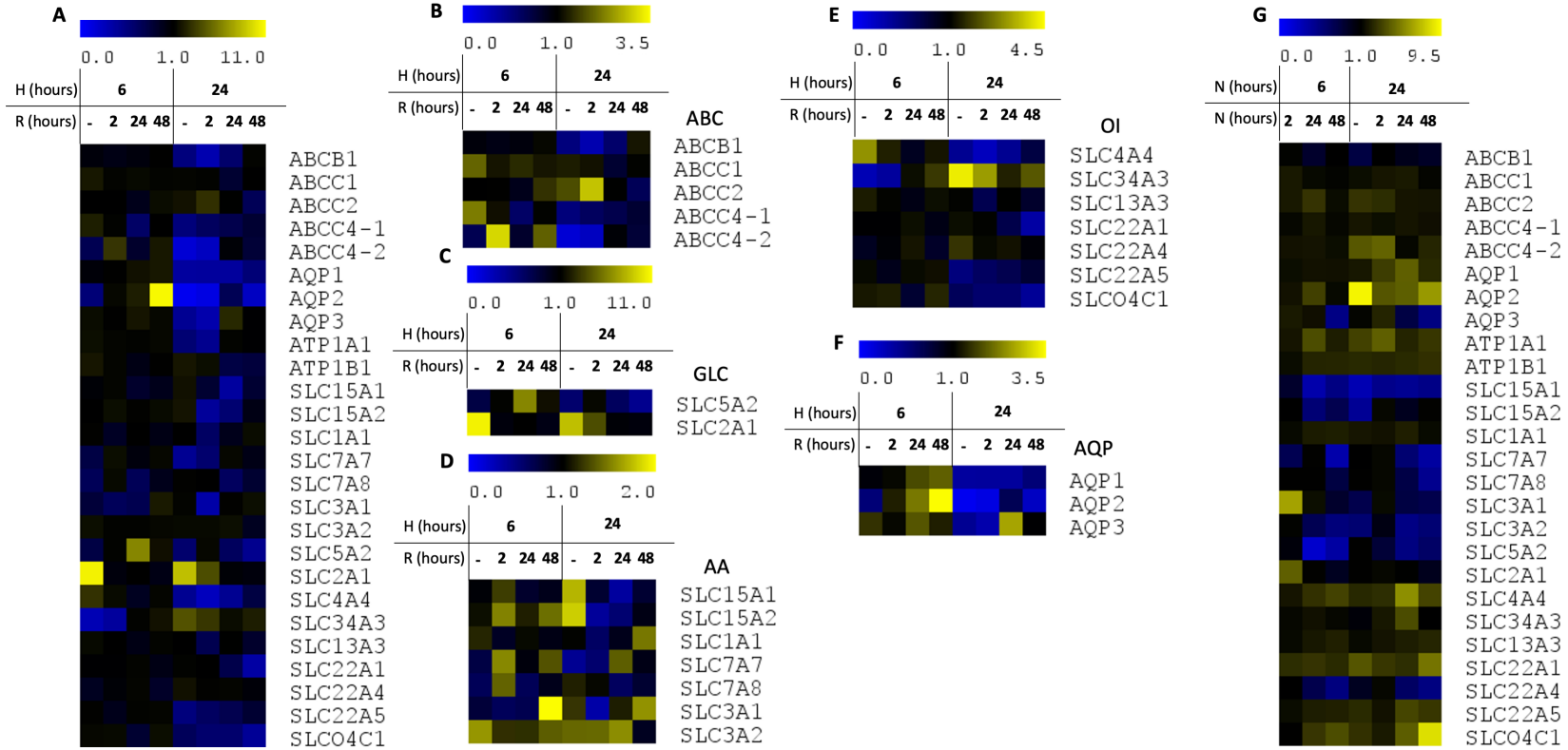

Figure 2

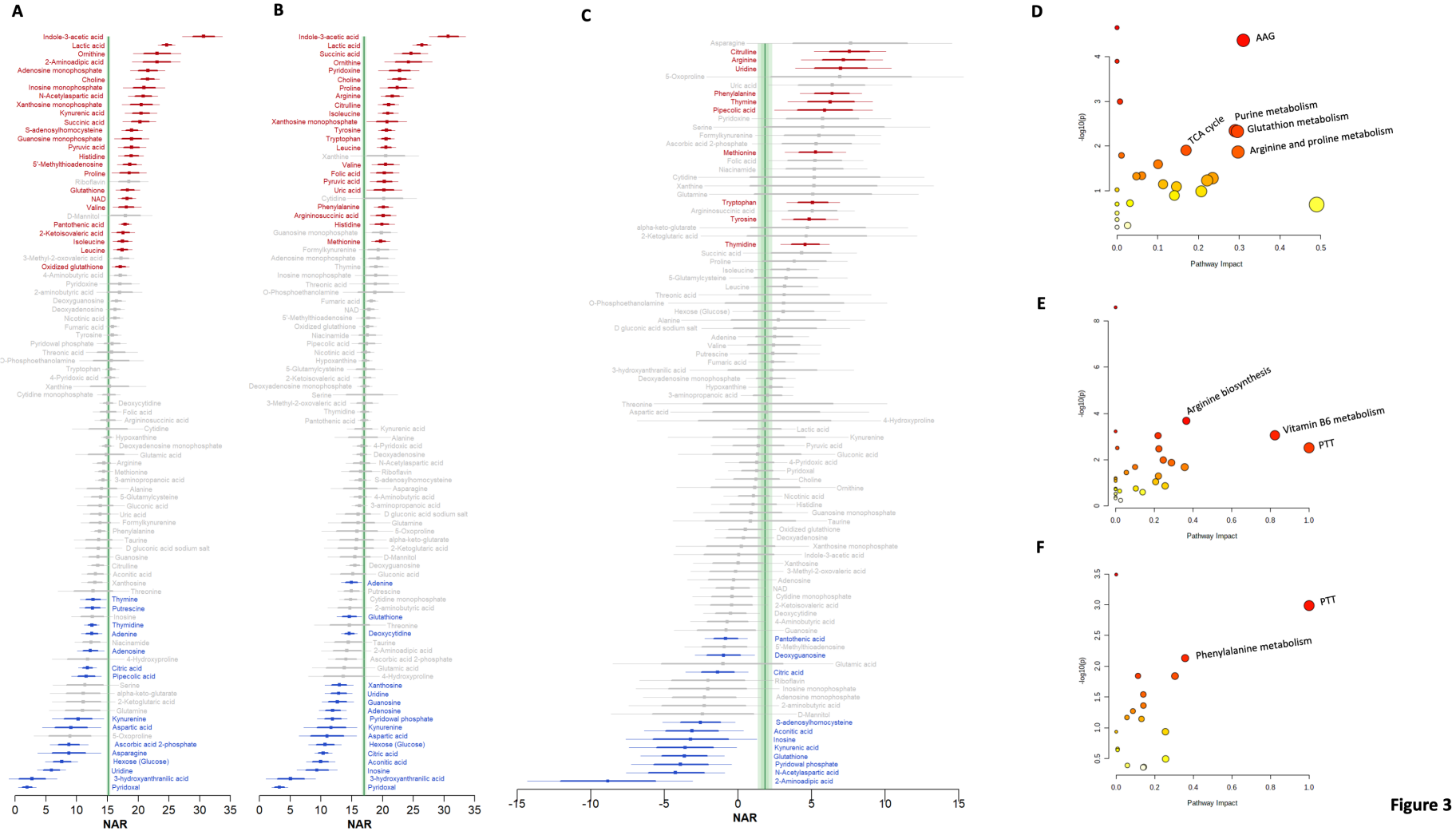

Figure 3

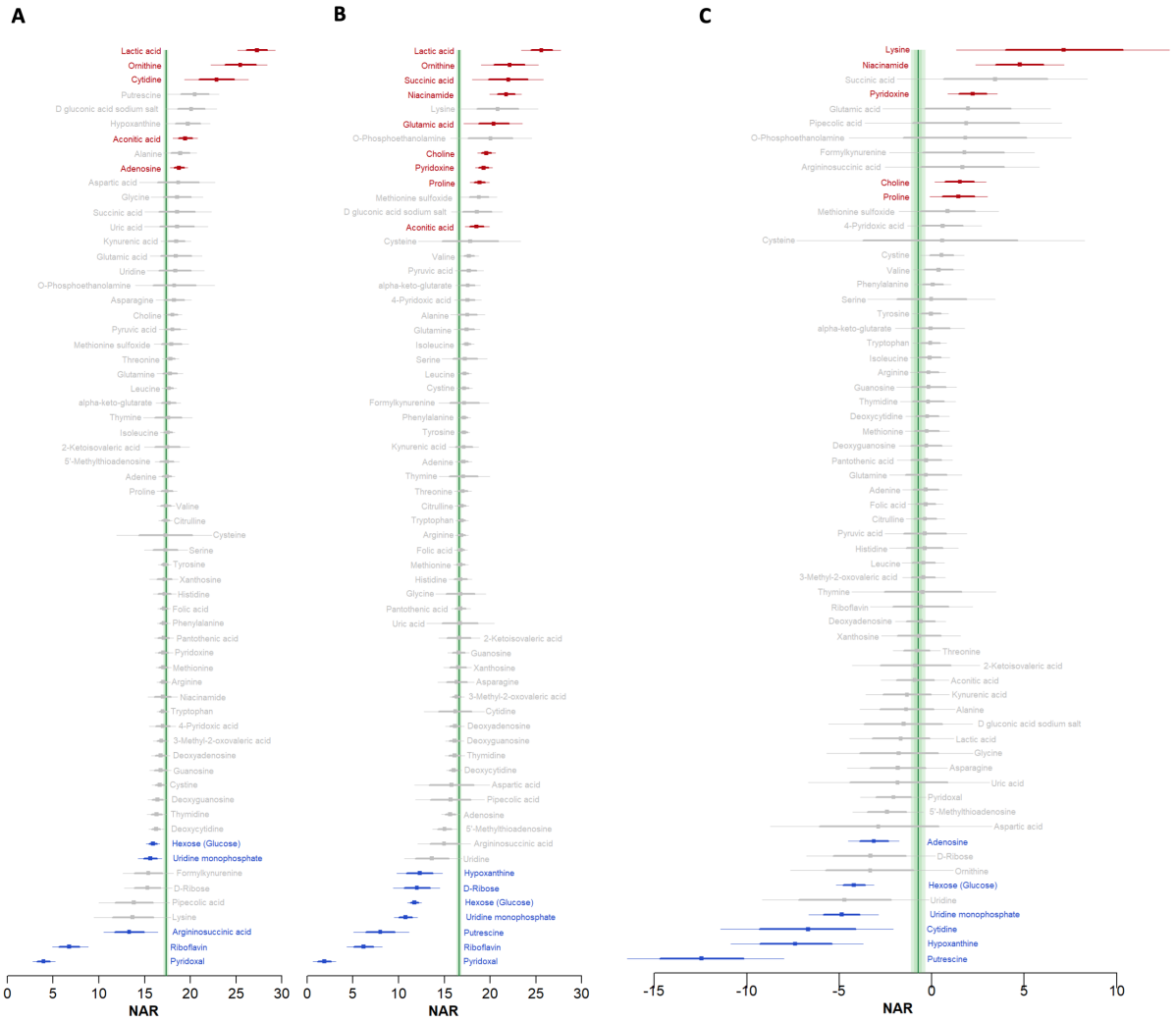

Figure 4

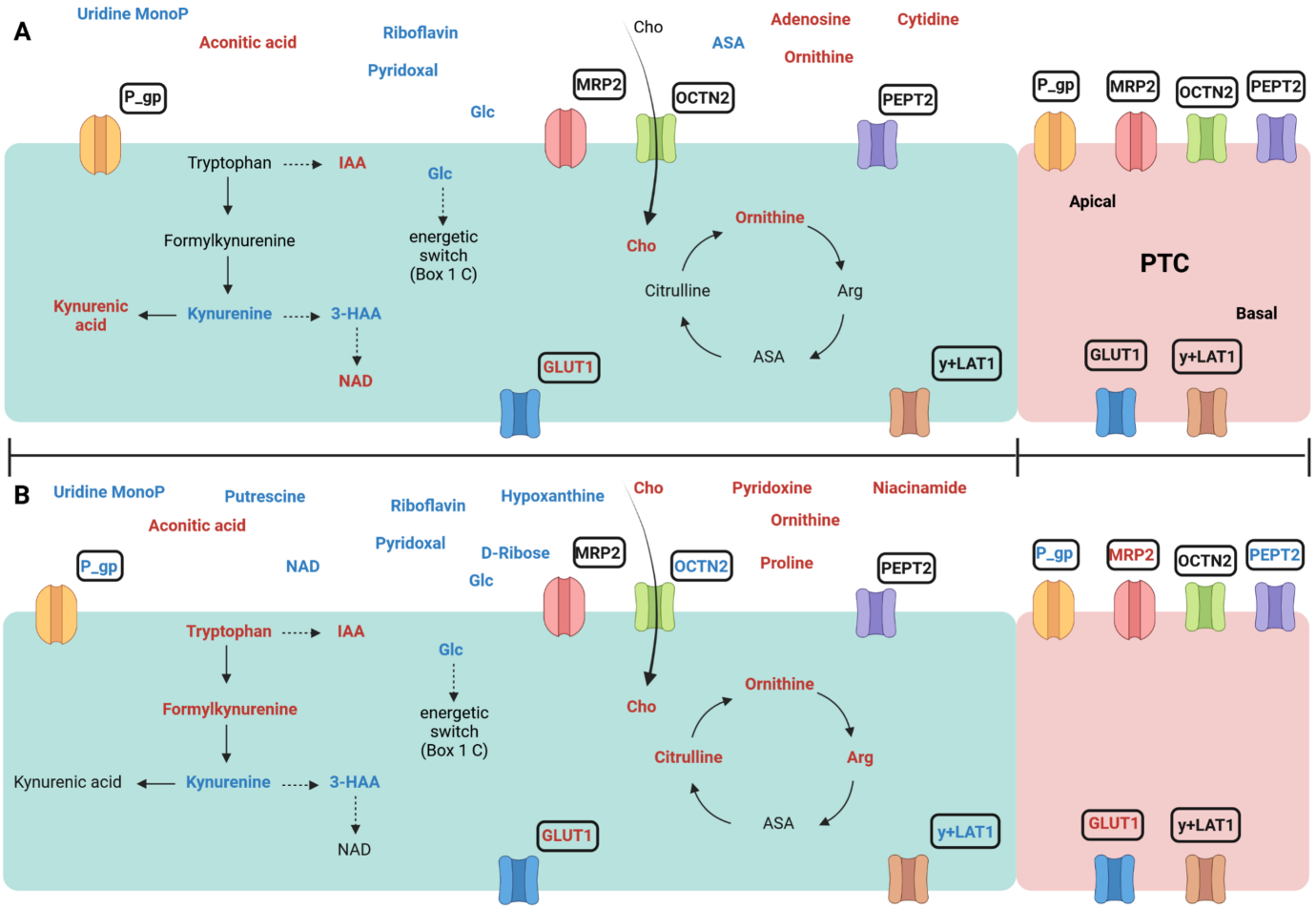

Figure 5

Rendered using BioRender.com

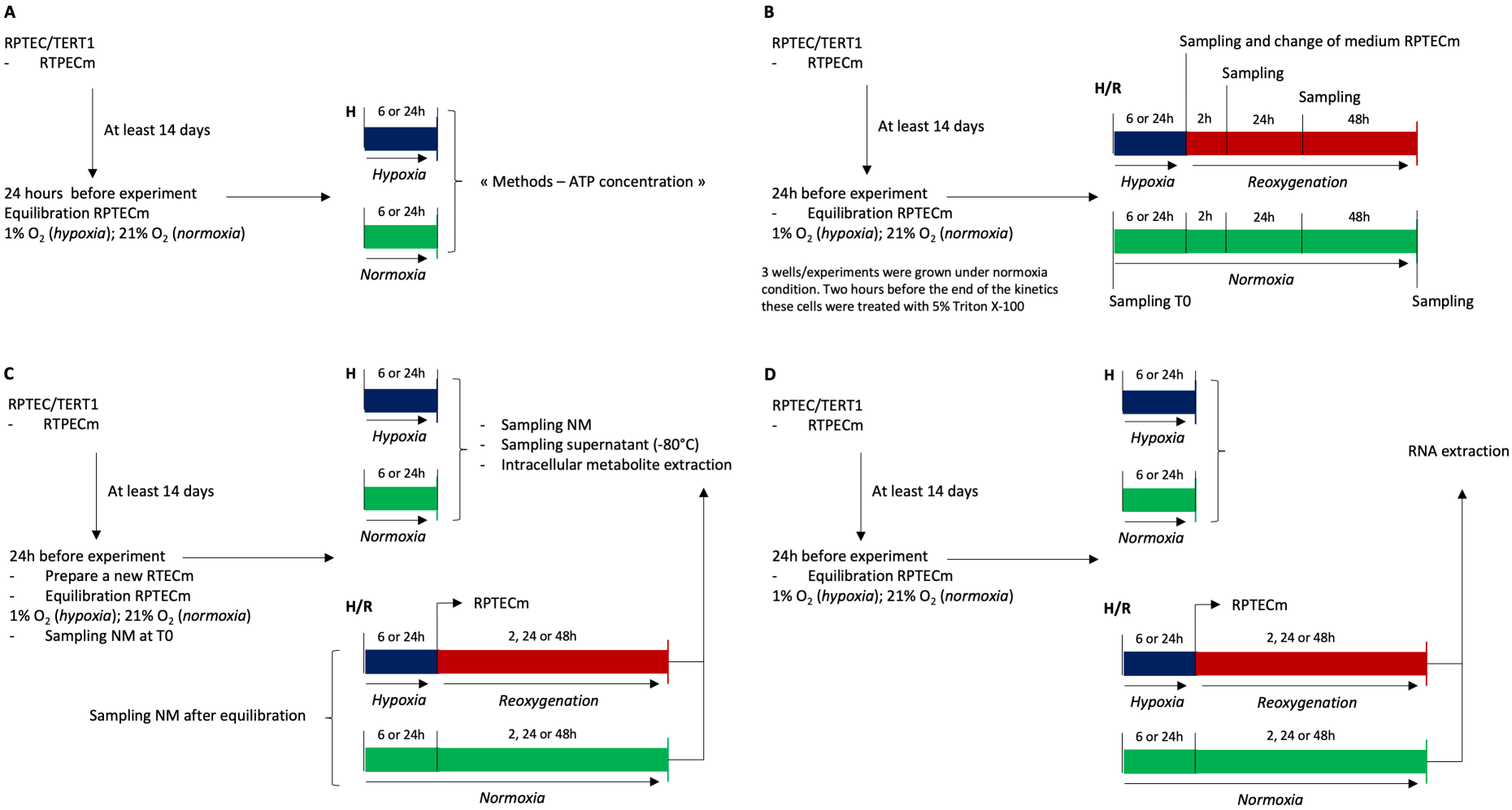

Figure 6

$$NAR_i = \frac{AR_{Hi}}{\sum_{i=1}^{3} AR_{Hi} + AR_{Ni}} =$$

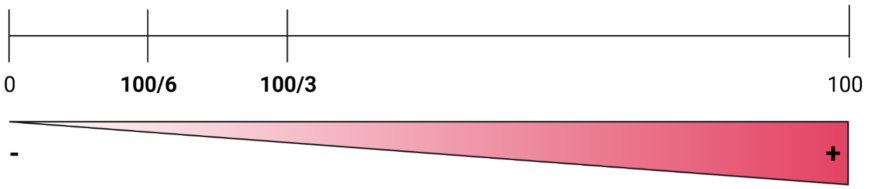

NAR = normalized area ratio
AR = area ratio
N = normoxic condition
H = hypoxic condition
i = replicate

Metabolite relative quantity under hypoxia (reoxygenation) conditions

Rendered using BioRender.com

Figure 7

II.3.3. Discussion et perspectives

II.3.3.1. Étude du transport transcellulaire transporteur-dépendant *in vitro*

II.3.3.1.1. Lignée cellulaire immortalisée et faible expression des transporteurs tubulaires

Les objectifs initiaux de notre étude fondamentale étaient d'évaluer, chez l'Homme, l'impact de l'hypoxie et de la réoxygénation sur l'expression et la localisation des transporteurs tubulaires. Nous souhaitions également caractériser l'efficacité du transport transcellulaire transporteur-dépendant lors de la cinétique de réoxygénation. Cependant, nous nous sommes heurtés aux limites des modèles cellulaires immortalisés.

En accord avec nos objectifs, nous avons sélectionné la lignée cellulaire la plus appropriée : les cellules RPTEC/TERT1. Cette lignée cellulaire immortalisée humaine présente des caractéristiques morphologiques (des microvillosités denses et des cils solitaires), fonctionnelles (production d'AMPc après stimulation avec la parathormone et pas avec l'arginine-vasopressine) et structurelles (potentiel trans-épithélial et expression de l'E-cadhérine) quasi-similaires à celles des lignées primaires[90]. Une étude avait pour but d'étudier l'expression des transporteurs de la super-famille des SLCs et ABCs pertinents pour le transport de xénobiotiques sur ce modèlecellulaire. L'expression transcriptomique de quelques transporteurs SLC (*i.e*. OCT2/3, MATE1/2, OCTN2, OAT1/2/3/4) et ABC (*i.e.* MRP2/4/5, BCRP, P-gp) avait été démontrée dans cette étude[91]. Pour autant, nous n'avons pas identifié les transporteurs OCT2/3, MATE1/2, OAT1/2/3/4 et BCRP dans nos analyses. Dans cette même étude, des études d'efflux P-gp-dépendant de substrats fluorescents, avec ou sans inhibiteurs spécifiques, avaient validé l'activité de ce transporteur. De plus, une étude de transport du substrat test (4-Di-1-ASP) sur insert de culture (Figure 7 A) avait démontré leur polarisation et leur capacité de transport trans-épithélial des cations organiques[91]. Des résultats similaires ont été rapportés par Secker et coll. avec le même substrat test[92]. Dans ces deux études, un minimum de 24 heures de culture était nécessaire pour détecter l'apparition du 4-Di-1-ASP dans le compartiment receveur. En revanche, les auteurs n'ont pas observé de transport du PAH[91] ou de la *luciferase yellow*[92], deux substrats tests du transport anionique OAT-dépendant. En accord avec nos résultats, Secker et coll. n'ont pas détecté la présence de transcrits codant pour OAT1/3 et 4 indiquant une discordance vis-à-vis de l'expression des transporteurs par ce modèle cellulaire. Dans ces deux études, les auteurs ont étudié le transport transcellulaire polarisé sans mettre en évidence son caractère transporteur-dépendant médié par OCT2 (basal) et MATE1 (apical). La longue durée d'incubation nécessaire pour objectiver le transport rend difficile la conservation des propriétés compétitives d'un inhibiteur spécifique. L'utilisation d'un autre substrat test et/ou d'une technique de détection plus sensible, avec l'objectif de diminuer la durée d'incubation, pourrait

favoriser les études de compétition substrat/inhibiteur. En ce sens, nous avons souhaité mettre au point une méthode de transport plus efficiente basée sur un substrat endogène physiologique (créatinine) *a contrario* d'un substrat exogène manufacturé (4-Di-1-ASP). Celle-ci reposait sur une méthode de dosage plus sensible, par spectrométrie de masse. Cependant, nous n'avons pas observé un transport plus rapide de la créatinine que du 4-Di-1-ASP. Nous souhaitions amplifier la capacité de transport, pour diminuer la durée d'incubation, en utilisant des milieux de transports spécifiques à chaque compartiment (concentration ionique ; pH), comme préconisé[93]. Cette méthode ne s'est pas révélée efficace. La majorité des études de transport sur inserts de culture ont recourt à des modèles cellulaires transfectés pour le(s) transporteur(s) ciblé(s)[93–95]. Ce principe n'était pas adapté à l'analyse globale des systèmes de transport membranaire de notre étude. En revanche, l'utilisation de siRNA (*small interfering RNA*) spécifiques de transcrits codant pour OCT2 et MATE1 serait envisageable afin d'induire une perte d'expression complète d'un ou des transporteurs et d'attester du caractère transporteur-dépendant lors de l'étude de transport[96–98].

Une étude récente démontre que les cellules RPTEC/TERT1 cultivées dans un système de sandwich tridimensionnel (3D) en matrigel (Figure 7 B) forment un réseau de structures tubulaires avec des cellules tubulaires hautement polarisées et une augmentation de la quantité d'ARNm codant pour des transporteurs membranaires (ex. MATE1/2 et OAT3). Des tests d'absorption ont démontré l'efficacité du transport de cations et, pour la première fois, du transport d'anions organiques, objectivé par la *luciferase yellow*[99]. Cette étude prouve que l'organisation tridimensionnelle et l'ancrage matriciel accroissent la différenciation cellulaire et la communication cellule-environnement. Cependant, ce système de culture ne permet pas d'évaluer le transport transcellulaire et se rapporte plus à l'étude de criblage de médicaments à effets néphrotoxiques. Une autre solution envisagée consistait à utiliser des cultures tubulaires primaires humaines[100]. Pour notre étude, les problématiques logistiques pour l'approvisionnement en cellules et leur dédifférenciation après un nombre limité de passages auraient rendu leur emploi trop complexe. De plus, ces cellules présentent une variabilité entre donneurs et sont prélevées sur des organes qui présentent un stade pathologique avancé et dont les structures cellulaires sont potentiellement endommagées[101].

Cette limite de l'étude globale du transport transcellulaire transporteur-dépendant sur modèle cellulaire ne devrait pas être considérée comme une fatalité inhérente à l'expérimentation *in vitro*. Au contraire, divers modèles cellulaires ou d'ingénierie émergent et la transition vers ces avancées doit être entreprise pour améliorer la pertinence des modèles expérimentaux.

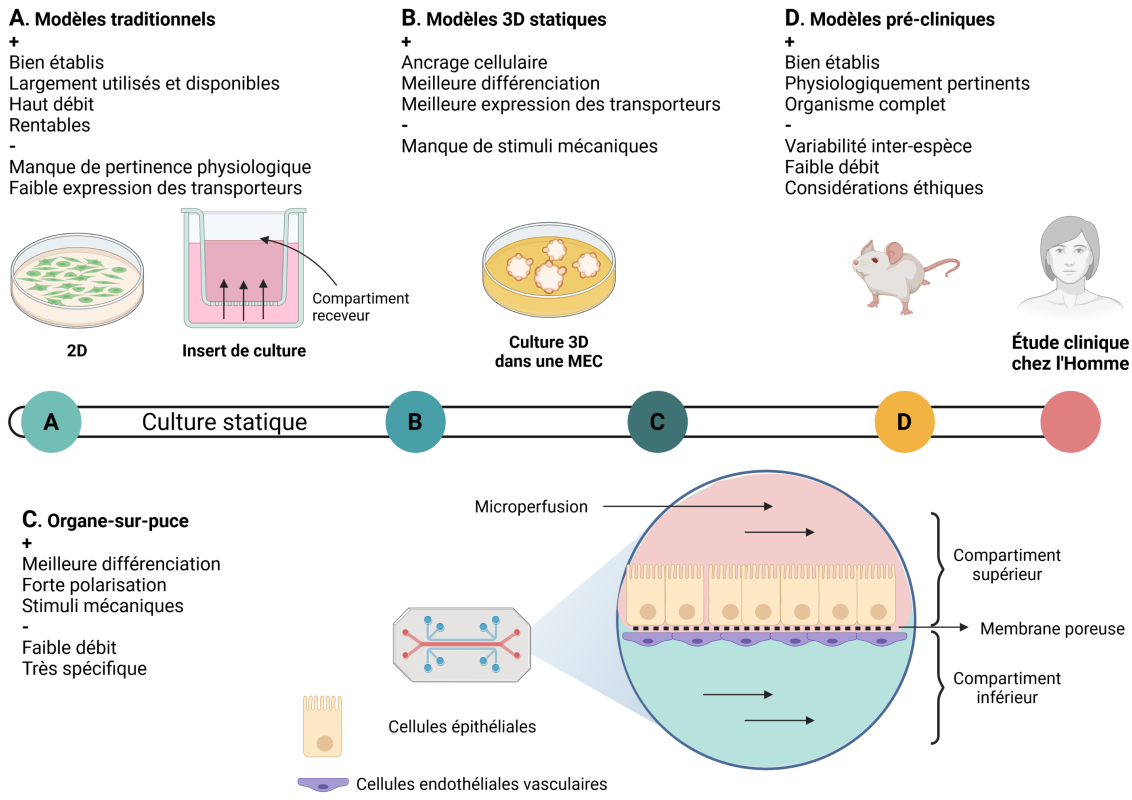

Figure 7 : Différents modèles d'études du transport tubulaire
L'illustration a été réalisée avec BioRender.com. MEC, matrice extracellulaire.

II.3.3.1.2. Organe-sur-puce (organ-on-chip)

L'organe-sur-puce (*organ-on-chip*) correspond à des cultures ou co-cultures bi-compartimentées à échelle réduite soumises à des stimuli mécaniques générés par un système micro-fluidique (Figure 8 A). Traditionnellement, l'expérimentation *in vitro* est réalisée en condition statique. Or, les cellules tubulaires proximales en conditions physiologiques sont soumises à une force de cisaillement continu (*fluid shear stress* (FSS)) et à un gradient osmotique épithélial. Chez l'Homme, nous estimons que le FSS en condition physiologique est proche de 1 dyne/cm^2 [102–104]. Des études démontrent que la présence et les variations du flux induisent des changements dans l'organisation du cytosquelette, les interactions cellule-cellule, l'expression des transporteurs ioniques et le transport de xénobiotiques[105,106]. La configuration de rein-sur-puce (*kidney-on-chip*) la plus utilisée est une culture 2D de cellules épithéliales tubulaires sur une membrane poreuse recouverte de MEC (matrice extracellulaire) et imbriquée dans des microcanaux en polydiméthylsiloxane (PDMS)[102,106,107] (Figure 8 B). Sur ce modèle, Jang et coll. ont démontré que la présence du FSS induit une augmentation de l'expression du transporteur SGLT1 et du transport trans-épithélial du glucose. La capacité d'efflux P-gp-dépendante en présence du FSS est plus forte qu'en condition statique[106]. Ces résultats laissent supposer que les processus de réabsorption et de sécrétion tubulaire des

cellules tubulaires sont améliorés avec ce système. Vormann et coll. ont développé un système de tubule proximal (TP)-sur-puce haut-débit, applicable au criblage de xénobiotiques. Celui-ci repose sur la culture de cellules tubulaires humaines immortalisées, aux capacités de transport P-gp/MRP et SGLT2-dépendant démontrées[108] (Figure 8 C). La mise au point de ce système était l'une des étapes du développement d'une plateforme microfluidique tridimensionnelle à haut débit, appelée *Nephroscreen*, utilisable pour l'étude de néphrotoxicité médicamenteuse[109]. Récemment, Yin et coll. ont mis au point un modèle de TP-sur-puce avec une co-culture de cellules endothéliales des capillaires péritubulaires cultivées dans une chambre distincte[110] (Figure 8 D). Les auteurs ont utilisé leur modèle pour une étude de cytotoxicité médicamenteuse et n'ont pas déterminé l'expression des transporteurs tubulaires et la capacité de transport trans-épithélial. Toutefois, cette co-culture épi/endothéliale renforce le caractère physiologique des modèles de TP-sur-puce.

Weber et coll. ont mis au point un système de micro-perfusion dans lequel des cellules primaires humaines de tubule proximal se fixent à une MEC et s'assemblent pour former une structure tubulaire en 3D. Le transport trans-épithélial transporteur-dépendant d'anions organiques (PAH, indoxyle sulfate) a été validé sur ce système[111]. Jansen et coll. ont cultivé des cellules tubulaires immortalisées sur des membranes fibreuses et poreuses en configuration tubulaire avec un système microfluidique (Figure 8 E). Ils ont démontré un transport cationique OCT2-dépendant efficient[112] et une sécrétion de toxines urémiques dépendante de OAT1, BCRP et MRP4[113]. Ces études prouvent que la structure et la composition des puces ne sont pas figées et que leur conceptualisation initiale est adaptable.

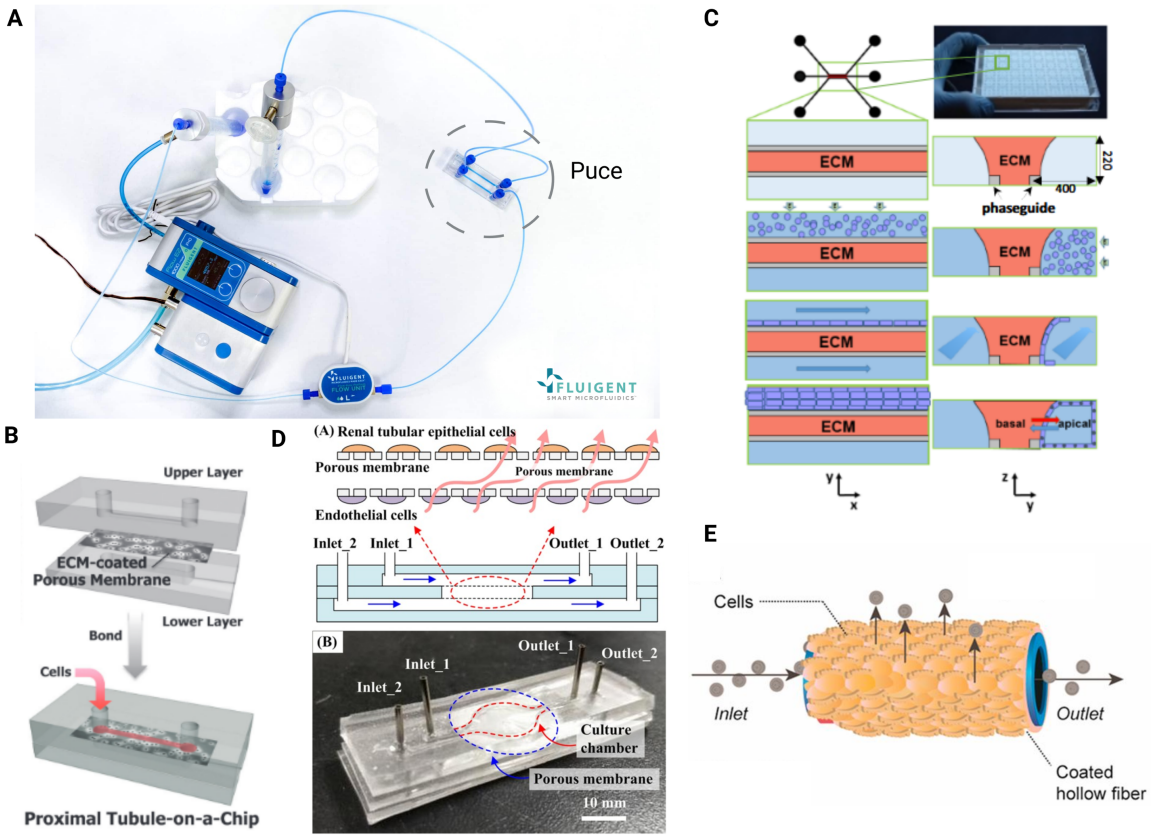

Figure 8 : Différents modèles de TP-sur-puce
(**A**) Système de micro-fluidique commercialisé par Fluigent™ © Fluigent. (**B**) Système de TP-sur-puce développé par Jang et coll.[106]. (**C**) TP-sur-puce haut-débit mis au point par Vormann et coll.[108]. (**D**) TP-sur-puce avec co-culture de cellules endothéliales proposé par Yin et coll.[110]. (**E**) TP-sur-puce en configuration tubulaire *via* l'utilisation d'une membrane fibreuse et poreuse (*Coated hollow fiver*) utilisé par Jansen et coll.[114]. Chaque figure présentée est issue de la référence associée dans la légende. L'illustration a été réalisée avec BioRender.com. ECM ; *extracellular matrix*.

II.3.3.1.3. Cellules souches induites à la pluripotence [induced pluripotent stem cell (iPSC)]

Les cellules souches induites à la pluripotence (iPSC) ont été mises au point par Takashi et Yamanaka en 2006[115]. Ils ont établi un protocole d'induction de cellules souches pluripotentes à partir de fibroblastes embryonnaires ou adultes de souris. Les iPSC correspondent à des cellules semblables aux cellules souches embryonnaires, générées par la dédifférenciation de cellules adultes provenant de tissus[101]. Ce travail a ouvert la voie à l'utilisation d'iPSC humaines, qui s'affranchissent des problèmes éthiques soulevés par l'utilisation des cellules embryonnaires humaines. De nombreux protocoles sont aujourd'hui disponibles pour la différenciation des iPSC en progéniteurs rénaux[101,116]. Des groupes de recherche ont rapporté la génération d'organoïdes rénaux à partir d'iPSC[101]. Ces organoïdes contiennent différentes structures rénales (ex. glomérulaire, tubulaire proximale et distale, et anse de Henlé). Plusieurs limitations sont à noter, notamment la présence de cellules

non-rénales à hauteur de 20% et un manque de maturité dans le processus de différenciation[101]. Ces limitations empêchent, à l'heure actuelle, l'utilisation de ces organoïdes dans le cadre de thérapies cellulaires régénératives.

Des progrès ont été réalisés afin de générer des organoïdes plus petits appelés micro-organoïdes[117]. Cette démarche a pour objectif de développer des monocultures de cellules spécifiques. Kandasamy et coll. ont établi un protocole dédié à la génération de cellules de type HPTC (*human proximal tubular cell*) dérivées de hiPSC (*human* iPSC)[118]. Ces cellules présentent des profils d'expression génique, des caractéristiques fonctionnelles et morphologiques typiques des cellules tubulaires proximales primaires. Ces cellules expriment les transporteurs OAT3, GLUT1, SGLT1 et PEPT1. De plus, l'utilisation d'inhibiteurs spécifiques de OAT1/3 (probénécide) et OCT2 (cimétidine) ont réduit la toxicité de la citrinine et de la rifampicine, respectivement substrats de OAT1/3 et OCT2. Ces résultats suggèrent que ce modèle de HPTC dérivé de hiPSC présente des capacités de transport tubulaire transporteur-dépendant. Plus récemment, Chandrasekaran et coll. ont développé un modèle de cellules tubulaires dérivé d'iPSC avec un protocole différent, dans lequel la capacité d'efflux P-gp-dépendante était similaire à des cellules primaires[119]. Toutefois, seule l'expression de quelques transporteurs a été évaluée dans ces études. À l'avenir, l'expression d'autres transporteurs devra être testée pour améliorer la caractérisation de ces modèles, d'autant plus que la variabilité inter-patients des hiPSC utilisées influence la différenciation tubulaire[118].

II.3.3.1.4. Bio-impression (Bioprinting)

La bio-impression (*bioprinting*) est un procédé de fabrication additive basé sur la disposition précise de biomatériaux pour produire artificiellement des tissus biologiques. Les techniques (ex. bio-impression assistée par pression, stéréolithographie, bio-impression électromagnétique) et les biomatériaux (ex. polymères thermoplastiques, hydrogels, résines) utilisés sont multiples. Ces dernières années, l'utilisation de ces technologies pour la biofabrication de modèles *in vitro* a considérablement augmenté. Le développement de ces systèmes est difficile et demande un effort logistique important. Toutefois, la mise au point récente de modèles *in vitro* de tubule proximal est encourageante. Nous présenterons ici uniquement les modèles de tubule proximal *in vitro* générés par bio-impression. Pour plus d'informations sur le domaine de la bio-impression, nous recommandons la référence[120].

Face au manque de géométrie tridimensionnelle des modèles de reins-sur-puce traditionnel, Homan et coll. ont mis au point un modèle micro-perfusé avec une architecture tubulaire contournée[121] (Figure 9 A). Dans ce modèle, les cellules tubulaires proximales exhibaient une morphologie épithéliale, une polarisation, une différenciation et des propriétés fonctionnelles caractéristiques de ces cellules. Lin et coll. ont développé un modèle de tubule

proximal vascularisé en 3D, composé de canaux indépendamment perfusés en cycle fermé, imbriqué dans une matrice extracellulaire et tapissés d'un épithélium ou d'un endothélium confluent l, appelé *3D VasPT* pour *3D vascularizedPT*[122] (Figure 9 B). Grâce à leur méthode d'impression, les auteurs ont pu créer une structure plus complexe au moyen de TP contournés avec une lumière ouverte et composés de cellules RPTEC/TERT1. Ils ont validé le processus de réabsorption tubulaire du glucose et la diaphonie épithélium-endothélium. Plusieurs vidéos de leur méthode de bio-impression sont disponibles dans la section *Supporting Information via* le DOI (https://doi.org/10.1073/pnas.1815208116).

Par l'utilisation d'une technique d'impression spécifique, Singh et coll. ont développé des tubes micro-fluidiques creux formant un parenchyme de tubules et de vaisseaux juxtaposés, composés de cellules épithéliales et endothéliales tubulaires rénales, respectivement[123] (Figure 9 C). Dans ces études, la capacité sécrétrice des cellules tubulaires proximales n'a pas été évaluée. Néanmoins, elles montrent l'intérêt des techniques de bio-impression pour favoriser la conception biomimétique de modèles de complexité croissante.

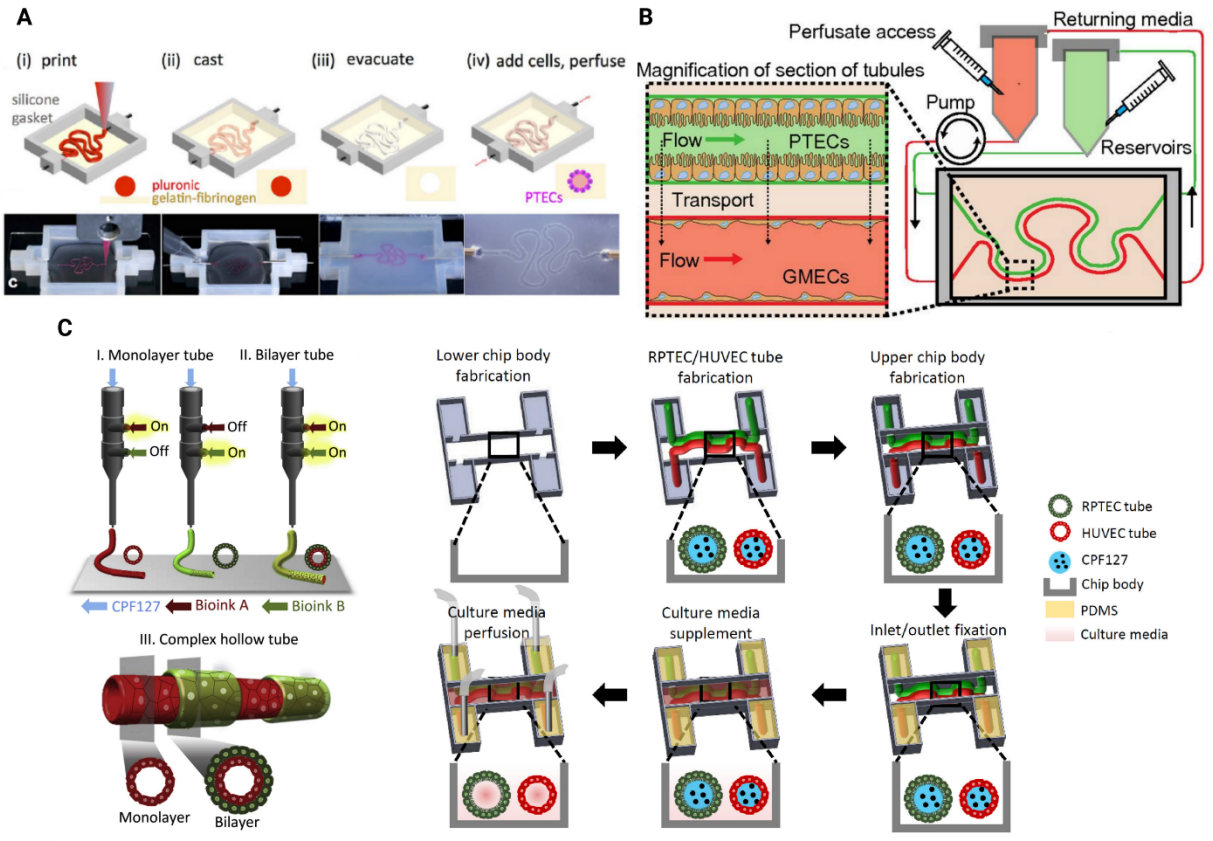

Figure 9 : Différents modèles de tubule proximal générés par bio-impression

(**A**) Modèle de tubule proximal contourné proposé par Homan et coll.[121]. (**B**) Modèle *3D VasPT* développé par Lin et coll.[122]. (**C**) Modèle de tube proximal creux et perfusé mis au point par Singh et coll.[123]. Chaque figure présentée est issue de la référence associée dans la légende. L'illustration a été réalisée avec BioRender.com. CPF127, *$CaCl_2$ solution* ; GMEC, *glomerular microvascular endothelial cells* ; HUVEC, *human umbilical vein endothelial cells* ; (R)PTEC, *(renal) proximal tubular epithelial cells* ; PDMS, *polydimethylsiloxane*.

Cette liste non-exhaustive de perspectives concernant les modèles cellulaires et les techniques d'ingénieries a pour but de mettre en lumière les opportunités d'amélioration de la robustesse des modèles in-vitro. Au niveau pharmacologique, de nombreuses études sont menées sur la biodisponibilité, la toxicité et la clairance des xénobiotiques. Les cellules épithéliales en contact avec les divers bio-fluides de l'organisme (ex. hépatocytes, entérocytes, cellules tubulaires proximales) sont d'une importance capitale dans les processus cités plus haut. Elles ont une structure et une fonctionnalité hautement dépendantes de l'environnement polarisé et dynamique dans lequel elles évoluent. En ce sens, les modèles micro-perfusés et bi-compartimentaux améliorent considérablement leur différenciation et tendent à réduire l'écart avec leurs propriétés physiologiques. La généralisation de ces modèles accroîtra la fiabilité, la précision et la reproductibilité des études pharmacologiques sur modèle cellulaire. Un phénomène déjà observé pour l'étude de toxicité et de criblage de médicaments.

Progressivement, des systèmes plus complexes émergent : les multi-organes-sur-puce (*multi-organs-on-chip*) avec la perspective du corps/humain–sur-puce (*body/human-on-chip*) (Figure 10). Ces modèles visent à simuler un corps entier en connectant, par micro-perfusion, plusieurs microsystèmes cellulaires entre eux. Bien que le développement et la standardisation d'un tel modèle soient soumis à de nombreuses contraintes, celui-ci favorisera la mise en route d'études de pharmacologie de système et apportera plus de précisions sur le devenir et la toxicité des médicaments dans l'organisme[124,125]. Ces modèles permettront, en outre, de réduire la dépendance de la recherche préclinique aux modèles animaux. Pour la transposition vers la clinique, des modèles de patients-sur-puce (*patients-on-chip*) sont envisagés. Schutgens et coll. ont mis au point un protocole pour la génération de « tubuloïdes » à partir de cellules humaines isolées de tissus rénaux et d'urines[126]. Dans ce travail, un système de tubuloïdes-sur-puce fonctionnel a été développé. Encore plus intéressant, les auteurs ont démontré que les tubuloïdes rénaux dérivés de l'urine d'un patient souffrant de mucoviscidose permettent d'évaluer *ex vivo* l'efficacité d'un traitement correcteur de cette pathologie.

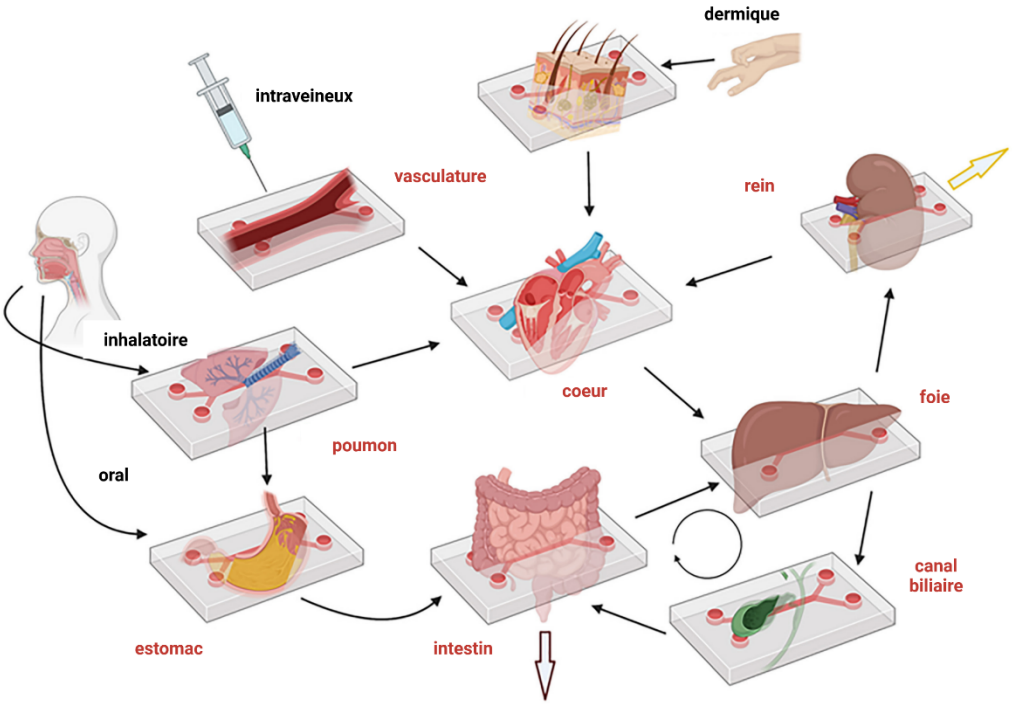

Figure 10 : Multi-organes-sur-puce et perspectives en pharmacologie de système
Principales voies d'exposition (texte noir) pour les produits pharmaceutiques et chimiques et leur distribution et leur élimination dans les systèmes d'organes pertinents (texte rouge) à évaluer par un système potentiel multi-organes-sur-puce. La figure et la légende sont adaptées de la référence [125]. L'illustration a été réalisée avec BioRender.com.

II.3.3.2. Machine de perfusion et administration thérapeutique

Les technologies de perfusion d'organes (HMP et NMP) offrent également les avantages d'une plateforme pour l'administration de thérapies pré-greffe. Une revue récente recense les avancées dans l'application des thérapies régénératives et des agents biologiques ciblant l'IRI et le rejet aigu pendant la perfusion rénale[127]. Ces thérapies incluent des nanoparticules, des agents anti-inflammatoires et des anticorps monoclonaux. D'un point de vue clinique, seules quelques études ont été effectuées. Une étude sur les effets de cinq agents vasoactifs (la prostaglandine E1, la trifluopérazine, le vérapamil, la papavérine et le mannitol) sur des reins issus d'ECD a montré que seule la prostaglandine E1 améliorait la fonction rénale précoce[128]. De nouvelles études doivent être menées pour identifier des candidats thérapeutiques efficaces, y compris par ciblage à haut débit. La modulation fonctionnelle des transporteurs pendant la période ischémique pourrait diminuer l'efficacité thérapeutique de certaines thérapies pré-greffe, ou au contraire constituer une stratégie préventive additionnelle.

Discussion et perspectives générales

Ce travail de thèse à visée exploratoire avait pour but d'étudier l'impact de l'ischémie et de l'hypoxie/réoxygénation sur l'expression et la fonctionnalité des transporteurs tubulaires rénaux.

Pour répondre à ces problématiques nous avons opté pour une approche translationnelle de la clinique vers la recherche fondamentale et *vice-versa*. Sur un modèle cellulaire humain, nous avons montré l'existence d'un mécanisme de régulation transcriptionnel différentiel et hypoxie-dépendant des transporteurs tubulaires proximaux. Ce mécanisme a divers effets (sur/sous-expression), il n'affecte pas tous les transporteurs, il est dépendant de la durée d'hypoxie et il peut être maintenu qu'à court terme au cours de la réoxygénation. Sur une cohorte de patients transplantés, nous avons observé que l'expression transcriptionnelle des transporteurs, en période pré-implantatoire, n'était pas prédictive de la fonction rénale post-greffe. Toutefois, l'estimation de cette fonction (IGF ou non-IGF) était rapportée à l'évaluation de la créatininémie à J7, un paramètre majoritairement associé au débit de filtration glomérulaire qui ne reflète pas spécifiquement la fonction tubulaire rénale. Pour statuer sur le rôle prédictif des transporteurs tubulaires en transplantation rénale, l'étude de leur fonctionnalité en période post-implantatoire serait plus pertinente. L'utilisation d'un critère d'évaluation de la sécrétion tubulaire, équivalent aux marqueurs exogènes (inuline et iohexol) fréquemment utilisés pour mesurer le débit de filtration glomérulaire, permettrait de positionner la fonction tubulaire comme un critère d'évaluation à part entière de la fonction rénale post-greffe. Aussi, l'évaluation de la fonction tubulaire permettrait de mieux caractériser la DGF dont la définition est reconnue comme imparfaite. En ce sens, une attention particulière a récemment été accordée à la sécrétion tubulaire en tant que fonction rénale sous-estimée dans l'évolution de l'insuffisance rénale chronique[129–132]. L'impact de la durée d'hypoxie sur l'expression transcriptionnelle des transporteurs, constaté *in vitro* à +37°C, n'est pas confirmé avec les organes conservés sur machine de perfusion à +4°C puis transplantés chez les patients de l'étude RENALIFE. En revanche, l'étude clinique a permis de mettre en évidence une forte variabilité interindividuelle de la modulation d'expression transcriptionnelle des transporteurs, qui reste donc inexpliquée. Toutefois, l'expression transcriptionnelle ne préjuge pas à elle seule de la modulation fonctionnelle des transporteurs.

Dans notre revue de littérature, nous avions mis en avant une perturbation d'expression et de fonctionnalité des transporteurs, durable lors de la reperfusion. À l'inverse des modèles précliniques d'ischémie chaude, l'expression transcriptionnelle des transporteurs tubulaires a montré que cette modulation disparaissait au bout 48 heures de réoxygénation sur cultures cellulaires isolées. L'ischémie chaude, réalisée *in vivo* par clampage artériel, entraîne une

privation en oxygène, en nutriments et un arrêt du flux circulant. Dans notre modèle, seul l'absence d'oxygène en condition statique a été étudiée. Par conséquent, nous supposons que la régulation transcriptionnelle des transporteurs observés n'est gouvernée que par l'hypoxie. Des expérimentations de *Chip-Seq* permettraient d'étudier la relation entre HIF-1α et les gènes codant pour les transporteurs, ainsi que d'identifier le mécanisme sous-jacent de cette régulation[133].

Nous souhaitions étudier la fonctionnalité des transporteurs dans leur ensemble. Pour couvrir un large spectre de substrats pris en charge par les transporteurs, nous avons opté pour une approche métabolomique semi-ciblée dans les perfusats de greffon et sur culture cellulaire isolée. Cependant, les métabolites impactés par la durée d'ischémie ou d'hypoxie n'étaient pas corrélés à l'expression transcriptionnelle des transporteurs tubulaires, et n'étaient pas des substrats connus de ces transporteurs. Au niveau cellulaire, l'étude des profils métabolomiques extra/intracellulaires a révélé que la réoxygénation cellulaire s'accompagne d'un retour rapide à un état d'équilibre. L'absence de variation dans les échanges cellule-environnement lors de la réoxygénation souligne que ce phénomène n'affecte pas la fonctionnalité des systèmes de transport dans leur ensemble. La présence de profils d'expression différents pour les différents transporteurs, couplée à la nature multi-spécifique de certains substrats suggère des mécanismes de transport inter-transporteurs compensatoires qui tendent à favoriser l'homéostasie métabolique.

Le recours à une approche métabolomique semi-ciblée visant à identifier plusieurs substrats potentiels, et par conséquent augmenter le nombre de transporteurs étudiés, s'est révélé peu adapté. Il nous a amené à appréhender ce sujet sous un angle soit trop restreint, soit trop large. Les déséquilibres métaboliques inhérents à un dysfonctionnement des transporteurs pourraient ne représenter qu'une variation métabolique minime, auquel cas cette approche n'est pas adaptée. À l'inverse, la méthode métabolomique semi-ciblée ne concernait pas un grand nombre de substrats des transporteurs. L'absence de données métabolomiques plus conséquentes, non ciblées, est une limite importante à l'identification de biomarqueurs prédictifs dans notre cohorte. Les métabolites endogènes impactés par une modulation des transporteurs pourraient alimenter le métabolisme cellulaire et se révéler indétectables à un temps donné. Finalement, dans cette étude, l'absence de données d'expression protéique et de localisation des transporteurs, ainsi que le manque de tests de fonctionnalité n'a pas permis de statuer quant à l'impact de l'hypoxie/réoxygénation sur la fonctionnalité des transporteurs tubulaires.

Nous proposons donc d'aborder à l'avenir cette problématique par une approche ciblée. Nous conseillons de sélectionner des couples de transporteurs (SLCs et/ou ABCs) impliqués dans un transport vectoriel et d'étudier l'impact de l'ischémie et de l'IR sur leur fonctionnalité,

leur expression et leur localisation. Bien que nous ayons démontré un mécanisme transcriptionnel hypoxie-dépendant, l'altération éventuelle de la fonction de transport à court terme serait d'avantage associée à une perturbation protéique, qu'elle soit une dégradation ou une perte de distribution membranaire. L'utilisation de substrats hautement spécifiques de ces couples de transporteurs apporterait une réponse claire quant à leur perturbation fonctionnelle. L'utilisation de substrats endogènes radiomarqués permettrait également de déterminer l'impact de cette modulation sur le métabolome de façon plus spécifique. Enfin, d'autres substrats endogènes et exogènes tels que les toxines urémiques et xénobiotiques pourraient être considérés pour étudier l'éventuelle compétitivité synergique entre substrats.

Protocoles expérimentaux proposés

Ici, nous proposons des perspectives pour compléter nos travaux et statuer quant à la modulation IR-dépendante des transporteurs tubulaires et ses conséquences en transplantation rénale.

Chez l'Homme

Pour étudier l'impact de l'ischémie sur le transport tubulaire transporteur-dépendant, la conduite d'une étude clinique menée sur des reins non-transplantables avec l'utilisation de substrats tests spécifiques sera nécessaire (Figure 11). Cette étude visera à déterminer la fonctionnalité des transporteurs tubulaires au cours de la conservation du greffon. Le liquide urinaire devra être collecté au fur et à mesure de la conservation et le(s) substrat(s) test(s) supplémenté(s) dans le liquide de perfusion. Ce dernier devra circuler en cycle fermé pour maintenir l'état d'hypothermie des tissus rénaux et pour accentuer l'exposition des cellules tubulaires aux substrats tests. Des tissus sains non-ischémiés devront être collectés comme contrôles, pour déterminer l'expression et la localisation physiologique des transporteurs.

Les transporteurs OAT1/3 et BCRP pourrait être évalués dans le cadre du transport d'anions organiques et les transporteurs OCT2, MATE1 et P-gp pour le transport de cations organiques avec des substrats spécifiques (l'indoxyl sulfate (IS) pour le transport d'anions, le tétraéthyl ammonium (TEA) pour le transport de cations). Les concentrations de substrats seront mesurées en fin de perfusion dans le perfusat et les urines par LC-MS[134]. Ces expériences de transport *ex vivo* devront être complétées par l'utilisation de métabolites marqués par des isotopes, à l'instar des travaux de Nath et coll.[135,136]. L'utilisation de ces métabolites renseignera sur l'impact de l'ischémie sur le transport tubulaire et l'influence de cette modulation sur le flux métabolique. Le rôle des transporteurs tubulaires dans l'activité métabolique du greffon lors de sa conservation sera alors clarifié. Dans notre revue de littérature, nous avions mis en avant divers mécanismes responsables de cette modulation

(ex. perturbation du gradient de concentration, privation en ATP, modification de la cyto-architecture et facteurs de transcription). L'étude combinée de l'expression, de la localisation et de la fonctionnalité des transporteurs apportera des indications sur le mécanisme sous-jacent prédominant et orientera les recherches futures à visée thérapeutique. Cependant, un tel projet pourrait se heurter à des contraintes logistiques majeures limitant sa faisabilité. En outre, l'utilisation de reins jugés non-transplantables suppose des altérations importantes des structures histologiques, représentant un biais potentiel vis-à-vis de la fonctionnalité des transporteurs tubulaires.

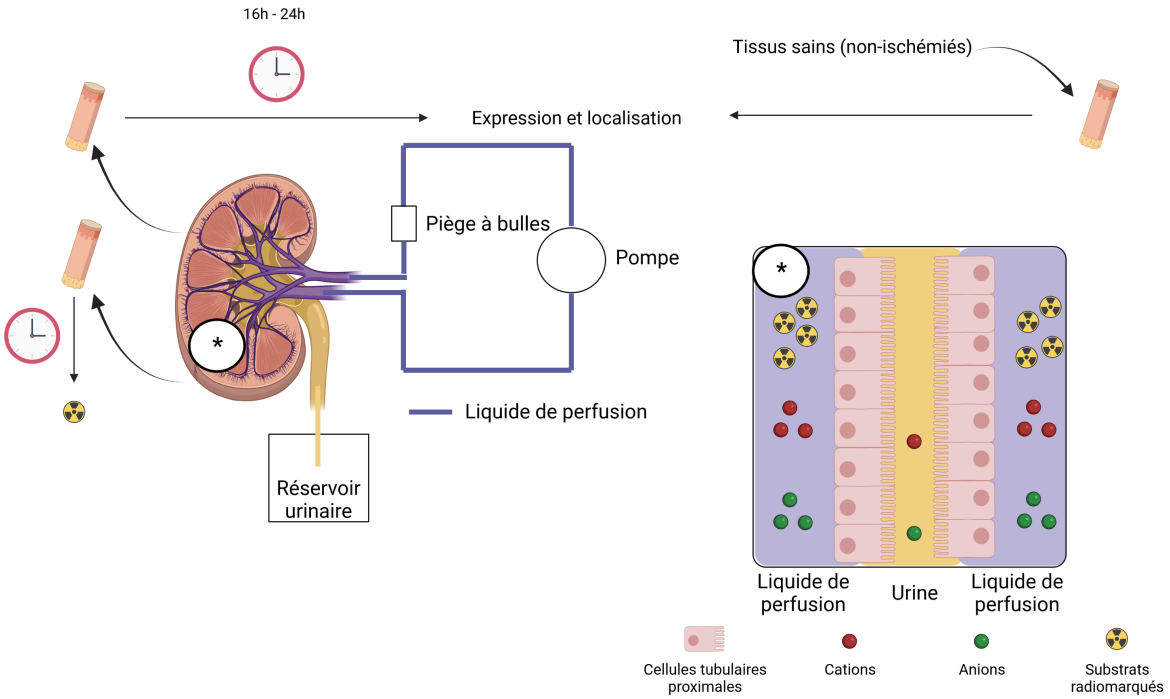

Figure 11 : Modèle d'étude de la fonction tubulaire transporteur-dépendante chez l'Homme
L'illustration a été réalisée avec BioRender.com.

Sur modèle préclinique

Une étude *ex-vivo* et *in-vivo* sur un modèle d'auto-transplantation porcin est à considérer. Elle pourra être inspirée des travaux de, ou en collaboration avec, l'unité de transplantation rénale et pancréatique des Cliniques universitaires Saint-Luc dirigée par le Pr. Michel Mourad[76–78] ou de l'unité du Dr. Zoltan Czigany de l'Hôpital universitaire RWTH Aacheen[137]. Le protocole envisagé est présenté en Figure 12. Cette étude aura pour objectif de déterminer l'effet de l'ischémie et de l'IR, dans le contexte de la transplantation rénale, sur l'expression, la localisation et la fonctionnalité des transporteurs tubulaires OAT1 (slc22a6) et BCRP (abcg2). Ici, nous avons développé un protocole basé sur ce couple de transporteur, d'autres couples pourraient être considéré avec l'utilisation de substrats spécifiques. Pour évaluer l'influence de l'oxygénation tissulaire pendant la perfusion rénale sur la modulation des

transporteurs tubulaires, des modèles de conservation HMP et $HMPO_2$ seront comparés. Concernant le protocole expérimental, le prélèvement d'une biopsie rénale devra être réalisé en amont de la procédure chirurgicale pour déterminer l'expression et la localisation basale des transporteurs. Pour mimer un donneur DCD, un clampage artériel devra être effectué 30 minutes avant le prélèvement de l'organe. L'organe prélevé devra être conservé sur l'une des machines de perfusion pendant 15h (en France en 2020, la durée moyenne d'ischémie froide était de 15,1h[3]). Une biopsie devra être prélevée en fin de perfusion pour étudier l'impact de l'ischémie sur l'expression et la localisation des transporteurs ciblés. Après la procédure chirurgicale d'auto-transplantation orthotopique, des biopsies devront être prélevées à différents temps de reperfusion pour étudier la cinétique d'évolution des transporteurs. En parallèle, des données cliniques de référence telles que la créatininémie, la créatininurie et l'évaluation anatomopathologique devront être collectées afin d'étudier la corrélation entre les critères d'évaluation standard et la modulation des transporteurs tubulaires, c'est-à-dire la corrélation ou non entre l'efficacité de la filtration glomérulaire et de la sécrétion tubulaire.

L'étude de l'excrétion tubulaire OAT/BCRP-dépendante impliquera l'intégration d'une cohorte de référence incluant des modèles précliniques pseudo-opérés. Elle sera inspirée des travaux de Bush et coll.[138] et devra consister en la perfusion sanguine de d'IS. La clairance de l'IS (mL/min) devra être ensuite calculée *via* la formule suivante [(concentration d'IS urinaire × volume urinaire) / (concentration d'IS plasmatique × temps)]. Le mesure des concentrations plasmatiques et urinaires sera réalisé par LC-MS[134]. Pour prendre en compte la cinétique de réoxygénation, deux groupes d'étude devront être constitués : un premier groupe dont la fonctionnalité sera évaluée après 1 jour de reperfusion et un second après 7 jours. Le premier informera sur la modulation à court terme, tandis que le second permettra de multiplier les prélèvements biopsiques et de comparer la fonctionnalité excrétrice tubulaire avec la créatininémie à J7.

Parmi les limites d'une telle approche : la variabilité inter-individuelle et inter-espèce inhérente au modèle préclinique affaiblira l'extrapolation *in vivo*/clinique des résultats ; les considérations éthiques mises en avant par la réglementation européenne récente visant à réduire le recours à des modèles animaux pourrait constituer un frein pour la mise en œuvre de ce protocole (https://www.europarl.europa.eu/doceo/document/TA-9-2021-0387_EN.html).

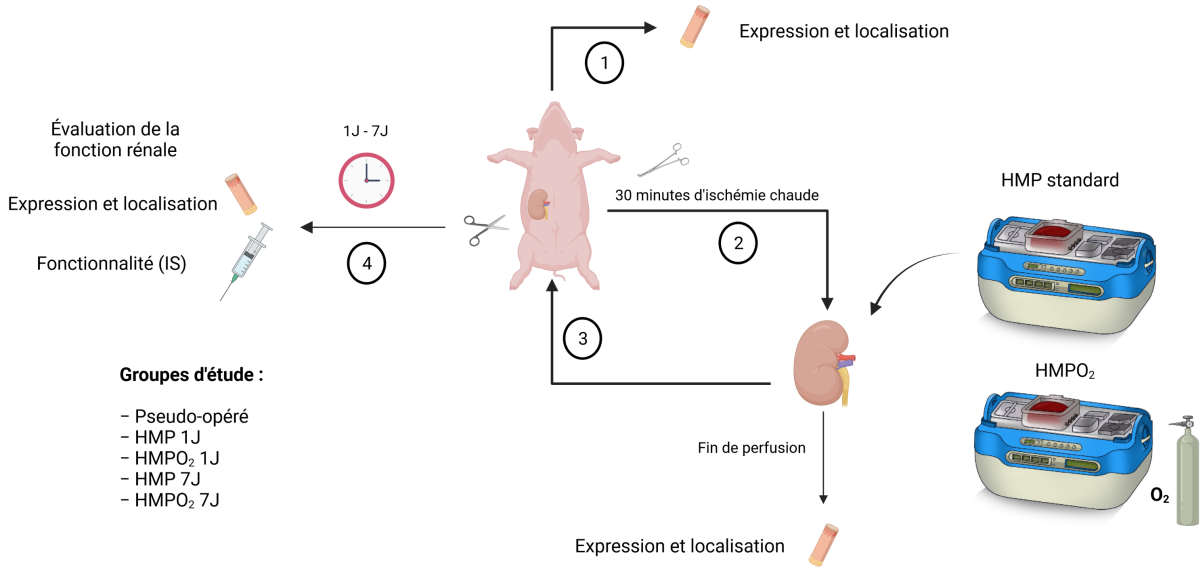

Figure 12 : Modèle d'auto-transplantation orthotopique chez le porc pour l'étude de l'influence de l'IR sur la fonction tubulaire transporteur-dépendante
(**1**) Prélèvement de référence en amont de l'acte chirurgical, (**2**) induction d'une ischémie chaude et mise du greffon sur machine, (**3**) procédure d'auto-transplantation orthotopique et (**4**) suivi post-greffe. L'illustration de la machine de perfusion est issue de la référence [139]. Un aperçu de la procédure chirurgicale d'auto-transplantation orthotopique réalisée dans l'étude [137] est disponible *via* le DOI (10.3791/61591). L'illustration a été réalisée avec BioRender.com. IS, *indoxyl sulfate*.

Sur modèle cellulaire

L'utilisation d'un organe-sur-puce couplé à un système de perfusion hypoxique semble être le modèle le plus approprié. Le plan expérimental envisagé est présenté en Figure 13. En premier lieu, les HPTC dérivées de hiPSC devront être mises au point en s'appuyant sur le protocole proposé par Chandrasekaran et coll.[119] (Figure 13 A). Les hiPSC, disponibles auprès de la *European Bank for induced Pluripotent stem cells* (https://cells.ebisc.org/), seront cultivées en routine sur une surface d'adhésion spécifique (*Geltrex™ Basement Membrane Matrix*) dans un milieu commercialisé (mTeSR1) permettant l'auto-renouvèlement et le maintien de la pluripotence. La différenciation des hiPSC en HPTC est un protocole multi-étapes incluant des milieux de culture différents et l'ajout de molécules spécifiques. Brièvement, les hiPSC seront traitées à l'accutase puis ensemencées sur une surface d'adhésion spécifique avec un milieu de différenciation (Annexe 3 : milieu de différenciation des hiPSC).
La phase I correspond à la sortie de pluripotence et à l'induction du mésoderme intermédiaire néphrogénique. Cette induction sera générée par la supplémentation du milieu avec du CHIR99021 (un inhibiteur spécifique de la glycogène synthase kinase 3β qui active la signalisation Wnt canonique) et du TTNPB (un agoniste du récepteur de l'acide rétinoïque)[140].

La phase II correspond à l'engagement tubulaire des cellules. Celles-ci seront alors incubées dans un milieu de culture spécifique des cellules tubulaires proximales (Annexe 3) supplémenté avec du FGF9 (facteur de croissance fibroblastique).
La phase III est une phase de stabilisation d'une durée de 7 jours avec des changements de milieu tous les 2-3 jours sans ajout de FGF9. Les critères de jugement initiaux pour la validation du modèle cellulaire HPTC devront être centrés sur l'évaluation morphologique et cyto-architecturale, ainsi que sur la mesure de marqueurs de différenciation tubulaire spécifiques (ex. expression de la mégaline et réponse à la PTH). L'expression des transporteurs cibles (OAT1/3, MRP2/4, OCT2, MATE1 et P-gp) devra être évaluée.

Chandrasekaran et coll. ont montré que leur modèle HPTC pouvait être cultivé après au moins un passage, en présence de *GW788388 hydrate*, de FCS (*fetal calf serum*) et de *Rock inhibitor* sans que cela affecte leurs caractéristiques. Les HPTC pourront alors être ensemencées sur puce : sur une membrane poreuse recouverte de MEC avec un milieu spécifique. La puce que nous proposons mime une architecture tubulaire contournée avec une bi-compartimentation reliée au système de micro-perfusion (Figure 13 B). Le compartiment « urinaire » devra lui-aussi être complété par ce milieu spécifique. Des tests de transport pourront être réalisés sur ce modèle pour déterminer la capacité de transport transcellulaire transporteur-dépendant des HPTC. Les substrats utilisés pourront être le PAH pour le transport OAT/MRP-dépendant et le TEA pour le transport OCT/MATE-dépendant. Ces substrats devront être administrés dans le compartiment « systémique » et dosés dans le compartiment « systémique » et « urinaire ». La faible quantité de cellules ensemencées sur les puces est une limite pour l'étude de l'expression protéique. La méthode traditionnelle du *western blot* est très gourmande en protéines. D'autre méthodes, adaptées à de plus faibles quantités, devront être envisagées. La méthode de spectrométrie de masse développée par King et coll. pour l'analyse protéomique ciblée d'OAT1, d'OAT3, d'OCT2, et de P-gp pourra être considérée[141].

Par la suite, il conviendra de tester l'influence de l'hypoxie/réoxygénation sur le transport tubulaire. Pour établir le système micro-fluidique mimant une perfusion ischémique extracorporelle suivie d'une reperfusion oxygénée, nous pourrons nous appuyer sur les propositions récemment formulées par Giraud et coll. dans une revue de littérature[142] (Figure 13 C). Les HPTC dérivées des hiPSC cultivées sur ce système permettront d'étudier l'impact de l'hypoxie et de l'hypoxie/réoxygénation sur l'expression, la localisation et la fonctionnalité des transporteurs tubulaires.

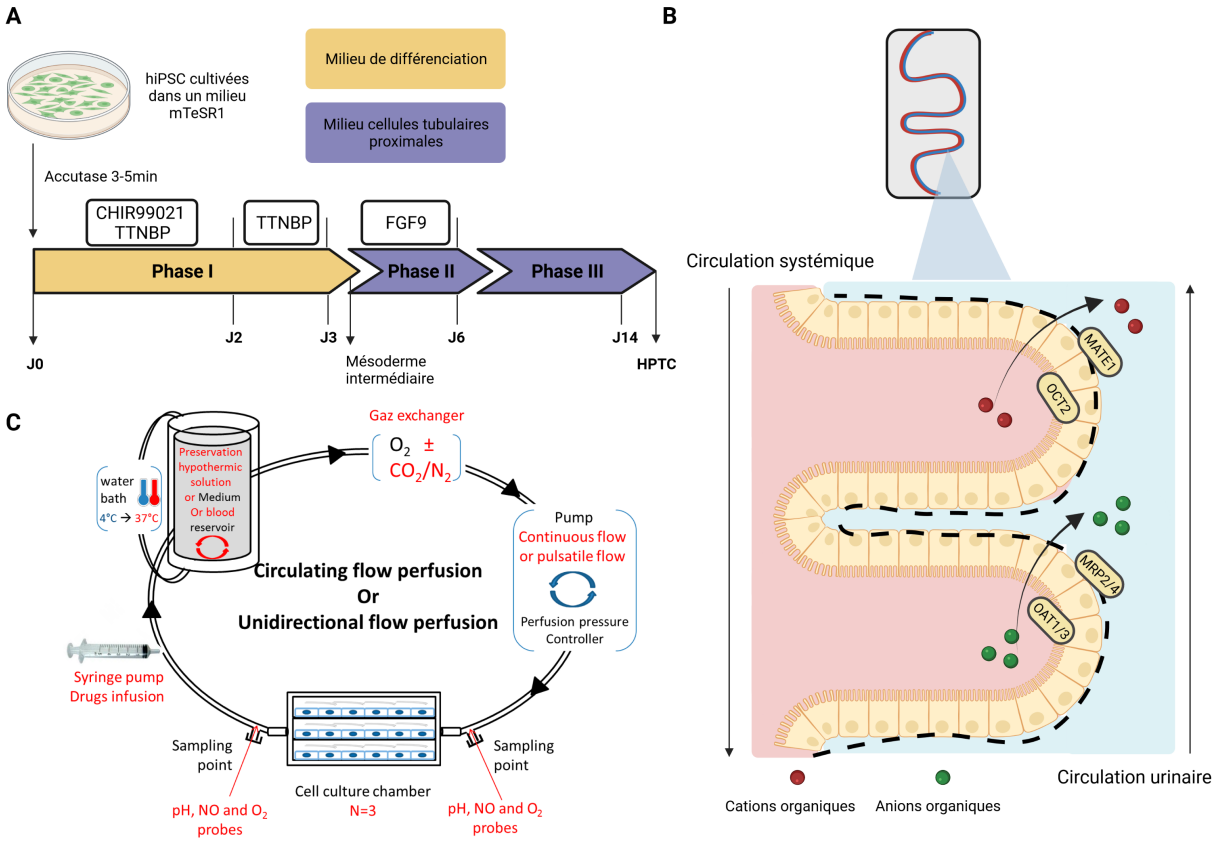

Figure 13 : Modèle de HPTC dérivées des hiPSC-sur-puce intégrant un système micro-fluidique adapté à l'étude de l'hypoxie/réoxygénation

(**A**) Flux de travail utilisé pour générer des HPTC dérivées des hiPSC développées par Chandrasekaran et coll.[119]. (**B**) Modèle de HPTC-sur-puce incluant une architecture tubulaire et une bi-compartimentation. (**C**) Proposition d'un modèle de perfusion hypothermique et hypoxique proposé par Giraud et coll.[142]. La Figure C est issue de la référence citée dans la légende. L'illustration a été réalisée avec BioRender.com.

Conclusion

Notre travail de thèse avait l'ambition d'étudier l'impact de l'hypoxie/réoxygénation sur le transport tubulaire transporteur-dépendant dans sa globalité. L'identification d'une modulation transcriptionnelle différentielle des transporteurs lors d'une privation en oxygène renforce l'hypothèse d'un mécanisme de régulation génique hypoxie-dépendant. Cette perturbation transcriptionnelle n'est pas prédictive de la fonction rénale post-greffe et n'est pas corrélée aux variations du métabolome endogène. L'appréciation de la modulation IR-dépendante des transporteurs tubulaires devra s'orienter vers une approche ciblée avec l'étude de caractéristiques plus pertinentes : leur fonctionnalité, leur expression protéique et leur localisation sur les cellules tubulaires proximales.

Dans la conclusion de notre revue de littérature, nous évoquions que l'amélioration de la survie du greffon s'appuie sur une stratégie de traitements multiples à différents temps du prélèvement, de la conservation et de la transplantation de l'organe. L'essor des machines de perfusion a redonné un élan à la recherche d'améliorations pour la conservation du greffon. L'utilisation de ces machines permet d'envisager des stratégies thérapeutiques effectives au cours de la conservation de l'organe, agrandissant par la même occasion la fenêtre d'action thérapeutique pré-transplantation. Récemment, Jochmans, Inaa. ; Nicholson, Michael L. and Hosgood, Sarah A. évoquaient "*In the future, we may progress toward organ-tailored preservation whereby high-risk kidneys can undergo assessment and repair before transplantation*."[143]. Les altérations éventuelles de la fonctionnalité des transporteurs tubulaires au cours de la conservation pourraient constituer une cible thérapeutique directe et/ou complémentaire, ainsi qu'un témoin des lésions ischémiques.
En post-opératoire, une modulation de l'activité des transporteurs pourrait mener à une perturbation métabolique systémique et une perte d'efficacité thérapeutique ou une surexposition médicamenteuse. D'un point de vue prédictif, l'estimation combinée de la filtration glomérulaire et de la réabsorption/sécrétion tubulaire permettrait d'affiner l'évaluation des fonctions rénales en période post-greffe immédiate.

Nous avons pu constater au cours de ce travail que l'étude du transport tubulaire transporteur-dépendant était très complexe, du fait de la multitude de transporteurs et de substrats impliqués. Dans le contexte de la transplantation rénale, cette complexité est accentuée par l'échelle de temps inhérente à cette procédure thérapeutique. La théorie RSST suggère que l'altération des transporteurs tubulaires lors de la transplantation pourrait avoir des effets délétères au sein de l'organisme. L'étude de la modulation IR-dépendante des transporteurs tubulaires en transplantation rénale est à considérer à diverses échelles, protéique, temporelle et de l'organisme, pour en saisir la globalité.

Références bibliographiques

1. Liyanage, T. *et al.* Worldwide access to treatment for end-stage kidney disease: a systematic review. *The Lancet* **385**, 1975–1982 (2015).

2. WHO | Projections of mortality and causes of death,
2016 to 2060. *WHO* http://www.who.int/healthinfo/global_burden_disease/projections/en/.

3. Agence de la biomédecine. Rapport annuel d'activité de l'agence de la biomédecine relatif à la greffe rénale (2020). https://rams.agence-biomedecine.fr/sites/default/files/pdf/2021-08/ABM_PG_Organes_Rein2020.pdf (2021).

4. Zhao, H., Alam, A., Soo, A. P., George, A. J. T. & Ma, D. Ischemia-Reperfusion Injury Reduces Long Term Renal Graft Survival: Mechanism and Beyond. *EBioMedicine* **28**, 31–42 (2018).

5. Tullius, S. G. *et al.* Contribution of prolonged ischemia and donor age to chronic renal allograft dysfunction. *J. Am. Soc. Nephrol. JASN* **11**, 1317–1324 (2000).

6. Wong, G. *et al.* The Impact of Total Ischemic Time, Donor Age and the Pathway of Donor Death on Graft Outcomes After Deceased Donor Kidney Transplantation. *Transplantation* **101**, 1152–1158 (2017).

7. Di Paolo, S. *et al.* Hypertension is an independent predictor of delayed graft function and worse renal function only in kidneys with chronic pathological lesions. *Transplantation* **73**, 623–627 (2002).

8. Yarlagadda, S. G., Coca, S. G., Formica, R. N., Poggio, E. D. & Parikh, C. R. Association between delayed graft function and allograft and patient survival: a systematic review and meta-analysis. *Nephrol. Dial. Transplant. Off. Publ. Eur. Dial. Transpl. Assoc. - Eur. Ren. Assoc.* **24**, 1039–1047 (2009).

9. Humar, A. *et al.* Risk factors for slow graft function after kidney transplants: a multivariate analysis. *Clin. Transplant.* **16**, 425–429 (2002).

10. Gill, J., Dong, J., Rose, C. & Gill, J. S. The risk of allograft failure and the survival benefit of kidney transplantation are complicated by delayed graft function. *Kidney Int.* **89**, 1331–1336 (2016).

11. Cohen, D. J., St Martin, L., Christensen, L. L., Bloom, R. D. & Sung, R. S. Kidney and pancreas transplantation in the United States, 1995-2004. *Am. J. Transplant. Off. J. Am. Soc. Transplant. Am. Soc. Transpl. Surg.* **6**, 1153–1169 (2006).

12. Doshi, M. D., Garg, N., Reese, P. P. & Parikh, C. R. Recipient risk factors associated with delayed graft function: a paired kidney analysis. *Transplantation* **91**, 666–671 (2011).

13. Moers, C. *et al.* Machine perfusion or cold storage in deceased-donor kidney transplantation. *N. Engl. J. Med.* **360**, 7–19 (2009).

14. Peng, P. *et al.* Hypothermic Machine Perfusion Versus Static Cold Storage in Deceased Donor Kidney Transplantation: A Systematic Review and Meta-Analysis of Randomized Controlled Trials. *Artif. Organs* **43**, 478–489 (2019).

15. Tingle, S. J. *et al.* Hypothermic machine perfusion is superior to static cold storage in deceased donor kidney transplantation: A meta-analysis. *Clin. Transplant.* e13814 (2020) doi:10.1111/ctr.13814.

16. Bon, D. *et al.* New strategies to optimize kidney recovery and preservation in transplantation. *Nat. Rev. Nephrol.* **8**, 339–347 (2012).

17. Nieuwenhuijs-Moeke, G. J. *et al.* Ischemia and Reperfusion Injury in Kidney Transplantation: Relevant Mechanisms in Injury and Repair. *J. Clin. Med.* **9**, 253 (2020).

18. Chen, C.-C., Chapman, W. C. & Hanto, D. W. Ischemia-reperfusion injury in kidney transplantation. *Front. Biosci. Elite Ed.* **7**, 117–134 (2015).

19. Nieuwenhuijs-Moeke, G. J. *et al.* Ischemia and Reperfusion Injury in Kidney Transplantation: Relevant Mechanisms in Injury and Repair. *J. Clin. Med.* **9**, (2020).

20. Kalogeris, T., Baines, C. P., Krenz, M. & Korthuis, R. J. Cell biology of ischemia/reperfusion injury. *Int. Rev. Cell Mol. Biol.* **298**, 229–317 (2012).

21. Peng, T.-I. & Jou, M.-J. Oxidative stress caused by mitochondrial calcium overload. *Ann. N. Y. Acad. Sci.* **1201**, 183–188 (2010).

22. Vanden Hoek, T. L. *et al.* Reperfusion injury on cardiac myocytes after simulated ischemia. *Am. J. Physiol.* **270**, H1334-1341 (1996).

23. Li, C. & Jackson, R. M. Reactive species mechanisms of cellular hypoxia-reoxygenation injury. *Am. J. Physiol. Cell Physiol.* **282**, C227-241 (2002).

24. Hara, S. Cell mediated rejection revisited: Past, current, and future directions. *Nephrol. Carlton Vic* **23 Suppl 2**, 45–51 (2018).

25. Picard, N. & Marquet, P. The influence of pharmacogenetics and cofactors on clinical outcomes in kidney transplantation. *Expert Opin. Drug Metab. Toxicol.* **7**, 731–743 (2011).

26. Benkali, K. *et al.* Tacrolimus population pharmacokinetic-pharmacogenetic analysis and Bayesian estimation in renal transplant recipients. *Clin. Pharmacokinet.* **48**, 805–816 (2009).

27. Mertens, I. *et al.* Urinary Protein Biomarker Panel for the Diagnosis of Antibody-Mediated Rejection in Kidney Transplant Recipients. *Kidney Int. Rep.* **5**, 1448–1458 (2020).

28. Van Loon, E. *et al.* Development and validation of a peripheral blood mRNA assay for the assessment of antibody-mediated kidney allograft rejection: A multicentre, prospective study. *EBioMedicine* **46**, 463–472 (2019).

29. Lamoureux, F. *et al.* Quantitative proteomic analysis of cyclosporine-induced toxicity in a human kidney cell line and comparison with tacrolimus. *J. Proteomics* **75**, 677–694 (2011).

30. Descazeaud, V., Mestre, E., Marquet, P. & Essig, M. Calcineurin regulation of cytoskeleton organization: a new paradigm to analyse the effects of calcineurin inhibitors on the kidney. *J. Cell. Mol. Med.* **16**, 218–227 (2012).

31. B, B. *et al.* Cyclosporine A inhibits MRTF-SRF signaling through Na +/K + ATPase inhibition and actin remodeling. *FASEB BioAdvances* **1**, (2019).

32. Woillard, J.-B., Labriffe, M., Debord, J. & Marquet, P. Tacrolimus Exposure Prediction Using Machine Learning. *Clin. Pharmacol. Ther.* **110**, 361–369 (2021).

33. Wu, H. *et al.* Preconditioning with recombinant high-mobility group box 1 protein protects the kidney against ischemia-reperfusion injury in mice. *Kidney Int.* **85**, 824–832 (2014).

34. Lin, Y. *et al.* Berberine protects renal tubular cells against hypoxia/reoxygenation injury via the Sirt1/p53 pathway. *J. Nat. Med.* **72**, 715–723 (2018).

35. Tan, X.-H. *et al.* Fibroblast growth factor 2 protects against renal ischaemia/reperfusion injury by attenuating mitochondrial damage and proinflammatory signalling. *J. Cell. Mol. Med.* **21**, 2909–2925 (2017).

36. Goncharov, R. G., Rogov, K. A., Temnov, A. A., Novoselov, V. I. & Sharapov, M. G. Protective role of exogenous recombinant peroxiredoxin 6 under ischemia-reperfusion injury of kidney. *Cell Tissue Res.* (2019) doi:10.1007/s00441-019-03073-z.

37. Chatterjee, P. K. Novel pharmacological approaches to the treatment of renal ischemia-reperfusion injury: a comprehensive review. *Naunyn. Schmiedebergs Arch. Pharmacol.* **376**, 1–43 (2007).

38. Fouad, A. A., Qureshi, H. A., Al-Sultan, A. I., Yacoubi, M. T. & Al-Melhim, W. N. Nephroprotective effect of telmisartan in rats with ischemia/reperfusion renal injury. *Pharmacology* **85**, 158–167 (2010).

39. Nigwekar, S. U., Navaneethan, S. D., Parikh, C. R. & Hix, J. K. Atrial natriuretic peptide for management of acute kidney injury: a systematic review and meta-analysis. *Clin. J. Am. Soc. Nephrol. CJASN* **4**, 261–272 (2009).

40. Fuller, T. F. *et al.* Protein kinase C inhibition ameliorates posttransplantation preservation injury in rat renal transplants. *Transplantation* **94**, 679–686 (2012).

41. Sohotnik, R. *et al.* Phosphodiesterase-5 inhibition attenuates early renal ischemia-reperfusion-induced acute kidney injury: assessment by quantitative measurement of urinary NGAL and KIM-1. *Am. J. Physiol. Renal Physiol.* **304**, F1099-1104 (2013).

42. Boudjema, K., Robin, F., Jeddou, H., Sulpice, L. & Flecher, E. Avancées de la conservation des greffons destinés à la transplantation. *Bull. Académie Natl. Médecine* **205**, 49–57 (2021).

43. Legendre, C. *La transplantation rénale*. (Lavoisier, 2011).

44. Legeai, C., Durand, L., Savoye, E., Macher, M.-A. & Bastien, O. Effect of preservation solutions for static cold storage on kidney transplantation outcomes: A National Registry Study. *Am. J. Transplant. Off. J. Am. Soc. Transplant. Am. Soc. Transpl. Surg.* **20**, 3426–3442 (2020).

45. O'Callaghan, J., Leuvenink, H. G. D., Friend, P. J. & Ploeg, R. J. Chapter 9 - Kidney Preservation. in *Kidney Transplantation–Principles and Practice (Seventh Edition)* (eds. Morris, P. J. & Knechtle, S. J.) 130–141 (W.B. Saunders, 2014). doi:10.1016/B978-1-4557-4096-3.00009-X.

46. Venema, L. H. *et al.* Effects of Oxygen During Long-term Hypothermic Machine Perfusion in a Porcine Model of Kidney Donation After Circulatory Death. *Transplantation* **103**, 2057–2064 (2019).

47. Gallinat, A., Efferz, P., Paul, A. & Minor, T. One or 4 h of 'in-house' reconditioning by machine perfusion after cold storage improve reperfusion parameters in porcine kidneys. *Transpl. Int. Off. J. Eur. Soc. Organ Transplant.* **27**, 1214–1219 (2014).

48. Nath, J. *et al.* Metabolic differences between cold stored and machine perfused porcine kidneys: A 1H NMR based study. *Cryobiology* **74**, 115–120 (2017).

49. O'Callaghan, J. M., Morgan, R. D., Knight, S. R. & Morris, P. J. Systematic review and meta-analysis of hypothermic machine perfusion versus static cold storage of kidney allografts on transplant outcomes. *Br. J. Surg.* **100**, 991–1001 (2013).

50. Hosgood, S. A. & Nicholson, M. L. First in man renal transplantation after ex vivo normothermic perfusion. *Transplantation* **92**, 735–738 (2011).

51. Elliott, T. R., Nicholson, M. L. & Hosgood, S. A. Normothermic kidney perfusion: An overview of protocols and strategies. *Am. J. Transplant. Off. J. Am. Soc. Transplant. Am. Soc. Transpl. Surg.* **21**, 1382–1390 (2021).

52. Minor, T. *et al.* First-in-man controlled rewarming and normothermic perfusion with cell-free solution of a kidney prior to transplantation. *Am. J. Transplant. Off. J. Am. Soc. Transplant. Am. Soc. Transpl. Surg.* **20**, 1192–1195 (2020).

53. Mueller, T. F. *et al.* The transcriptome of the implant biopsy identifies donor kidneys at increased risk of delayed graft function. *Am. J. Transplant. Off. J. Am. Soc. Transplant. Am. Soc. Transpl. Surg.* **8**, 78–85 (2008).

54. Druml, W. Protein metabolism in acute renal failure. *Miner. Electrolyte Metab.* **24**, 47–54 (1998).

55. Watanabe, M. *et al.* Consequences of low plasma histidine in chronic kidney disease patients: associations with inflammation, oxidative stress, and mortality. *Am. J. Clin. Nutr.* **87**, 1860–1866 (2008).

56. Posada-Ayala, M. *et al.* Identification of a urine metabolomic signature in patients with advanced-stage chronic kidney disease. *Kidney Int.* **85**, 103–111 (2014).

57. de Vries, L. V. *et al.* The tryptophan/kynurenine pathway, systemic inflammation, and long-term outcome after kidney transplantation. *Am. J. Physiol. Renal Physiol.* **313**, F475–F486 (2017).

58. Zhang, Z.-H. *et al.* Metabolomics insights into chronic kidney disease and modulatory effect of rhubarb against tubulointerstitial fibrosis. *Sci. Rep.* **5**, 14472 (2015).

59. Li, R., Dai, J. & Kang, H. The construction of a panel of serum amino acids for the identification of early chronic kidney disease patients. *J. Clin. Lab. Anal.* **32**, (2018).

60. Sun, J. *et al.* Serum metabolomic profiles from patients with acute kidney injury: a pilot study. *J. Chromatogr. B Analyt. Technol. Biomed. Life. Sci.* **893–894**, 107–113 (2012).

61. Malagrino, P. A. *et al.* Metabolomic characterization of renal ischemia and reperfusion in a swine model. *Life Sci.* **156**, 57–67 (2016).

62. Wei, Q., Xiao, X., Fogle, P. & Dong, Z. Changes in metabolic profiles during acute kidney injury and recovery following ischemia/reperfusion. *PloS One* **9**, e106647 (2014).

63. Jouret, F. *et al.* Nuclear Magnetic Resonance Metabolomic Profiling of Mouse Kidney, Urine and Serum Following Renal Ischemia/Reperfusion Injury. *PloS One* **11**, e0163021 (2016).

64. Chihanga, T. *et al.* NMR spectroscopy and electron microscopy identification of metabolic and ultrastructural changes to the kidney following ischemia-reperfusion injury. *Am. J. Physiol. Renal Physiol.* **314**, F154–F166 (2018).

65. Bon, D. *et al.* Analysis of perfusates during hypothermic machine perfusion by NMR spectroscopy: a potential tool for predicting kidney graft outcome. *Transplantation* **97**, 810–816 (2014).

66. Guy, A. J. *et al.* Metabolomic analysis of perfusate during hypothermic machine perfusion of human cadaveric kidneys. *Transplantation* **99**, 754–759 (2015).

67. Stryjak, I., Warmuzińska, N., Bogusiewicz, J., Łuczykowski, K. & Bojko, B. Monitoring of the influence of long-term oxidative stress and ischemia on the condition of kidney using solid phase microextraction chemical biopsy coupled with liquid chromatography high resolution mass spectrometry. *J. Sep. Sci.* (2020) doi:10.1002/jssc.202000032.

68. Nigam, S. K., Bush, K. T., Bhatnagar, V., Poloyac, S. M. & Momper, J. D. The Systems Biology of Drug Metabolizing Enzymes and Transporters: Relevance to Quantitative Systems Pharmacology. *Clin. Pharmacol. Ther.* **108**, 40–53 (2020).

69. Nigam, S. K. & Bush, K. T. Uraemic syndrome of chronic kidney disease: altered remote sensing and signalling. *Nat. Rev. Nephrol.* **15**, 301–316 (2019).

70. Mihaila, S. M. *et al.* Drugs Commonly Applied to Kidney Patients May Compromise Renal Tubular Uremic Toxins Excretion. *Toxins* **12**, 391 (2020).

71. Barin-Le Guellec, C., Largeau, B., Bon, D., Marquet, P. & Hauet, T. Ischemia/reperfusion-associated tubular cells injury in renal transplantation: Can metabolomics inform about mechanisms and help identify new therapeutic targets? *Pharmacol. Res.* **129**, 34–43 (2018).

72. Zou, L. *et al.* Molecular Mechanisms for Species Differences in Organic Anion Transporter 1, OAT1: Implications for Renal Drug Toxicity. *Mol. Pharmacol.* **94**, 689–699 (2018).

73. Wishart, D. S. Metabolomics for Investigating Physiological and Pathophysiological Processes. *Physiol. Rev.* **99**, 1819–1875 (2019).

74. Darius, T., Nath, J. & Mourad, M. Simply Adding Oxygen during Hypothermic Machine Perfusion to Combat the Negative Effects of Ischemia-Reperfusion Injury: Fundamentals and Current Evidence for Kidneys. *Biomedicines* **9**, 993 (2021).

75. Thuillier, R. *et al.* Benefits of active oxygenation during hypothermic machine perfusion of kidneys in a preclinical model of deceased after cardiac death donors. *J. Surg. Res.* **184**, 1174–1181 (2013).

76. Darius, T. *et al.* Influence of Different Partial Pressures of Oxygen During Continuous Hypothermic Machine Perfusion in a Pig Kidney Ischemia-reperfusion Autotransplant Model. *Transplantation* **104**, 731–743 (2020).

77. Darius, T. *et al.* Brief O2 uploading during continuous hypothermic machine perfusion is simple yet effective oxygenation method to improve initial kidney function in a porcine autotransplant model. *Am. J. Transplant. Off. J. Am. Soc. Transplant. Am. Soc. Transpl. Surg.* **20**, 2030–2043 (2020).

78. Darius, T. *et al.* The effect on early renal function of various dynamic preservation strategies in a preclinical pig ischemia–reperfusion autotransplant model. *Am. J. Transplant.* **19**, 752–762 (2019).

79. Darius, T. *et al.* Influence of Different Partial Pressures of Oxygen During Continuous Hypothermic Machine Perfusion in a Pig Kidney Ischemia-reperfusion Autotransplant Model. *Transplantation* **104**, 731–743 (2020).

80. Jochmans, I. *et al.* Oxygenated versus standard cold perfusion preservation in kidney transplantation (COMPARE): a randomised, double-blind, paired, phase 3 trial. *Lancet Lond. Engl.* **396**, 1653–1662 (2020).

81. Meister, F. A. *et al.* Hypothermic Oxygenated Machine Perfusion of Extended Criteria Kidney Allografts from Brain Dead Donors: Protocol for a Prospective Pilot Study. *JMIR Res. Protoc.* **8**, e14622 (2019).

82. Ravaioli, M. *et al.* Hypothermic Oxygenated Perfusion Versus Static Cold Storage for Expanded Criteria Donors in Liver and Kidney Transplantation: Protocol for a Single-Center Randomized Controlled Trial. *JMIR Res. Protoc.* **9**, e13922 (2020).

83. Hosgood, S. A. *et al.* A pilot study assessing the feasibility of a short period of normothermic preservation in an experimental model of non heart beating donor kidneys. *J. Surg. Res.* **171**, 283–290 (2011).

84. Gage, F. *et al.* Room temperature pulsatile perfusion of renal allografts with Lifor compared with hypothermic machine pump solution. *Transplant. Proc.* **41**, 3571–3574 (2009).

85. Kay, M. D. *et al.* Static normothermic preservation of renal allografts using a novel nonphosphate buffered preservation solution. *Transpl. Int. Off. J. Eur. Soc. Organ Transplant.* **20**, 88–92 (2007).

86. Nicholson, M. L. & Hosgood, S. A. Renal transplantation after ex vivo normothermic perfusion: the first clinical study. *Am. J. Transplant. Off. J. Am. Soc. Transplant. Am. Soc. Transpl. Surg.* **13**, 1246–1252 (2013).

87. Kaths, J. M. *et al.* Continuous Normothermic Ex Vivo Kidney Perfusion Is Superior to Brief Normothermic Perfusion Following Static Cold Storage in Donation After Circulatory Death Pig Kidney Transplantation. *Am. J. Transplant. Off. J. Am. Soc. Transplant. Am. Soc. Transpl. Surg.* **17**, 957–969 (2017).

88. McEvoy, C. M. *et al.* Normothermic Ex-vivo Kidney Perfusion in a Porcine Auto-Transplantation Model Preserves the Expression of Key Mitochondrial Proteins: An Unbiased Proteomics Analysis. *Mol. Cell. Proteomics* 100101 (2021) doi:10.1016/j.mcpro.2021.100101.

89. Urbanellis, P. *et al.* Transcriptome Analysis of Kidney Grafts Subjected to Normothermic Ex Vivo Perfusion Demonstrates an Enrichment of Mitochondrial Metabolism Genes. *Transplant. Direct* **7**, e719 (2021).

90. Wieser, M. *et al.* hTERT alone immortalizes epithelial cells of renal proximal tubules without changing their functional characteristics. *Am. J. Physiol. Renal Physiol.* **295**, F1365-1375 (2008).

91. Aschauer, L., Carta, G., Vogelsang, N., Schlatter, E. & Jennings, P. Expression of xenobiotic transporters in the human renal proximal tubule cell line RPTEC/TERT1. *Toxicol. Vitro Int. J. Publ. Assoc. BIBRA* **30**, 95–105 (2015).

92. Secker, P. F., Schlichenmaier, N., Beilmann, M., Deschl, U. & Dietrich, D. R. Functional transepithelial transport measurements to detect nephrotoxicity in vitro using the RPTEC/TERT1 cell line. *Arch. Toxicol.* **93**, 1965–1978 (2019).

93. Müller, F., Weitz, D., Mertsch, K., König, J. & Fromm, M. F. Importance of OCT2 and MATE1 for the Cimetidine-Metformin Interaction: Insights from Investigations of Polarized

Transport in Single- And Double-Transfected MDCK Cells with a Focus on Perpetrator Disposition. *Mol. Pharm.* **15**, 3425–3433 (2018).

94. König, J., Zolk, O., Singer, K., Hoffmann, C. & Fromm, M. F. Double-transfected MDCK cells expressing human OCT1/MATE1 or OCT2/MATE1: determinants of uptake and transcellular translocation of organic cations. *Br. J. Pharmacol.* **163**, 546–555 (2011).

95. Sato, T. *et al.* Transcellular transport of organic cations in double-transfected MDCK cells expressing human organic cation transporters hOCT1/hMATE1 and hOCT2/hMATE1. *Biochem. Pharmacol.* **76**, 894–903 (2008).

96. Kong, Y. *et al.* Celecoxib antagonizes the cytotoxicity of oxaliplatin in human esophageal cancer cells by impairing the drug influx. *Eur. J. Pharm. Sci.* **81**, 137–148 (2016).

97. Ingoglia, F. *et al.* Functional characterization of the organic cation transporters (OCTs) in human airway pulmonary epithelial cells. *Biochim. Biophys. Acta* **1848**, 1563–1572 (2015).

98. Miakotina, O. L., Agassandian, M., Shi, L., Look, D. C. & Mallampalli, R. K. Adenovirus stimulates choline efflux by increasing expression of organic cation transporter-2. *Am. J. Physiol. Lung Cell. Mol. Physiol.* **288**, L93-102 (2005).

99. Secker, P. F., Luks, L., Schlichenmaier, N. & Dietrich, D. R. RPTEC/TERT1 cells form highly differentiated tubules when cultured in a 3D matrix. *ALTEX* **35**, 223–234 (2018).

100. Lash, L. H., Putt, D. A. & Cai, H. Membrane transport function in primary cultures of human proximal tubular cells. *Toxicology* **228**, 200–218 (2006).

101. Fransen, M. F. J. *et al.* Bioprinting of kidney in vitro models: cells, biomaterials, and manufacturing techniques. *Essays Biochem.* EBC20200158 (2021) doi:10.1042/EBC20200158.

102. Wilmer, M. J. *et al.* Kidney-on-a-Chip Technology for Drug-Induced Nephrotoxicity Screening. *Trends Biotechnol.* **34**, 156–170 (2016).

103. Essig, M., Terzi, F., Burtin, M. & Friedlander, G. Mechanical strains induced by tubular flow affect the phenotype of proximal tubular cells. *Am. J. Physiol. Renal Physiol.* **281**, F751-762 (2001).

104. Duan, Y. *et al.* Shear-induced reorganization of renal proximal tubule cell actin cytoskeleton and apical junctional complexes. *Proc. Natl. Acad. Sci. U. S. A.* **105**, 11418–11423 (2008).

105. Essig, M. & Friedlander, G. Tubular Shear Stress and Phenotype of Renal Proximal Tubular Cells. *J. Am. Soc. Nephrol.* **14**, S33–S35 (2003).

106. Jang, K.-J. *et al.* Human kidney proximal tubule-on-a-chip for drug transport and nephrotoxicity assessment. *Integr. Biol.* **5**, 1119–1129 (2013).

107. Snouber, L. C. *et al.* Analysis of transcriptomic and proteomic profiles demonstrates improved Madin-Darby canine kidney cell function in a renal microfluidic biochip. *Biotechnol. Prog.* **28**, 474–484 (2012).

108. Vormann, M. K. *et al.* Nephrotoxicity and Kidney Transport Assessment on 3D Perfused Proximal Tubules. *AAPS J.* **20**, 90 (2018).

109. Vriend, J. *et al.* Nephroscreen: A robust and versatile renal tubule-on-a-chip platform for nephrotoxicity assessment. *Curr. Opin. Toxicol.* **25**, 42–48 (2021).

110. Yin, L. *et al.* Efficient Drug Screening and Nephrotoxicity Assessment on Co-culture Microfluidic Kidney Chip. *Sci. Rep.* **10**, 6568 (2020).

111. Weber, E. J. *et al.* Development of a microphysiological model of human kidney proximal tubule function. *Kidney Int.* **90**, 627–637 (2016).

112. Jansen, J. *et al.* Human proximal tubule epithelial cells cultured on hollow fibers: living membranes that actively transport organic cations. *Sci. Rep.* **5**, 16702 (2015).

113. Jansen, J. *et al.* Bioengineered kidney tubules efficiently excrete uremic toxins. *Sci. Rep.* **6**, 26715 (2016).

114. Jansen, J. *et al.* Remote sensing and signaling in kidney proximal tubules stimulates gut microbiome-derived organic anion secretion. *Proc. Natl. Acad. Sci. U. S. A.* **116**, 16105–16110 (2019).

115. Takahashi, K. & Yamanaka, S. Induction of pluripotent stem cells from mouse embryonic and adult fibroblast cultures by defined factors. *Cell* **126**, 663–676 (2006).

116. Chuah, J. K. C. & Zink, D. Stem cell-derived kidney cells and organoids: Recent breakthroughs and emerging applications. *Biotechnol. Adv.* **35**, 150–167 (2017).

117. Kumar, S. V. *et al.* Kidney micro-organoids in suspension culture as a scalable source of human pluripotent stem cell-derived kidney cells. *Dev. Camb. Engl.* **146**, dev172361 (2019).

118. Kandasamy, K. *et al.* Prediction of drug-induced nephrotoxicity and injury mechanisms with human induced pluripotent stem cell-derived cells and machine learning methods. *Sci. Rep.* **5**, 12337 (2015).

119. Chandrasekaran, V. *et al.* Generation and characterization of iPSC-derived renal proximal tubule-like cells with extended stability. *Sci. Rep.* **11**, 11575 (2021).

120. Mota, C., Camarero-Espinosa, S., Baker, M. B., Wieringa, P. & Moroni, L. Bioprinting: From Tissue and Organ Development to in Vitro Models. *Chem. Rev.* **120**, 10547–10607 (2020).

121. Homan, K. A. *et al.* Bioprinting of 3D Convoluted Renal Proximal Tubules on Perfusable Chips. *Sci. Rep.* **6**, 34845 (2016).

122. Lin, N. Y. C. *et al.* Renal reabsorption in 3D vascularized proximal tubule models. *Proc. Natl. Acad. Sci.* **116**, 5399–5404 (2019).

123. Singh, N. K. *et al.* Three-dimensional cell-printing of advanced renal tubular tissue analogue. *Biomaterials* **232**, 119734 (2020).

124. Park, D., Lee, J., Chung, J. J., Jung, Y. & Kim, S. H. Integrating Organs-on-Chips: Multiplexing, Scaling, Vascularization, and Innervation. *Trends Biotechnol.* **38**, 99–112 (2020).

125. van Berlo, D., van de Steeg, E., Amirabadi, H. E. & Masereeuw, R. The potential of multi-organ-on-chip models for assessment of drug disposition as alternative to animal testing. *Curr. Opin. Toxicol.* (2021) doi:10.1016/j.cotox.2021.05.001.

126. Schutgens, F. *et al.* Tubuloids derived from human adult kidney and urine for personalized disease modeling. *Nat. Biotechnol.* **37**, 303–313 (2019).

127. Hosgood, S. A., Hoff, M. & Nicholson, M. L. Treatment of transplant kidneys during machine perfusion. *Transpl. Int. Off. J. Eur. Soc. Organ Transplant.* **34**, 224–232 (2021).

128. Woodside, K. J. *et al.* Enhancing kidney function with thrombolytic therapy following donation after cardiac death: a multicenter quasi-blinded prospective randomized trial. *Clin. Transplant.* **29**, 1173–1180 (2015).

129. Risso, M. A. *et al.* The Importance of Tubular Function in Chronic Kidney Disease. *Int. J. Nephrol. Renov. Dis.* **12**, 257–262 (2019).

130. Lowenstein, J. & Grantham, J. J. The rebirth of interest in renal tubular function. *Am. J. Physiol.-Ren. Physiol.* **310**, F1351–F1355 (2016).

131. Leong, S. C. *et al.* Residual Function Effectively Controls Plasma Concentrations of Secreted Solutes in Patients on Twice Weekly Hemodialysis. *J. Am. Soc. Nephrol.* **29**, 1992–1999 (2018).

132. Chen, Y. *et al.* Kidney Clearance of Secretory Solutes Is Associated with Progression of CKD: The CRIC Study. *J. Am. Soc. Nephrol. JASN* **31**, 817–827 (2020).

133. Kushida, N. *et al.* Hypoxia-Inducible Factor-1α Activates the Transforming Growth Factor-β/SMAD3 Pathway in Kidney Tubular Epithelial Cells. *Am. J. Nephrol.* **44**, 276–285 (2016).

134. van Gelder, M. K. *et al.* Protein-Bound Uremic Toxins in Hemodialysis Patients Relate to Residual Kidney Function, Are Not Influenced by Convective Transport, and Do Not Relate to Outcome. *Toxins* **12**, (2020).

135. Patel, K. *et al.* The Effects of Oxygenation on Ex Vivo Kidneys Undergoing Hypothermic Machine Perfusion. *Transplantation* **103**, 314–322 (2019).

136. Nath, J. *et al.* (13)C glucose labelling studies using 2D NMR are a useful tool for determining ex vivo whole organ metabolism during hypothermic machine perfusion of kidneys. *Transplant. Res.* **5**, 7 (2016).

137. Liu, W.-J. *et al.* Orthotopic Kidney Auto-Transplantation in a Porcine Model Using 24 Hours Organ Preservation And Continuous Telemetry. *J. Vis. Exp. JoVE* (2020) doi:10.3791/61591.

138. Bush, K. T., Singh, P. & Nigam, S. K. Gut-derived uremic toxin handling in vivo requires OAT-mediated tubular secretion in chronic kidney disease. *JCI Insight* **5**, (2020).

139. Ayala-García, M. A., Hernández, M. Á. P., Ramírez-Barba, É. J., Encalada, J. M. S. & Yebra, B. G. *Preservation of Renal Allografts for Transplantation*. *Renal Transplantation - Updates and Advances* (IntechOpen, 2012). doi:10.5772/27231.

140. Araoka, T. *et al.* Efficient and Rapid Induction of Human iPSCs/ESCs into Nephrogenic Intermediate Mesoderm Using Small Molecule-Based Differentiation Methods. *PLoS ONE* **9**, e84881 (2014).

141. King, S. M. *et al.* 3D Proximal Tubule Tissues Recapitulate Key Aspects of Renal Physiology to Enable Nephrotoxicity Testing. *Front. Physiol.* **8**, 123 (2017).

142. Giraud, S., Thuillier, R., Cau, J. & Hauet, T. In Vitro/Ex Vivo Models for the Study of Ischemia Reperfusion Injury during Kidney Perfusion. *Int. J. Mol. Sci.* **21**, 8156 (2020).

143. Jochmans, I., Nicholson, M. L. & Hosgood, S. A. Kidney perfusion: some like it hot others prefer to keep it cool. *Curr. Opin. Organ Transplant.* **22**, 260–266 (2017).

Annexes

Annexe 1. Solutions de conservation en transplantation rénale

Composition des différentes solutions de conservation commercialisées.

Composition	UW (Viaspan®)	*KPS®*	*CELSIOR®*	*HTK (Custodiol®)*	IGL-1®	SCOT® 15
Ions (mM)						
Na^+	30	80	100	15	125	118
K^+	125	25	15	10	30	5
Mg^{2+}	5	5	13	4	5	1,20
Ca^{2+}	-	0,5	0,25	0,015	-	1,75
Cl^-	-	0,5	-	50	-	-
Tampon (mM)						
SO_4^{2-}	5	-	1,2	-	5	-
$H_2PO_4^{2-}$	25	25	-	-	25	-
HCO_3^-	25	-	-	-	-	25
HEPES	-	10	-	-	-	-
Glucose	-	10	-	-	-	11
Raffinose	30	-	-	-	30	-
Ribose	-	5	-	-	-	-
Lactobionate	100	-	80	-	100	-
Adenosine	5	5	-	-	5	-
Glutathion	4	4	3	-	3	-
Allopurinol	-	1	-	-	1	-
Histidine	-	-	30	180	-	-
Mannitol	-	30	60	30	-	-
Glutamate	-	-	20	-	-	-
Tryptophane	-	-	-	2	-	-
A-cétoglutarate	-	-	-	1	-	-
Colloïdes (g/L)						
HES	50	50	-	-	-	-
PEG 20kDA	-	-	-	-	-	30
PEG 35kDA	-	-	-	-	1	-
Physicochimie						
pH	7,3	7,4	7,3	7,2	7,3	7,3
Viscosité (cSt)	2,4	3,15	0,7	0,7	0,7	1,6
Osmolarité (mOsm)	320	320	320	310	320	320

Tableau adapté de la référence [43]. HES, *hydroxyethyl starch* ; PEG, *polyethylene glycol* ; cSt, *centistokes* ; mOsm, *milliosmole*

Annexe 2. Anatomie du néphron

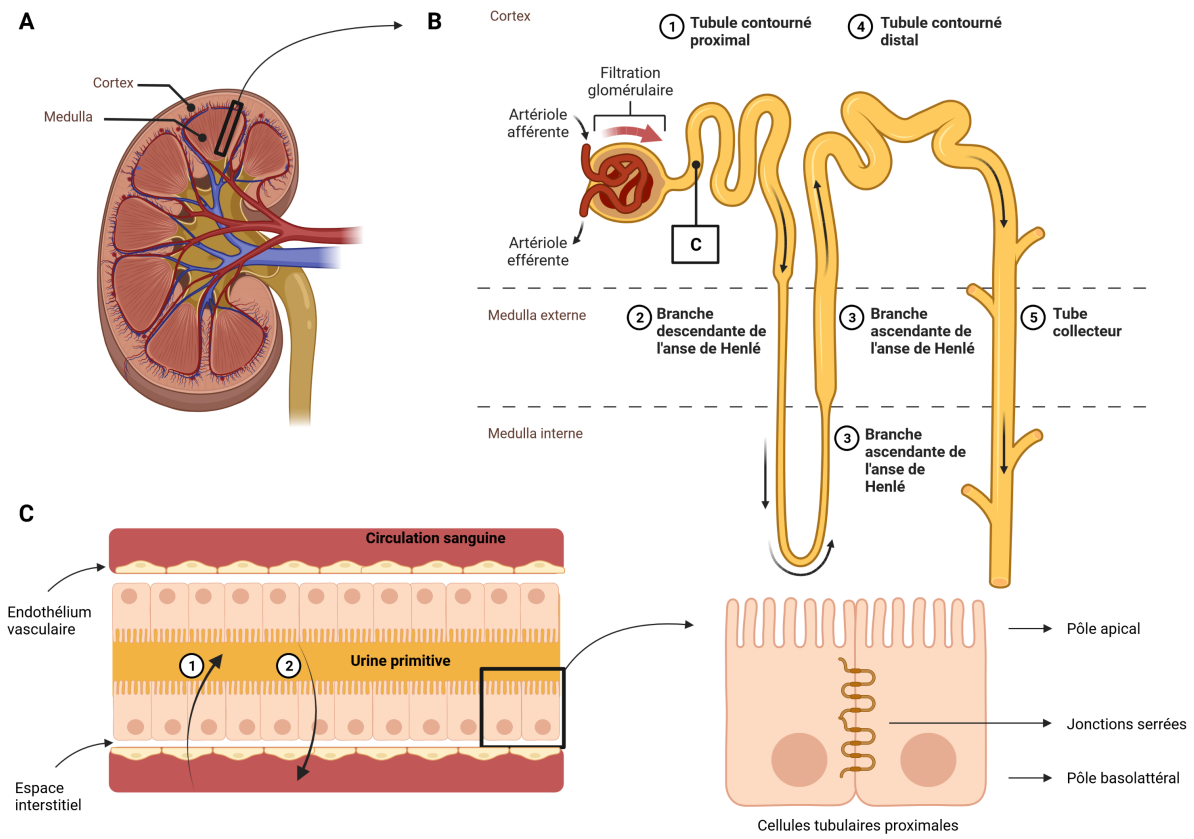

Localisation anatomique des cellules tubulaires proximales
(**A**) Coupe transversale de rein avec vascularisation. (**B**) Architecture du néphron. (**C**) Présentation du tubule proximal à l'échelle cellulaire : 1 : réabsorption tubulaire ; 2 : sécrétion tubulaire. L'illustration a été réalisée avec BioRender.com.

Annexe 3. Contenu supplémentaire de l'article expérimentale 1

Annexe 3.1. Article expérimental 1 : Supplemental Digital Content

Supplemental Digital Content

SDC, Materials and Methods:

1. **Study design :**

This two year prospective study relied on 38 kidney transplants from the Orléans Regional Hospital and University Hospital of Tours (France), within the framework of the clinical research project named RENALIFE, registered under ClinicalTrials.gov (NCT03024229). Patients were included if they met the following selection criteria: Donor aged at least 18 years, expressed non-opposition, dead brain deceased, and met the expanded criteria for renal retrieval (a donor aged either more than 50 or 60 years old, with two of the following criteria: a history of high blood pressure, a plasmatic creatinine greater than or equal to 1.5 mg/L, death resulting from a stroke). Immediately after the kidneys had been retrieved from the donor, they were stored on HMP, LifePort® Kidney Transporter 1.0 (Organ Recovery Systems). The organ preservation solution used in this device was KPS-1® solution (Organ Recovery System). The parameters of perfusion machine (i.e. temperature, flow, resistance) were recorded during kidney conservation. When the receiver was ready for transplantation, the graft was removed from the machine. An aliquot of the perfusion fluid was taken and immediately centrifuged at 3000g for 10 min then stored at -20°C. Just before transplantation, a systematic graft biopsy was also performed with a 16 Gauge gun (directed in order to sample the renal cortex). The biopsy was split transversely into two fragments: the first one was fixed in Bouin's solution (picric acid, acetic acid, formalin) or in AFA (acetic alcohol formalin) depending on the date of inclusion and then included in paraffin to carry out pathological classification, according to the revised Banff classification 2013; the second fragment was stored at -20°C. Each recipient benefited from a clinical and biological follow-up, including daily creatininemia measurement until day 7 and a collection of clinical events, which was

carried out during the entire follow-up period, i.e. 3 months post-transplantation. The primary endpoints for graft recovery were Immediate Graft Function (IGF), characterized by a creatininemia at day 7 ≤ 250 µmol/L without the necessity for dialysis and Delayed Graft Function (DGF), characterized by the necessity for dialysis within 7 days.

2. Reagents

Discovery HS F5-3 column (150 x 2.1 mm d.i., 3 µm) (#567503-U), 2-Isopropylmalic acid (#333115), α-ketoglutaric acid (#75890), D-gluconic acid sodium salt (#G9005), D-Mannitol (#M4125), D-Ribose (#R7500), L-Carnitine (#8.40092), Magnesium D-gluconate hydrate (#G9130), P-Aminohippuric acid (#A1422) and Taurine (#T0625) were purchased from Sigma-Aldrich. Creatinine (27910) was purchased from Fluka. Taqman Low Density Array® (TLDA) cards were purchased from Thermofisher. The list of probe sets and manufacturer's code for TaqMan probes are listed in Supplementary Table 1.

3. Metabolomics analysis of graft preservation samples

3.1. **LC-MS/MS-metabolomic analysis**

Mass spectrometry analysis of perfusion fluids was performed using LCMS-8060 (Shimadzu) tandem mass spectrometer and the LC-MS/MS "Method Package for Cell Culture Profiling Ver.2" (Shimadzu). In order to analyze compounds not initially included in this kit, an infusion of pure substances was performed and the corresponding transitions were added to the list of compounds to analyze. Briefly, 200 µL of acetonitrile and 20 µL of internal standard (2-Isopropylmalic acid [0.5 mmol/L]) were added to 100 µL of preservative solution from each patient. After centrifugation at room temperature for 15 minutes at 15,000 g, the supernatant was diluted 1/10th in ultrapure water and transferred to a vial before injection of 3µL into the analytical system. For each transition analyzed, only well-defined chromatographic peaks were considered. Each sample was analyzed in duplicate. Quality controls were prepared by

mixing an equal volume of each patient's sample and were injected three times in all the series. Metabolites with a coefficient variation (CV) > 30% in quality controls were not retained for subsequent metabolomics analysis. Native KPS-1 was also injected to determine its basal metabolic composition. Raw spectrometric data sets were normalized in relation to the intensity of 2-Isopropylmalic acid as internal standard. Regarding the LC-MS/MS parameters: Chromatographic separation of the compounds was carried out with a Discovery HS F5-3 column (150 x 2.1 mm d.i., 3 µm) column thermostated at 40°C, at a flow rate of 350 µL/min according to the following linear mobile phase gradient: 0-1.4 min : 0% B ; 1.4-3.5 min : 0 to 25% B ; 3.5-7.5 min ; 25 to 35% B ; 7.5 to 10.3 min : 35 to 95% B; 10.3-13.7: 95%B; 13.7-13.8 min: 95 to 0% B; 13.8-17 min: 0%B where A is a 0.1% solution of formic acid in water and B is a 0.1% solution of formic acid in acetonitrile. Detection was performed by electrospray ionization using the following source conditions: Nebulizing gas flow rate; 3 mL/min; Drying gas flow rate: 10 mL/min; Heating gas flow rate: 10 mL/min; Interface temperature: 300°C; Desolvation line temperature: 250°C; block heater temperature: 400°C; Compounds were detected in scheduled MRM (Multi Reaction Monitoring) mode alternately in positive and negative modes, used for compound identification: one transition for quantification and a minimum of one transition for confirmation and relative retention time (Supplementary Table 2).

3.2. **Assessment of other biochemical compounds**

COBAS 6000 analyzer (Roche Diagnostics) was used to determine sodium, potassium, calcium, phosphate, chloride, bicarbonate, urea, creatinine and glucose concentrations. The quantifiable features were then added to the list of metabolites measured by LC-MS/MS for subsequent analyses.

4. Transcriptional expression of tubular transporter

Frozen pre-implantation biopsies were used for RNA extraction, using the Nucleospin RNA/Protein kit (Macherey-Nagel), according to the manufacturer's instructions. RNA was then quantified using Qubit 4.0 with the Qubit RNA HS Assay kit (Thermofisher). RNA quality was assessed by RNA Integrity Number (RIN), determined with a Bioanalyzer 21 000 (Agilent). Agilent RNA 6000 Pico or Agilent RNA 6000 Nano kits were used according to RNA concentration. 200ng of RNA were then reverse transcribed into complementary DNA (cDNA) using the High capacity cDNA Reverse Transcription kit (ThermoFisher), according to the manufacturer's instructions. The TLDA card used enabled the quantification of 35 membrane tubular transporters , 3 aquaporins, 2 Na/K-ATPase subunits, and 4 housekeeping genes candidates (*NME4*, *CHFR*, *C16ORF62* and *NASP)* chosen according to the literature. For each sample, a mix containing all the cDNA diluted in RNAse-free water q.s. 55µL and 55 µL TaqMan® Universal Master Mix II was prepared. 100 µL of this reaction mix was then loaded onto each slot of the TLDA card. After double centrifugation at 1,200 rpm for 1 minute, the card was sealed and subsequently analyzed using Polymerase Chain Reaction (PCR) QuantStudio 12K with mix-UNG Amperase following the program conditions: 50°C for 2 min, 95°C for 10 min and 40 cycles of 95°C for 15 s followed by 60°C for 1 min. Undetermined or > 35 Ct values were replaced by 35. Renal transporters expression was then analyzed by the comparative $2^{-\Delta Ct}$ method with ΔCt = Ct (target gene) **–** Ct (mean of the housekeeping genes finally retained). $2^{-\Delta Ct}$ were then normalized by log 2 transformation. Housekeeping genes finally retained for the $2^{-\Delta Ct}$ method (*NME4*, *CHFR* and *C16ORF62*) were selected using Genorm and Normfinder.

5. Statistical analyzes

The study had three objectives: (i) explore the impact of ischemia duration on the metabolomic content of perfusion liquids and on renal tubular transporters expression, (ii) explore relationships between metabolomic profiles and renal tubular transporters expression during HPM and (iii) find new biomarkers of IGF by comparing several parameters between patients with IGF or non-IGF. For the first objective, grafts were allocated to 1 out of 3 groups according to the perfusion duration in the machine: < 12h, between 12 and 20h, and > 20h. Metabolites intensities or concentrations (for those analysed with Cobas instrument) were normalized by the sum of all features and then log transformed. Auto scaling was performed prior to statistical analyses, in accordance with standard approaches for metabolomic analysis. A two-step statistical approach was performed for each objective. Univariate analyzes were performed using non-parametric tests, i.e. Wilcoxon and Kruskall-Wallis for two or more groups, respectively. P values were corrected for multiple statistical tests using the False Discovery Rate (FDR) method. Concerning multivariate exploration, unsupervised analysis by Principal Component Analyses (PCA) was performed prior to the use of different machine learning approaches (e.g. partial least-squares discriminant analysis (PLS-DA) and Random-Forest (RF)). Pathway analyzes were performed for metabolites identified as discriminant during multivariate analyzes. Correlation between normalized metabolites values and membrane transporters' expression ($\log2(2^{-\Delta Ct})$) was evaluated by Partial Least Squares regression (PLS). The MetaboAnalyst 5.0 computational platform (www.metaboanalyst.ca/faces/home.xhtml) was used for all the statistical analyzes except for the PLS analysis which was used to study the correlation between transporter expression and metabolite content, performed using the MixOmics package (version 1.6.3) in the R software (version 4.0.2).

SDC, Figures:

Figure S1: Pathway analysis based on metabolites only detected in perfusates.

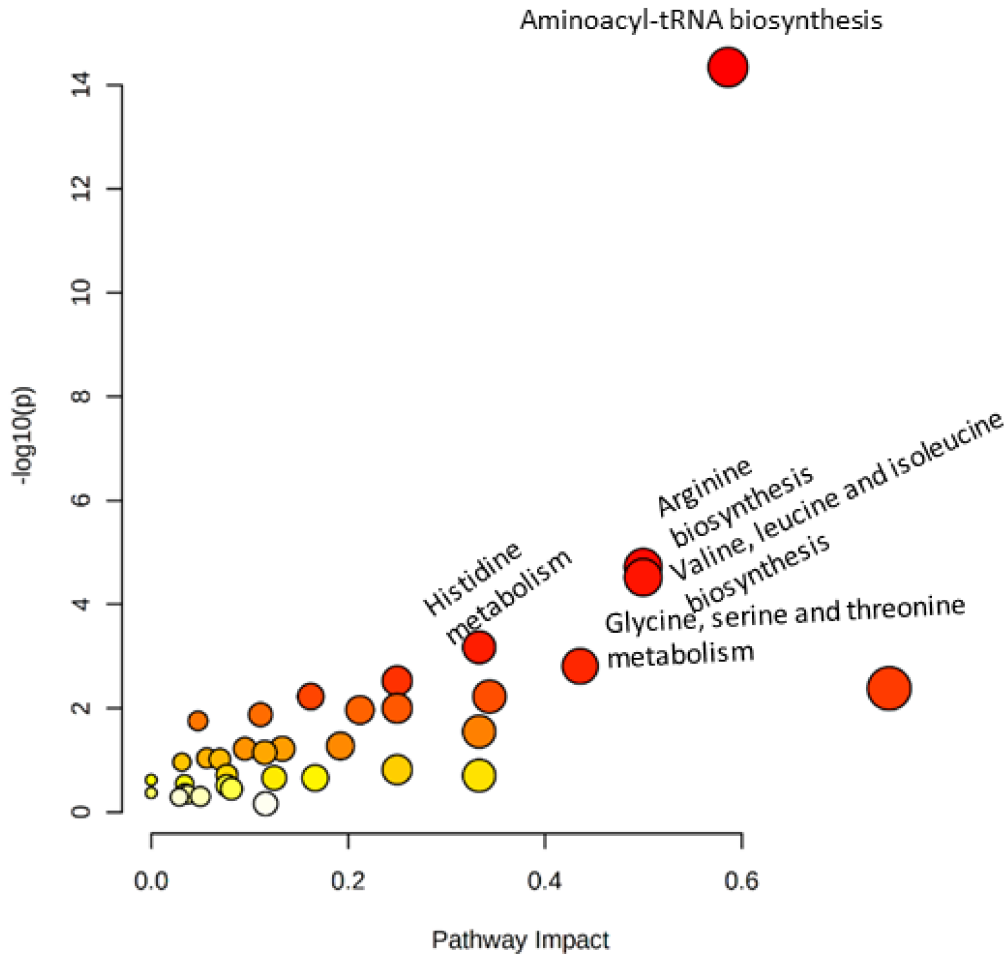

Figure S2: Correlation matrix between transporters found in pre-implantation biopsies. The dark red and dark blue colors indicate positive and negative correlations, respectively.

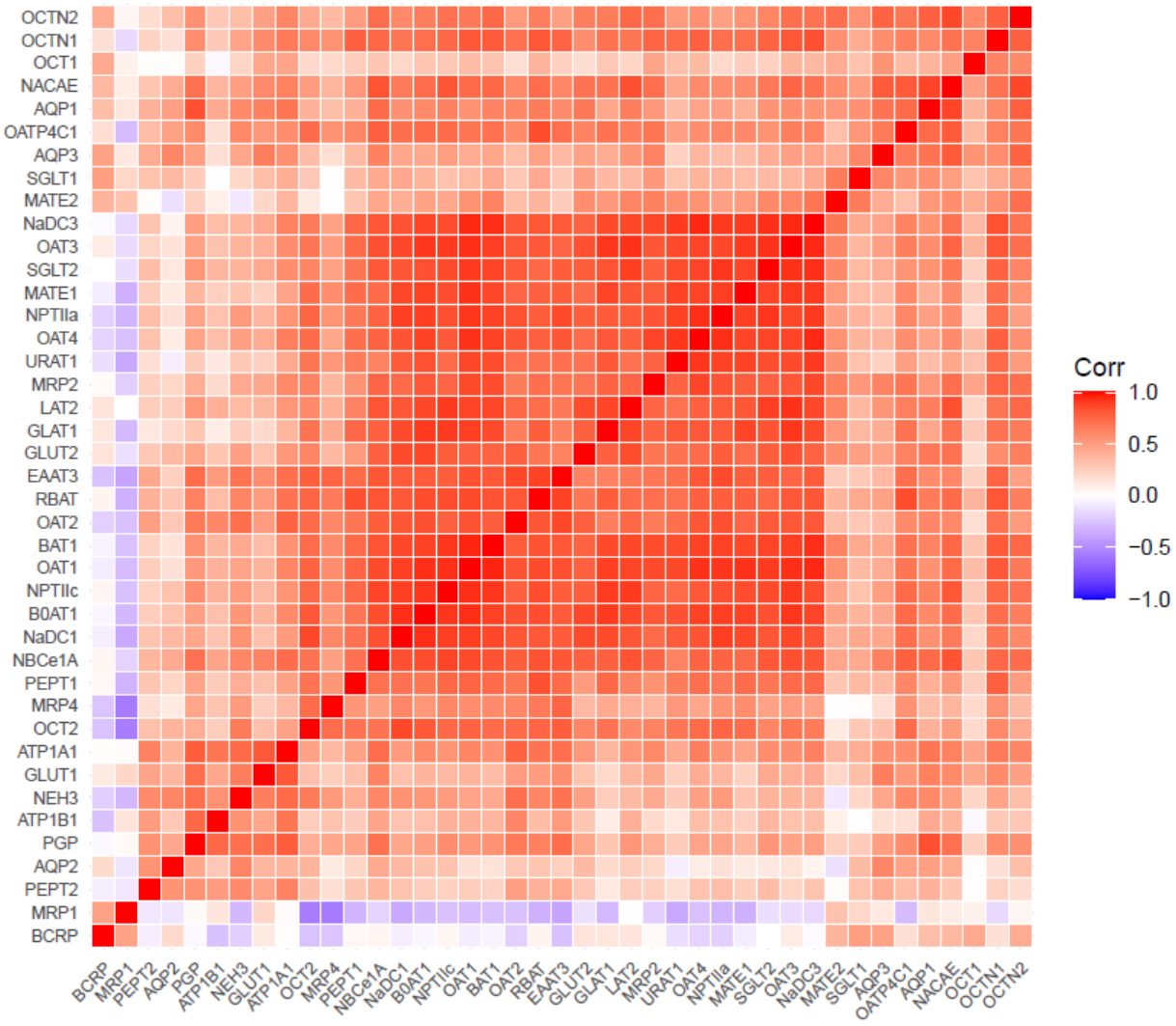

Figure S3: Dot plot of pathway enrichment analysis based on the most important metabolites, determined by Annova test, according to the perfusion time.

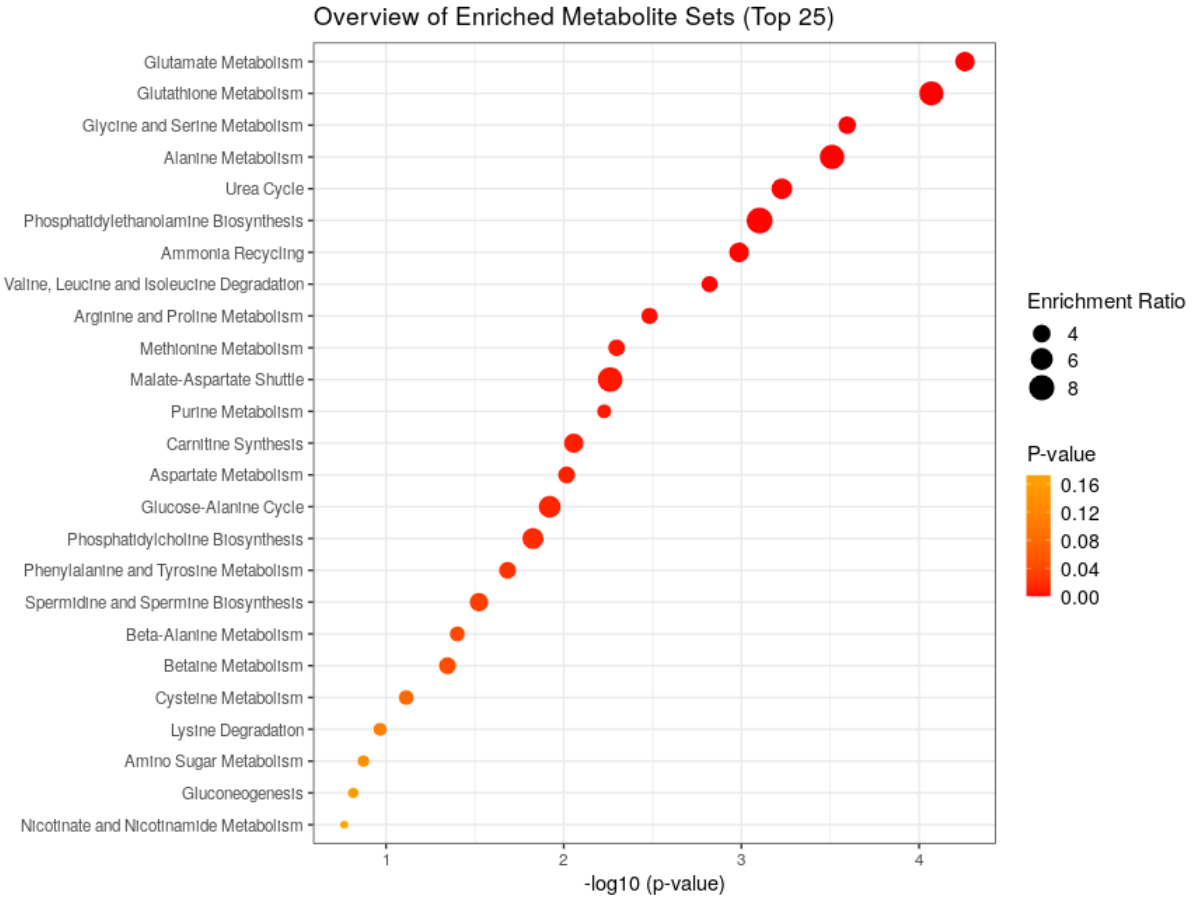

SDC, Tables:

Table S1: Custom-Designed TaqMan Low Density Array Card.

Assay ID	Gene Symbol(s)	Amplicon Length
Hs00537914_m1	*SLC22A6*	68
Hs00198527_m1	*SLC22A7*	69
Hs00188599_m1	*SLC22A8*	144
Hs01056646_m1	*SLC22A8*	76
Hs00945829_m1	*SLC22A11*	82
Hs00427552_m1	*SLC22A1*	79
Hs01010726_m1	*SLC22A2*	70
Hs00268200_m1	*SLC22A4*	76
Hs00929869_m1	*SLC22A5*	65
Hs00217320_m1	*SLC47A1*	74
Hs99999905_m1	*GAPDH*	0
Hs00945652_m1	*SLC47A2*	63
Hs00960489_m1	*ABCC2*	62
Hs00988720_g1	*ABCC4*	86
Hs00988721_m1	*ABCC4*	141
Hs01053790_m1	*ABCG2*	83
Hs00184500_m1	*ABCB1*	67
Hs01030727_m1	*SLC22A12*	64
Hs00192639_m1	*SLC15A1*	76
Hs01113665_m1	*SLC15A2*	69
Hs00903842_m1	*SLC9A3*	77
Hs00919316_g1	*SLC13A2*	72
Hs00955744_m1	*SLC13A3*	68
Hs01092910_m1	*SLC34A1*	84
Hs02341453_g1	*SLC34A3*	94
Hs00698884_m1	*SLCO4C1*	77
Hs01573793_m1	*SLC5A1*	60

Hs00894642_m1	*SLC5A2*	75
Hs00892681_m1	*SLC2A1*	76
Hs01096908_m1	*SLC2A2*	65
Hs00933601_m1	*ATP1A1*	76
Hs00426868_g1	*ATP1B1*	89
Hs01028916_m1	*AQP1*	96
Hs00292214_s1	*AQP2*	87
Hs00185020_m1	*AQP3*	63
Hs01047033_m1	*SLC4A4*	68
Hs01561483_m1	*ABCC1*	65
Hs01384157_m1	*SLC6A19*	70
Hs00909948_m1	*SLC7A7*	79
Hs00794796_m1	*SLC7A8*	87
Hs00374243_m1	*SLC3A2*	77
Hs00942976_m1	*SLC3A1*	66
Hs00204638_m1	*SLC7A9*	50
Hs00188172_m1	*SLC1A1*	76
Hs00943494_m1	*CHFR*	67
Hs00359037_m1	*NME4*	70
Hs01032748_g1	*NASP*	65
Hs00220422_m1	*C16ORF62*	82

Table S2: MRM transitions, retention time and mass spectrometric conditions of metabolites

Compound	Ionisation mode	Precursor ion	Product ion				Retention time (min)
			1	2	3	4	
		m/z	m/z	m/z	m/z		
2-Isopropylmalic acid	Negative	175.15	113.05	115.05			5.2
1-Methylhistidine	Positive	170.00	83.10	124.05			2.0
2-Aminoethanol	Positive	62.15	27.10	44.10			1.8

2-Ketoisovaleric acid	Negative	115.20	43.20	59.20	71.05	4.8
3-Methyl-2-oxovaleric acid	Negative	129.20	57.00	85.10	111.00	4.9
4-Aminobenzoic acid	Positive	138.25	65.10	77.10		5.3
4-Hydroxyproline	Positive	132.10	68.05	86.05		1.3
4-Pyridoxic acid	Positive	184.00	148.10	166.10		4.8
5-Glutamylcysteine	Positive	251.10	84.10	122.10		3.0
5'-Methylthioadenosine	Positive	298.10	119.10	136.10		6.2
Adenine	Positive	136.00	65.00	119.05		4.9
Adenosine	Positive	268.10	119.00	136.05		5.0
Alanine	Positive	89.90	44.10	45.30		1.4
alpha-keto-glutarate	Negative	145.30	40.95	73.00	83.00	1.3
Anthranilic acid	Positive	138.00	65.05	120.10		5.3
Arginine	Positive	175.20	60.10	70.10	116.00	1.8
Aspartic acid	Positive	134.00	70.10	74.05	88.10	1.3
Biotin	Positive	245.10	97.05	226.95		6.0
Choline	Positive	104.10	45.10	60.05		2.7
Creatinine	Positive	114.10	43.10	44.20	86.20	2.9
Cystathionine	Positive	223.00	88.05	134.00		1.3
Cystine	Positive	241.00	73.90	119.95	151.95	1.3
Deoxycytidine monophosphate	Positive	308.10	95.10	112.05		1.3
D-Mannitol	Negative	181.10	71.05	89.15	101.10	1.3
D-Ribose	Negative	149.30	59.05	71.15	89.05	1.3
Gluconic acid	Negative	195.20	74.90	99.00	129.05	1.2
Glucosamine	Positive	180.00	72.10	162.10		2.0
Glutamic acid	Positive	147.90	56.10	84.10		1.4
Glutamine	Negative	145.20	109.00	127.15		1.4
Glutathione	Positive	308.00	130.10	179.10	276.00	3.2
Glycine	Positive	75.90	30.15			1.3
Guanosine	Positive	284.00	110.00	135.00	152.00	4.8
Hexose (Glucose)	Negative	179.20	59.05	89.10		1.2
Histidine	Positive	155.90	56.10	82.70	110.10	1.7
Hypoxanthine	Positive	137.00	55.05	110.00		3.1

Inosine	Positive	269.10	110.00	118.95	137.05		4.8
Isoleucine	Positive	132.10	41.20	44.20	69.15	86.20	5.2
Kynurenine	Positive	209.10	94.10	118.10	145.90	192.05	5.9
Lactic acid	Negative	89.30	43.10	45.10	71.10	89.05	2.0
L-Carnitine	Positive	162.30	60.10	103.15			3.2
Leucine	Positive	132.10	30.05	43.35	86.05		5.3
Lysine	Positive	147.20	56.10	84.20	130.10		2.0
Methionine	Positive	149.90	56.10	104.10			3.2
Methionine sulfoxide	Positive	166.00	55.95	74.10	102.00		1.4
Niacinamide	Positive	123.10	53.10	77.00	80.05		3.5
O-Phosphoethanolamine	Positive	142.10	44.20				1.2
Ornithine	Positive	133.10	70.10	116.05			1.6
Oxidized glutathione	Negative	611.10	143.05	306.00			4.8
PAH	Positive	195.00	65.20	92.20	120.15		5.0
Phenylalanine	Positive	166.10	77.10	103.10	120.10		5.7
Pipecolic acid	Positive	130.10	56.10	84.05	112.10		2.6
Proline	Positive	116.10	28.05	43.20	70.15		1.7
Riboflavin	Positive	377.00	172.00	197.00	243.05		5.2
Serine	Positive	105.90	42.30	60.10	70.10		1.3
Taurine	Negative	124.35	64.10	79.95			1.2
Threonine	Positive	120.10	56.05	74.15	102.10		1.3
Thymidine	Positive	243.10	109.00	116.00	127.10		4.8
Thymine	Positive	127.10	54.05	110.05			4.8
Tryptophan	Positive	205.10	91.00	118.00	146.10	188.15	6.8
Tyrosine	Positive	182.10	77.10	91.10	136.10		4.9
Uracil	Positive	113.00	70.00				2.1
Uric acid	Negative	167.10	96.20	123.95			2.4
Uridine	Positive	245.00	70.00	96.00	113.05		3.2
Valine	Positive	118.00	55.10	57.10			2.9
Xanthine	Negative	151.00	42.00	108.00			3.1
Xanthosine	Positive	284.90	135.95	153.05			4.8

Annexe 3.2. Méthode RMN

Soixante µL d'une solution contenant du D2O (tampon phosphate pH = 7,45) ainsi qu'une référence interne (TSP) de concentration finale 152,4 µM ont été ajoutés à 150 µL de chaque liquide de conservation. D'un point de vue analytique, la séquence d'acquisition (1H) utilisée est la séquence noesypr1d avec un délai de 20s et un nombre de scans de 64. Les métabolites ont été identifiés à l'aide du logiciel ChenomX NMR suite 7.7.

Annexe 4. Contenu supplémentaire de l’article expérimental 2

Supplementary data

Supplementary data "Materiel and Methods"

LC-MS/MS settings for metabolomics analyses

Chromatographic separation of the compounds was carried out with a Discovery HS F5-3 column (150 x 2.1 mm d.i., 3 µm) at 40°C, at a flow rate of 350 µL/min according to the following linear mobile phase gradient: 0-1.4 min : 0% B ; 1.4-3.5 min : 0 to 25% B ; 3.5-7.5 min ; 25 to 35% B ; 7.5 to 10.3 min : 35 to 95% B; 10.3-13.7: 95%B; 13.7-13.8 min: 95 to 0% B; 13.8-17 min: 0%B where A is a 0.1% solution of formic acid in water and B is a 0.1% solution of formic acid in acetonitrile. Detection was performed by electrospray ionization using the following source conditions: nebulizing gas flow rate; 3 mL/min; drying gas flow rate: 10 mL/min; heating gas flow rate: 10 mL/min; interface temperature: 300°C; desolvation line temperature: 250°C; block heater temperature: 400°C. The compounds were detected in the scheduled MRM (Multi Reaction Monitoring) mode in the positive and negative polarities alternately. One quantification and a minimum of one confirmation transition, as well as the relative retention time were used for compound identification (Supplementary Table 2).

Supplementary Tables

Supplementary Table 1: Summary of fold-changes in the transcriptomic study

Numbers in blue indicate downregulation (fold-change ≤ 0.5) and numbers in red upregulation (fold-change ≥ 2).

Part 1: Fold-changes after hypoxia (H) and hypoxia/reoxygenation (R)									
	H (hours)	6				24			
	R (hours)	0	2	24	48	0	2	24	48
ABC	ABCB1	0,95	0,92	0,95	1,08	0,51	**0,30**	0,58	1,22
	ABCC1	**2,00**	1,21	1,42	1,22	1,29	1,20	0,80	1,04
	ABCC2	1,01	1,03	0,89	1,50	1,78	**2,93**	1,00	0,66
	ABCC4-1	**2,23**	1,17	0,60	1,04	0,52	0,63	0,70	0,80
	ABCC4-2	0,68	**3,11**	0,82	1,97	**0,17**	**0,24**	0,98	0,78
AQP	AQP1	0,97	1,09	1,73	1,95	**0,37**	**0,38**	**0,39**	0,54
	AQP2	0,54	1,32	**2,20**	**10,77**	**0,06**	**0,11**	0,66	**0,23**
	AQP3	1,51	1,09	1,86	1,32	**0,42**	**0,32**	**2,63**	0,99
ATP	ATP1A1	1,59	1,29	1,17	1,39	0,55	**0,44**	1,24	0,99
	ATP1B1	1,91	1,29	0,92	1,11	1,91	1,54	0,73	0,75
AA	SLC15A1	0,97	1,25	0,82	0,89	1,72	0,81	**0,37**	0,79
	SLC15A2	1,06	1,52	1,13	1,44	1,80	**0,40**	0,56	0,92
	SLC1A1	1,15	0,85	1,04	0,91	1,02	0,61	0,89	1,47
	SLC7A7	0,73	1,53	0,94	1,33	**0,42**	0,57	1,37	0,91

	SLC7A8	0,65	1,39	0,66	0,90	1,13	1,03	0,63	0,81
	SLC3A1	0,77	0,65	0,68	**2,08**	1,21	**0,33**	1,12	1,58
	SLC3A2	1,59	1,19	1,19	1,37	1,41	1,42	1,56	0,87
GLC	SLC5A2	0,73	1,19	**6,29**	1,70	0,57	1,33	0,64	**0,44**
	SLC2A1	**10,56**	0,94	1,06	0,92	**8,58**	**4,11**	0,98	0,94
	SLC4A4	**3,03**	1,47	0,87	1,30	**0,44**	**0,26**	**0,43**	0,74
	SLC34A3	**0,29**	**0,38**	1,19	1,77	**4,26**	**3,17**	1,49	**2,21**
	SLC13A3	1,40	1,08	0,92	1,20	1,06	0,69	0,99	0,82
OI	SLC22A1	0,99	0,99	1,21	0,91	1,18	1,06	0,71	**0,36**
	SLC22A4	0,87	0,97	1,29	0,84	1,72	1,15	1,27	0,96
	SLC22A5	1,14	0,89	1,16	1,24	0,51	0,63	0,70	0,79
	SLCO4C1	1,36	1,42	0,80	1,52	0,65	0,58	0,57	**0,41**

Part 2: Fold-changes after 6-hour normoxia

	N (hours)	6				24				6				24			
	N (hours)	0	2	24	48	0	2	24	48	0	2	24	48	0	2	24	48
	ABCB1	1,00	1,16	0,83	1,03	0,74	1,03	0,89	0,85	0,95	1,07	0,78	1,11	**0,38**	**0,31**	0,52	1,03
	ABCC1	1,00	1,87	1,34	1,17	1,45	1,77	1,93	1,22	**2,00**	**2,27**	1,91	1,43	1,87	**2,11**	1,54	1,27
ABC	ABCC2	1,00	1,90	**2,76**	1,41	**2,74**	**2,52**	1,73	1,69	1,01	1,95	**2,47**	**2,12**	**4,87**	**7,39**	1,72	1,12
	ABCC4-1	1,00	1,28	1,84	1,32	1,80	1,52	1,71	1,57	**2,23**	1,50	1,11	1,37	0,93	0,96	1,20	1,25
	ABCC4-2	1,00	1,64	1,67	1,44	**3,99**	**4,34**	1,29	**2,30**	0,68	**5,10**	1,37	**2,83**	0,66	1,05	1,26	1,79

	AQP1	1,00	1,46	1,65	1,61	1,84	**3,09**	**4,23**	**2,40**	0,97	1,59	**2,85**	**3,14**	0,69	1,18	1,64	1,29
AQP	AQP2	1,00	1,66	**3,16**	1,34	**9,22**	**3,93**	**4,20**	**6,08**	0,54	**2,19**	**6,95**	**14,38**	0,57	**0,43**	**2,79**	1,39
	AQP3	1,00	1,93	1,58	**0,48**	1,24	2,23	0,73	**0,49**	1,51	**2,09**	**2,95**	**0,63**	0,53	0,71	1,91	**0,49**
	ATP1A1	1,00	1,70	**3,65**	**2,02**	**3,23**	**4,26**	**2,24**	**2,83**	1,59	**2,19**	**4,26**	**2,81**	1,79	1,86	**2,77**	**2,79**
ATP	ATP1B1	1,00	1,42	**2,26**	**2,30**	**2,42**	**2,29**	**2,47**	**2,66**	1,91	1,83	**2,07**	**2,56**	**4,63**	**3,53**	1,80	**2,01**
	SLC15A1	1,00	0,82	**0,32**	**0,49**	**0,29**	**0,46**	**0,43**	**0,47**	0,97	1,02	**0,27**	**0,43**	**0,50**	**0,37**	**0,16**	**0,38**
	SLC15A2	1,00	1,02	0,54	0,69	**0,42**	1,31	0,88	1,12	1,06	1,55	0,61	1,00	0,75	0,52	0,49	1,02
	SLC1A1	1,00	1,34	1,95	**2,04**	1,73	1,64	**2,08**	1,38	1,15	1,14	**2,03**	1,87	1,77	1,00	1,86	**2,04**
AA	SLC7A7	1,00	0,68	1,11	**0,33**	1,04	1,33	0,56	**0,37**	0,73	1,04	1,04	**0,44**	**0,44**	0,75	0,77	**0,33**
	SLC7A8	1,00	1,08	1,08	0,74	1,09	1,31	0,72	**0,44**	0,65	1,51	0,71	0,66	1,23	1,35	**0,46**	**0,35**
	SLC3A1	1,00	**6,45**	1,50	0,82	0,70	1,40	0,74	0,70	0,77	**4,18**	1,03	1,71	0,85	**0,47**	0,83	1,11
	SLC3A2	1,00	1,16	0,67	0,52	0,56	0,92	**0,47**	0,55	1,59	1,38	0,80	0,71	0,79	1,30	0,74	**0,47**
GLC	SLC5A2	1,00	0,96	**0,19**	**0,36**	1,07	0,78	**0,49**	0,60	0,73	1,14	1,22	0,62	0,61	1,03	**0,31**	**0,26**
	SLC2A1	1,00	**4,26**	1,13	0,87	1,07	1,27	1,00	0,89	**10,56**	**4,01**	1,20	0,80	**9,21**	**5,21**	0,97	0,84
	SLC4A4	1,00	1,73	**2,69**	**3,24**	**2,36**	**2,56**	**5,78**	**3,32**	**3,03**	**2,55**	**2,34**	**4,21**	1,02	0,66	**2,49**	**2,46**
	SLC34A3	1,00	1,31	1,63	1,27	0,97	1,80	**3,57**	1,01	**0,29**	**0,49**	1,94	**2,25**	**4,12**	**5,70**	**5,31**	**2,24**
	SLC13A3	1,00	1,36	1,82	**2,16**	1,37	1,69	**2,00**	**2,29**	1,40	1,47	1,67	**2,59**	1,45	1,16	1,99	1,87
IO	SLC22A1	1,00	**2,53**	**2,74**	**2,45**	**3,92**	**2,85**	**2,55**	**4,91**	0,99	**2,49**	**3,32**	**2,23**	**4,63**	**3,01**	1,82	1,76
	SLC22A4	1,00	1,02	0,70	0,50	0,86	1,27	0,61	0,50	0,87	1,00	0,90	0,42	1,48	1,46	0,78	**0,48**
	SLC22A5	1,00	1,42	**2,02**	**2,16**	**2,45**	1,64	**3,36**	**2,84**	1,14	1,27	**2,35**	**2,68**	1,24	1,02	**2,34**	**2,25**

SLCO4C1	1,00	1,08	**2,80**	**3,61**	**2,67**	1,91	**4,13**	**8,46**	1,36	1,53	**2,24**	**5,50**	1,73	1,10	**2,36**	**3,45**

Supplementary Table 2: Custom-Designed TaqMan Low Density Array Card.

Assay ID	Gene Symbol(s)	Amplicon Length
Hs00537914_m1	*SLC22A6*	68
Hs00198527_m1	*SLC22A7*	69
Hs00188599_m1	*SLC22A8*	144
Hs01056646_m1	*SLC22A8*	76
Hs00945829_m1	*SLC22A11*	82
Hs00427552_m1	*SLC22A1*	79
Hs01010726_m1	*SLC22A2*	70
Hs00268200_m1	*SLC22A4*	76
Hs00929869_m1	*SLC22A5*	65
Hs00217320_m1	*SLC47A1*	74
Hs99999905_m1	*GAPDH*	0
Hs00945652_m1	*SLC47A2*	63
Hs00960489_m1	*ABCC2*	62
Hs00988720_g1	*ABCC4*	86
Hs00988721_m1	*ABCC4*	141
Hs01053790_m1	*ABCG2*	83
Hs00184500_m1	*ABCB1*	67
Hs01030727_m1	*SLC22A12*	64
Hs00192639_m1	*SLC15A1*	76
Hs01113665_m1	*SLC15A2*	69
Hs00903842_m1	*SLC9A3*	77
Hs00919316_g1	*SLC13A2*	72
Hs00955744_m1	*SLC13A3*	68
Hs01092910_m1	*SLC34A1*	84
Hs02341453_g1	*SLC34A3*	94
Hs00698884_m1	*SLCO4C1*	77
Hs01573793_m1	*SLC5A1*	60
Hs00894642_m1	*SLC5A2*	75
Hs00892681_m1	*SLC2A1*	76
Hs01096908_m1	*SLC2A2*	65
Hs00933601_m1	*ATP1A1*	76
Hs00426868_g1	*ATP1B1*	89
Hs01028916_m1	*AQP1*	96
Hs00292214_s1	*AQP2*	87

Hs00185020_m1	*AQP3*	63
Hs01047033_m1	*SLC4A4*	68
Hs01561483_m1	*ABCC1*	65
Hs01384157_m1	*SLC6A19*	70
Hs00909948_m1	*SLC7A7*	79
Hs00794796_m1	*SLC7A8*	87
Hs00374243_m1	*SLC3A2*	77
Hs00942976_m1	*SLC3A1*	66
Hs00204638_m1	*SLC7A9*	50
Hs00188172_m1	*SLC1A1*	76
Hs00943494_m1	*CHFR*	67
Hs00359037_m1	*NME4*	70
Hs01032748_g1	*NASP*	65
Hs00220422_m1	*C16ORF62*	82

Supplementary Table 3: MRM transitions, retention time and mass spectrometric conditions of metabolomics analyses

Compound	Ionisation mode	Precursor ion	Product ion				Retention time (min)
			1	2	3	4	
		m/z	m/z	m/z	m/z		
2-Isopropylmalic acid	Negative	175.15	113.05	115.05			5.2
2-Aminoadipic acid	Positive	162.15	55.15	116.20			1.9
2-aminobutyric acid	Positive	104.00	43.10	58.10			1.5
2-Ketoisovaleric acid	Negative	115.20	43.20	59.20	71.05		4.8
3-aminopropanoic acid	Positive	90.05	30.15	72.15			1.8
3-hydroxyanthranilic acid	Positive	154.05	80.10	136.10			5.0
3-Methyl-2-oxovaleric acid	Negative	129.20	57.00	85.10	111.00		4.9
4-Aminobutyric acid	Positive	104.00	45.00	68.95			2.2
4-Hydroxyproline	Positive	132.10	68.05	86.05			1.3
4-Pyridoxic acid	Positive	184.00	148.10	166.10			4.8
5-Glutamylcysteine	Positive	251.10	84.10	122.10			3.2
5'-Methylthioadenosine	Positive	298.10	119.10	136.10			6.2
5-Oxoproline	Negative	128.20	81.90	84.05			1.5
Aconitic acid	Negative	173.00	85.15	111.00			3.0
Adenine	Positive	136.00	65.00	119.05			4.9
Adenosine	Positive	268.10	119.00	136.05			5.0
Adenosine monophosphate	Positive	348.00	94.10	109.10	136.05	250.10	2.0
Alanine	Positive	89.90	44.10	45.30			1.4
alpha-keto-glutarate	Negative	145.30	40.95	73.00	83.00		1.3
Arginine	Positive	175.20	60.10	70.10	116.00		1.8
Argininosuccinic acid	Positive	291.10	70.05	116.05			1.8
Ascorbic acid 2-phosphate	Negative	254.90	78.80	237.0			1.0
Asparagine	Positive	133.10	28.05	74.05	87.15		1.3
Aspartic acid	Positive	134.00	70.10	74.05	88.10		1.3
Choline	Positive	104.10	45.10	60.05			2.7
Citric acid	Negative	191.20	67.05	87.05	111.10		1.9

Citrulline	Positive	176.10	70.05	113.05	159.05		2.2
Creatinine	Positive	114.10	43.10	44.20	86.20		2.9
Cystathionine	Positive	223.00	88.05	134.00			1.3
Cysteine	Positive	122.00	59.00	76.05	87.05	105.05	1.3
Cystine	Positive	241.00	73.90	119.95	151.95		1.3
Cytidine	Positive	244.10	95.00	112.05			4.2
Cytidine monophosphate	Positive	324.00	67.10	95.00	112.05		1.5
Cytosine	Positive	112.00	95.05				1.9
Deoxyadenosine	Positive	252.10	119.00	136.15			5.0
Deoxyadenosine monophosphate	Positive	332.10	81.10	136.20			3.0
Deoxycytidine	Positive	228.10	95.05	112.10			5.0
Deoxyguanosine	Positive	268.10	135.10	152.15			4.8
D-Mannitol	Negative	181.10	71.05	89.15	101.10		1.3
D-Ribose	Negative	149.30	59.05	71.15	89.05		1.3
Folic acid	Positive	442.00	120.05	176.05	295.15		5.1
Formylkynurenine	Positive	237.00	118.15	146.05			5.4
Fumaric acid	Negative	115.00	26.95	46.25	71.10		3.2
Gluconic acid	Negative	195.20	74.90	99.00	129.05		1.2
Glutamic acid	Positive	147.90	56.10	84.10			1.4
Glutamine	Negative	145.20	109.00	127.15			1.4
Glutathione	Positive	308.00	130.10	179.10	276.00		3.3
Glycine	Positive	75.90	30.15				1.3
Glycyl-glutamine	Positive	204.00	58.00	84.10	130.10		1.8
Guanine	Negative	150.00	66.10	133.00			3.7
Guanosine	Positive	284.00	110.00	135.00	152.00		4.8
Guanosine monophosphate	Positive	364.00	135.00	152.05			1.8
Hexose (Glucose)	Negative	179.20	59.05	89.10			1.2
Histidine	Positive	155.90	56.10	82.70	110.10		1.7
Hypoxanthine	Positive	137.00	55.05	110.00			3.1
Indole-3-acetic acid	Positive	176.00	103.05	130.20			7.0
Inosine	Positive	269.10	110.00	118.95	137.05		4.8
Inosine monophosphate	Positive	349.05	119.20	137.10			1.5

Isoleucine	Positive	132.10	41.20	44.20	69.15	86.20	5.2
Kynurenic acid	Positive	190.15	89.10	144.10			5.5
Kynurenine	Positive	209.10	94.10	118.10	145.90	192.05	5.9
Lactic acid	Negative	89.30	43.10	45.10	71.10	89.05	2.0
Leucine	Positive	132.10	30.05	43.35	86.05		5.3
Lysine	Positive	147.20	56.10	84.20	130.10		2.0
Methionine	Positive	149.90	56.10	104.10			3.2
Methionine sulfoxide	Positive	166.00	55.95	74.10	102.00		1.4
N-Acetylaspartic acid	Positive	175.90	88.05	134.05			2.1
NAD	Positive	664.00	136.10	428.15			3.2
Niacinamide	Positive	123.10	53.10	77.00	80.05		3.5
Nicotinic acid	Positive	124.05	78.05	80.05			2.8
O-Phosphoethanolamine	Positive	142.10	44.20				1.2
Ornithine	Positive	133.10	70.10	116.05			1.6
Oxidized glutathione	Negative	611.10	143.05	306.00			5.0
Pantothenic acid	Positive	220.10	90.15	184.10	202.10		4.8
Phenylalanine	Positive	166.10	77.10	103.10	120.10		5.7
Pipecolic acid	Positive	130.10	56.10	84.05	112.10		2.6
Proline	Positive	116.10	28.05	43.20	70.15		1.7
Putrescine	Positive	89.20	30.10	72.10			2.3
Pyridoxal	Positive	167.90	67.15	94.15	122.05	150.05	5.1
Pyridoxal phosphate	Positive	248.10	94.15	150.15			2.5
Pyridoxine	Positive	169.90	77.10	134.05	152.05		5.5
Pyruvic acid	Negative	86.90	42.95				1.8
Riboflavin	Positive	377.00	172.00	197.00	243.05		5.2
S-adenosylhomocysteine	Positive	385.10	134.10	136.15			6.0
Serine	Positive	105.90	42.30	60.10	70.10		1.3
Succinic acid	Negative	116.90	55.05	73.00	99.05		2.9
Taurine	Negative	124.35	64.10	79.95			1.5
Threonic acid	Negative	135.20	59.00	75.00			1.3
Threonine	Positive	120.10	56.05	74.15	102.10		1.3
Thymidine	Positive	243.10	109.00	116.00	127.10		5.0

Thymine	Positive	127.10	54.05	110.05			4.8
Tryptophan	Positive	205.10	91.00	118.00	146.10	188.15	6.8
Tyrosine	Positive	182.10	77.10	91.10	136.10		4.9
Uric acid	Negative	167.10	96.20	123.95			2.4
Uridine	Positive	245.00	70.00	96.00	113.05		3.2
Uridine monophosphate	Positive	325.05	97.10	113.05	136.05		2.0
Valine	Positive	118.00	55.10	57.10			2.9
Xanthine	Negative	151.00	42.00	108.00			3.1
Xanthosine	Positive	284.90	135.95	153.05			4.8
Xanthosine monophosphate	Positive	365.05	97.10	153.15			1.5

Tab S4 - Summary statistical analysis

Box1 A: ATP concentration

Unpaired t test				
Hypoxia	Comparison	p-value	p-value summary	t, df
6h	6N vs 6H	0,0002	***	t=13.06 df=4
24h	24N vs 24H	P<0.0001	***	t=26.18 df=4
Box1 B: LDH release				
Unpaired t test with Welch's correction				
Hypoxia	Comparison	p-value	p-value summary	Welch-corrected t, df
6h	T0	0,317	ns	t=1,025 df=21
	6N vs 6H	0,165	ns	t=1,447 df=18
	6N2N vs 6H2R	0,4982	ns	t=0,6953 df=14
	6N24N vs 6H24R	0,1509	ns	t=1,520 df=14
	6N48N vs 6H48R	0,4885	ns	t=0,7051 df=21
24h	T0	0,2484	ns	t=1,187 df=21
	24N vs 24H	0,2135	ns	t=1,283 df=21
	24N2N vs 24H2R	0,0025	**	t=3,624 df=15
	24N24N vs 24H24R	0,0116	*	t=3,021 df=11
	24N48N vs 24H48R	0,0162	*	t=2,795 df=12
Box 1 C: Intracellular metabolomic statistical analysis				
Unpair t-test Unpaired t test with Welch's correction				
Metabolite	Comparison	p-value	p-value summary	Welch-corrected t, df
Citric acid	6N vs 6H	< 0,0001	****	t=7,467 df=14
	24N vs 24H	0,0003	***	t=5,261 df=11
	6H vs 24H	0,0899	ns	t=1,813 df=15
keto-glutaric	6N vs 6H	0,0055	**	t=3,630 df=9
	24N vs 24H	0,6865	ns	t=0,4121 df=14
	6H vs 24H	0,0074	**	t=3,436 df=9
Fumaric acid	6N vs 6H	0,2901	ns	t=1,112 df=11

	24N vs 24H	0,0075	**	t=3,088 df=15
	6H vs 24H	0,0049	**	t=3,387 df=13
Succinic acid	6N vs 6H	0,0014	**	t=3,914 df=15
	24N vs 24H	< 0,0001	****	t=6,795 df=10
	6H vs 24H	0,0008	***	t=4,740 df=10
Hexoses	6N vs 6H	< 0,0001	****	t=7,949 df=9
	24N vs 24H	0,0002	***	t=5,126 df=14
	6H vs 24H	0,0636	ns	t=2,115 df=9
Pyruvic acid	6N vs 6H	0,0046	**	t=3,326 df=15
	24N vs 24H	0,0001	***	t=5,499 df=12
	6H vs 24H	0,0574	ns	t=2,058 df=15
Lactic acid	6N vs 6H	< 0,0001	****	t=12,08 df=10
	24N vs 24H	< 0,0001	****	t=16,22 df=10
	6H vs 24H	0,0005	***	t=4,371 df=15

H, hypoxia; N, normoxia; R, reoxygenation. For example, the 6H2R condition corresponds to 6-hour hypoxia followed by 2-hour reoxygenation.

Supplementary Table 5: Priors for each parameter of models used for metabolomic analysis

Prior	Type of priors	coefficient	group	dpar	source
	population				default
normal(100.0/6,4)	population	Intercept			user
	population	moreox_t			default
	population	moreox_t:oxie_t24			default
	population	oxie_t24			default
normal(0,3)	population			sigma	user
	population	metabolite*		sigma	default
exponential(1)	Intercept			sigma	user
student_t(3, 0, 2.5)	Standard deviation				default
normal(0,3)	Standard deviation		metabolite		user
	Standard deviation	Intercept	metabolite		default
	Standard deviation	oxie_t:reox_t **	metabolite		default
dirichlet(1)	Simplex monotonic	moreox_t:oxie_t241			default
dirichlet(1)	Simplex monotonic	moreox_t1			default

More information about priors in brms are in chapter 2.1 https://cran.r-project.org/web/packages/brms/vignettes/brms_overview.pdf

** There was one coefficient by metabolite to increase or decrease the standard deviation of the metabolite as compared to the population standard deviation.*

*** 8 coefficients: one by interaction of hypoxia and reoxygenation duration.*

Annexe 5. Milieux de culture utilisés pour la génération de HPTC dérivées de hiPSC

Annexe 5.1. Milieu de différenciation des hiPSC

Mélange 1:1 de DMEM:F12, 2 mM de glutamax , 5 µg/ml d'insuline, 5 µg/ml de transferrine et 5 ng/ml de sélénite de sodium.

Annexe 5.2. Milieu de culture spécifique des cellules tubulaires proximales

Mélange 1:1 de DMEM:F12, 2 mM de glutamax, 5 µg/ml d'insuline, 5 µg/ml de transferrine, 5 ng/ml de sélénite de sodium, 10 ng/ml de facteur de croissance épithéliale et 36 ng/ml d'hydrocortisone avec addition de 100 U/ml de pénicilline et 0.5% FCS (*fetal calf serum*).

Impact de l'hypoxie/réoxygénation sur l'expression et la fonctionnalité des transporteurs tubulaires rénaux

Pour répondre à la disparité croissante entre le nombre de donneurs en liste d'attente d'une greffe rénale et le nombre d'organes disponibles, la plupart des centres de transplantation ont recours à des donneurs « sous-optimaux ». L'utilisation de ces greffons est associée des lésions d'ischémie-reperfusion (IRI) plus fréquentes, qui nécessitent d'être mieux comprises pour mettre en place des méthodes préventives. Cette thèse s'intéresse aux effets de l'ischémie et de l'hypoxie/réoxygénation sur l'expression et la fonctionnalité des transporteurs membranaires exprimés à la surface des cellules tubulaires proximales. Ces cellules assurent des mouvements trans-cellulaires de divers composés, principalement régis par l'activité coordonnée de transporteurs membranaires des super-familles SLC (Solute Carriers) et ABC (ATP-Binding Cassette). Nous avons réalisé un état des lieux des connaissances relatives aux effets des lésions d'IR sur les transporteurs tubulaires, puis conduit une étude translationnelle ayant nécessité recherche clinique et recherche fondamentale. Nous avons démontré qu'il existe des modifications transcriptionnelles hypoxie-dépendantes, variables selon les transporteurs. Toutefois, cette réponse transcriptionnelle n'était pas prédictive de la fonction rénale post-greffe sur une cohorte de patients transplantés. Pour étudier les systèmes de transport tubulaire dans leur ensemble nous avons évalué les variations du métabolome endogène en condition d'hypoxie/réoxygénation. Malheureusement, nous n'avons pas identifié de variations métaboliques corrélées avec la modulation des transporteurs, in vitro et chez l'Homme. L'absence de données protéiques et de tests de fonctionnalité n'a pas permis de confirmer l'effet de l'hypoxie/réoxygénation sur la fonction des transporteurs tubulaires et ces approches complémentaires devront être considérées à l'avenir. Au vu de la complexité globale de l'étude des systèmes de transport tubulaire à laquelle nous avons fait face dans cette étude, nous proposons la conduite d'expérimentations ciblées sur des transporteurs présélectionnés, avec l'utilisation de substrats spécifiques.

Mots-clés : Transplantation rénale, Transporteurs tubulaires, Métabolomique, Hypoxie/réoxygénation, HMP

Impact of hypoxia/reoxygenation on the expression and the functionality of renal tubular transporters

Faced with the divergence between the need for kidney grafts and the number of organs available, more transplant centers accept "suboptimal" donors. The use of grafts from such high-risk donors has led to a growing incidence of ischemia-reperfusion injury (IRI), the mechanisms of which need to be better understood in order to develop preventive measures. The present thesis focuses on the effects of ischemia and hypoxia/reoxygenation on the expression and functionality of membrane transporters located at the membrane of proximal tubular cells (PTC). These transporters belong to either the solute carrier (SLC) or the ATP-binding cassette transporter (ATP) superfamilies, the coordinated functions of which govern the transcellular transport of a broad range of compounds. After having comprehensively reviewed the literature about the effects of IRI on tubular transporters, we conducted a translational study combining clinical and basic experiments. Particular attention was paid to the effects of ischemia and hypoxia/reoxygenation-induced on the transcriptional expression and function of transporters. We demonstrated that different PTC transporters had different mRNA expression responses to hypoxia. However, mRNA expression was not correlated with the immediate renal function recovery in a cohort of kidney transplant patients. We also studied the metabolome to look for dysfunctions among the tubular transport systems in hypoxia/reoxygenation conditions. Unfortunately, none of the metabolic variations found in vitro on in the perfusion liquid of explanted kidney grafts were significantly associated with the tubular transporter functions. The lack of protein data and functionality tests also prevented us from confirming the effect of hypoxia/reoxygenation on tubular transporter functions. Given the difficulty of thoroughly investigating tubular transport systems, we recommend conducting targeted experiments on pre-selected transporters using selective substrates.

Keywords : Kidney transplantation, Tubular transporters, Metabolomic, Hypoxia/reoxygenation, HMP